ZooKeys 1156: 1–14 (2023)
doi: 10.3897/zookeys.1156.98331
https://zookeys.pensoft.net

RESEARCH ARTICLE

A peer-reviewed open-access journal
ZooKeys
Launched to accelerate biodiversity research

Pholcid spiders of the *Pholcus phungiformes* species-group (Araneae, Pholcidae) from Liaoning Province, China: an overview, with description of a new species

Fangyu Zhao[1], Tian Jiang[1], Lan Yang[1], Qiaoqiao He[1,2,3], Guo Zheng[1,2,3], Zhiyuan Yao[1,2,3]

1 *College of Life Science, Shenyang Normal University, Shenyang 110034, Liaoning, China* **2** *Liaoning Key Laboratory of Evolution and Biodiversity, Shenyang 110034, Liaoning, China* **3** *Liaoning Key Laboratory for Biological Evolution and Agricultural Ecology, Shenyang 110034, Liaoning, China*

Corresponding authors: Zhiyuan Yao (yaozy@synu.edu.cn); Guo Zheng (zhengguo@synu.edu.cn); Qiaoqiao He (heqq@synu.edu.cn)

Academic editor: Gergin Blagoev | Received 5 December 2022 | Accepted 10 March 2023 | Published 24 March 2023

https://zoobank.org/CF00C07F-11E0-4D1C-957A-0B5EF9B2D552

Citation: Zhao F, Jiang T, Yang L, He Q, Zheng G, Yao Z (2023) Pholcid spiders of the *Pholcus phungiformes* species-group (Araneae, Pholcidae) from Liaoning Province, China: an overview, with description of a new species. ZooKeys 1156: 1–14. https://doi.org/10.3897/zookeys.1156.98331

Abstract

Species of the *Pholcus phungiformes* group exhibit high diversity in Liaoning Province of northeastern China. This paper summarizes the current knowledge on this species-group from this area. A checklist of 22 species recorded from this province is given, accompanied with a distribution map of the species. *Pholcus xiuyan* Zhao, Zheng & Yao, **sp. nov.** (♂♀) is described as new to science, and *P. yuhuangshan* Yao & Li, 2021 is reported from Liaoning for the first time.

Keywords

Biodiversity, daddy-long-legs spider, morphology, Northeast Asia, taxonomy

Introduction

The spider family Pholcidae C.L. Koch, 1850 currently contains 97 genera and 1896 species (World Spider Catalog 2022) classified within five subfamilies: Arteminae Simon, 1893, Modisiminae Simon, 1893, Ninetinae Simon, 1890, Pholcinae C.L. Koch, 1850, and Smeringopinae Simon, 1893 (Huber 2011a; Dimitrov et al. 2013; Eberle et al. 2018).

Pholcus Walckenaer, 1805 is the most diverse genus of the family, comprising 375 described species (World Spider Catalog 2022). These species belong to 21 species-groups, of which the *phungiformes* group is highly diverse and contains 94 species (Huber 2011b; Wang et al. 2020; Yao et al. 2021; Lu et al. 2022). This species-group is mainly distributed in northeastern China and the Korean Peninsula. Liaoning is a province in northeastern China and lies northwest of North Korea. The exploration of pholcid spiders from Liaoning was started rather recently, especially for the *phungiformes* species-group. Song and Ren (1994) were the first authors to record pholcids from Liaoning, and they described two species, *P. guani* Song & Ren, 1994 from Beizhen County and *P. gaoi* Song & Ren, 1994 from Kuandian County; the latter species belongs to the *phungiformes* species-group. Song et al. (1999) described the second species of this species-group, *P. suizhongicus* Zhu & Song, 1999, from Suizhong County. Nearly 10 years later, Zhang and Zhu (2009) described two species from Fenghuangshan Mountain, namely *P. fengcheng* Zhang & Zhu, 2009 and *P. phoenixus* Zhang & Zhu, 2009. During the following decade (2010–2019), only eight species of this group have been described from Liaoning (Tong and Ji 2010; Yao and Li 2012; Peng and Zhang 2013; Liu and Tong 2015). Wang et al. (2020) estimated that a large part of the *phungiformes* species-group diversity likely remains undiscovered in the Changbai Mountains in northeastern China, especially in Liaoning. For this reason, a one-month-long expedition to the Changbai Mountains was undertaken, which resulted in 11 new species being reported, including eight from Liaoning (Yao et al. 2021). To date, 20 species of this species-group have been recorded from Liaoning, most of which were collected from rock walls or at cave entrances.

The present study provides a checklist of the *phungiformes* species-group from Liaoning and a distribution map of all of the species (Figs 1, 2). This study also describes a species new to science and reports a species from this region for the first time.

Materials and methods

Specimens were examined and measured with a Leica M205 C stereomicroscope. The left male palp was photographed. The epigyne was photographed before dissection. The vulva was treated in a 10% warm solution of potassium hydroxide (KOH) to dissolve soft tissues before illustration. Images were captured with a Canon EOS 750D wide zoom digital camera (24.2 megapixels) mounted on the stereomicroscope mentioned above and assembled using Helicon Focus v. 3.10.3 image stacking software (Khmelik et al. 2005). All measurements are given in millimeters (mm). Leg measurements are shown as: total length (femur, patella, tibia, metatarsus, tarsus). Leg segments were measured on their dorsal side. The distribution map was generated with ArcGIS v. 10.2 (ESRI Inc.). The specimens studied are preserved in 75% ethanol and deposited in the College of Life Science, Shenyang Normal University (**SYNU**) in Liaoning, China.

Terminology and taxonomic descriptions follow Huber (2011b) and Yao et al. (2015, 2021). The following abbreviations are used in the descriptions: **ALE** = anterior lateral eye, **AME** = anterior median eye, **PME** = posterior median eye, **L/d** = length/

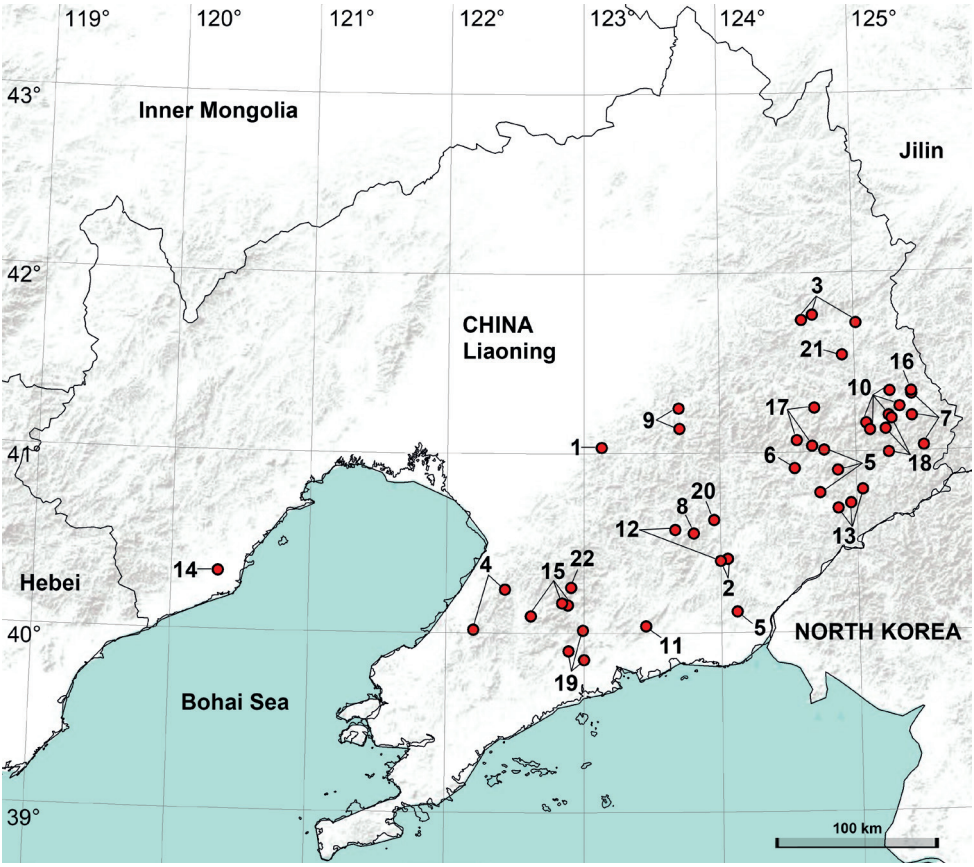

Figure 1. Distribution of the *Pholcus phungiformes* species-group in Liaoning, China: 1 = *P. decorus*, 2 = *P. fengcheng*, 3 = *P. foliaceus*, 4 = *P. gaizhou*, 5 = *P. gaoi*, 6 = *P. guanshui*, 7 = *P. hamatus*, 8 = *P. jiguanshan*, 9 = *P. jiuwei*, 10 = *P. longxigu*, 11 = *P. luoquanbei*, 12 = *P. phoenixus*, 13 = *P. shenshi*, 14 = *P. suizhongicus*, 15 = *P. tianmenshan*, 16 = *P. tongi*, 17 = *P. wangi*, 18 = *P. wangtian*, 19 = *P. xianrendong*, 20 = *P. yaoshan*, 21 = *P. yuhuangshan*, 22 = *P. xiuyan* sp. nov.

diameter ratio; used in the illustrations: **b** = bulb, **da** = distal apophysis, **e** = embolus, **fa** = frontal apophysis, **pa** = proximo-lateral apophysis, **pp** = pore plate, **pr** = procursus, **u** = uncus.

Taxonomic accounts

Family Pholcidae C.L. Koch, 1850
Subfamily Pholcinae C.L. Koch, 1850

Genus *Pholcus* Walckenaer, 1805

Type species. *Aranea phalangioides* Fuesslin, 1775.

Figure 2. *Pholcus xiuyan* sp. nov., living specimens and habitat **A, B** females and juveniles on rock walls **C** habitat, arrow indicates collecting site.

Pholcus phungiformes species-group from Liaoning Province

Diagnosis and description. See Huber (2011b) and Yao et al. (2021).

1. *Pholcus decorus* Yao & Li, 2012

Pholcus decorus Yao & Li, 2012: 14, figs 55A–D, 56A–E, 57A–E, 58A–D (♂♀).
Pholcus decorus Yao et al., 2021: S6, fig. 2B.1 (♂).

Distribution. China (Anshan in Liaoning; habitat: rock walls).

2. *Pholcus fengcheng* Zhang & Zhu, 2009

Pholcus fengcheng Zhang & Zhu, 2009: 28, fig. 11A–I (♂♀).
Pholcus fengcheng Yao & Li, 2012: 16, figs 63A–D, 64A–C (♂♀). Yao et al. 2021: S7, fig. 2B.2 (♂).

New material examined. 1♂ (SYNU-Ar00001F), roadside of G304 (40°24.667'N, 124°3.067'E, 139 m), near Fenghuangshan Mountain, Fengcheng, Dandong, **Liaoning**, **China**, 13 July 2020, Z Yao leg.

Distribution. China (Fengcheng in Liaoning; habitat: rock walls).

3. *Pholcus foliaceus* Peng & Zhang, 2013

Pholcus foliaceus Peng & Zhang, 2013: 75, figs 1A–G, 2A–F (♂♀).
Pholcus foliaceus Yao et al., 2021: S7, figs 2B.3, S4A–D (♂♀).

New material examined. 2♂ (SYNU-Ar00002F, Ar00003F) and 2♀ (SYNU-Ar00004F, Ar00005F), roadside of S202 (41°44.117'N, 124°36.867'E, 119 m), near Houshi National Forest Park, Muqi Town, Xinbin County, Fushun, **Liaoning**, **China**, 23 June 2020, Z Yao leg.

Distribution. China (Qingyuan County and Xinbin County in Liaoning; habitat: rock walls).

4. *Pholcus gaizhou* Yao & Li, 2021

Pholcus gaizhou Yao & Li in Yao et al. 2021: S8, figs 2B.4, S5A–D, S6A–H (♂♀).

New material examined. 2♂ (SYNU-Ar00006F, Ar00007F) and 3♀ (SYNU-Ar00008F–Ar00010F), roadside (40°1.167'N, 122°12.050'E, 257 m), near Xuemaoshan Scenic Spot, Jiuzhai Town, Gaizhou, Yingkou, **Liaoning**, **China**, 16 July 2020, Z Yao leg.

Distribution. China (Gaizhou in Liaoning; habitat: rock walls).

5. *Pholcus gaoi* Song & Ren, 1994

Pholcus gaoi Song & Ren, 1994: 20, figs 1–7 (♂♀).
Pholcus gaoi Song et al., 1999: 57, fig. 23L–O (♂♀). Zhang and Zhu 2009: 29, fig. 12A–G (♂♀). Yao and Li 2012: 17, figs 69A–D, 70A–C (♂♀). Yao et al. 2021: S9, fig. 2B.5 (♂).

New material examined. 2♂ (SYNU-Ar00011F, Ar00012F) and 1♀ (SYNU-Ar00013F), roadside of Sandaogoumen (40°53.950'N, 124°51.900'E, 431 m), Xinfeng Village, Dachuantou Town, Kuandian County, Dandong, **Liaoning**, **China**, 8 July 2020, Z Yao leg. 3♂ (SYNU-Ar00014F–Ar00016F) and 1♀ (SYNU-Ar00017F), roadside of X627 (41°0.633'N, 124°45.950'E, 520 m), Jiangjunling, Bahechuan Town, Kuandian County, Dandong, **Liaoning**, **China**, 8 July 2020, Z Yao leg.

Distribution. China (Kuandian County in Liaoning; habitat: rock walls).

6. *Pholcus guanshui* Yao & Li, 2021

Pholcus guanshui Yao & Li in Yao et al. 2021: S10, figs 2B.6, S7A–D, S8A–H (♂♀).

Distribution. China (Kuandian County in Liaoning; habitat: rock walls).

7. *Pholcus hamatus* Tong & Ji, 2010

Pholcus hamatus Tong & Ji, 2010: 98, figs 1a–c, j, 2a–g (♂♀).
Pholcus hamatus Yao et al., 2021: S11, figs 2B.7, S9A–D (♂♀).

New material examined. 1♂ (SYNU-Ar00018F) and 3♀ (SYNU-Ar00019F–Ar00021F), roadside of G506 (41°11.733'N, 125°25.100'E, 349 m), Huanggouli Village, Yahe Town, Huanren County, Benxi, **Liaoning**, **China**, 27 June 2020, Z Yao leg. 2♂ (SYNU-Ar00022F, Ar00023F) and 3♀(SYNU-Ar00024F–Ar00026F), roadside of G506 (41°1.783'N, 125°30.000'E, 179 m), Dawudaoyangcha, Gangouzi Village, Shajianzi Town, Huanren County, Benxi, **Liaoning**, **China**, 27 June 2020, Z Yao leg.

Distribution. China (Huanren County in Liaoning; habitat: rock walls).

8. *Pholcus jiguanshan* Yao & Li, 2021

Pholcus jiguanshan Yao & Li in Yao et al. 2021: S12, figs 2B.8, S10A–D, S11A–H (♂♀).

Distribution. China (Fengcheng in Liaoning; habitat: rock walls).

9. *Pholcus jiuwei* Tong & Ji, 2010

Pholcus jiuwei Tong & Ji, 2010: 99, figs 1d–f, k, 3a–g (♂♀).
Pholcus jiuwei Yao et al., 2021: S13, figs 2B.9, S12A–D (♂♀).

New material examined. 2♂ (SYNU-Ar00027F, Ar00028F) and 2♀ (SYNU-Ar00029F, Ar00030F), roadside (41°8.233'N, 125°42.217'E, 227 m), near Benxi Grand Canyon, Nanfen District, Benxi, **Liaoning**, **China**, 12 July 2020, Z Yao leg.

Distribution. China (Benxi and Pingshan County in Liaoning; habitat: rock walls).

10. *Pholcus longxigu* Yao & Li, 2021

Pholcus longxigu Yao & Li in Yao et al. 2021: S14, figs 2B.11, S13A–D, S14A–H (♂♀).

New material examined. 1♂ (SYNU-Ar00031F) and 3♀ (SYNU-Ar00032F–Ar00034F), roadside of S201 (41°20.117'N, 125°15.400'E, 291 m), Wudaohezi Village, Huanren Town, Huanren County, Benxi, **Liaoning**, **China**, 24 June 2020, Z Yao leg. 1♂ (SYNU-Ar00035F), roadside of G201 (41°14.867'N, 125°19.650'E, 294 m), Shihada Village, Yahe Town, Huanren County, Benxi, **Liaoning**, **China**, 26 June 2020, Z Yao leg. 1♂ (SYNU-Ar00036F) and 1♀ (SYNU-Ar00037F), roadside of G201 (41°11.967'N, 125°14.817'E, 276 m), near Lianhe Bridge, Lianhe Village, Yahe Town, Huanren County, Benxi, **Liaoning**, **China**, 26 June 2020, Z Yao leg. 2♂ (SYNU-Ar00038F, Ar00039F) and 1♀ (SYNU-Ar00040F), roadside of G201 (41°6.467'N, 125°7.217'E, 305 m), near Daqinggou Village, Pulepu Town, Benxi, **Liaoning**, **China**, 6 July 2020, Z Yao leg.

Distribution. China (Benxi and Huanren County in Liaoning; habitat: rock walls).

11. *Pholcus luoquanbei* Yao & Li, 2021

Pholcus luoquanbei Yao & Li in Yao et al. 2021: S15, figs 2B.12, S15A–D, S16A–H (♂♀).

Distribution. China (Xiuyan County in Liaoning; habitat: rock walls).

12. *Pholcus phoenixus* Zhang & Zhu, 2009

Pholcus phoenixus Zhang & Zhu, 2009: 69, figs 37A–I, 38A–I (♂♀).
Pholcus phoenixus Yao & Li, 2012: 30, figs 144A–D, 145A–C (♂♀). Yao et al. 2021: S17, fig. 2B.14 (♂).

New material examined. 3♂ (SYNU-Ar00041F–Ar00043F) and 2♀ (SYNU-Ar00044F, Ar00045F), roadside of Maqing Road (40°34.483'N, 123°40.050'E, 243 m), near Qingliangshan Scenic Spot, Qingliangshan Village, Qinglingshan Town, Xiuyan County, Anshan, **Liaoning**, **China**, 13 July 2020, Z Yao leg.

Distribution. China (Fengcheng and Xiuyan County in Liaoning; habitat: rock walls).

13. *Pholcus shenshi* Yao & Li, 2021

Pholcus shenshi Yao & Li in Yao et al. 2021: S18, figs 2B.15, S17A–D, S18A–H (♂♀).

New material examined. 1♂ (SYNU-Ar00046F) and 2♀ (SYNU-Ar00047F, Ar00048F), roadside of Kuanbei Road (40°42.883'N, 124°57.483'E, 315 m), Shanghaozigou Village, Hongshi Town, Kuandian County, Dandong, **Liaoning**, **China**, 7 July 2020, Z Yao leg. 1♂ (SYNU-Ar00049F) and 1♀ (SYNU-Ar00050F), roadside of Kuanbei Road (40°41.217'N, 124°51.867'E, 439 m), Shangchangyinzi Village, Shihugou Town, Kuandian County, Dandong, **Liaoning**, **China**, 7 July 2020, Z Yao leg.

Distribution. China (Kuandian County in Liaoning; habitat: rock walls).

14. *Pholcus suizhongicus* Zhu & Song, 1999

Pholcus suizhongicus Zhu & Song in Song et al. 1999: 59, fig. 25A–H (♂♀).
Pholcus suizhongicus Zhang & Zhu, 2009: 89, fig. 51A–H (♂♀). Yao and Li 2012: 33, figs 167A–D, 168A–C (♂♀).

Distribution. China (Suizhong County in Liaoning; habitat: unknown).

15. *Pholcus tianmenshan* Yao & Li, 2021

Pholcus tianmenshan Yao & Li in Yao et al. 2021: S19, figs 2B.17, S19A–D, S20A–H (♂♀).

New material examined. 2♂ (SYNU-Ar00051F, Ar00052F) and 2♀ (SYNU-Ar00053F, Ar00054F), roadside of Beitu Road (40°9.983'N, 122°50.567'E, 345 m), Taipingzhuang Village, Kuangdonggou Town, Gaizhou, Yingkou, **Liaoning**, **China**, 15 July 2020, Z Yao leg. 1♂ (SYNU-Ar00055F) and 3♀ (SYNU-Ar00056F–Ar00058F), roadside (40°5.617'N, 122°37.050'E, 227 m), near Chishan Scenic Spot, Wanfu Town, Gaizhou, Yingkou, **Liaoning**, **China**, 15 July 2020, Z Yao leg.

Distribution. China (Gaizhou and Zhuanghe in Liaoning; habitat: rock walls).

16. *Pholcus tongi* Yao & Li, 2012

Pholcus tongi Yao & Li, 2012: 34, figs 173A–D, 174A–E, 175A–D, 176A–D (♂♀).
Pholcus tongi Yao et al., 2021: S20, fig. 2B.18 (♂).

Distribution. China (Huanren County in Liaoning; habitat: rock walls).

17. *Pholcus wangi* Yao & Li, 2012

Pholcus wangi Yao & Li, 2012: 37, figs 191A–D, 192A–E, 193A–D, 194A–D (♂♀).
Pholcus wangi Yao et al., 2021: S21, fig. 2B.19 (♂).

New material examined. 1♂ (SYNU-Ar00059F) and 2♀ (SYNU-Ar00060F, Ar00061F), roadside of S309 (41°2.017'N, 124°40.667'E, 306 m), Liming Village, Shuangshanzi Town, Kuandian County, Dandong, **Liaoning**, **China**, 10 July 2020, Z Yao leg. 3♂ (SYNU-Ar00062F–Ar00064F) and 3♀ (SYNU-Ar00065F–Ar00067F), roadside of G506 (41°14.783'N, 124°42.000'E, 628 m), Dongyingfang Town, Benxi County, Benxi, **Liaoning**, **China**, 10 July 2020, Z Yao leg.

Distribution. China (Benxi County and Kuandian County in Liaoning; habitat: rock walls).

18. *Pholcus wangtian* Tong & Ji, 2010

Pholcus wangtian Tong & Ji, 2010: 102, figs 1g–i, l, 4a–f (♂♀).
Pholcus wangtian Yao et al., 2021: S23, figs 2B.21, S23A–D (♂♀).

New material examined. 1♂ (SYNU-Ar00068F) and 2♀ (SYNU-Ar00069F, Ar00070F), Fenglingu Forest Park (41°7.433'N, 125°13.400'E, 392 m), Xiangyang Town, Huanren County, Benxi, **Liaoning**, **China**, 26 June 2020, Z Yao leg. 2♂ (SYNU-Ar00071F, Ar00072F) and 2♀ (SYNU-Ar00073F, Ar00074F), roadside (40°59.683'N, 125°14.533'E, 212 m), near Manjiazhai, Qingshangou Village, Qingshangou Town, Kuandian County, Dandong, **Liaoning**, **China**, 7 July 2020, Z Yao leg.

Distribution. China (Huanren County and Kuandian County in Liaoning; habitat: rock walls and a cave entrance).

19. *Pholcus xianrendong* Liu & Tong, 2015

Pholcus xianrendong Liu & Tong, 2015: 32, figs 1A–J, 2A–F (♂♀).
Pholcus xianrendong Yao et al., 2021: S24, figs 2B.22, S24A–D (♂♀).

New material examined. 3♂ (SYNU-Ar00075F–Ar00077F) and 2♀ (SYNU-Ar00078F, Ar00079F), roadside of S203 (39°50.983'N, 123°0.150'E, 96 m), Dawangtun, Sijia Village, Daying Town, Zhuanghe, Dalian, **Liaoning**, **China**, 15 July 2020, Z Yao leg.

Distribution. China (Zhuanghe in Liaoning; habitat: rock walls).

20. *Pholcus yaoshan* Yao & Li, 2021

Pholcus yaoshan Yao & Li in Yao et al. 2021: S25, figs 2B.24, S27A–D, S28A–H (♂♀).

Distribution. China (Xiuyan County in Liaoning; habitat: rock walls).

21. *Pholcus yuhuangshan* Yao & Li, 2021

Pholcus yuhuangshan Yao & Li in Yao et al. 2021: S27, figs 2B.25, S1A, S29A–D, S30A–H (♂♀).

New material examined. 2♂ (SYNU-Ar00080F, Ar00081F) and 1♀ (SYNU-Ar00082F), roadside of S201 (41°32.400'N, 124°54.717'E, 118 m), Chaluzi Village, Yüshu Town, Xinbin County, Fushun, **Liaoning**, **China**, 24 June 2020, Z Yao leg. (New record for Liaoning)

Distribution. China (Xinbin County in Liaoning; habitat: rock walls).

22. *Pholcus xiuyan* Zhao, Zheng & Yao, sp. nov.
https://zoobank.org/5583C31D-4B7E-4C42-8A34-20BB8663778F
Figs 3, 4

Remarks. This new species is assigned to the *phungiformes* group by the following combination of characters: the male chelicerae with frontal apophyses (arrow fa in Fig. 4D), the male palpal tibia with a prolatero-ventral projection (Fig. 3A), the procursus with dorsal spines (arrows in Fig. 3D), the uncus with a "pseudo-appendix" (arrow 2 in Fig. 4C), and the epigyne with a knob (Fig. 4A).

Type material. ***Holotype*****:** ♂ (SYNU-Ar00251), Jiaxigou (40°15.200'N, 122°54.567'E, 318 m), Taipingling Village, Shihuiyao Town, Xiuyan County, Anshan, **Liaoning**, **China**, 13 July 2022, G Zheng, L Xiang & N Li leg. ***Paratypes*****:** 1♂ (SYNU-Ar00252) and 2♀ (SYNU-Ar00253, Ar00254), same data as for the holotype.

Etymology. The specific name refers to the type locality; noun in apposition.

Diagnosis. The new species resembles *P. brevis* Yao & Li, 2012 (Yao and Li 2012: 12, figs 39A–D, 40A–E, 41A–D, 42A–D) with similar bulbal apophyses (Fig. 4C) and epigynal plate (Fig. 4A), but it can be easily distinguished by the procursus with a sclerotized dorsal protrusion (arrow 2 in Fig. 3C; a flat dorsal sclerite in *P. brevis*), the strong male cheliceral frontal apophyses (arrow fa in Fig. 4D; frontal apophyses indistinct in *P. brevis*), the epigyne with a pair of lateral protrusions (arrow in Fig. 4A; absent in *P. brevis*), the wavy vulval anterior arch (Fig. 4B; slightly curved anterior arch in *P. brevis*), and the male clypeus without frontal apophysis (Fig. 4E; present in *P. brevis*); also distinguished from all of its known congeners in Xiuyan County by the following combination of characters: the procursus with sclerotized, raised prolateral edge bearing a spine-shaped distal apophysis (arrow 1 in Fig. 3C) and a sclerotized dorsal protrusion (arrow 2 in Fig. 3C), the semitransparent "pseudo-appendix" (arrow 2 in Fig. 4C), the strong male cheliceral frontal apophyses (arrow fa in Fig. 4D), the epigyne with a pair of lateral protrusions (arrow in Fig. 4A), and the wavy vulval anterior arch (Fig. 4B).

Description. Male (***holotype***, SYNU-Ar00251): total length 6.60 (6.73 with clypeus), prosoma 2.00 long, 2.15 wide, opisthosoma 4.60 long, 1.88 wide. Leg I: 49.82 (12.37, 0.91, 12.63, 20.90, 3.01), leg II: 34.84 (9.62, 0.85, 8.78, 13.65, 1.94), leg III: 19.07 (7.40, 0.73, 6.22, 3.33, 1.39), leg IV: 33.13 (9.62, 0.80, 8.46, 12.69, 1.56); tibia I L/d: 66. Eye interdistances and diameters: PME–PME 0.29, PME 0.17, PME–ALE 0.06, AME–AME 0.08, AME 0.11. Sternum width/length:1.43/1.08. Habitus as in Fig. 4E, F. Dorsal shield of prosoma yellowish, with brown radiating marks and marginal brown bands; ocular area yellowish, with median and lateral brown bands; clypeus and sternum yellowish, with brown marks. Legs overall yellowish, dark brown on patellae and whitish on distal parts of femora and tibiae, with darker rings on subdistal parts of femora and proximal and subdistal parts of tibiae. Opisthosoma yellowish, with dorsal and lateral black spots. Chelicerae (Fig. 4D) with pair of proximo-lateral apophyses, pair of distal apophyses with two teeth each (invisible in frontal view; cf. *P. tianmenshan*, fig. S20D in Yao et al. 2021), and pair of frontal apophyses.

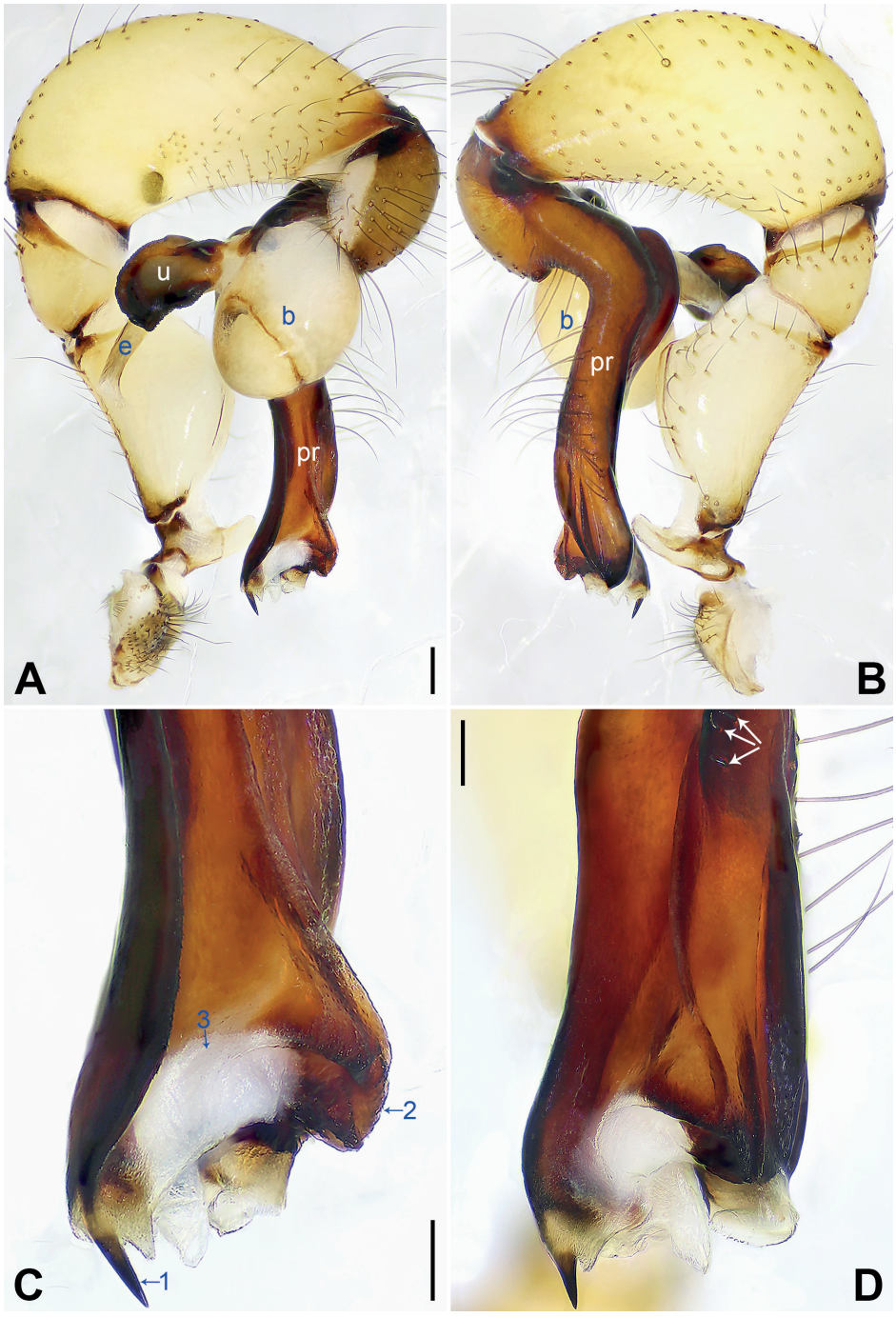

Figure 3. *Pholcus xiuyan* sp. nov., holotype male **A, B** palp (**A** prolateral view **B** retrolateral view) **C, D** distal part of procursus (**C** prolateral view, arrow 1 indicates spine-shaped distal apophysis, arrow 2 indicates sclerotized dorsal protrusion, arrow 3 indicates subdistal membranous process **D** dorsal view, arrows indicate dorsal spines). Abbreviations: b = bulb, e = embolus, pr = procursus, u = uncus. Scale bars: 0.20 mm (**A, B**); 0.10 mm (**C, D**).

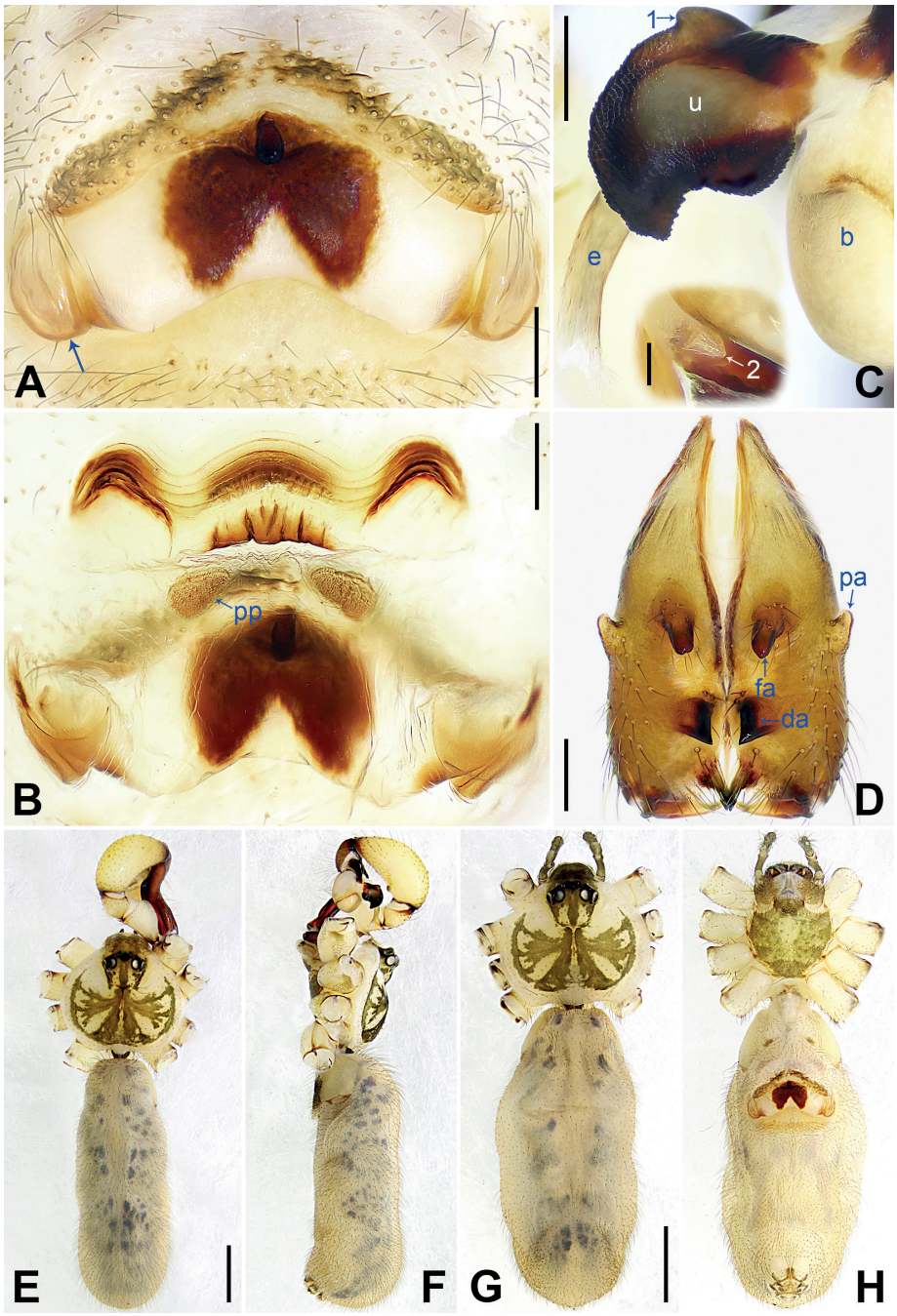

Figure 4. *Pholcus xiuyan* sp. nov., holotype male (**C–F**) and paratype female (**A, B, G, H**) **A** epigyne, ventral view, arrow indicates lateral protrusion **B** vulva, dorsal view **C** bulbal apophyses, prolateral view (the insert is retrolateral view of "pseudo-appendix"), arrow 1 indicates semicircular proximal apophysis, arrow 2 indicates "pseudo-appendix" **D** chelicerae, frontal view **E–H** habitus (**E, G** dorsal view **F** lateral view **H** ventral view). Abbreviations: b = bulb, da = distal apophysis, e = embolus, fa = frontal apophysis, pa = proximo-lateral apophysis, pp = pore plate, u = uncus. Scale bars: 0.20 mm (**A–D**); 0.05 mm (the insert in **C**); 1.00 mm (**E–H**).

Palp as in Fig. 3A, B; trochanter two times longer than wide, retrolaterally swollen; femur with small retrolatero-proximal protrusion and indistinct ventral protrusion; tibia with prolatero-ventral protrusion; procursus slender, simple proximally but complex distally, with sclerotized, raised prolateral edge bearing spine-shaped distal apophysis (arrow 1 in Fig. 3C), sclerotized dorsal protrusion (arrow 2 in Fig. 3C), subdistal membranous process (arrow 3 in Fig. 3C), and two strong and one slender dorsal spines (arrows in Fig. 3D); uncus curved, with scales and semicircular proximal apophysis (arrow 1 in Fig. 4C); "pseudo-appendix" short and semitransparent (arrow 2 in Fig. 4C); embolus weakly sclerotized, with some transparent distal projections (Fig. 4C). Retrolateral trichobothrium of tibia I at 3% proximally; legs with short vertical setae on tibiae, metatarsi, and tarsi; tarsus I with 38 distinct pseudosegments.

Female (***paratype***, SYNU-Ar00253): habitus as in Fig. 4G, H. Total length 5.80 (5.96 with clypeus), prosoma 1.72 long, 2.00 wide, opisthosoma 4.08 long, 1.78 wide; tibia I: 10.05; tibia I L/d: 57. Eye interdistances and diameters: PME–PME 0.22, PME 0.15, PME–ALE 0.04, AME–AME 0.06, AME 0.09. Sternum width/length: 1.22/0.94. Coloration generally as in male, except for dark brown clypeus.

Epigyne (Fig. 4A) postero-medially strongly curved, with median brown marks, short knob and pair of lateral protrusions (arrow in Fig. 4A). Vulva (Fig. 4B) with wavy, medially and laterally sclerotized anterior arch and pair of nearly triangular pore plates.

Variation. Tibia I in paratype male (SYNU-Ar00252): 11.67. Tibia I in another paratype female (SYNU-Ar00254): 9.81.

Natural history. The species was found on rock walls.

Distribution. China (Liaoning, type locality; Fig. 1).

Acknowledgements

The manuscript benefited greatly from comments by Gergin Blagoev, Alireza Zamani, Mikhail M. Omelko, Yanfeng Tong, and anonymous reviewers. Abid Ali kindly checked the English. This study was supported by the National Natural Science Foundation of China (NSFC-32170461, 31872193, 31970410) and the Liaoning Revitalization Talents Program (XLYC1907150, XLYC2002083). Part of the laboratory work was supported by the Shenyang Youth Science and Technology Project (RC200183).

References

Dimitrov D, Astrin JJ, Huber BA (2013) Pholcid spider molecular systematics revisited, with new insights into the biogeography and the evolution of the group. Cladistics 29(2): 132–146. https://doi.org/10.1111/j.1096-0031.2012.00419.x

Eberle J, Dimitrov D, Valdez-Mondragón A, Huber BA (2018) Microhabitat change drives diversification in pholcid spiders. BMC Evolutionary Biology 18(1): 1–141. https://doi.org/10.1186/s12862-018-1244-8

Huber BA (2011a) Phylogeny and classification of Pholcidae (Araneae): An update. The Journal of Arachnology 39(2): 211–222. https://doi.org/10.1636/CA10-57.1

Huber BA (2011b) Revision and cladistic analysis of *Pholcus* and closely related taxa (Araneae, Pholcidae). Bonner Zoologische Monographien 58: 1–509.

Khmelik VV, Kozub D, Glazunov A (2005) Helicon Focus 3.10.3. https://www.heliconsoft.com/heliconsoft-products/helicon-focus/ [Accessed 10 November 2022]

Liu Y, Tong Y (2015) A new species of the genus *Pholcus* Walckenaer, 1805 from Xianrendong National Forest Park, Liaoning Province, China (Araneae: Pholcidae). Acta Arachnologica Sinica 24(1): 31–34. https://doi.org/10.3969/j.issn.1005-9628.2015.01.008

Lu Y, Chu C, Zhang X, Li S, Yao Z (2022) Europe vs. China: *Pholcus* (Araneae, Pholcidae) from Yanshan-Taihang Mountains confirms uneven distribution of spiders in Eurasia. Zoological Research 43(4): 532–534 [Supplement 1–78]. https://doi.org/10.24272/j.issn.2095-8137.2022.103

Peng Y, Zhang F (2013) Two new *Pholcus* species from northern China (Araneae: Pholcidae). Acta Arachnologica 62(2): 75–80. https://doi.org/10.2476/asjaa.62.75

Song D, Ren L (1994) Two new species of the genus *Pholcus* from China (Araneae: Pholcidae). Journal of Hebei Normal University (Supplement): 19–23. [Natural Science Edition]

Song D, Zhu M, Chen J (1999) The Spiders of China. Hebei Science and Technology Publishing House, Shijiazhuang, 640 pp.

Tong Y, Ji L (2010) Three new species of the spider genus *Pholcus* (Araneae: Pholcidae) from Liaodong Mountain, China. Entomologica Fennica 21: 97–103. https://doi.org/10.33338/ef.84516

Wang X, Shaheen S, He Q, Yao Z (2020) Notes on two closely related spider species of the *Pholcus phungiformes* species group (Araneae, Pholcidae) from Beijing, China. ZooKeys 965: 1–16. https://doi.org/10.3897/zookeys.965.56199

World Spider Catalog (2022) World Spider Catalog, Version 23.5. Natural History Museum Bern. http://wsc.nmbe.ch [Accessed 22 November 2022]

Yao Z, Li S (2012) New species of the spider genus *Pholcus* (Araneae: Pholcidae) from China. Zootaxa 3289(1): 1–271. https://doi.org/10.11646/zootaxa.3289.1.1

Yao Z, Pham DS, Li S (2015) Pholcid spiders (Araneae: Pholcidae) from northern Vietnam, with descriptions of nineteen new species. Zootaxa 3909(1): 1–82. https://doi.org/10.11646/zootaxa.3909.1.1

Yao Z, Wang X, Li S (2021) Tip of the iceberg: species diversity of *Pholcus* spiders (Araneae, Pholcidae) in the Changbai Mountains, Northeast China. Zoological Research 42(3): 267–271 [Supplement 1–60]. https://doi.org/10.24272/j.issn.2095-8137.2021.037

Zhang F, Zhu M (2009) A review of the genus *Pholcus* (Araneae: Pholcidae) from China. Zootaxa 2037(1): 1–114. https://doi.org/10.11646/zootaxa.2037.1.1

ZooKeys 1156: 15–24 (2023)
doi: 10.3897/zookeys.1156.101396
https://zookeys.pensoft.net

RESEARCH ARTICLE

A peer-reviewed open-access journal
ZooKeys
Launched to accelerate biodiversity research

Larissimus nigricans sp. nov. (Hymenoptera, Braconidae), a new reared species of a rare neotropical genus recovered through biodiversity inventory in Ecuador

Pomona Carrington-Hoekstra[1], Jose Fernandez-Triana[2], Lee A. Dyer[3], James Whitfield[4]

1 *School of Integrative Biology, University of Illinois, Urbana, IL 61801 USA* **2** *Canadian National Collection of Insects, Ottawa, ON K1A 0C6 Canada* **3** *Department of Biology, University of Nevada, Reno, NV 89557 USA* **4** *Department of Entomology, University of Illinois, Urbana, IL 61801 USA*

Corresponding author: James Whitfield (jwhitfie@life.illinois.edu)

Academic editor: K. van Achterberg | Received 2 February 2023 | Accepted 5 March 2023 | Published 24 March 2023

https://zoobank.org/D11B957A-1BD5-4594-872C-CB6D9E0858EC

Citation: Carrington-Hoekstra P, Fernandez-Triana J, Dyer LA, Whitfield J (2023) *Larissimus nigricans* sp. nov. (Hymenoptera, Braconidae), a new reared species of a rare neotropical genus recovered through biodiversity inventory in Ecuador. ZooKeys 1156: 15–24. https://doi.org/10.3897/zookeys.1156.101396

Abstract

A new species of the rarely collected neotropical microgastrine braconid wasp genus *Larissimus* Nixon, represented previously by only a single described species, *L. cassander* Nixon, was recovered by the Caterpillars and Parasitoids of the Eastern Andes in Ecuador inventory project. *Larissimus nigricans* **sp. nov.** was reared from an unidentified species of arctiine Erebidae feeding on the common bamboo species *Chusquea scandens* Kunth at the Yanayacu Biological Station near Cosanga, Napo Province, Ecuador. The new species is described and diagnosed from *L. cassander* using both morphological and DNA barcode data.

Keywords

Arctiinae, bamboo, *Chusquea*, Erebidae, Lepidoptera, parasitoid

Introduction

The braconid parasitoid wasp subfamily Microgastrinae currently contains 81 recognized genera and roughly 3,000 described species (Fernandez-Triana et al. 2020), although the true species richness may perhaps be over 45,000 species when undescribed

species are included (Rodriguez et al. 2013). While clearly the ratio of undescribed to described species is large, this hyperdiverse group is nevertheless better understood than most in terms of higher classification and natural history (summarized by Whitfield et al. 2018). Undeniably, some of this understanding has resulted from focused historical specialization by taxonomists, as well as the ease of collecting adult species of the group using flight traps. Additionally, the rich data emerging from tropical inventories of caterpillars, their host plants, and parasitoids have provided an especially enlightening window into the ecology and diversity of the group (Forister et al. 2015).

The new reared species was discovered via the Caterpillars and Parasitoids of the Eastern Andes in Ecuador project, with fieldwork involving researchers from around the world for identification and description of host plants, caterpillars, and parasitoids. To date the project has produced 10,091 adult parasitoids, 3,648 of which are braconids belonging to 37 genera. For some genera, the project is greatly expanding knowledge of host biology over what was previously known from other regions.

The genus *Larissimus* was erected by Nixon (1965) for one neotropical species, *L. cassander* Nixon, from Brazil; the genus has been retained with essentially the same monotypic definition in subsequent treatments (Mason 1981; Whitfield et al. 2018; Fernandez-Triana et al. 2020). Penteado-Dias (1997) subsequently recorded the first host for *L. cassander*, *Bertholdia* sp. (Erebidae, Arctiinae) feeding on *Croton floribundus* (Euphorbiaceae). The newly reared species below is associated with a host from the same caterpillar subfamily; the presence of this genus in tropical forests beyond Brazil has been suspected (Whitfield et al. 2009) but not officially recorded with the described species.

Materials and methods

Field protocols for the Ecuador inventory

Adult parasitoids were reared from externally feeding larval Lepidoptera (i.e., caterpillars) that were collected by experienced parataxonomists, graduate students, undergraduate students, postdocs, Earthwatch volunteers, and principal investigators. To provide standardized estimates of caterpillar-parasitoid abundances and diversity, we employed survey methods currently in use at multiple sites across the Americas. Briefly, we document interaction diversity and collect all specimens within 5–30 m diameter plots along elevational gradients within a field site. This method includes intensive searches on specific host plants and documentation of caterpillar densities on individual plants, parasitoid loads on caterpillars, and quantitative data on species richness per leaf area. Plots were supplemented by general collecting of immature and adult Lepidoptera along the same elevational gradients. All collected caterpillars were reared using methods published elsewhere (Dyer et al. 2007; Wagner et al. 2021). Collecting and rearing took place continuously from 2000 to present, with a standard week consisting of four days of general collecting, 2–6 plots sampled, and daily rearing. Collections included caterpillars that were clearly parasitized.

Immature Lepidoptera were identified to family and to a morphospecies common name by field staff. Adult lepidopteran specimens (reared or collected as adults) were field-pinned, transported to the University of Nevada, then spread and curated using standard techniques. Vouchers examined by various taxonomic authorities, including newly established type specimens and undescribed species, are housed in collections of the taxonomists' preference to facilitate further systematic studies of the material. Voucher specimens of the focal plants and novel host records were collected and pressed to ensure accurate taxonomic identification, then deposited at national herbaria. Each plant, caterpillar, and parasitoid specimen collected was registered as a unique record in a detailed database currently in use by a collaborative team across the Americas (Forister et al. 2015).

When wasps emerged from any stages of lepidopteran hosts, they were killed and preserved directly into 95% ethanol. Data labels were included in the specimen vials with the full locality, dates of collection and emergence, and the collector's name. Rearing containers were checked frequently in order to find the parasitoids while they were still alive. Caterpillar remains were preserved when possible and were not detached from the substrate if they were attached.

Specimen study

Examination and photography of the Ecuador specimens was conducted with a Leica M205 C stereomicroscope fitted with a five-megapixel Leica DFC 425 digital microscope camera. Image stacking was performed using a motor drive on the scope and Zerene Stacker software v. 2.0 (http://zerenestacker.com). The Brazil specimens were photographed with a Keyence VHX-1000 digital microscope, using a lens with a range of 13–130×. Image stacking was performed using the software associated with the Keyence system. Morphological terminology follows that in Huber and Sharkey (1993) and Fernandez-Triana et al. (2014). A single midleg was removed from each specimen and processed for COI DNA barcode identification using standard protocols (Ratnasingham and Hebert 2007, 2013).

Descriptive taxonomy

The large body size, antennae with placodes mostly irregularly arranged on flagellomeres or in three disorganized rows, mostly highly polished body, large well-defined fore wing areolet, reduced and poorly set off hind wing vannal lobe, and elongate hourglass-shaped and relatively narrow first metasomal tergite combined with triangular second mediotergite clearly placed the species within *Larissimus* (Whitfield 1997), even without female genitalic characters available. The new species is conspicuously different from *L. cassander* and can be separated on the basis of color (mostly blackish dark brown with infuscate wings) and body size (over 5.0 mm, unusual for microgastrines) alone. While only male specimens were available, the available material of *Larissimus*–both described and undescribed–in collections shows little sexual dimorphism with respect to color. *Larissimus cassander* (Figs 3, 4) recorded from Brazil (states of Santa

Catarina and São Paulo) is bigger (body length 7.0–8.0 mm, fore wing length 8.0–9.0 mm) and much lighter colored in both sexes, with most of its body orange-yellow or reddish yellow, including bright yellow pterostigma. The new species of *Larissimus* from Ecuador is smaller (body length 5.5 mm, fore wing length 5.4 mm) and much darker, with most of its body black to dark brown but with some areas white (most of T1 and all laterotergites plus bordering areas of tergites) and dark brown pterostigma. The two species can also be distinguished by 12% base pair differences in their corresponding DNA barcodes and also in biology (see below for details on hosts).

Larissimus nigricans Carrington-Hoekstra & Whitfield, sp. nov.

https://zoobank.org/D333F68F-7921-4E3E-A9FC-6A4D23BD8E18
Fig. 1A–F

Description. Holotype male. Body length 5.5 mm: fore wing length 5.4 mm.

Color (Fig. 1A). Dark chestnut-brown, nearly black except: lighter brown clypeus, labrum, lateroventral portions of pronotum and propleuron, hind margin of propodeum, most of fore and mid legs and hind femur; whitish palpi, mid coxa, distoventral portions of hind coxa, anterior half and posterior margin of first metasomal tergite and lateral portions of metasomal tergites and sternites.

Head (Fig. 1B, C). Antenna slender and roughly same length as body; placodes on flagellomeres roughly arranged in somewhat disorganized rows (typically three proximally). Face and eyes moderately setose, less so in an area posterior to the antenna and anterior to the ocelli. Labrum large and contrastingly colored (pale against a dark frons), with indentation dividing the labrum into a smaller dorsal section and larger ventral section. Ocelli arranged in low triangle (anterior edge of lateral ocelli on more or less same transverse line as posterior edge of anterior ocellus); lateral ocellus slightly truncated laterally due to overlapping cuticle.

Mesosoma (Fig. 1A, C, D). Pronotum laterally mostly smooth and hairless with setae mostly confined dorsal portion; ventral groove broad and smooth, dorsal groove indistinct. Mesoscutum convex, nearly smooth over most of surface with denser setae and faint punctation anteriorly and laterally. Scutellum smooth, convex, and subtriangular. Mesopleuron hairless centrally, with smooth shallow concavity in posterior half. Propodeum smooth with sharply defined medial carina over entire length.

Wings (Fig. 1E). Fore wing areolet of moderate size, strongly triangular. Vein 2r exiting the pterostigma at nearly a right angle (vs much more strongly angled to distal end in *L. cassander*) and straight to juncture with 1Rs. Height and length of triangular areolet nearly equal. Hind wing: Cu and cu-a bending slightly distally/"outward" at juncture with M + Cu. Vein 3M as strong as 2M. Vein r vaguely spectral or absent. 2r-m weak, unpigmented.

Legs (Fig. 1A, D). Middle leg: inner tibial spur much longer than outer and nearly as long as basitarsus. Hind leg: proximal end of femur marked with a very narrow light band (matching trochanter); tibial spurs both long, inner longer than outer and roughly 0.75 as long as basitarsus.

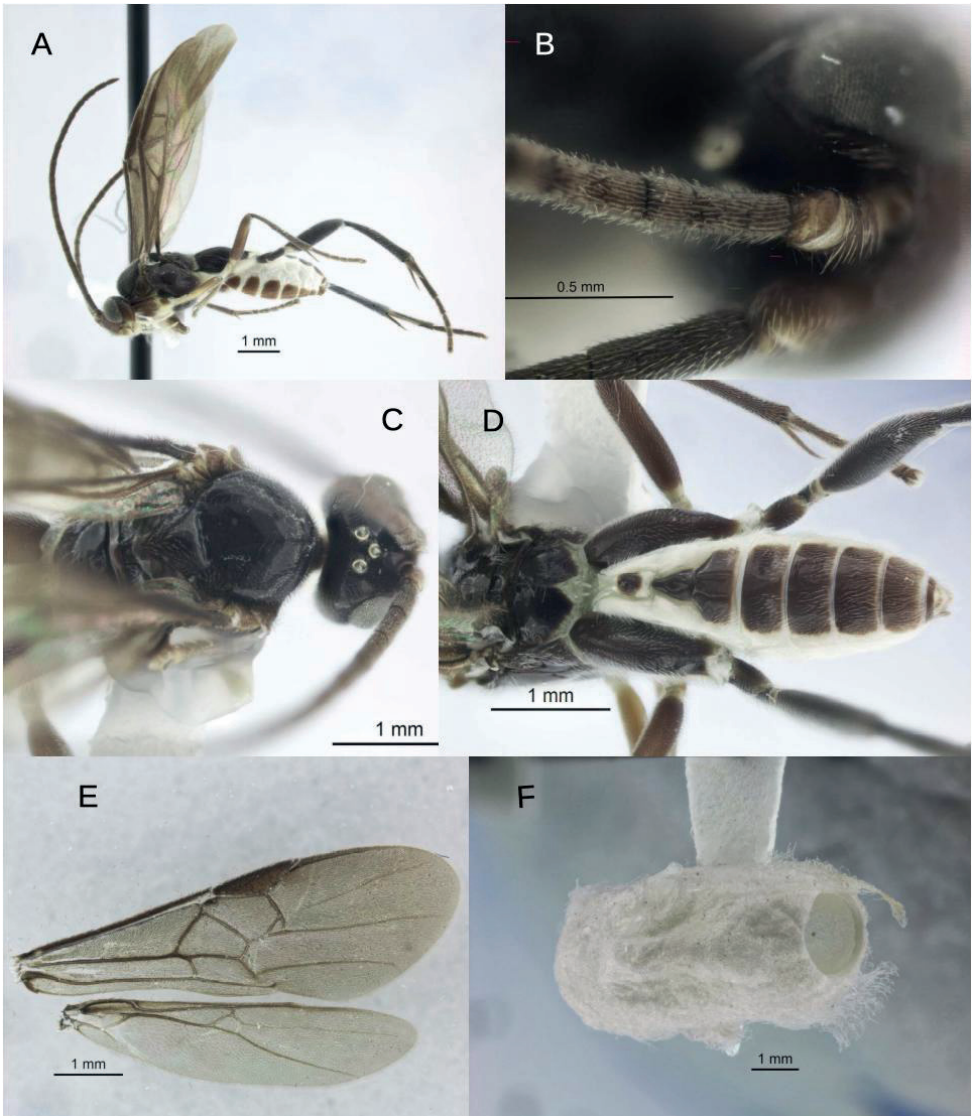

Figure 1. *Larissimus nigricans* sp. nov., male **A** lateral habitus **B** proximal regions of left antenna **C** dorsal view, head and mesosoma **D** dorsal view, propodeum and metasoma **E** wings **F** emerged cocoon.

Metasoma (Fig. 1D, known only from male): tergite I smooth, more than twice as long as broad (narrowest just before midlength), with medial groove strongest anteriorly. Tergite II smooth, strongly triangular and longer than maximum width, more than twice as broad posteriorly as anteriorly. Laterotergites strongly whitish and matching lateral band of white on Tergite III and more posterior tergites. Tergite III rectangular over posterior half but with anterolateral corners angled; central third polished and slightly raised and set off from more setose lateral portions by longitudinal grooves. Tergites IV–V roughly rectangular with a small medial patch of hairlessness surrounded by light setae.

Figure 2. Host and host plant of *L. nigricans* sp. nov. **A** parasitized caterpillar of lithosiine (Arctiinae, Erebidae) moth on *Chusquea* leaf **B** unparasitized caterpillar of the same species, showing healthy color, and from which the adult was reared and identified as *Ardonea* sp. **C** a stand of *Chusquea scandens* Kunth from which the host caterpillars were reared.

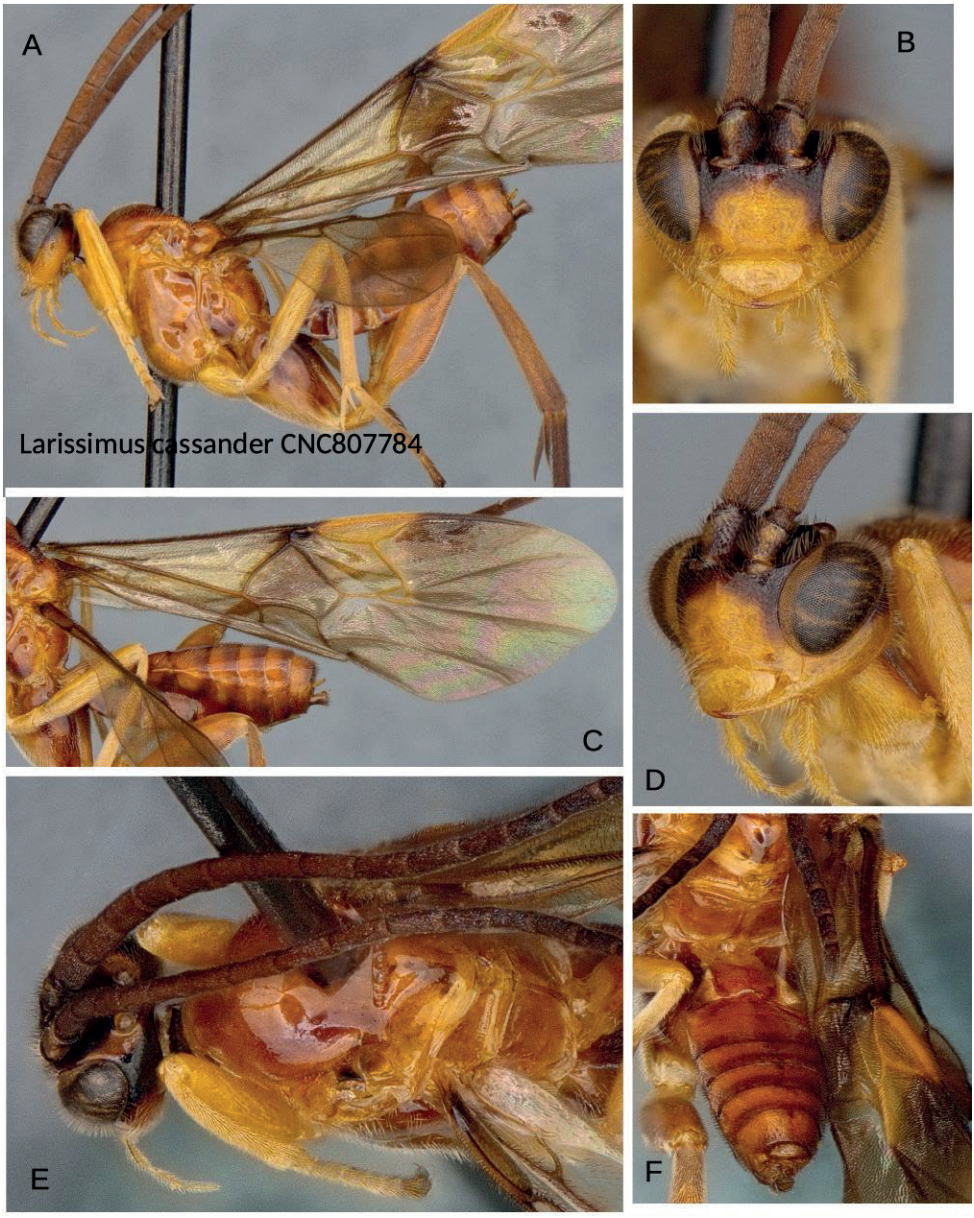

Figure 3. *Larissimus cassander* Nixon, male, Brazil **A** lateral habitus **B** head, frontal view **C** fore wing **D** head, view from left side, showing malar suture **E** dorsal view, head and mesosoma **F** dorsal view, metasoma.

Female. Unknown.

Variation. The two males available are extremely similar despite arising from different rearings in different years. The paratype male is slightly larger than the holotype.

Cocoon (Fig. 1F). White, bluntly oval, spun from dense silk with loose strands externally.

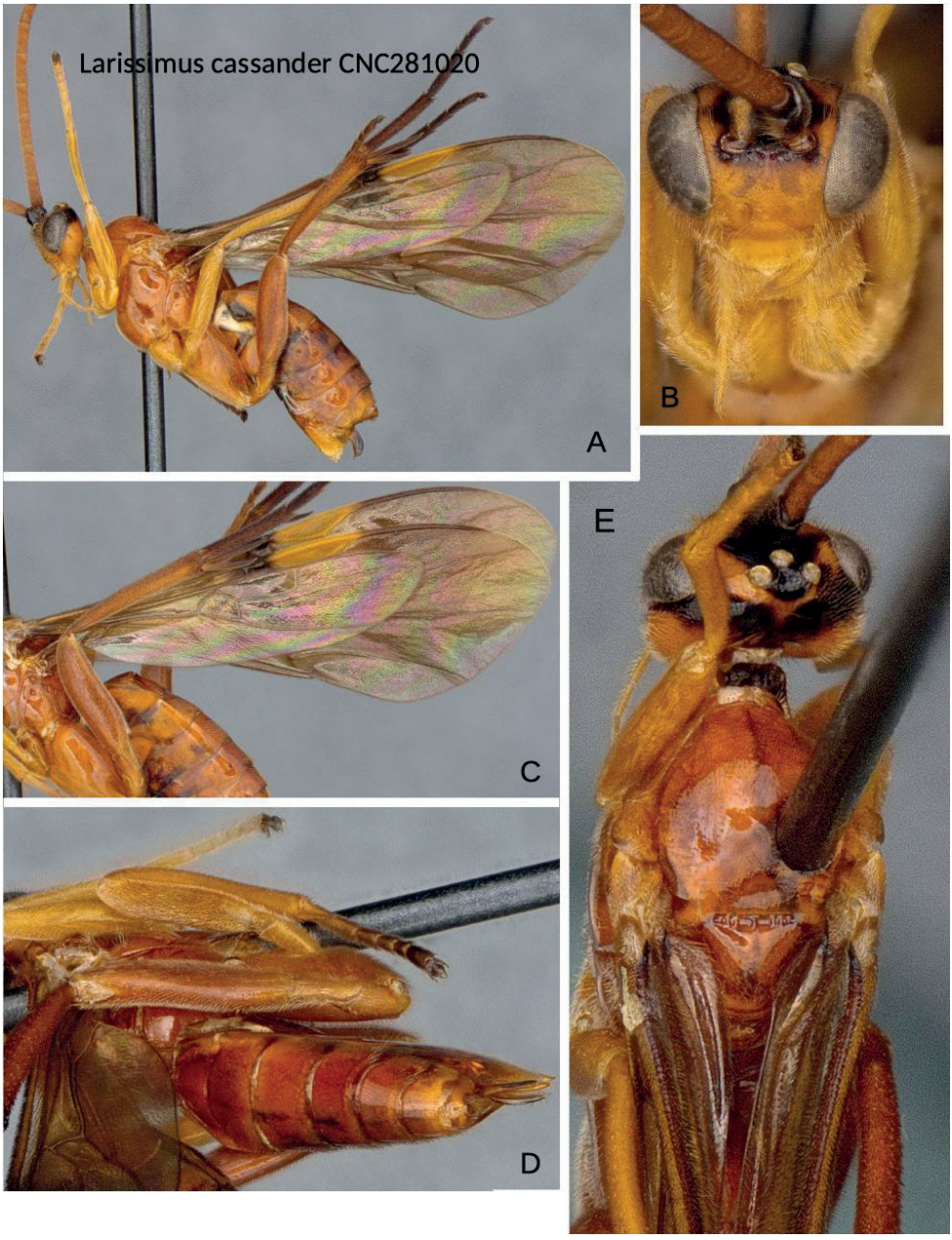

Figure 4. *Larissimus cassander* Nixon, female, Brazil **A** lateral habitus **B** head, frontal view **C** wings (especially showing hind wing) **D** dorsal view, metasoma **E** dorsal view, head and mesosoma.

Hosts. Unidentified species of *Ardonea* Walker (Erebidae, subfamily Arctiinae, tribe Lithosiini) caterpillar (Fig. 2A, B) feeding on *Chusquea scandens* Kunth (Poaceae), a common and widespread Andean bamboo (Fig. 2C).

Material examined. ***Holotype*** male: Ecuador: Napo Prov., Yanayacu Biological Station, bamboo trail 2051, –0.5833, –77.8978, 218 m elev., collected 12 February 2011, rearing code 55036. ***Paratype*****:** same data as holotype but collected on yy road 2100, –0.5667, –77.8667, 21 April 2009, rearing code 38108. Both holotype and paratype deposited in Canadian National Collection of Insects, Ottawa (CNC).

Etymology. From the Latin "nigricans", meaning "blackish". JFT and JBW have seen additional undescribed species of *Larissimus* (primarily in the Canadian National Insect Collection) with different color patterns, but not predominantly blackish ones.

Comments. Despite the dramatically different color combination and pattern, this new species is not strikingly different morphologically from *L. cassander*, at least based on the two males we have seen. Most structural differences are in minor shape proportions of structures (metasomal tergites narrower in the new species) and in wing vein angles (e.g., as mentioned above, compare angle of 2r in Figs 1E, 3C).

Molecular data. Cytochrome c oxidase subunit 1 barcode sequence (sequence code BCNCC047-22 in the Barcode of Life (BOLD) database (Ratnasingham and Hebert 2007, 2013) consists of 614 bp and is 12% different in base pair identity from that of *L. cassander* (BOLD BIN BOLD:ABU6476).

Acknowledgements

LAD and JBW thank the National Science Foundation for funding the Caterpillars and Parasitoids of the Eastern Andes in Ecuador project under grants DEB 0346712, DEB 0717402, DEB 1020510, DEB 1146119 and EN 2133818. We thank Wilmer Simbaña for collection and rearing specimens. PC-H and JBW would like to thank Dr Joshua Gibson for assistance with the photography and image-stacking in Illinois.

References

Dyer LA, Singer MS, Lill JT, Stireman JO, Gentry GL, Marquis RJ, Ricklefs RE, Greeney HF, Wagner DL, Morais HC, Diniz IR, Kursar TA, Coley PD (2007) Host specificity of Lepidoptera in tropical and temperate forests. Nature 448(7154): 696–699. https://doi.org/10.1038/nature05884

Fernandez-Triana JL, Whitfield JB, Rodriguez JJ, Smith MA, Janzen DH, Hallwachs MD, Hajibabaei M, Burns JM, Solis MA, Brown J, Cardinal S, Goulet H, Hebert PDN (2014) Review of *Apanteles* sensu stricto (Hymenoptera, Braconidae, Microgastrinae) from Area de Conservacion Guanacaste, northwest Costa Rica, with keys to all described species from Mesoamerica. ZooKeys 383: 1–565. https://doi.org/10.3897/zookeys.383.6418

Fernandez-Triana JL, Shaw MR, Boudrault C, Beaudin M, Broad GR (2020) Annotated world checklist of Microgastrinae parasitoid wasps (Hymenoptera: Braconidae). ZooKeys 920(1–2): 1–1089. https://doi.org/10.3897/zookeys.920.39128

Forister ML, Novotny V, Panorska AK, Baje L, Basset Y, Butterill PT, Cizek L, Coley PD, Dem F, Diniz IR, Drozd P, Fox M, Glassmire AE, Hazen R, Hrcek J, Jahner JP, Kaman O, Kozubowski TJ, Kursar TA, Lewis OT, Lill J, Marquis RJ, Miller SE, Morais HC, Murakami M, Nickel H, Pardikes NA, Ricklefs RE, Singer MS, Smilanich AM, Stireman JO, Villamarin-Cortez S, Vodka S, Volf M, Wagner DL, Walla T, Weiblen GD, Dyer LA (2015) The global distribution of diet breadth in insect herbivores. Proceedings of the National Academy of Sciences of the United States of America 112(2): 442–447. https://doi.org/10.1073/pnas.1423042112

Huber JT, Sharkey MJ (1993) Structure. In: Goulet H, Huber JT (Eds) Hymenoptera of the World: An Identification Guide to Families. Centre for Land and Biological Resources Research, Ottawa, 13–59.

Mason WRM (1981) The polyphyletic nature of *Apanteles* Foerster (Hymenoptera: Braconidae): a phylogeny and reclassification of Microgastrinae. Memoirs of the Entomological Society of Canada 113(S115): 1–147. https://doi.org/10.4039/entm113115fv

Nixon GEJ (1965) A reclassification of the tribe Microgasterini (Hymenoptera: Braconidae). Bulletin of the British Museum (Natural History). Entomology Series (Supplement 2): 1–284. https://doi.org/10.5962/p.144036

Penteado-Dias AM (1997) First host record for the genus *Larissimus* (Hymenoptera: Braconidae). Entomological News 108: 1–66.

Ratnasingham S, Hebert PDN (2007) BOLD: The Barcode of Life Data System (www.barcodinglife.org). Molecular Ecology Notes 7(3): 355–364. https://doi.org/10.1111/j.1471-8286.2007.01678.x

Ratnasingham S, Hebert PDN (2013) A DNA-based registry for all animal species: The Barcode Index Number (BIN) System. PLoS ONE 8(8): e66213. https://doi.org/10.1371/journal.pone.0066213

Rodriguez JJ, Fernandez-Triana JL, Smith MA, Janzen DH, Hallwachs W, Erwin TL, Whitfield JB (2013) Extrapolations from field studies and known faunas converge on dramatically increased estimates of global microgastrine parasitoid wasp species richness (Hymenoptera: Braconidae). Insect Conservation and Diversity 6: 530–536. https://doi.org/10.1111/icad.12003

Wagner DL, Fox R, Salcido DM, Dyer LA (2021) A window to the world of global insect declines: Moth biodiversity trends are complex and heterogeneous. Proceedings of the National Academy of Sciences of the United States of America 118(2): e2002549117. https://doi.org/10.1073/pnas.2002549117

Whitfield JB (1997) Subfamily Microgastrinae. In: Wharton RA, Marsh PM, Sharkey MJ (Eds) Identification Manual to the New World Genera of the Family Braconidae (Hymenoptera). Special Publication 1. International Society of Hymenopterists, Washington DC, 333–364.

Whitfield JB, Rodriguez JJ, Masonick PK (2009) Reared microgastrine wasps (Hymenoptera: Braconidae) from the Yanayacu Biological Station and environs (Napo Province, Ecuador): diversity and host specialization. Journal of Insect Science 9(31): 1–31. https://doi.org/10.1673/031.009.3101

Whitfield JB, Austin A, Fernandez-Triana JL (2018) Systematics, biology and evolution of microgastrine parasitoid wasps. Annual Review of Entomology 63(1): 389–406. https://doi.org/10.1146/annurev-ento-020117-043405

ZooKeys 1156: 25–31 (2023)
doi: 10.3897/zookeys.1156.97364
https://zookeys.pensoft.net

SHORT COMMUNICATION

A peer-reviewed open-access journal
ZooKeys
Launched to accelerate biodiversity research

Two new host records for *Centrodora italica* Ferrière (Hymenoptera, Aphelinidae) from eggs of Tettigoniidae (Orthoptera, Ensifera) in northeastern Italy

Giacomo Ortis[1], Serguei V. Triapitsyn[2], Luca Mazzon[1]

1 *Department of Agronomy, Food, Natural Resources, Animals and Environment (DAFNAE), University of Padova, Legnaro, Italy* **2** *Entomology Research Museum, Department of Entomology, University of California, Riverside, California, USA*

Corresponding author: Giacomo Ortis (giacomo.ortis@unipd.it)

Academic editor: Zachary Lahey | Received 9 November 2022 | Accepted 20 January 2023 | Published 24 March 2023

https://zoobank.org/BB0073D4-7EE0-482E-8E8E-6526ABE727CB

Citation: Ortis G, Triapitsyn SV, Mazzon L (2023) Two new host records for *Centrodora italica* Ferrière (Hymenoptera, Aphelinidae) from eggs of Tettigoniidae (Orthoptera, Ensifera) in northeastern Italy. ZooKeys 1156: 25–31. https://doi.org/10.3897/zookeys.1156.97364

Abstract

The egg parasitoid *Centrodora italica* Ferrière is reported for the first time from sentinel eggs of two species of Tettigoniidae (Orthoptera), *Pachytrachis gracilis* (Brunner von Wattenwyl) and *Eupholidoptera schmidti* (Fieber). In Italy, only two hosts of this parasitic wasp are known, one of which is a tettigoniid species. Exposure of sentinel eggs represented a useful method to detect new host associations of this parasitoid species that can search for their host's eggs in the ground. The parasitoids were identified by comparing our specimens with those of the type series, and the original description of *C. italica*.

Keywords

Aphelinid, egg parasitoid, Mediterranean region, parasitic wasp, sentinel eggs, tettigoniid

Introduction

The genus *Centrodora* Förster, 1878 (Hymenoptera, Aphelinidae) is cosmopolitan and includes parasitoids which develop on insects belonging to different orders (Hayat 1974; Polaszek 1991; Viggiani 1994; Bocca et al. 2020). In particular, some members of *Centrodora* are known to parasitize eggs of Orthoptera and Hemiptera, whereas other species can attack nymphs of Hemiptera, and pupae of Diptera, Hymenoptera and Coleoptera.

The checklist of the Italian fauna includes four species of *Centrodora*: *C. brevifuniculata* Viggiani, 1972, *C. cicadae* Silvestri, 1918, *C. italica* Ferrière, 1968 and *C. livens* (Walker, 1851) (www.faunaitalia.it). Three of these species are recorded from hemipteran hosts at egg or pupal stage, while only *C. italica* was reared from eggs or pupae of species belonging to various orders including *Uromenus brevicollis* (Fischer, 1853) (Orthoptera, Tettigoniidae), *Saperda carcharias* (L., 1758) (Coleoptera, Cerambycidae), *Euderus caudatus* Thomson, 1878 (Hymenoptera, Eulophidae) (Cavalcaselle 1968; Noyes 2019). Recently, *C. livens* was reared in Italy from eggs of the introduced Nearctic pest *Metcalfa pruinosa* Say, 1830 (Hemiptera, Flatidae) (Raspi and Canovai 2003).

Here we report new host records for *C. italica* from sentinel eggs of two tettigoniid species.

Materials and methods

During summer 2021, five species of Tettigoniidae were collected in multiple localities in the Euganean and Berici Hills of the Veneto Region of Italy: *Pachytrachis gracilis* (Brunner von Watternwyl, 1861), *Pholidoptera littoralis* (Fieber, 1853), *Pholidoptera fallax* (Fischer, 1853), *Eupholidoptera schmidti* (Fieber, 1861) and *Decticus albifrons* (F., 1775). About thirty total individuals of both sexes were reared in cages in a greenhouse with temperature gradually fluctuating between 19 °C and 35 °C in relation to natural photoperiod (15 h light) and relative humidity cycling between 70% and 80%. Each cage contained, at the bottom, a tray filled with washed sand for egg laying. Adults were fed with branches of *Rubus* sp., various fruits and vegetables, and also with dry cat food. On 6 August 2021, eggs of all five tettigoniid species (at least 13 for each species) were sifted from sand and placed in a permanent meadow in the Friuli Venezia Giulia Region, Italy (Udine Province, near Godia: 46°06'21.9"N, 13°16'38.5"E, 127 m a.s.l.) under bushes of *Rubus* sp., approximately 2 cm beneath the soil surface. To prevent damage by predators, sentinel eggs of each species were placed in one soil-filled plastic cup (10 × 10 × 5 cm) covered with a nylon net of 0.9 mm mesh. The bottom of the cup was removed and replaced with a nylon net to allow for rainwater flow. All the eggs were retrieved on 25 September 2021 and incubated in a laboratory at room temperature in plastic vials on moist filter paper. All collecting and rearing was done by G. Ortis.

The parasitoids were subsequently identified by S. V. Triapitsyn as *C. italica* by directly comparing them with the type series of this species and the original description, since it was made after the publication of the key to the European species of the genus by Ferrière (1965).

Results

On 22 November 2021, seven adult parasitoids hatched from each of two eggs of *Eupholidoptera schmidti* and seven adult parasitoids hatched from each of two eggs of *Pachytrachis gracilis*. Although females reared by us have a relatively shorter and less

protruding ovipositor (Fig. 1) than those of the type series of *C. italica* from another tettigoniid host, we consider that likely to be subject of intraspecific variability rather than warranting description of a new species in the genus where recognition of species worldwide, including Europe, is already extremely difficult. Females of *C. italica* from our study are illustrated here (Fig. 1) to facilitate their recognition.

Taxonomic remarks

Ferrière (1968) described *C. italica* from the holotype female from Sardinia and several paratypes of both sexes from Sardinia and Rome, Italy. In the collection of Muséum

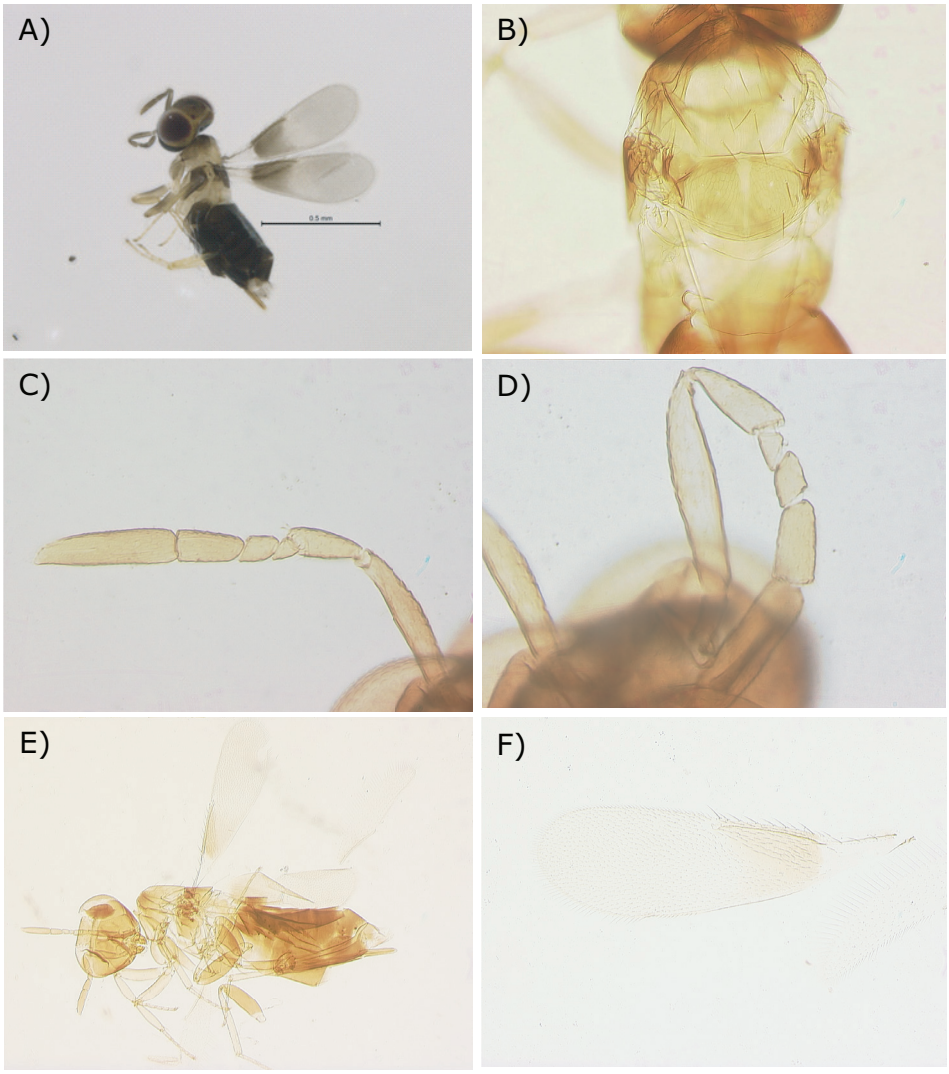

Figure 1. *Centrodora italica* from this study **A** habitus of female (in ethanol) **B** mesosoma **C** antenna **D** antenna **E** habitus (slide-mounted specimen) **F** fore wing. Scale bar: 0.5 mm.

d'Histoire Naturelle de la Ville de Genève, Geneva, Switzerland (**MHNG**), the type series of this species is mounted on five slides, four of which are labeled identically as follows: (1) "Sardaigne 1965 Cavalcaselle Ex *Uromenus brevicollis*", (2) "Aphelinidae *Centrodora italica* sp. n. Ch. Ferrière."; the remaining slides are labeled as follows: (3) "Italie Rome 1965 Cavalcaselle Ex *Uromenus brevicollis*", and (4) "Aphelinidae *Centrodora italica* sp. n. Ch. Ferrière.". Apparently, B. Cavalcaselle was the collector in Sardinia, but the exact type locality on the island is unknown. All specimens are in very poor condition, being dissected and slide-mounted without prior clearing and missing most of the antennae. Because the holotype was not marked, it is impossible now to decide which one of those specimens from Sardinia was the actual primary type. The best preserved and most complete slide-mounted female (1) is illustrated here (Fig. 2) for comparing purposes. Proper recognition of *C. italica* would require support from molecular evidence, as morphologically this species, particularly females from Sardinia and Rome, seem to be very similar to the widespread European species *C. amoena* Förster, 1878 (Fig. 3). The distinguishing features between these two nominal species mentioned by Ferrière (1968) in the diagnosis of *C. italica* are all of minor nature and eventually may be proven to be within the range of intraspecific variability of *C. amoena*.

Other material examined

Centrodora amoena (specimens in the National Museum of Natural History, Washington DC, USA [USNM]): France, Alpes-de-Haute-Provence, Manosque, 1959, H. L. Parker, "mass rearing alfalfa stems", 1 female. Russia, with the following labels: "Ural, 1931", "Egg pods of Locustids", "Rec'd from M. N. Nikolskaya let[ter]., 5-17-1935", 6 females.

Centrodora italica (specimen in the Entomology Research Museum, University of California, Riverside, California, USA [UCRC]): Italy, Campania, Caserta Province, SE end of Lago del Matese, 41°24.41'N, 14°24.20'E, 1050 m, 7.vi.2003, M. Bologna, J. Munro, A. Owen, J. D. Pinto, 1 male.

Discussion

Here we report the first record of *Centrodora italica* from northeastern Italy and two new host records of this species. Both *Eupholidoptera schmidti* and *Pachytrachis gracilis* occur from northeastern Italy and southernmost Austria across parts of the Balkans to Bulgaria and Greece, and are usually found in the transition zone of shrubs and small clearings (IUCN 2021). The wide distributional area of these hosts suggests that this parasitoid could be present also in other areas in the Mediterranean region.

While the common collection methods for micro-hymenopterous parasitoids, such as Malaise traps, yellow pan traps, sweep netting or Berlese funnels, allow for the capture of these wasps at adult stage, they are not suitable to detect their host

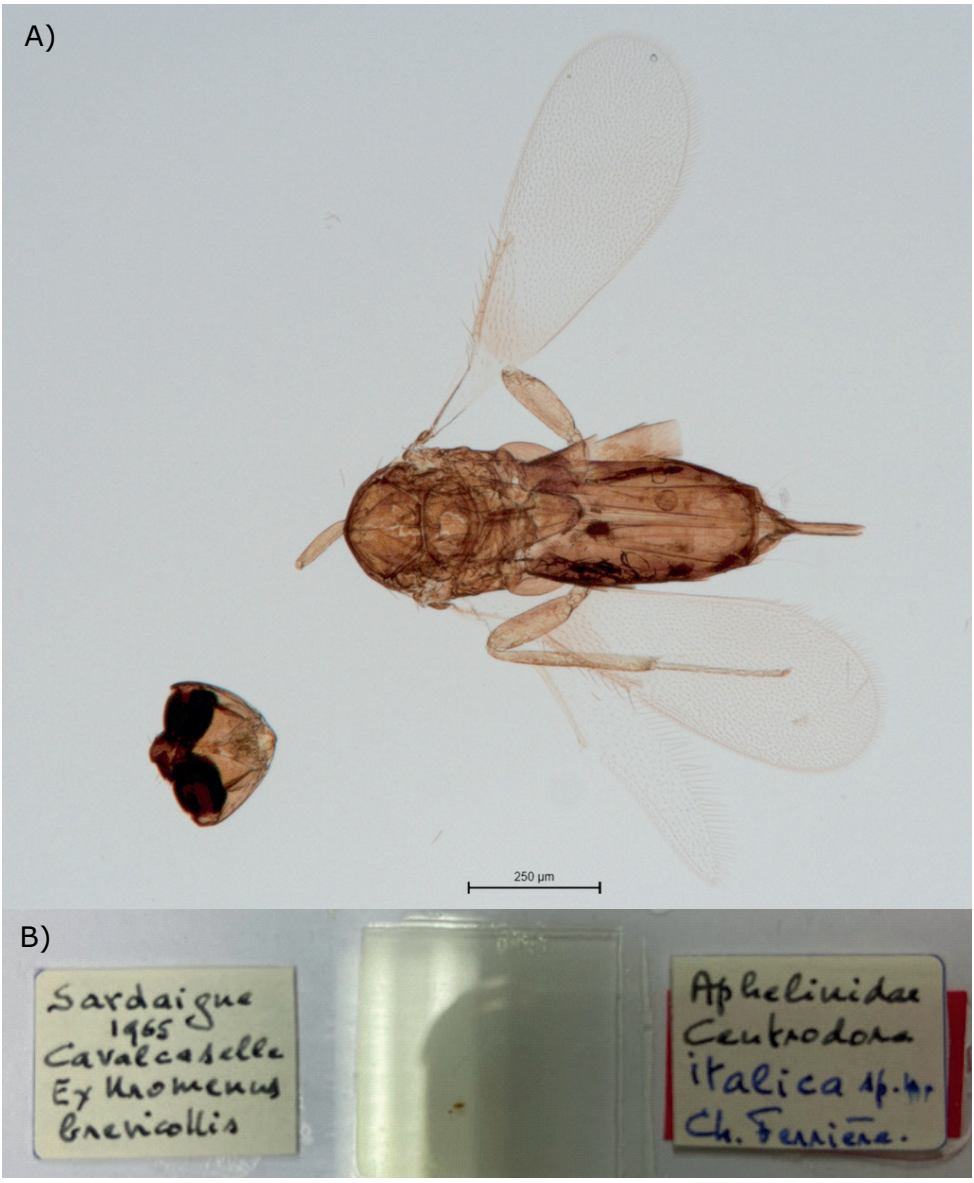

Figure 2. *Centrodora italica*, female of the type series **A** habitus **B** slide. Scale bar: 0.25 mm.

associations, in particular for those species that search for their hosts in the ground (Ortis et al. 2020). Because we placed sentinel eggs in August, we can hypothesize that the activity of this parasitoid takes place during summer after, or during, the oviposition period of most tettigoniid species (Ingrisch 1986; Ortis et al. 2022). It will be worth, for future studies, to provide genetic data for species delimitation within this genus *Centrodora*.

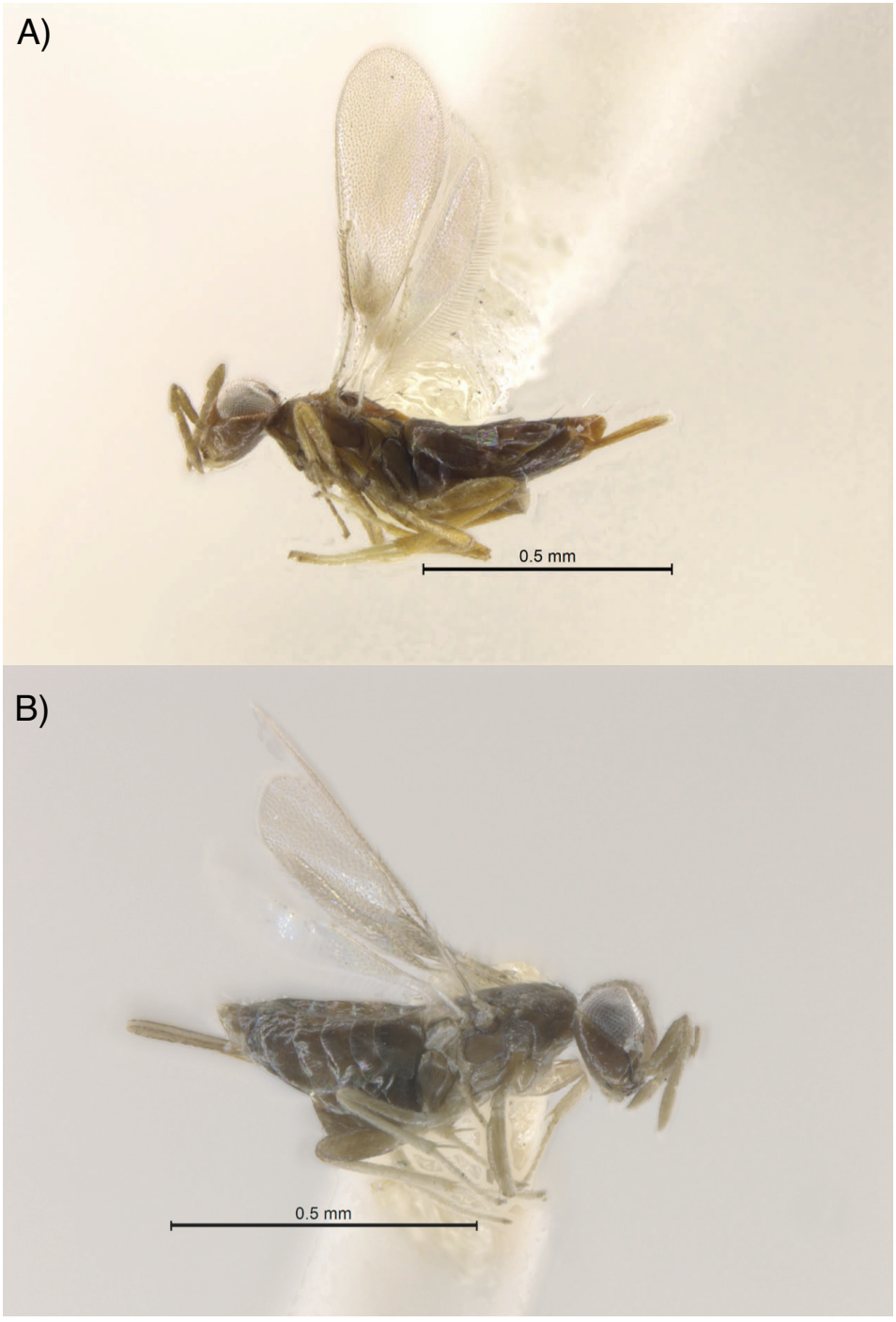

Figure 3. *Centrodora amoena*: **A** *C. amoena* female from Manosque, France **B** *C. amoena* female from Ural area, Russia. Scale bar: 0.5 mm.

Acknowledgements

We thank Bernard Landry (MHNG) for kindly providing digital images of the type series of *C. italica* and help with access to specimens under his care.

References

Bocca FM, Picciau L, Laudonia S, Alma A (2020) Palaearctic egg parasitoids interaction to three grapevine exotic pests in Northwestern Italy: A new association involving *Metcalfa pruinosa*. Insects 11(9): e610. https://doi.org/10.3390/insects11090610

Cavalcaselle B (1968) Un interessante caso di adattamento ad ospiti diversi da parte di un parassita oofago. Entomophaga 13(4): 319–322. https://doi.org/10.1007/BF02371913

Ferrière C (1965) Hymenoptera Aphelinidae d'Europe et du Bassin Méditerranéen. Faune de l'Europe et du Bassin Méditerranéen 1, Masson et Cie, Paris, 206 pp.

Ferrière C (1968) Notes sur quelques chalcidiens nouveaux ou peu connus (Hym.). Mitteilungen der Schweizerische Entomologische Gesellschaft 40: 240–248.

Hayat M (1974) Host-parasite catalogue of the egg-inhabiting aphelinid genera *Centrodora* Foerster, 1878 and *Tumidiscapus* Girault, 1911 (Hymenoptera, Chalcidoidea). Polskie Pismo Entomologiczne 44: 287–298.

Ingrisch S (1986) The plurennial life cycles of the European Tettigoniidae (Insecta: Orthoptera) – 1. The effect of temperature on embryonic development and hatching. Oecologia 70(4): 606–616. https://doi.org/10.1007/BF00379913

IUCN (2021) The IUCN Red List of Threatened Species. Version 2021-3. https://www.iucnredlist.org [Accessed 21 July 2022]

Noyes JS (2019) Universal Chalcidoidea Database. World Wide Web electronic publication. http://www.nhm.ac.uk/chalcidoids [Accessed 3 November 2022]

Ortis G, Triapitsyn SV, Cavaletto G, Martinez-Sañudo I, Mazzon L (2020) Taxonomic identification and biological traits of *Platystethynium triclavatum* (Donev & Huber, 2002), comb. n. (Hymenoptera, Mymaridae), a newly recorded egg parasitoid of the Italian endemic pest *Barbitistes vicetinus* Galvagni & Fontana, 1993 (Orthoptera, Tettigoniidae). PeerJ 8: e9667. https://doi.org/10.7717/peerj.9667

Ortis G, Marini L, Cavaletto G, Mazzon L (2022) Increasing temperatures affect multiyear life cycle of the outbreak bush-cricket *Barbitistes vicetinus* (Orthoptera, Tettigoniidae). Insect Science 0: 1–9. https://doi.org/10.1111/1744-7917.13094

Polaszek A (1991) Egg parasitism in Aphelinidae (Hymenoptera: Chalcidoidea) with special reference to *Centrodora* and *Encarsia* species. Bulletin of Entomological Research 81(1): 97–106. https://doi.org/10.1017/S0007485300053293

Raspi A, Canovai R (2003) *Centrodora livens* (Walker)-aphelinid egg parasitoid of *Metcalfa pruinosa* (Say) in Italy. Informatore Fitopatologico (Italy) 53: 49–51. [*Ulmus campestris* L.-Tuscany]

Viggiani G (1994) Lotta Biologica e Integrata nella Difesa Fitosanitaria. Liguori, 517 pp.

ZooKeys 1156: 33–52 (2023)
doi: 10.3897/zookeys.1156.94589
https://zookeys.pensoft.net

RESEARCH ARTICLE

A peer-reviewed open-access journal
ZooKeys
Launched to accelerate biodiversity research

New records of Nitidulidae (Nitidulidae, Coleoptera) species in Canada, Ontario, and Manitoba

Sharon E. Reed[1], David Dutkiewicz[2], Fiona Ross[3], Jennifer Llewellyn[4], Hannah Fraser[4]

1 *Ontario Forest Research Institute, Ministry of Natural Resources, and Forestry, 1235 Queen Street, Sault Ste. Marie, Canada* **2** *Invasive Species Centre, Sault Ste Marie, Canada* **3** *Manitoba Natural Resources and Northern Development, Winnipeg, Canada* **4** *Ontario Ministry of Agriculture, Food, and Rural Affairs, Guelph, Canada*

Corresponding author: Sharon E. Reed (Sharon.reed@ontario.ca)

Academic editor: A. Kirejtshuk | Received 8 September 2022 | Accepted 3 March 2023 | Published 24 March 2023

https://zoobank.org/95B624A8-3622-4429-BD5A-4E643C6C6367

Citation: Reed SE, Dutkiewicz D, Ross F, Llewellyn J, Fraser H (2023) New records of Nitidulidae (Nitidulidae, Coleoptera) species in Canada, Ontario, and Manitoba. ZooKeys 1156: 33–52. https://doi.org/10.3897/zookeys.1156.94589

Abstract

Nitidulidae trapping performed from 2018 to 2021 to characterize flight behaviors of potential vectors of the oak wilt pathogen yielded three new species records for Canada, six new species records for Ontario, and three new species records for Manitoba. The new records for Canada include *Carpophilus* (*Ecnomorphus*) *corticinus* reported from Ontario, *C.* (*Myothorax*) *nepos* reported from Ontario and Manitoba, and *Glischrochilus* (*Librodor*) *obtusus* reported from Ontario. In addition, the following species are first recorded in Ontario: *Carpophilus* (*Ecnomorphus*) *antiquus*, *C.* (*Megacarpolus*) *sayi*, *Stelidota coenosa*; and also in Manitoba: *Carpophilus* (*Megacarpolus*) *lugubris* and *Cychramus adustus*. Collection data is provided for the two provinces and national records.

Keywords

Bretziella fagacearum, *Carpophilus*, *Cychramus*, *Glischrochilus*, oak wilt, *Stelidota*

Introduction

The family Nitidulidae occurs globally with at least 4,500 species, of which, 173 species are found in North America (Habeck 2002; Marske and Ivie 2003). Also known as sap beetles or picnic beetles, Nitidulidae feed on flowers, fruits, fungi, stored products, de-

caying and fermenting plant tissues, carrion, and other insects. Feeding on fermenting sugars of fruits and vegetation is most common. Feeding by the beetles introduces fungi and bacteria to damaged plant tissues, resulting in further decay and fermentation. This appetite attracts the beetles of several Nitidulidae genera to the fruit-like smell of fungal mats produced by the oak wilt pathogen, *Bretziella fagacearum* (T.W. Bretz) J Hunt, which is an invasive species of fungus affecting oak trees (*Quercus* spp.) (Downie and Arnett 1996). Nitidulids become contaminated with fungal spores when they visit oak wilt mats. New infections occur when contaminated beetles leave the oak wilt mats and fly to fresh wounds on healthy oak trees, spreading the disease across the landscape (Jagemann et al. 2018). Identifying beetle species associated with movement of the fungus is important for establishing management criteria.

Oak wilt has been killing oak trees in the United States for more than half a century, spreading to 24 states and residing within 1 km of Canada on Belle Island, Michigan (Juzwik et al. 2008; USDA-FS 2019). Oak trees are susceptible to this fungus with some species dying within weeks of the initial infection. Oak wilt can infect neighboring trees through root-to-root contact (Bruhn et al. 1991), however transmission by nitidulids is considered more concerning because of the potential for transmission over greater distances and the formation of many new infection epicenters (DiGirolomo et al. 2020).

Overland spread of oak wilt by nitidulid beetles can be reduced by avoiding oak wounding when nitidulids are most active. A multi-year study of Nitidulidae beetle flight behavior was carried out at 21 localities in the following three Canadian provinces, Manitoba, Ontario, and New Brunswick. The study also aimed to describe the diversity of nitidulids that could be involved in oak wilt transmission. Beetles were collected using flight interruption traps. In total, there were 49 nitidulid species collected across the three provinces with three new records in Manitoba, six new records in Ontario, and three new records for Canada from Ontario and Manitoba. No new records are reported for New Brunswick.

Materials and methods

Traps were deployed at 14 localities in Ontario, four in Manitoba, and three in New Brunswick (Fig. 1). Flight intercept traps were installed in Manitoba in or near Winnipeg. These four localities are in the Interlake Plain and Lake Manitoba ecoregions (Smith et al. 1998). Both ecoregions experience short, warm summers and long, cold winters with slightly warmer temperatures in the Lake Manitoba Ecoregion. Deciduous and coniferous forest remain but large areas have been cleared for agriculture. Localities included an airport and three provincial parks. Bur oak (*Quercus macrocarpa* Michx.) is the only oak species that occurs in these ecoregions (Farrar 1995).

All New Brunswick localities were in the Grand Lake Lowlands (Fig. 1; Province of New Brunswick 2007). This ecoregion has a longer growing season and warmer sum-

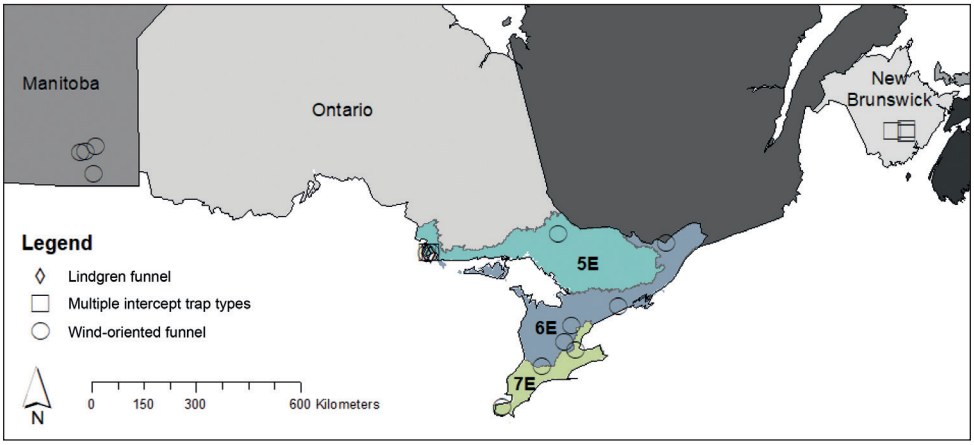

Figure 1. Geographic localities in Canada and Ontario ecoregions where flight intercept traps were used to collect Nitidulidae. Abbreviations: 5E – ecoregion 5, Georgina Bay.; 6E – ecoregion 6, Lake Simcoe-Rideau; 7E – ecoregion 7, Lake Erie-Lake Ontario.

mer temperatures than the rest of the province due the presence of the Grand Lake. The area is dominated by coniferous and mixed forests, but deciduous forests do occur. Trees are present in 70% of the ecoregion. Northern red oak (*Quercus rubra* L.) and bur oak are found in New Brunswick (Farrar 1995).

Ontario localities were in three ecoregions classified as 5E, 6E and 7E (Fig. 1). Six localities were in Ecoregion 5E, the Georgina Bay Ecoregion (Crins et. al 2009). Localities were mixed hardwood forests, a residential property with oak trees, and a forest edge next to a field. The climate of 5E is cool-temperate and humid. The area is dominated by mixed, deciduous, and coniferous forests typical of the Great lakes–St Lawrence Forest region. Predominant tree species are red pine (*Pinus resinosa* Sol. Ex Aiton), eastern white pine (*Pinus strobus* L.), eastern hemlock (*Tsuga canadensis* (L.) Carrière), yellow birch (*Betulae alleghansiensis* Britt.), maple (*Acer* spp.) and oak (northern red oak, bur oak). To the south is the Lake Simcoe-Rideau Ecoregion (i.e., Ecoregion 6E) which extends from the eastern shore of Lake Huron to the Ottawa River (Crins et al. 2009). Study localities within Ecoregion 6E included a mixed hardwood forest, a park containing hardwoods, and an oak plantation. The climate is mild and moist. More than half of the ecoregion has been converted to agriculture fields. The remaining treed areas are deciduous, coniferous, and mixed forests characteristic of the Great Lakes-St Lawrence Forest region. Oak species that may be found in Ecoregion 6E include northern red oak, bur oak, black oak (*Quercus velutina* Lam.), white oak (*Q. alba* L.), swamp white oak (*Q. bicolor* Willd.), and chinquapin oak (*Q. muelhlenbergii* Engelm.) (Farrar 1995).

Ecoregion 7E, the Lake Erie-Lake Ontario Ecoregion, is the most southerly area of Ontario (Crins et al. 2009). It incorporates shorelines from lakes Huron, Erie, and Ontario. The entire Carolinian forest region, dominated by beech, maple, black

walnut, hickory, and oak forests, occurs here. This area is considered unique to Canada because it is the northern edge of the deciduous forest in North America, which does not occur elsewhere in Canada. The area experiences cool winters and long, hot, humid summers. Nearly 80% of the area has been converted to agriculture fields. Deciduous forests cover approximately 10% of the ecoregion. In addition to the oak species found in Ecoregion 6E, 7E may contain northern pin (*Quercus ellipsoidalis* E.J. Hill), Shumard (*Q. shumardii* Buckl.), dwarf Chinquapin (*Q. prinoides* Willd.) and swamp pin oak (*Q. palustris* Muenchh.) (Farrar 1995). Ecoregion 7E is warmer than 6E and 5E and has a longer average growing season. The three ecoregions share a similar range in precipitation. Study localities were a mixed hardwood forest and two plantations in urban areas.

Flying beetles were collected using four types of traps; wind-oriented funnel traps, 12-unit Lindgren funnel traps, 12-unit modified Lindgren funnel traps, and 5-unit Synergy multitraps (Synergy Semiochemical Corp. Delta, BC). Wind-oriented funnel traps are also referred to as PVC pipe traps and wind-oriented pipe traps (Dowd et al. 1992; DiGirolomo et al. 2020). Three traps were placed at least 10 m apart at 16 localities in Ontario and Manitoba. Traps were hung from poles approximately 1.0–1.5 m in height from the ground and placed within 10 m of a red oak (*Quercus rubra*) or a bur oak (*Q. macrocarpa*). Wind-oriented traps were solely used at 14 localities and 12-unit Lindgren traps used at two localities. At four localities near Sault Ste Marie, Ontario and Fredericton, New Brunswick, five of each, wind-oriented funnel, Synergy multitrap, Lindgren funnel, and modified Lindgren funnel, were placed 20 m apart in hardwood stands containing *Quercus* species. At one additional site in New Brunswick, the same design was used except no Synergy multitraps were deployed. These traps were also hung from poles, at the same height from the ground.

The wind-oriented funnel traps (Dowd et al. 1992) included a collection chamber with insecticidal strips (19.2% Diclovos, "Ortho Home Defence Max No-Pest Insecticide Strip") and a lure chamber containing fermenting flour dough plus commercial lure for *Carpophilus* (*Megacarpolus*) *sayi* Parsons, 1943 and *Colopterus truncatus* (Randall, 1938) beetles (Great Lakes IPM, Vestaburg MI) (Jagemann et al. 2018). The yeast dough was replaced every week, the pheromone lures every four weeks, and the insecticidal strips each month. Lindgren-funnel traps (Lindgren 1983), modified Lindgren traps (Miller et al. 2013), and Synergy multitraps were set up and maintained with the same lures and schedule as the wind-oriented funnel traps. Lures and baits were hung inside the top funnel for modified traps and outside for non-modified traps (Miller et al. 2013). The funnel cups were filled with a saltwater solution with several drops of dish detergent and replaced after every collection (Webster et al. 2012). Collections were made weekly from March to October. Samples were stored at -20 °C until they could be sorted and identified.

Specimens were initially sorted and identified by technicians (Sylvia Greifenhagen, Ontario Forest Research Institute (**OFRI**) and DD, Invasive Species Centre) and lead research scientist (SR, OFRI), later identifications were confirmed

by Cucujoidea specialist (Gareth Powell, Florida State Collection of Arthropods). All specimens are deposited at OFRI in Sault Ste Marie, Ontario, except for New Brunswick collections which are held at the Atlantic Forestry Centre collection in Fredericton, NB. The generic attribution of the *Carpophilus* species was used after the papers by Kirejtshuk (2008, 2018). Information on the number of specimens recorded and collections where specimens were deposited is included in parentheses () after each record.

All species are listed with their current known distribution in Canada (Bousquet et al. 2013; Webster et al. 2016, 2022), using abbreviations from the province/territory. New records for Ontario, Manitoba are indicated in bold. The following abbreviations are used in the text and table for the used toponyms:

AB Alberta;
BC British Columbia;
MB Manitoba;
NB New Brunswick;
NF & LB Newfoundland & Labrador;
NS Nova Scotia;
NT Northwest Territories;
NU Nunavut;
ON Ontario;
PE Prince Edward Island;
QC Quebec;
SK Saskatchewan;
YT Yukon Territory.

Other abbreviations used in the text are:

BG BugGuide.net (https://bugguide.net);
IN iNaturalist (https://www.inaturalist.org/);
MNRF Ministry of Natural Resources and Forestry;
OFRI Ontario Forest Research Institute.

Results

In this account, six species are reported for the first time in the province of Ontario and three species are reported for the first time in Manitoba. Reports for three species are new records for Canada (Table 1). The following are the locality data and collection dates of the new Nitidulidae records reported during this study in Ontario and Manitoba. All new species records are based on information in Bousquet et al. (2013), Webster et al. (2016, 2022), Pentinsaari et al. (2019).

Table 1. Distribution of *Carpophilus*, *Cychramus*, *Glischrochilus*, and *Stelidota* species reported for Canada. * = new to Canada; bold = to province, distribution from Bousquet et al. (2013) and Webster et al. (2016, 2022).

Taxa	Geographic distribution in Canada
Family Nitidulidae	
Subfamily Carpophilinae Erichson, 1842	
(Subgenus Caplothorax Kirejtshuk, 1997)	
Carpophilus melanopterus Erichson, 1843	ON, QC
(Subgenus Carpophilus Stephens,1829)	
Carpophilus hemipterus (Linnaeus, 1758)	BC, AB, MB, ON, QC, NB
(Subgenus Ecnomorphus Motchulsky, 1858)	
Carpophilus antiquus Melsheimer, 1844	**ON**, QC
Carpophilus brachypterus (Say, 1825)	MB, ON, QC, NB, NS, PE
Carpophilus corticinus Erichson, 1843*	**ON**
Carpophilus discoideus LeConte, 1858	BC, ON
(Subgenus Megacarpolus Reitter, 1919)	
Carpophilus lugubris Murray, 1864	BC, AB, SK, **MB**, ON
Carpophilus sayi Parsons, 1943	SK, MB, **ON**, QC, NB, NS
(Subgenus Myothorax Murray, 1864)	
Carpophilus dimidiatus (Fabricius, 1792)	BC, SK, MB, ON, QC, NB
Carpophilus mutilatus Erichson, 1843	BC
Carpophilus nepos Murray, 1864*	**MB**, **ON**
(Subgenus Semocarpolus Kirejtshuk, 2008)	
Carpophilus marginellus Motschulsky, 1858	SK, MB, ON, QC, NB, NS, PE
Subfamily Nitidulinae Latreille, 1802	
Tribe Cychramini Gistel, 1848	
Cychramus adustus Erichson, 1843	**MB**, ON, QC, NB
Tribe Nitidulini Latreille, 1802	
Stelidota coenosa Erichson, 1843	**ON**, NB
Stelidota geminata (Say, 1825)	ON, QC
Stelidota octomaculata (Say, 1825)	ON, QC, NB, NS
Subfamily Cryptarchinae C.G. Thomson, 1859	
Tribe Cryptarchini C.G. Thomson, 1859	
(Subgenus Glischrochilus Reitter, 1873)	
Glischrochilus confluentus (Say, 1823)	BC, AB, SK, MB, ON, QC, NB, NS
Glischrochilus lecontei W.J. Brown, 1932	BC, MB,
Glischrochilus moratus W.J. Brown, 1932	BC, AB, SK, MB, ON, QC, NB, NS, PE
Glischrochilus vittatus (Say, 1835)	BC, AB, MB, ON, QC, NB, NS, PE
(Subgenus Librodor Reitter, 1884)	
Glischrochilus fasciatus (Olivier, 1790)	BC, MB, ON, QC, NB, NS, PE
Glischrochilus obtusus (Say, 1835)*	**ON**
Glischrochilus quadrisignatus (Say, 1835)	BC, AB, SK, MB, ON, QC, NB, NS, PE, NF
Glischrochilus sanguinolentus sanguinolentus (Olivier, 1790)	BC, AB, ON, QC, NB, NS, PE
Glischrochilus siepmanni W.J. Brown, 1932	BC, AB, SK, MB, ON, QC, NB, NS, PE

Taxonomy

Family NITIDULIDAE Latreille, 1802
Subfamily Carpophilinae Erichson, 1842

Carpophilus (*Ecnomorphus*) *antiquus* (Melsheimer, 1844)

Notes. This species has only been recorded in Quebec, Canada (Bousquet et al. 2013) and is prevalent across much of the eastern United States including states that border

with Canada (Parsons 1943; Price and Young 2006; Morris 2020). Neither BugGuide (BG), an online entomological database hosted by Iowa State University, or iNaturalist, a citizen science database, list Ontario when reporting the distribution of the species. However, Ontario is listed under the distribution of this species in Downie and Arnett (1996) but without supporting data. Here, we recorded *C.* (*E.*) *antiquus* for the first time in Ontario from two localities in 2018.

New records. Ontario: Windsor, ON, Maidstone Conservation Area off lakeshore Rd. 209, 42.2130°N, 82.7911°W, 8-v-2018 (19, OFRI); ibidem, 15-v-2018 (2, OFRI). All samples were taken from wind-oriented funnel traps, in hardwood forest next to *Quercus* sp.

London, ON, Fanshawe Conservation Area off Fanshawe Park Rd, East, 43.0507°N, 81.1818°W, 4-ix-2018, wind-oriented funnel trap, plantation forest next to *Quercus* sp. (1, OFRI).

Distribution in Canada. MB, **ON**, QC (Bousquet et al. 2013).

Carpophilus (*Ecnomorphus*) *corticinus* Erichson, 1843

Notes. This is a new record for Canada and Ontario. *Carpophilus* (*Ecnomorphus*) *corticinus* was collected in four different localities across the Southern region of Ontario in 2018, 2019, and 2020. There are no other records of this species for Canada in either BN or IN. However, Ontario is listed under the distribution description for Price's (2003) thesis of Kateretidae and Nitidulidae of Wisconsin. *Carpophilus* (*Ecnomorphus*) *corticinus* has been recorded from US states bordering Canada, including New York, Ohio, and Michigan as well as south to Texas and Georgia (Parsons 1943; Downie and Arnett 1996).

New records. Canada, Ontario: Windsor, ON, Maidstone Conservation Area off lakeshore Rd. 209, 42.2130°N, 82.7911°W, 17-iv-2018 (21, OFRI); ibidem, 24-iv-2018 (3, OFRI); ibidem, 8-v-2018 (7, OFRI); ibidem, 29-v-2018 (3, OFRI); ibidem, 5-vi-2018 (1, OFRI); ibidem, 19-vi-2018 (1, OFRI). All samples taken from wind-oriented funnel traps, in hardwood forest next to *Quercus* sp.

London, ON, Fanshawe Conservation Area off Fanshawe Park Rd, East, 43.0507°N, 81.1818°W, 29-v-2018 wind-oriented funnel trap, plantation forest next to *Quercus* sp. (4, OFRI).

Hamilton, ON, Royal Botanical Gardens, off Homestead Ave, 43.2882°N, 79.9069°W, 8-v-2019 (4, OFRI); ibidem, 22-v-2019 (1, OFRI); ibidem, 29-v-2019 (2, OFRI); ibidem, 12-vi-2019 (1, OFRI); ibidem, 19-vi-2019 (5, OFRI); ibidem, 3-vii-2019 (2, OFRI); ibidem, 24-vii-2019 (1, OFRI) ; ibidem, 31-vii-2019 (1, OFRI); ibidem, 14-viii-2019 (1, OFRI). All samples taken from wind-oriented funnel traps, in planted hardwood forest next to *Quercus* sp.

London, ON, Fanshawe Conservation Area off Fanshawe Park Rd, East, 43.0507°N, 81.1818°W, 10-iv-2019 (1, OFRI); ibidem, 24-iv-2019 (1, OFRI), note: specimen damaged; ibidem, 29-v-2019 (10, OFRI); ibidem, 5-vi-2019 (8, OFRI); ibidem, 12-vi-2019 (3, OFRI); ibidem, 19-vi-2019 (3, OFRI); ibidem, 16-

vi-2019 (1, OFRI); ibidem, 17-vii-2019 (1, OFRI); ibidem, 18-ix-2019 (1, OFRI); ibidem, 25-ix-2019 (1, OFRI); ibidem, 2-x-2019 (1, OFRI); ibidem, 16-x-2019 (1, OFRI). All samples taken from wind-oriented funnel traps, in plantation forest next to *Quercus* sp.

Hamilton, ON, Royal Botanical Gardens, off Homestead Ave, 43.2882°N, 79.9069°W, 28-v-2020 (3, OFRI); ibidem, 3-vi-2020 (4, OFRI); ibidem, 11-vi-2020 (4, OFRI); ibidem, 18-vi-2020 (4, OFRI); ibidem, 25-vi-2020 (1, OFRI); ibidem, 8-vii-2020 (2, OFRI); ibidem, 16-vii-2020 (1, OFRI); ibidem, 30-vii-2020 (1, OFRI); ibidem, 26-viii-2020 (1, OFRI); ibidem, 17-ix-2020 (3, OFRI). All samples taken from wind-oriented funnel traps, in planted hardwood forest next to *Quercus* sp.

London, ON, Fanshawe Conservation Area off Fanshawe Park Rd, East, 43.0507°N, 81.1818°W, 27-v-2020 (13, OFRI); ibidem, 10-vi-2020 (7, OFRI); ibidem, 17-vi-2020 (4, OFRI); ibidem, 24-vi-2020 (2, OFRI); ibidem, 8-vii-2020 (1, OFRI); ibidem, 15-vii-2020 (3, OFRI); ibidem, 12-viii-2020 (2, OFRI); ibidem, 28-x-2020 (1, OFRI). All samples taken from wind-oriented funnel traps, in plantation forest next to *Quercus* sp.

Guelph, ON, The Arboretum, University of Guelph, 43.5436°N, 80.2205°W, 25-vi-2020 (1, OFRI); ibidem, 8-vii-2020 (1, OFRI); ibidem, 3-ix-2020 (1, OFRI). All samples taken from wind-oriented funnel traps, in *Quercus rubra* plantation.

Distribution in Canada. ON (new Canadian record).

Carpophilus (*Megacarpolus*) *lugubris* Murray, 1864

Notes. This species is recorded for much of central and western Canada from British Columbia to Saskatchewan and Ontario (Bousquet et al. 2013). Here, we report *Carpophilus* (*Megacarpolus*) *lugubris* for the first time in Manitoba from three localities in 2019, 2020, and 2021. This species being found in Manitoba was not unexpected since it is present in the bordering provinces of Saskatchewan and Ontario. Downie and Arnett (1996) record *C.* (*M.*) *lugubris* occurring across the United States. There are several records of this species in Canada reported on the IN website, from BC, ON, and QC (Lugubris 2023).

New records. Manitoba: Birds Hill Provincial Park, MB, Roscoe Rd. 50.0436°N, 96.8719°W, 10-ix-2019 wind-oriented funnel trap, mixed hardwood forest next to *Quercus* sp. (1, OFRI).

Beaudry Provincial Park, MB, Roblin Blvd, 49.8576°N, 97.4638°W, 11-viii-2020 (1, OFRI), ibidem, 18-viii-2020 (1, OFRI); ibidem, 2-ix-2020 (2, OFRI); ibidem, 23-ix-2020 (1, OFRI); ibidem, 30-ix-2020 (1, OFRI). All samples were collected from wind-oriented funnel traps, riparian hardwood forest next to *Quercus* sp.

Saint Malo, St Malo Provincial Park, MB, 49.3229°N, 96.9355°W, 29-vii-2021, wind-oriented funnel trap, mixed hardwood forest next to *Quercus* sp. (1, OFRI).

Distribution in Canada. BC, AB, SK, **MB**, ON (Bousquet et al. 2013).

***Carpophilus* (*Myothorax*) *nepos* Murray, 1864**

Notes. This is the first record for *Carpophilus* (*Myothorax*) *nepos* in Canada, obtained from five localities in Ontario in 2018, 2019, and 2020 and four localities in Manitoba in 2019 and 2021. This species, associated with stored grain products, is almost cosmopolitan and its distribution is poorly understood due to its synonym with *Carpophilus freemani* Dobson, 1956 (Kirejtshuk 1996). Peck and Thomas (1998) mention that this species has been recorded in the United States and Price (2003) provides records for the state of Wisconsin. *Carpophilus* (*Myothorax*) *nepos* has not been recorded in Canada according to Bousquet et al. (2013).

New records. Canada, Ontario: Windsor, ON, Maidstone Conservation Area off lakeshore Rd. 209, 42.2130°N, 82.7911°W, 15-v-2018, wind-oriented funnel trap, hardwood forest next to *Quercus* sp. (1, OFRI).

Ottawa, ON, Elmhurst Park, off Alpine Ave, 45.3591°N, 75.7861°W, 23-viii-2019, wind-oriented funnel trap, in a hardwood forest next to *Quercus* sp. (2, OFRI).

Hamilton, ON, Royal Botanical Gardens, off Homestead Ave, 43.2882°N, 79.9069°W, 3-vii-2019 (1, OFRI); ibidem, 18-ix-2019 (1, OFRI); ibidem, 2-x-2019 (2, OFRI). All samples taken from wind-oriented funnel traps, in a planted hardwood forest, next to *Quercus* sp.

London, ON, Fanshawe Conservation Area off Fanshawe Park Rd, East, 43.0507°N, 81.1818°W, 4-ix-2019 (1, OFRI); ibidem, 11-ix-2019 (1, OFRI); ibidem, 24-ix-2019 (1, OFRI). All samples taken from wind-oriented funnel traps, in a plantation forest, next to *Quercus* sp.

Guelph, ON, The Arboretum, University of Guelph, 43.5436°N, 80.2205°W, 3-vii-2019 (1, OFRI); ibidem, 43.5436°N, 80.2205°W, 18-ix-2019 (1, OFRI). All samples taken from wind-oriented funnel traps in a *Quercus rubra* plantation.

Ottawa, ON, Elmhurst Park, off Alpine Ave, 45.3591°N, 75.7861°W, 27-viii-2020 wind-oriented funnel trap in hardwood forest next to *Quercus* sp. (1, OFRI).

Hamilton, ON, Royal Botanical Gardens, off Homestead Ave, 43.2882°N, 79.9069°W, 30-vii-2020 (1, OFRI); ibidem, 5-viii-2020 (1, OFRI); ibidem, 12-viii-2020 (1, OFRI); ibidem, 17-ix-2020 (1, OFRI). All samples taken from wind-oriented funnel traps, in a planted hardwood forest, next to *Quercus* sp.

London, ON, Fanshawe Conservation Area off Fanshawe Park Rd, East, 43.0507°N, 81.1818°W, 15-vii-2020 (2, OFRI); ibidem, 22-vii-2020 (2, OFRI); ibidem, 28-x-2020 (1, OFRI). All samples taken from wind-oriented funnel traps, in a plantation forest, next to *Quercus* sp.

Guelph, ON, The Arboretum, University of Guelph, 43.5436°N, 80.2205°W, 12-vii-2020 (4, OFRI); ibidem, 10-ix-2020 (2, OFRI); ibidem, 24-ix-2020 (3, OFRI). All samples taken from wind-oriented funnel traps, in a *Quercus rubra* plantation.

New records. Canada, Manitoba: Birds Hill Provincial Park, MB, Roscoe Rd. 50.0436°N, 96.8719°W, 2-vii-2019, wind-oriented funnel trap, mixed hardwood forest next to *Quercus* sp. (2, OFRI).

Beaudry Provincial Park, MB, Roblin Blvd, 49.8576°N, 97.4638°W, 11-vi-2019, wind-oriented funnel trap, riparian hardwood forest next to *Quercus* sp. (2, OFRI).

Winnipeg, MB, Winnipeg James Armstrong Richardson International Airport off Wihuri Rd., 49.8996°N, 97.2538°W, 11-vi-2019 (1, OFRI); ibidem, 25-vi-2019 (1, OFRI); ibidem, 14-viii-2019 (2, OFRI); ibidem, 22-viii-2019 (1, OFRI). All samples taken from wind-oriented funnel traps, in a mixed hardwood forest next to *Quercus* sp.

Saint Malo, MB, St Malo Provincial Park, 49.3229°N, 96.9355°W, 3-vi-2021, wind-oriented funnel trap, mixed hardwood forest next to *Quercus* sp. (1, OFRI).

Distribution in Canada. ON, **MB** (new Canadian record).

Carpophilus (*Megacarpolus*) *sayi* Parsons, 1943

Notes. Here, we report *Carpophilus* (*Megacarpolus*) *sayi* for the first time in Ontario from 12 localities in 2018, 2019, 2020, and 2021. The species is found throughout central Canada excluding Ontario (Bousquet et al. 2013) and along the northern United States bordering Canada (Downie and Arnett 1996). These records suggest that this species could be found throughout Ontario. BugGuide does not specifically exclude Ontario from its distribution; however, Downie and Arnett (1996) include Ontario in their distribution description. iNaturalist does include one locality of *C.* (*M.*) *sayi* near Kitchener, Ontario (Jakubowski 2021) with a photo attached. The photo submitted to IN could be *Carpophilus* (*Megacarpolus*) *sayi* or *C.* (*M.*) *lugubris*. The two species sometimes look similar enough that Parsons (1943) suggested they could hybridize. According to Parsons (1943) the males of *C.* (*M.*) *lugubris* have two, deep, circular depressions on the hypopygidium and females have a pygidium that is blunt carinate, shining, and tuberculiform at the apex. In contrast, the males of *C.* (*M.*) *sayi* have two, large, vague, shallow depression on the hind margin of their hypopygidium and females have a distinct, blunt carina on the pygidium (Parsons 1943). Price (2003) also points out that *C.* (*M.*) *sayi* has rectangular humeral angles while the elytral humerals of *C.* (*M.*) *lugubris* are rounded or obtuse.

New records. Ontario: Sault Ste. Marie, ON, Wattswood Park and Ski Trails off Mt. Pleasant Ct., 46.3356°N, 84.2527°W, 14-v-2018 (10, OFRI); ibidem, 20-v-2018 (11, OFRI); ibidem, 27-v-2018 (123, OFRI); ibidem,, 6-vi-2018 (31, OFRI); ibidem, 10-vi-2018 (4, OFRI); ibidem, 25-vi-2018 (11, OFRI); ibidem, 1-vii-2018 (1, OFRI); ibidem, 4-vii-2018 (3, OFRI); ibidem, 11-vii-2018 (1, OFRI); ibidem, 18-vii-2018 (2, OFRI); ibidem, 28-vii-2018 (15, OFRI). All samples were taken from wind-oriented funnel traps, in a mixed hardwood forest, next to *Quercus* sp.

Peterborough, ON Northumberland County Forest off Dunbar Rd., 17-v-2018 (5, OFRI); ibidem, 24-v-2018 (15, OFRI); ibidem, 31-v-2018 (11, OFRI); ibidem, 14-vi-2018 (20, OFRI); ibidem, 19-vi-2018 (18, OFRI); ibidem, 29-vi-2018 (6, OFRI); ibidem, 6-vii-2018 (25, OFRI); ibidem, 13-vii-2018 (4, OFRI); ibidem, 19-vii-2018 (1, OFRI); ibidem, 26-vii-2018 (4, OFRI). All samples were taken from wind-oriented funnel traps, in a mixed hardwood forest, next to *Quercus* sp.

Sault Ste. Marie, ON, Hiawatha Highlands off Fish Hatchery Rd., 46.3436°N, 84.1705°W, 15-v-2019 (2, OFRI); ibidem, 29-v-2019 (28, OFRI); ibidem, 5-vi-2019 (7, OFRI); ibidem, 12-vi-2019 (90, OFRI); ibidem, 19-vi-2019 (16, OFRI); ibidem, 26-vi-2019 (10, OFRI); ibidem, 3-vii-2019 (4, OFRI); ibidem, 9-vii-2019 (1, OFRI); ibidem, 17-vii-2019 (6, OFRI); ibidem, 31-vii-2019 (4, OFRI); ibidem, 8-viii-2019 (4, OFRI); ibidem, 14-viii-2019 (16, OFRI); ibidem, 21-viii-2019 (3, OFRI); ibidem, 28-viii-2019 (2, OFRI). All samples were taken from wind-oriented funnel traps, in mixed hardwood forest, next to *Quercus* sp.

Ottawa, ON, Elmhurst Park, off Alpine Ave, 45.3591°N, 75.7861°W, 8-v-2019 (1, OFRI); ibidem, 12-vi-2019 (1, OFRI); ibidem, 25-vi-2019 (1, OFRI); ibidem, 31-vii-2019 (1, OFRI); ibidem, 7-viii-2019 (1, OFRI). All samples were taken from wind-oriented funnel traps, in a hardwood forest, next to *Quercus* sp.

Hamilton, ON, Royal Botanical Gardens, off Homestead Ave, 43.2882°N, 79.9069°W, 22-v-2019 (3, OFRI); ibidem, 29-v-2019 (61, OFRI); ibidem, 5-vi-2019 (6, OFRI); ibidem, 12-vi-2019 (3, OFRI); ibidem, 19-vi-2019 (12, OFRI); ibidem, 26-vi-2019 (1, OFRI); ibidem, 3-vii-2019 (5, OFRI); ibidem, 10-vii-2019 (1, OFRI). All samples were taken from wind-oriented funnel traps, in a planted hardwood forest, next to *Quercus* sp.

North Bay, ON, Canadore College trails, off College Dr., 46.3427°N, 79.5033°W, 30-v-2019 (15, OFRI); ibidem, 6-vi-2019 (5, OFRI); ibidem, 13-vi-2019 (70, OFRI); ibidem, 20-vi-2019 (10, OFRI); ibidem, 27-vi-2019 (10, OFRI); ibidem, 4-vii-2019 (8, OFRI); ibidem, 11-vii-2019 (3, OFRI); ibidem, 18-vii-2019 (5, OFRI); ibidem, 25-vii-2019 (1, OFRI); ibidem, 12-ix-2019 (1, OFRI). All samples were taken from wind-oriented funnel traps, in a mixed hardwood forest, next to *Quercus* sp.

London, ON, Fanshawe Conservation Area off Fanshawe Park Rd, East, 43.0507°N, 81.1818°W, 15-vi-2019 (1, OFRI); ibidem, 26-vi-2019 (1, OFRI). Both samples were taken from wind-oriented funnel traps, in a mixed hardwood forest, next to *Quercus* sp.

Guelph, ON, The Arboretum, University of Guelph, 43.5436°N, 80.2205°W, 5-vi-2019 (2, OFRI); ibidem, 12-vi-2019 (2, OFRI); ibidem, 19-vi-2019 (4, OFRI). All samples were taken from wind-oriented funnel traps, in a *Quercus rubra* plantation.

Sault Ste. Marie, ON, Hiawatha Highlands off Fish Hatchery Rd., 46.3436°N, 84.1705°W, 19-v-2020 (18, OFRI); ibidem, 20-v-2020 (14, OFRI); ibidem, 25-v-2020 (18, OFRI); ibidem, 27-v-2020 (8, OFRI); ibidem, 1-vi-2020 (28, OFRI); ibidem, 2-vi-2020 (8, OFRI); ibidem, 3-vi-2020 (3, OFRI); ibidem, 4-vi-2020 (6, OFRI); ibidem, 5-vi-2020 (3, OFRI); ibidem, 8-vi-2020 (5, OFRI); ibidem, 10-vi-2020 (6, OFRI); ibidem, 14-vi-2020 (2, OFRI); ibidem, 15-vi-2020 (3, OFRI); ibidem, 16-vi-2020 (8, OFRI); ibidem, 17-vi-2020 (2, OFRI); ibidem, 25-vi-2020 (3, OFRI); ibidem, 26-vi-2020 (1, OFRI); ibidem, 3--vi-2020 (1, OFRI); ibidem, 8-vii-2020 (3, OFRI); ibidem, 15-vii-2020 (9, OFRI); ibidem, 22-vii-2020 (11, OFRI); ibidem, 29-vii-2020 (7, OFRI); ibidem, 5-viii-2020 (13, OFRI); ibidem, 12-viii-2020 (17, OFRI); ibidem, 19-viii-2020 (22, OFRI); ibidem, 26-viii-2020 (9, OFRI); ibidem, 2-ix-2020 (2, OFRI); ibidem, 9-ix-2020 (3, OFRI); ibidem, 17-ix-2020 (1, OFRI); Sault Ste. Marie, ON, Hiawatha Highlands off Fish Hatchery Rd.,

46.5601°N, 84.4193°W, 19-v-2020 (3, OFRI). Almost all samples were taken from the wind-oriented funnel trap, in a mixed hardwood forest, next to *Quercus* sp., but the sample of 19-v-2020 was collected from the Lindgren funnel trap, in a mixed regenerated forest, next to *Quercus* sp.

Sault Ste. Marie, ON, Maki Rd., 46.5601°N, 84.4193°W, 18-v-2020 (1, OFRI); ibidem, 20-v-2020 (1, OFRI); ibidem, 21-v-2020 (24, OFRI); ibidem, 22-v-2020 (34, OFRI); ibidem, 23-v-2020 (20, OFRI); ibidem, 24-v-2020 (15, OFRI); ibidem, 25-v-2020 (17, OFRI); ibidem, 27-v-2020 (10, OFRI); ibidem, 28-v-2020 (6, OFRI); ibidem, 2-vi-2020 (1, OFRI); ibidem, 3-vi-2020 (3, OFRI); ibidem, 4-vi-2020 (5, OFRI); ibidem, 8-vi-2020 (8, OFRI); ibidem, 9-vi-2020 (12, OFRI); ibidem, 10-vi-2020 (4, OFRI); ibidem, 14-vi-2020 (4, OFRI); ibidem, 15-vi-2020 (5, OFRI); ibidem, 16-vi-2020 (4, OFRI); ibidem, 17-vi-2020 (1, OFRI); ibidem, 19-vi-2020 (3, OFRI); ibidem, 20-vi-2020 (1, OFRI); ibidem, 21-vi-2020 (1, OFRI); ibidem, 8-vii-2020 (8, OFRI); ibidem, 15-vii-2020 (2, OFRI); ibidem, 21-vii-2020 (2, OFRI); ibidem, 29-vii-2020 (4, OFRI); ibidem, 5-viii-2020 (1, OFRI); ibidem, 12-viii-2020 (6, OFRI); ibidem, 18-viii-2020 (1, OFRI); ibidem, 2-ix-2020 (1, OFRI); ibidem, 16-ix-2020 (1, OFRI); ibidem, 30-ix-2020 (1, OFRI). All samples were taken from Lindgren funnel traps, in a mixed regenerated forest, next to *Quercus* sp.

Sault Ste. Marie, ON, Retta St., 46.5061°N, 84.2945°W, 24-v-2020 (2, OFRI); ibidem, 25-v-2020 (12, OFRI); ibidem, 27-v-2020 (10, OFRI); ibidem, 1-vi-2020 (14, OFRI); ibidem, 2-vi-2020 (9, OFRI); ibidem, 3-vi-2020 (16, OFRI); ibidem, 4-vi-2020 (11, OFRI); ibidem, 5-vi-2020 (5, OFRI); ibidem, 8-vi-2020 (14, OFRI); ibidem, 9-vi-2020 (26, OFRI); ibidem, 10-vi-2020 (8, OFRI); ibidem, 16-vi-2020 (3, OFRI); ibidem, 17-vi-2020 (4, OFRI); ibidem, 18-vi-2020 (2, OFRI); ibidem, 20-vi-2020 (1, OFRI); ibidem, 1-vii-2020 (9, OFRI); ibidem, 8-vii-2020 (34, OFRI); ibidem, 15-vii-2020 (8, OFRI); ibidem, 22-vii-2020 (12, OFRI); ibidem, 29-vii-2020 (9, OFRI); ibidem, 5-viii-2020 (3, OFRI); ibidem, 19-viii-2020 (2, OFRI); ibidem, 12-viii-2020 (4, OFRI); ibidem, 30-ix-2020 (1, OFRI). All samples were taken from Lindgren funnel traps, among residential hardwood trees (*Quercus* sp.).

Ottawa, ON, Elmhurst Park, off Alpine Ave, 45.3591°N, 75.7861°W, 29-v-2020 (9, OFRI); ibidem, 4-v-2020 (1, OFRI); ibidem, 11-v-2020 (17, OFRI); ibidem, 19-v-2020 (1, OFRI); ibidem, 24-v-2020 (1, OFRI); ibidem, 10-vii-2020 (2, OFRI); ibidem, 24-vii-2020 (1, OFRI). All samples were taken from wind-oriented funnel traps, in a hardwood forest, next to *Quercus* sp.

Hamilton, ON, Royal Botanical Gardens, off Homestead Ave, 43.2882°N, 79.9069°W, 28-v-2020 (21, OFRI); ibidem, 3-vi-2020 (48, OFRI); ibidem, 11-vi-2020 (58, OFRI); ibidem, 18-vi-2020 (31, OFRI); ibidem, 25-vi-2020 (8, OFRI); ibidem, 2-vii-2020 (11, OFRI); ibidem, 8-vii-2020 (2, OFRI); ibidem, 16-vii-2020 (14, OFRI); ibidem, 23-vii-2020 (6, OFRI); ibidem, 30-vii-2020 (3, OFRI); ibidem, 5-viii-2020 (8, OFRI); ibidem, 12-viii-2020 (1, OFRI); ibidem, 26-viii-2020 (1, OFRI); ibidem, 17-ix-2020 (1, OFRI). All samples were taken from wind-oriented funnel traps, in a planted hardwood forest, next to *Quercus* sp.

North Bay, ON, Canadore College trails, off College Dr., 46.3427°N, 79.5033°W, 20-v-2020 (3, OFRI); ibidem, 27-v-2020 (193, OFRI); ibidem, 3-vi-2020 (3, OFRI);

ibidem, 10-vi-2020 (34, OFRI); ibidem, 17-vi-2020 (9, OFRI); ibidem, 24-vi-2020 (6, OFRI); ibidem, 1-vii-2020 (14, OFRI); ibidem, 8-vii-2020 (15, OFRI); ibidem, 15-vii-2020 (1, OFRI); ibidem 29-vii-2020 (7, OFRI). ; ibidem, 5-viii-2020 (2, OFRI). All samples were taken from wind-oriented funnel traps, in a mixed hardwood forest, next to *Quercus* sp.

London, ON, Fanshawe Conservation Area, 43.0507°N, 81.1818°W, 24-vi-2020 wind-oriented funnel trap, plantation forest, next to *Quercus* sp. (1, OFRI).

Guelph, ON, The Arboretum, University of Guelph, 43.5436°N, 80.2205°W, 3-vi-2020; ibidem, 11-vi-2020 (1, OFRI); ibidem, 16-vii-2020 (1, OFRI); ibidem, 30-vii-2020 (1, OFRI). All samples were taken from wind-oriented funnel traps, in a *Quercus rubra* plantation.

Sault Ste. Marie, Goulais Ave, Crimson Ridge golf course, 46.5767°N, 84.3799°W, 18-v-2021, Lindgren funnel (71, OFRI), modified Lindgren funnel (40, OFRI), synergy multitrap (120, OFRI), wind-oriented funnel trap (55, OFRI); ibidem,, 25-v-2021, Lindgren funnel (159, OFRI), modified Lindgren funnel (59, OFRI), synergy multitrap (200, OFRI), wind-oriented funnel trap (73, OFRI); ibidem,46.5767°N, 84.3799°W, 1-vi-2021, Lindgren funnel (166, OFRI), modified Lindgren funnel (35, OFRI), synergy multitrap (75, OFRI), wind-oriented funnel trap (21, OFRI); ibidem, 8-vi-2021, Lindgren funnel (162, OFRI), modified Lindgren funnel (81, OFRI), synergy multitrap (155, OFRI), wind-oriented funnel trap (35, OFRI); ibidem, 15-vi-2021, Lindgren funnel (34, OFRI), modified Lindgren funnel (18, OFRI), synergy multitrap (25, OFRI), wind-oriented funnel trap (3, OFRI); ibidem, 22-vi-2021, Lindgren funnel (25, OFRI), modified Lindgren funnel (16, OFRI), synergy multitrap (37, OFRI), wind-oriented funnel trap (6, OFRI); ibidem, 29-vi-2021, Lindgren funnel (7, OFRI), modified Lindgren funnel (4, OFRI), synergy multitrap (8, OFRI), wind-oriented funnel trap (7, OFRI); ibidem, 6-vii-2021, Lindgren funnel (5, OFRI), modified Lindgren funnel (4, OFRI), wind-oriented funnel trap (7, OFRI); ibidem, 13-vii-2021, Lindgren funnel (8, OFRI), modified Lindgren funnel (8, OFRI), synergy multitrap (8, OFRI), wind-oriented funnel trap (6, OFRI); ibidem, 20-vii-2021, Lindgren funnel (16, OFRI), modified Lindgren funnel (2, OFRI), synergy multitrap (7, OFRI), wind-oriented funnel trap (3, OFRI); ibidem, 27-vii-2021, Lindgren funnel (9, OFRI), modified Lindgren funnel (3, OFRI), synergy multitrap (5, OFRI), wind-oriented funnel trap (1, OFRI); ibidem, 3-viii-2021, modified Lindgren funnel (2, OFRI); ibidem, 10-viii-2021, Lindgren funnel (2, OFRI), synergy multitrap (1, OFRI); ibidem, 17-viii-2021, synergy multitrap (1, OFRI), wind-oriented funnel trap (1, OFRI); ibidem, 22-ix-2021, synergy multitrap (1, OFRI). All samples were collected from a mixed hardwood forest, next to *Quercus* sp.

Sault Ste. Marie, ON, Landslide Rd., 46.5792°N, 84.2802°W, 18-v-2021, Lindgren funnel trap (340, OFRI), modified Lindgren funnel trap (183, OFRI), synergy multitrap (468, OFRI), wind-oriented funnel trap (340, OFRI); ibidem, 18-v-2021, Lindgren funnel (276, OFRI), modified Lindgren funnel (160, OFRI), synergy multitrap (299, OFRI), wind-oriented funnel trap (174, OFRI); ibidem, 1-vi-2021, Lindgren funnel (151, OFRI), modified Lindgren funnel (77, OFRI),

synergy multitrap (210, OFRI), wind-oriented funnel trap (33, OFRI); ibidem, 8-vi-2021, Lindgren funnel (148, OFRI), modified Lindgren funnel (198, OFRI), synergy multitrap (277, OFRI), wind-oriented funnel trap (54, OFRI ; ibidem, 15-vi-2021, Lindgren funnel (69, OFRI), modified Lindgren funnel (27, OFRI), synergy multitrap (67, OFRI), wind-oriented funnel trap (15, OFRI); ibidem, 22-v-2021, Lindgren funnel (23, OFRI), modified Lindgren funnel (18, OFRI), synergy multitrap (59, OFRI),wind-oriented funnel trap (17, OFRI); ibidem, 29-vi-2021, Lindgren funnel (22, OFRI), modified Lindgren funnel (23, OFRI), synergy multitrap (29, OFRI), wind-oriented funnel trap (12, OFRI); ibidem, 6-vii-2021, Lindgren funnel (12, OFRI), modified Lindgren funnel (15, OFRI), synergy multitrap (30, OFRI), wind-oriented funnel trap (6, OFRI); ibidem, 13-vii-2021, Lindgren funnel (9, OFRI), modified Lindgren funnel (20, OFRI), synergy multitrap (29, OFRI), wind-oriented funnel trap (10, OFRI); ibidem, 20-vii-2021, Lindgren funnel (17, OFRI), modified Lindgren funnel (18, OFRI), synergy multitrap (28, OFRI), wind-oriented funnel trap (5, OFRI; ibidem, 27-vii-2021, Lindgren funnel (4, OFRI), modified Lindgren funnel (10, OFRI), synergy multitrap (10, OFRI), wind-oriented funnel trap (4, OFRI); ibidem, 3-viii-2021, Lindgren funnel (1, OFRI), modified Lindgren funnel (2, OFRI), synergy multitrap (2, OFRI), wind-oriented funnel trap (2, OFRI); ibidem, 10-viii-2021 (1, OFRI); ibidem, 17-viii-2021 (3, OFRI); ibidem, 24-viii-2021, Lindgren funnel (1, OFRI), synergy multitrap (3, OFRI); ibidem, 7-ix-2021 (1, OFRI). All samples were collected from a mixed hardwood forest, next to *Quercus* sp.

Distribution in Canada. SK, MB, **ON**, QC, NB, NS (Bousquet et al. 2013).

Subfamily Nitidulinae Latreille, 1802
Tribe Cychramini Gistel, 1848

Cychramus adustus (Erichson, 1843)

Notes. This is the first record of *Cychramus adustus* for Manitoba found in three localities in 2019. The McNamara (1991) checklist of Nitidulidae recorded *C. adustus* present in Ontario and Quebec. Majka et al. (2008) recorded *C. adustus* in New Brunswick, and Webster et al. (2022) recorded *C. adustus* in Prince Edward Island. There are five records for *C. adustus* on the IN website that are mostly collected in eastern Ontario and near Montreal, Quebec (Adustus 2023). The BN website references Bousquet et al. (2013) when describing the range of *C. adustus* as eastern North America.

New records. Manitoba: Birds Hill Provincial Park, MB, Roscoe Rd. 50.0436°N, 96.8719°W, 14-v-2019 (4, OFRI); ibidem, 22-v-2019 (9, OFRI); ibidem, 4-vi-2019 (4, OFRI); ibidem, 11-vi-2019 (4, OFRI); ibidem, 17-vi-2019 (3, OFRI); ibidem, 25-vi-2019 (5, OFRI); ibidem, 2-vii-2019 (3, OFRI); ibidem, 31-vii-2019 (1, OFRI); ibidem, 6-viii-2019 (2, OFRI); ibidem, 28-viii-2019 (2, OFRI); ibidem, 10-ix-2019 (2, OFRI). All samples were taken from wind-oriented funnel traps, in a mixed hardwood forest, next to *Quercus* sp.

Beaudry Provincial Park, MB, Roblin Blvd, 49.8576°N, 97.4638°W, 14-v-2019 (2, OFRI); ibidem, 29-v-2019 (14, OFRI); ibidem, 4-vi-2019 (3, OFRI); ibidem, 11-vi-2019 (14, OFRI); ibidem, 25-vi-2019 (1, OFRI); ibidem, 8-vii-2019 (1, OFRI); ibidem, 16-vii-2019 (1, OFRI); ibidem, 6-viii-2019 (2, OFRI); ibidem, 28-viii-2019 (1, OFRI); ibidem, 10-ix-2019 (2, OFRI). All samples were taken from wind-oriented funnel traps, in a riparian hardwood forest, next to *Quercus* sp.

Winnipeg, MB, Winnipeg James Armstrong Richardson International Airport off Wihuri Rd., 49.8996°N, 97.2538°W, 22-v-2019 (1, OFRI); ibidem, 4-vi-2019 (4, OFRI); ibidem, 11-v-2019 (3, OFRI); ibidem, 17-vi-2019 (3, OFRI); ibidem, 25-vi-2019 (2, OFRI); ibidem, 8-vii-2019 (1, OFRI); ibidem, 31-vii-2019 (1, OFRI); ibidem, 14-viii-2019 (1, OFRI). All samples were taken from wind-oriented funnel traps, in a mixed hardwood forest, next to *Quercus* sp.

Distribution in Canada. MB, ON, QC, NB, PE (Bousquet et al. 2013; Webster et al. 2022).

Tribe Nitidulini Latreille, 1802

Stelidota coenosa Erichson, 1843

Notes. This is the first record of *Stelidota coenosa* for Ontario. It was collected at one locality in the province in 2021. The species was first reported from boletus mushrooms in a *Pinus banksiana* forest in Northumberland Co., New Brunswick by Webster et al. (2016). It has also been recorded from several states along the eastern United States from New York to Florida (Parsons 1943). *Stelidota coenosa* was collected as far west as Wisconsin, south to Arizona and can be found in subtropical and tropical areas of Central and South America (Galford et al. 1991). The IN website does not have any record for *S. coenosa* in Canada while the website, BG references the report from New Brunswick (Webster et al. 2016).

New record. Ontario: Guelph, ON, The Arboretum, University of Guelph, 43.5436°N, 80.2205°W, 5-viii-2021, wind-oriented funnel trap, in *Quercus rubra* plantation (1, OFRI).

Distribution in Canada. ON, NB (Bousquet et al. 2013; Webster et al. 2016).

Subfamily Cryptarchinae C.G. Thomson, 1859
Tribe Cryptarchini C.G. Thomson, 1859

Glischrochilus (*Librodor*) *obtusus* (Say, 1835)

Notes. This 2018 collection is the first record of *Glischrochilus* (*Librodor*) *obtusus* in Canada and a new provincial record for Ontario. This species can be found throughout the eastern United States including the northern border states with Canada; Maine, New York, Michigan, and Wisconsin (Downie and Arnett 1996; Price and Young 2006). IN recorded locality information by Nenadov (2021) in Comber, Ontario on July 6, 2021.

New record. Ontario: Peterborough, ON, Northumberland County Forest off Dunbar Rd., 44.0636°N, 78.0331°W, 19-vi-2018, wind-oriented funnel trap, in a mixed hardwood forest, next to *Quercus* sp. (2, OFRI).

Distribution in Canada. ON (New Canadian record).

Discussion

In 2013, Bousquet et al. (2013) reported 99 species of Nitidulidae from Canada. This included 45 species from Manitoba and 63 from Ontario. In addition, three Palaearctic species were recently recorded in Canada, the first one from New Brunswick (Webster et al. 2016), the second one from Prince Edward Island (Webster et al. 2022), and the third one from Ontario (Pentinsaari et al. 2019). Brunke et al. (2019) suggested that the total number of Nitidulidae species in Canada is even higher. They used an analysis of BOLD barcode index numbers to estimate that as many as 12 Nitidulidae species from Canada have not been described or reported. Here, we report six new species for Ontario, *Carpophilus* (*Megacarpolus*) *sayi*, *C.* (*Ecnomorphus*) *antiquus*, *C.* (*E.*) *corticinus*, *C.* (*Myothorax*) *nepos*, *Glischrochilus* (*Librodor*) *obtusus*, and *Stelidota coenosa* bringing the total to 70, and three species for Manitoba, *Carpophilus* (*Megacarpolus*) *lugubris*, *C.* (*M.*) *nepos*, and *Cychramus adustus*, bringing the total to 48. Three of these reports, *Carpophilus* (*Ecnomorphus*) *corticinus*, *C.* (*Myothorax*) *nepos*, and *Glischrochilus obstusus* are new reports for Canada bringing the total to 104 or 105 depending on the inclusion of Cybocephalinae as a subfamily in the family of Nitidulidae (Kirejtshuk 2008; Kirejtshuk and Mantič 2015) or consideration of this group as a separate family (Cline et al. 2014; Smith 2022).

The new records fill gaps in our knowledge of these species' distributions. Of the new species found in Ontario, *Carpophilus* (*Megacarpolus*) *sayi* was the most frequently reported species with records at 13 of 14 survey localities. *Carpophilus* (*Myothorax*) *nepos* also appears widespread, being reported at numerous localities throughout southern Ontario (i.e., ecoregions 6 and 7) and in Manitoba.

Four new records occurred only in southern Ontario (i.e., ecoregions 6E, 7E), indicating that more surveys in this region could increase our knowledge of Nitidulidae diversity in Canada. One reason may be that part of this region contains the northernmost extent of the deciduous forest type, sometimes called the Carolinian Forest Region or the Deciduous Forest Region (Crins et al. 2009). The diversity of flora and fauna is greater here than in other parts of Canada. This region is warmer and has a longer growing season than the rest of Ontario because of its proximity to three large lakes and its southern position (Crins et al. 2009). In addition, further surveying in Manitoba is needed to clarify if *Carpophilus* (*Megacarpolus*) *lugubris*, *C.* (*Myothorax*) *nepos*, and *Cychramus adustus* occur outside the greater Winnipeg area. No new records were made for New Brunswick, suggesting that recent efforts to more fully describe the beetle diversity of this province have been reasonably complete (Majka et al. 2008; Webster et al. 2016).

The new species recorded in this study have been collected from fungi or sap flows and some are known to transmit fungal spores and fragments of mycelia (Price 2003). New detections of mycetophagous beetles in Canada are important, further elucidating how fungi and fungal diseases are spread across Canada's treed landscapes. Especially species of *Carpophilus*, *Glischrochilus*, *Cychramus*, *Stelidota*, and others that have been found at oak wilt mats or other fungal structures (Price 2003).

Acknowledgements

We would like to acknowledge the hard work and dedication of Sylvia Greifenhagen, Ontario Ministry of Natural Resources, and Forestry (MNRF) who was instrumental in organizing, collecting, and beetle identification. Thank you to Jon Sweeney of Natural Resources Canada for overseeing New Brunswick sampling. We would like to thank the Ontario MNRF forest health technicians, Ariel Ilic and Rebecca Lidster for assistance with beetle collections. Thank you to other collectors, Cory Hughes of Natural Resources Canada, John Enright and Brandon Williamson of Upper Thames Conservation Authority, Todd Farrell of Northumberland County Forest, Robert Davies and Dan Lebdyk of Essex Region Conservation Authority, Jason Pollard of City of Ottawa, Jeremy St. Onge and Stephen Romaniuk of Canadore College, and Monique Wester of MNRF. Taxonomic guidance for Manitoba and Ontario collections was assisted by Kevin Barber from Natural Resources Canada, Great Lakes Forestry Centre and Gareth Powell from Florida State Collection of Arthropods. We would also like to thank Christine St. Jules, Brittany Cote, and Corey Schmitt of Ontario MNRF for sorting and identification of beetles. Funding was provided by the Canadian Food Inspection Agency and Manitoba Natural Resources and Northern Development through SERG-I and from the International Society of Arboriculture-Ontario.

References

Adustus (2023) Observations of *Cychramus adustus* in Canada. https://inaturalist.ca/observations?place_id=6712&subview=map&taxon_id=174084 [Accessed February 2023]

Bousquet Y, Bouchard P, Davies AE, Sikes DS (2013) Checklist of beetles (Coleoptera) of Canada and Alaska (2nd edn.). Pensoft, Sofia, 402 pp. https://doi.org/10.3897/zookeys.360.4742

Bruhn JN, Pickens JB, Stanfield DG (1991) Probit analysis of oak wilt transmission through root grafts in red oak stands. Journal of Forest Science 37: 28–44.

Brunke AJ, Bouchard P, Douglas HB, Pentinsaari M (2019) Coleoptera of Canada. In: Langor DW, Sheffield CS (Eds) The Biota of Canada – A Biodiversity Assessment. Part 1: The Terrestrial Arthropods. ZooKeys 819: 361–376. https://doi.org/10.3897/zookeys.819.24724

Cline AR, Smith TR, Miller K, Moulton M, Whiting M, Audisio P (2014) Molecular phylogeny of Nitidulidae: assessment of subfamilial and tribal classification and formalization

of the family Cybocephalidae (Coleoptera: Cucujoidea). Systematic Entomology 39(4): 758–772. https://doi.org/10.1111/syen.12084

Crins WJ, Gray PA, Uhlig PWC, Wester MC (2009) The ecosystems of Ontario, Part 1: Ecozones and Ecoregions. Ontario Ministry of Natural Resources, Inventory, Monitoring and Assessment, Peterborough ON. SIB TER IMA TR- 01, 71 pp.

DiGirolomo MF, Munck IA, Dodds KJ, Cancelliere J (2020) Sap beetles (Coleoptera: Nitidulidae) in oak forests of two northeastern states: A comparison of trapping methods and monitoring for phoretic fungi. Journal of Economic Entomology 113(6): 2758–2771. https://doi.org/10.1093/jee/toaa195

Dowd PF, Bartelt RJ, Wicklow DT (1992) Novel insect trap useful in capturing sap beetles (Coleoptera: Nitidulidae) and other flying insects. Journal of Economic Entomology 85(3): 772–778. https://doi.org/10.1093/jee/85.3.772

Downie NM, Arnett RH (1996) The Beetles of Northeastern North America: Polyphaga, Superfamily Bostrichidae, Through Curculionidae (Vol. 2). The Sandhill Crane Press, Florida, 880 pp. https://doi.org/10.1201/9781420041231

Farrar JL (1995) Trees in Canada. Fitzhenry & Whiteside Limited, Markham, ON and Natural Resources Canada, Canadian Forest Service, Ottawa, 502 pp.

Galford JR, Williams RN, Beacom M (1991) Notes on the Biology and Host of *Stelidota ferruginea* (Coleoptera: Nitidulidae). Res. Pap. NE-654. Radnor, PA: US Department of Agriculture, Forest Service, Northeastern Forest Experiment Station, Radnor, 4 pp. https://doi.org/10.2737/NE-RP-654

Habeck DH (2002) Nitidulidae. In: Arnett RH, Thomas MC, Skelley PE, Frank JH (Eds) American Beetles (Vol. 2) Polyphaga: Scarabaeoidae through Curculionoidae. CRC Press, Florida, 311–315. https://doi.org/10.1201/9781420041231

Jagemann SM, Juzwik J, Tobin PC, Raffa KF (2018) Seasonal and regional distributions, degree-day models, and phoresy rates of the major sap beetle (Coleoptera: Nitidulidae) vectors of the oak wilt fungus, *Bretziella fagacearum*, in Wisconsin. Environmental Entomology 47(5): 1152–1164. https://doi.org/10.1093/ee/nvy080

Jakubowski R (2021) *Carpophilus* (*Megacarpolus*) *sayi*. https://inaturalist.ca/observations/85864145 [Accessed February 2023]

Juzwik J, Harrington TC, MacDonald WL, Appel DN (2008) The origin of *Ceratocystis fagacearum*, the oak wilt fungus. Annual Review of Phytopathology 46(1): 13–26. https://doi.org/10.1146/annurev.phyto.45.062806.094406

Kirejtshuk AG (1996) Some results of study on the Nitidulidae from Namibia and adjacent territories. Part 1 (Coleoptera, Cucujoidea, Nitidulidae). Mitteilungen aus dem Zoologischen Museum in Berlin 72(1): 21–52. https://doi.org/10.1002/mmnz.19960720106

Kirejtshuk AG (2008) A current generic classification of sap beetles (Coleoptera, Nitidulidae). Zoosystematica Rossica 17(1): 107–122. https://doi.org/10.31610/zsr/2008.17.1.107

Kirejtshuk AG (2018) New Taxa of Carpophilinae (Coleoptera, Nitidulidae) from the Himalaya and Northern Indochina. Part 1. Entomological Review 98(9): 1186–1216. https://doi.org/10.1134/S0013873818090063

Kirejtshuk AG, Mantič M (2015) On systematics of the subfamily Cybocephalinae (Coleoptera: Nitidulidae) with description of new species and generic taxa. Trudy Zoologicheskogo Instituta RAN 319(2): 196–214. https://doi.org/10.31610/trudyzin/2015.319.2.196

Lindgren BS (1983) A multiple funnel trap for scolytid beetles (Coleoptera). The Canadian Entomologist 115(3): 299–302. https://doi.org/10.4039/Ent115299-3

Lugubris (2023) Observations of *Carpophilus* (*Megacarpolus*) *lugubris* in Canada. https://inaturalist.ca/observations?locale=en-US&place_id=6712&preferred_place_id=6712&subview=map&taxon_id=1281051 [Accessed February 2023]

Majka CG, Webster R, Cline AR (2008) New records of Nitidulidae and Kateretidae (Coleoptera) from New Brunswick, Canada. ZooKeys 2: 337–356. https://doi.org/10.3897/zookeys.2.23

Marske KA, Ivie MA (2003) Beetle fauna of the United States and Canada. Coleopterists Bulletin 57(4): 495–503. https://doi.org/10.1649/663

McNamara J (1991) Family Nitidulidae: sap beetles. In: Bousquet Y (Ed.) Checklist of Beetles in Canada and Alaska. Agriculture Canada Research Branch Publication 1861/E: 214–217.

Miller DR, Crowe CM, Barnes BF, Gandhi KJ, Duerr DA (2013) Attaching lures to multiple-funnel traps targeting saproxylic beetles (Coleoptera) in pine stands: Inside or outside funnels? Journal of Economic Entomology 106(1): 206–214. https://doi.org/10.1603/EC12254

Morris OR (2020) Seasonal activity and phoresy rates of sap beetles (Coleoptera: Nitidulidae) in oak wilt infection centers, volatile organic compounds related to the oak wilt cycle, and long-term evaluation of red oak provenances. Masters Thesis, Michigan State University, East Lansing, MI, 97 pp.

Nenadov M (2021) Observation of *Glischrochilus* (*Libridor*) *obtusus*. https://inaturalist.ca/observations/85960611 [accessed July 2022]

Parsons CT (1943) A review of Nearctic Nitidulidae (Coleoptera). Bulletin of the Museum of Comparative Zoology at Harvard College 92: 121–278.

Peck S, Thomas M (1998) A distributional checklist of the beetles (Coleoptera) of Florida and neighboring land areas. Florida Department of Agriculture and Consumer Services, Gainsville 16: 1–180.

Pentinsaari M, Anderson R, Borowiec L, Bouchard P, Brunke A, Douglas H, Smith A, Hebert P (2019) DNA barcodes reveal 63 overlooked species of Canadian beetles (Insecta, Coleoptera). ZooKeys 894: 53–150. https://doi.org/10.3897/zookeys.894.37862

Price MB (2003) A comprehensive survey of the sap and short-winged flower beetles of Wisconsin (Coleoptera: Nitidulidae, Kateretidae). M.Sc. thesis. University of Wisconsin-Madison, Madison, Wisconsin, 407 pp.

Price MB, Young DK (2006) An annotated checklist of Wisconsin sap and short-winged flower beetles (Coleoptera: Nitidulidae, Kateretidae). Insecta Mundi 1: 69–84.

Province of New Brunswick (2007) Our Landscape Heritage: The story of ecological land classification in New Brunswick (2nd ed.). Province of New Brunswick, Department of Natural Resources, Fredericton, New Brunswick, 359 pp.

Smith TR (2022) Review of the Cybocephalidae (Coleoptera) of North America and the West Indies with descriptions of two new species of *Cybocephalus* Erichson. Insecta Mundi 0950: 1–35.

Smith RE, Veldhuis H, Mills GF, Eilers RG, Fraser WR, Lelyk GW (1998) Terrestrial Ecozones, Ecoregions, and Ecodistricts, An ecological stratification of Manitoba's Landscape. Agriculture and Agri-Food Canada, Land Resource Unit, Brandon Research Centre, Research Branch, Winnipeg, MB. Technical Bulletin 98-9E, 319 pp.

USDA-FS [United States Department of Agriculture Forest Service] (2019) Oak wilt – *Ceratocystis fagacearum* (Bretz) J. Hunt. Alien Forest Pest Explorer – species map. United States

Department of Agriculture Forest Service Northern Research Station and Forest Health Protection. https://www.fs.fed.us/nrs/tools/afpe/maps/pdf/OW.pdf [Accessed February 2021]

Webster RP, Smetana A, Sweeney JD, Demerchant I (2012) New Staphylinidae (Coleoptera) records with new collection data from New Brunswick and an addition to the fauna of Quebec: Staphylininae. ZooKeys 186: 293–348. https://doi.org/10.3897/zookeys.186.2469

Webster RP, Webster VL, Alderson CA, Hughes CC, Sweeney JD (2016) Further contributions to the Coleoptera fauna of New Brunswick with an addition to the fauna of Nova Scotia, Canada. ZooKeys 573: 265–335. https://doi.org/10.3897/zookeys.573.7327

Webster RP, Hughes CC, Sweeney JD (2022) The Coleoptera of the Province of Prince Edward Island, Canada: 295 new records from Lindgren funnel traps and a checklist to species, Canada. ZooKeys 1107: 1–158. https://doi.org/10.3897/zookeys.1107.82976

ZooKeys 1156: 53–69 (2023)
doi: 10.3897/zookeys.1156.86786
https://zookeys.pensoft.net

RESEARCH ARTICLE

A peer-reviewed open-access journal
ZooKeys
Launched to accelerate biodiversity research

New species and records of the genus *Antocha* Osten Sacken (Diptera, Limoniidae) from Tibet, China with a key to species in Qinghai-Tibet region

Hanhuiying Lv[1,2], Juan Sun[1], Ning Wang[2], Ding Yang[3], Xiao Zhang[1]

1 *Shandong Engineering Research Center for Environment-Friendly Agricultural Pest Management, College of Plant Health and Medicine/College of Grassland Science, Qingdao Agricultural University, Qingdao 266109, China* **2** *Key Laboratory of Biohazard Monitoring and Green Prevention and Control in Artificial Grassland, Ministry of Agriculture and Rural Affairs, Institute of Grassland Research, Chinese Academy of Agricultural Sciences, Hohhot 010010, China* **3** *College of Plant Protection, China Agricultural University, Beijing 100193, China*

Corresponding authors: Ning Wang (wangningis@163.com); Xiao Zhang (xzhang_cn@163.com)

Academic editor: Pavel Starkevic | Received 20 May 2022 | Accepted 17 March 2023 | Published 24 March 2023

https://zoobank.org/0EA9E43B-A5BF-4232-A297-B341861E835D

Citation: Lv H, Sun J, Wang N, Yang D, Zhang X (2023) New species and records of the genus *Antocha* Osten Sacken (Diptera, Limoniidae) from Tibet, China with a key to species in Qinghai-Tibet region. ZooKeys 1156: 53–69. https://doi.org/10.3897/zookeys.1156.86786

Abstract

Thirty-four known species and subspecies of the genus *Antocha* Osten Sacken, 1860 have been recorded from China, of which four occur in Tibet. Herein, two new *Antocha* species, *A.* (*Antocha*) *curvativa* **sp. nov.** and *A.* (*A.*) *tibetana* **sp. nov.**, are described and illustrated from Tibet. The new species are distinguished from congeners mainly by their male genitalia. *Antocha* (*A.*) *spiralis* Alexander, 1932 and *A.* (*A.*) *setigera* Alexander, 1933, which are newly recorded in Tibet, are redescribed and illustrated. A key to *Antocha* species in the Qinghai-Tibet region of China is also presented.

Keywords

Chinese fauna, crane flies, Limoniinae, Qinghai-Tibet Plateau, taxonomy

Introduction

The genus *Antocha* Osten Sacken, 1860 is a medium-sized genus of 161 described species and subspecies in the family Limoniidae (Oosterbroek 2023). It is known from the Oriental (83 species and subspecies), Palaearctic (56 species and subspecies), Afrotropic (21 species), Nearctic (seven species), Australasian (three species), and Neotropic (one species) regions (Oosterbroek 2023). A conspicuous feature of the genus is that the anal angle of the wing is nearly right-angled, and detailed features for the recognition of the genus were given by Osten Sacken (1860), Alexander (1968), and Markevičiūtė et al. (2019, 2021). In the past three decades, many taxonomic studies have been carried out on Asian *Antocha*, mainly focusing on the species in Japan (Torii 1992a, 1992b, 1992c, 1996), China (Podenas and Young 2015; Markevičiūtė et al. 2019, 2021), South Korea (Podenas and Byun 2014), North Korea (Podenas 2015), and Indonesia (Young 1994).

Tibet is located in the Qinghai-Tibet region of China, which also includes all of Qinghai, western Sichuan, and small parts of Gansu, Xinjiang, and Yunnan. The main body of the region is the Qinghai-Tibet Plateau, which is known as the "roof of the world" because of its high terrain and extensive grasslands. The Qinghai-Tibet region is also the source of many rivers in China.

At present, 34 *Antocha* species and subspecies are recorded from China, of which 22 are known in the Qinghai-Tibet region, while only four are distributed in Tibet (Oosterbroek 2023). In this study, specimens of *Antocha* from Tibet have been examined, and four species are added to the fauna of Tibet (Fig. 1), of which *A.* (*A.*) *curvativa* sp. nov. and *A.* (*A.*) *tibetana* sp. nov. are described and illustrated as new to science, and *A.* (*A.*) *spiralis* Alexander, 1932 and *A.* (*A.*) *setigera* Alexander, 1933 are newly recorded from Tibet. More comprehensive redescriptions and illustrations for the two known species, as well as a key to the *Antocha* crane flies in Qinghai-Tibet region, are also presented.

Materials and methods

All specimens for this study were collected from Tibet, China by various entomologists in 2014–2018. Type specimens are deposited in Entomological Museum of China Agricultural University, Beijing, China (**CAU**). The holotype of *A.* (*A.*) *setigera*, deposited in the National Museum of Natural History, Smithsonian Institution, Washington, DC, USA (**USNM**), was also examined. Genitalic preparations of males were made by macerating the apical portion of the abdomen in cold 10% hydroxide (NaOH) for 12–15 hours. Observations and illustrations were made using a ZEISS Stemi 2000-C stereomicroscope. Photographs were taken with a Canon EOS 90D digital camera through a macro lens. Details of coloration were examined in specimens immersed in 75% ethanol (C_2H_5OH).

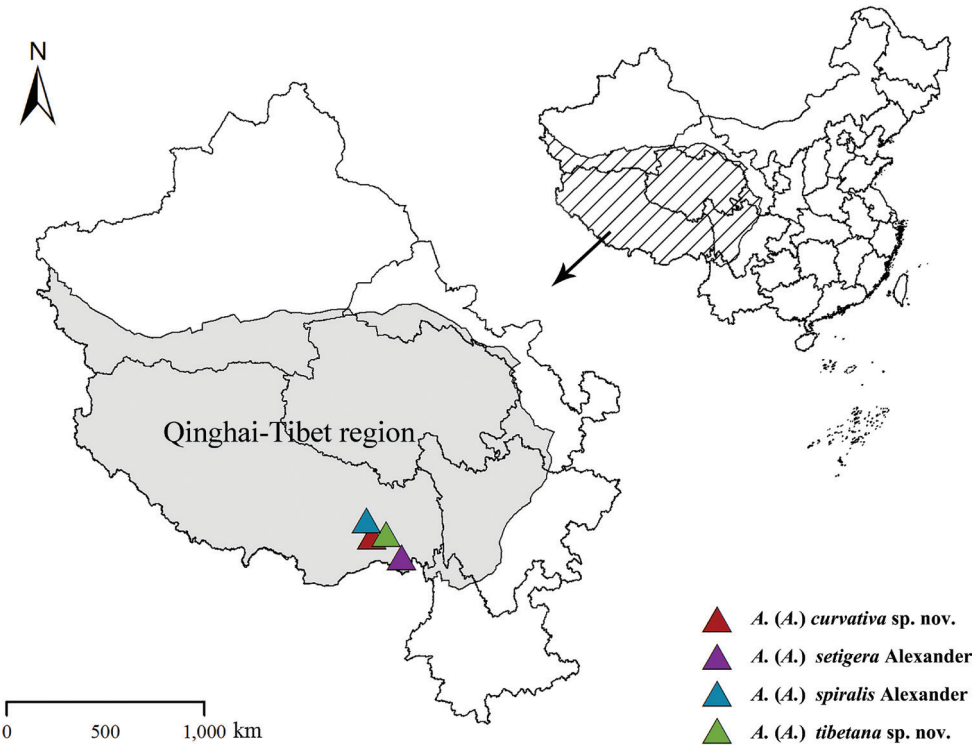

Figure 1. Collecting sites of *Antocha* species in China.

The morphological terminology mainly follows Cumming and Wood (2017) and de Jong for wing venation (2017). The term "inner branch of paramere" is adopted from Kato and Tachi (2019). The general distribution of species is given according to Oosterbroek (2023).

The following abbreviations in figures are used: aed = aedeagus, app = apical part of paramere, bp = base of paramere, cerc = cercus, goncx = gonocoxite, hyp vlv = hypogynial valve, i gonst = inner gonostylus, ib = interbase, ibp = inner branch of paramere, o gonst = outer gonostylus, pm = paramere, tg 9 = tergite 9, tg 10 = tergite 10.

Checklist of *Antocha* crane flies in Qinghai-Tibet region of China

New province records in bold

Antocha (*Antocha*) *bella* Markevičiūtė & Podenas, 2019 (Sichuan)
Antocha (*Antocha*) *bidens* Alexander, 1932 (Sichuan)
Antocha (*Antocha*) *bifida* Alexander, 1924 (Sichuan, Guangdong, Taiwan; Russia; Kazakhstan; Mongolia; North Korea; South Korea; Japan; Philippines)

Antocha (*Antocha*) *constricta* Alexander, 1932 (Sichuan)
Antocha (*Antocha*) *curvativa* Lv & Zhang sp. nov. (Tibet)
Antocha (*Antocha*) *emarginata* Alexander, 1938 (Sichuan)
Antocha (*Antocha*) *flavidibasis* Alexander, 1938(Sichuan)
Antocha (*Antocha*) *fortidens* Alexander, 1933 (Sichuan, Tibet)
Antocha (*Antocha*) *indica* Brunetti, 1912 (Sichuan, Zhejiang; India; Malaysia)
Antocha (*Antocha*) *lacteibasis* Alexander, 1935 (Sichuan)
Antocha (*Antocha*) *minuticornis* Alexander, 1931 (Sichuan)
Antocha (*Antocha*) *multidentata* Alexander, 1932 (Sichuan)
Antocha (*Antocha*) *nebulipennis immaculata* Alexander, 1938 (Sichuan; Myanmar)
Antocha (*Antocha*) *nebulipennis nebulipennis* Alexander, 1931 (Gansu, Sichuan, Tibet; India; Nepal; Tajikistan; Afghanistan)
Antocha (*Antocha*) *nigribasis* Alexander, 1932 (Sichuan)
Antocha (*Antocha*) *pallidella* Alexander, 1933 (Sichuan)
Antocha (*Antocha*) *picturata* Alexander, 1936 (Sichuan)
Antocha (*Antocha*) *pterographa* Alexander, 1953 (Tibet)
Antocha (*Antocha*) *pulchra* Markevičiūtė & Podenas, 2021 (Sichuan)
Antocha (*Antocha*) *quadrifurca* Alexander, 1971 (Sichuan; India)
Antocha (*Antocha*) *setigera* Alexander, 1933 (Sichuan, **Tibet**)
Antocha (*Antocha*) *spiralis* Alexander, 1932 (Sichuan, **Tibet**; India)
Antocha (*Antocha*) *tibetana* Lv & Zhang sp. nov. (Tibet)
Antocha (*Antocha*) *yatungensis* Alexander, 1963 (Tibet)

Taxonomy

Key to *Antocha* species from Qinghai-Tibet region of China

1 Wing with distinct brown or dark gray stigma **2**
– Wing without stigma or with indistinct stigma (Figs 2d, 4d, 6d, 8d) **9**
2 Crossvein m-cu long before fork of M, distance about its own length **3**
– Crossvein m-cu at or short before fork of M, distance less than half of own length (Figs 2d, 4d, 6d, 8d) **4**
3 Prescutum and presutural scutum uniformly light yellow. Crossvein m-cu more than one and half times its own length, before fork of M. Posterior margin of tergite 9 with median emarginate (Alexander 1932; Markevičiūtė et al. 2019, 2021) ..... ***A.* (*A.*) *nigribasis***
– Prescutum and presutural scutum grey with three brown stripes. Crossvein m-cu a little less than its own length, before fork of M. Posterior margin of tergite 9 without median emarginate (Alexander 1953) ..... ***A.* (*A.*) *pterographa***
4 Cell m_1 longer than cell dm (Figs 4d, 6d, 8d) **5**
– Cell m_1 almost as long as or shorter than cell dm (Fig. 2d) **6**

5 Prescutum and presutural scutum grey, with a brown stripe. Vein Sc ending nearly fork of Rs (Alexander 1936) ..... ***A.* (*A.*) *picturata***

– Prescutum and presutural scutum uniformly yellowish gray, without stripes. Vein Sc ending a greater distance before fork of Rs (Alexander 1931; Markevičiūtė et al. 2019, 2021) ..... ***A.* (*A.*) *nebulipennis nebulipennis***

6 Apex of outer gonostylus not bifid **7**

– Apex of outer gonostylus bifid **8**

7 Inner branch of paramere with outer tooth shorter than inner tooth (Alexander 1932; Markevičiūtė et al. 2019) ..... ***A.* (*A.*) *multidentata***

– Inner branch of paramere with outer tooth longer than inner tooth (Alexander 1971; Markevičiūtė et al. 2021) ..... ***A.* (*A.*) *quadrifurca***

8 Posterior margin of tergite 9 with two small lobes far away from each other, middle flat (Alexander 1932; Markevičiūtė et al. 2019, 2021) ***A.* (*A.*) *bidens***

– Posterior margin of tergite 9 with two close lobes, middle concave (Alexander 1933a; Markevičiūtė et al. 2019, 2021) ..... ***A.* (*A.*) *fortidens***

9 Crossvein m-cu long before fork of M, distance about its own length **10**

– Crossvein m-cu at or short before fork of M, distance less than half of its own length (Figs 2d, 4d, 6d, 8d) **11**

10 Basal section of R_5 slightly longer than r-m. Posterior margin of tergite 9 with two small lobes, middle flat (Alexander 1933b; Markevičiūtė et al. 2021) ..... ***A.* (*A.*) *pallidella***

– Basal section of R_5 nearly twice as long as r-m. Posterior margin of tergite 9 with two big lobes, middle concave (Alexander 1963) ..... ***A.* (*A.*) *yatungensis***

11 Vein Sc ending before fork of Rs (Figs 2d, 6d, 8d) **12**

– Vein Sc ending at or beyond fork of Rs (Fig. 4d) **19**

12 Prescutum and presutural scutum without stripe (Fig. 6c) **13**

– Prescutum and presutural scutum with stripe(s) (Figs 2c, 4c, 8c) **14**

13 Apical part of paramere with three small branches (Alexander 1932; Markevičiūtė et al. 2019, 2021) ..... ***A.* (*A.*) *constricta***

– Apical part of paramere slender and twisted into spiral, without branches (Figs 6e, 7) ..... ***A.* (*A.*) *spiralis***

14 Antennae with scape yellow, remaining segments black **15**

– Antennae black, dark brown, or brown throughout (Figs 2b, 8b) **16**

15 Basal section of M_3 as long as m-m. Posterior margin of tergite 9 flat. Inner gonostylus narrowed to obtuse tip (Brunetti 1912; Markevičiūtė et al. 2019, 2021) ..... ***A.* (*A.*) *indica***

– Basal section of M_3 twice as long as m-m. Posterior margin of tergite 9 with two rounded lobes. Inner gonostylus with tip dilated (Alexander 1938a; Markevičiūtė et al. 2019, 2021) ..... ***A.* (*A.*) *nebulipennis immaculata***

16 Basal section of M_3 shorter than one and half times length of m-m (Alexander 1938a) ..... ***A.* (*A.*) *flavidibasis***

– Basal section of M_3 as long as or longer than twice length of m-m (Figs 2d, 8d) **17**

17 Tip of inner branch of paramere bifid (Figs 8e, 9).....***A.* (*A.*) *tibetana* sp. nov.**
– Tip of inner branch of paramere not bifid (Figs 2e, 3, 4e, 5).....**18**
18 Basal section of M_3 four times as long as m-m (Fig. 2d). Outer gonostylus with tip inflated and blunt (Figs 2e, 3).....***A.* (*A.*) *curvativa* sp. nov.**
– Basal section of M_3 twice as long as m-m. Outer gonostylus narrowed to acute tip (Alexander 1935; Markevičiūtė et al. 2019, 2021).....***A.* (*A.*) *lacteibasis***
19 Tip of outer gonostylus bifid (Markevičiūtė et al. 2021: Figs 10, 15) **20**
– Tip of outer gonostylus not bifid **21**
20 Posterior margin of tergite 9 with two teeth (Alexander 1924; Markevičiūtė et al. 2019, 2021) .....***A.* (*A.*) *bifida***
– Posterior margin of tergite 9 without teeth (Markevičiūtė et al. 2021) ....***A.* (*A.*) *pulchra***
21 Inner branch of paramere spiral (Markevičiūtė et al. 2019, 2021)....***A.* (*A.*) *bella***
– Inner branch of paramere straight (Figs 4e, 5).....**22**
22 Posterior margin of tergite 9 with a deep, U-shaped, median concavity (Alexander 1938b; Markevičiūtė et al 2019, 2021) .....***A.* (*A.*) *emarginata***
– Posterior margin of tergite 9 with a gentle median concavity (Fig. 5).....**23**
23 Tip of aedeagus not bifid (Alexander 1931; Markevičiūtė et al. 2019, 2021). .....***A.* (*A.*) *minuticornis***
– Tip of aedeagus bifid (Figs 4e, 5) .....***A.* (*A.*) *setigera***

***Antocha* (*Antocha*) *curvativa* Lv & Zhang, sp. nov.**
https://zoobank.org/CE9CC4CC-B440-40E5-979D-35F2A4843FEB
Figs 2, 3

Type material. ***Holotype*:** China • ♂; Tibet Autonomous Region, Medog County, Bari village; 29°20'13"N, 95°21'54"E; 1680 m a.s.l.; 29 July 2014; Yan Li leg; CAU. ***Paratypes*:** China • 2 ♂♂ 2 ♀♀; same data as holotype; CAU.

Diagnosis. *Antocha* (*A.*) *curvativa* sp. nov. can be recognized by thorax with four more or less confluent stripes, wing having no stigma, basal section of M_3 which is about four times as long as m-m, posterior margin of tergite 9 having shallow median emargination and specific, stout outer gonostylus with tip distinctly flattened and nearly funnel-shaped. Aedeagal complex with interbase elongated, distally oval; paramere apically slender and curved ventrally; inner branch of paramere elongated, tip rounded.

Description. Male. Body length 4.8–5.5 mm, wing length 4.3–4.8 mm, antenna length 0.9–1.1 mm.

Head (Fig. 2b). Dark brown, with brown setae. Antenna dark brown. Scape cylindrical; pedicel oval; flagellomeres oval, apically tapering and shortened. Setae on antenna brown. Rostrum light brown; palpus brown to dark brown; setae on rostrum and palpus brown.

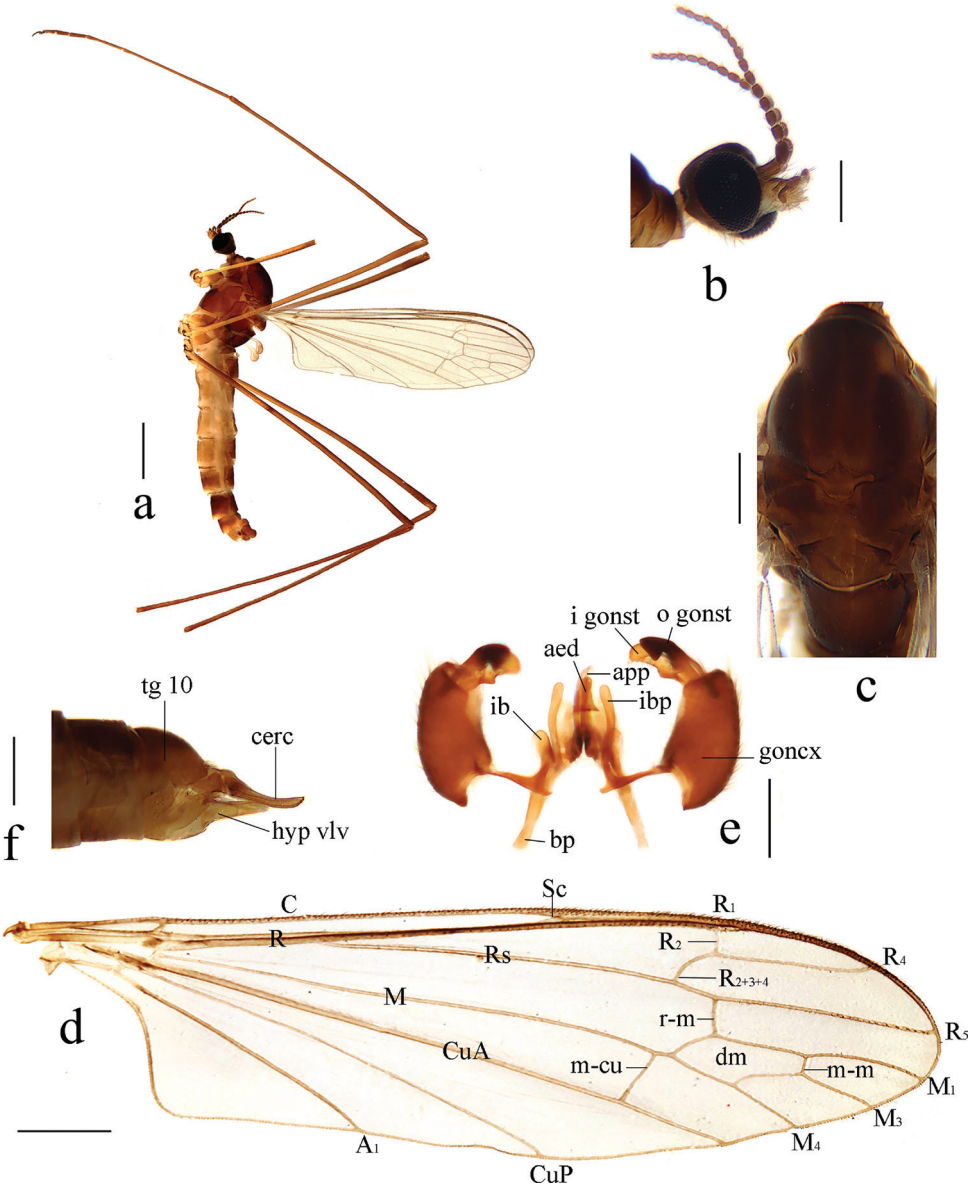

Figure 2. *Antocha* (*Antocha*) *curvativa* sp. nov. **a** habitus of male, lateral view **b** male head, lateral view **c** male thorax, dorsal view **d** male wing **e** aedeagal complex with gonocoxite and gonostyli, dorsal view **f** female ovipositor, lateral view. Scale bars: 1.0 mm (**a**); 0.3 mm (**b, c**); 0.5 mm (**d**); 0.2 mm (**e, f**).

Thorax (Fig. 2c). Pronotum dark brown. Prescutum and presutural scutum brown, with four more or less confluent dark brown stripes. Postsutural scutum brown; scutal lobes each with a darker brown spot. Scutellum brown, with side edges dark brown.

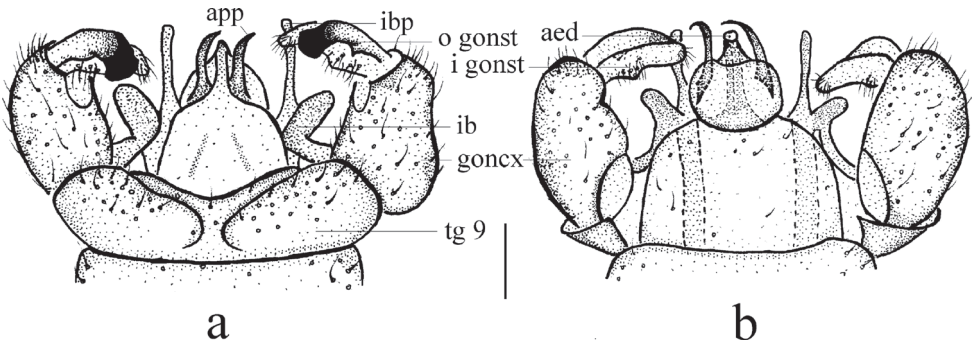

Figure 3. *Antocha* (*Antocha*) *curvativa* sp. nov. **a** male hypopygium, dorsal view **b** male hypopygium, ventral view. Scale bar: 0.1 mm.

Mediotergite dark brown. Pleuron brown (Fig. 2a). Legs with light brown coxae; trochanters light yellow with side edges brown; femora yellowish, becoming brown towards apex; tibiae and tarsal segments brown. Setae on legs brown. Wing light brown, without stigma; anal angle nearly right-angled (Fig. 2d). Veins light brown. Venation: Sc ending before fork of Rs, at about 2/3 of Rs; basal section of R_5 about as long as r-m; m-cu shortly before fork of M, distance approximately 1/4 its own length; basal section of M_3 about four times as long as m-m; cell m_1 about as long as cell dm. Halter with stem pale.

Abdomen. Tergites 1–6 brown, tergites 7 and 8 dark brown. Sternites 1–6 light brown, sternites 7 and 8 dark brown.

Hypopygium (Figs 2e, 3). Brown. Posterior margin of tergite 9 with broad and shallow emargination (Fig. 3a). Gonocoxite nearly cylindrical, with long yellow setae (Figs 2e, 3). Outer gonostylus stout, apical half sclerotized, tip distinctly curved, flattened, nearly funnel-shaped. Inner gonostylus thick and fleshy. Interbase nearly V-shaped, distal part elongate and oval (Figs 2e, 3). Paramere with base rod-shaped, apical part slender, curved ventrally, and with tip sharp. Inner branch of paramere in the shape of elongated lobe with tip rounded (Figs 2e, 3). Aedeagus rod-shaped, curved ventrally (Figs 2e, 3).

Female. Body length 5.0–5.5 mm, wing length 4.5–5.0 mm. Generally similar to male by body coloration.

Ovipositor (Fig. 2f). Tergite 10 dark brown, caudal part paler. Cercus brown with base darker, tip raised and tapering. Hypogynial valve light brown, reaching approximately 3/5 of cercus.

Etymology. The specific name refers to the curved apical part of paramere.

Distribution. China (Tibet).

Remarks. The new species is similar to *A.* (*A.*) *lacteibasis* from China in having similar apical part of paramere and tip of inner branch of paramere being not bifid, but it can be easily distinguished by the basal section of vein M_3 being about four times as long as m-m (Fig. 2d) and the stout outer gonostylus with the tip sclerotized, funnel-shaped, inflated, and blunt (Figs 2e, 3). In *A.* (*A.*) *lacteibasis*, the basal section of vein M_3 is about twice as long as m-m, and the outer gonostylus narrow with acute tip (Alexander 1935; Markevičiūtė et al. 2019, 2021).

***Antocha* (*Antocha*) *setigera* Alexander**
Figs 4, 5

Antocha (*Antocha*) *setigera* Alexander 1933b: 369 (original description).

Type material examined. *Holotype*: China • ♂; Sichuan province, Mount Omei; 2134 m a.s.l.; 17 July 1931; Franck leg; USNM. **Other material examined:** China • 8 ♂♂ 6 ♀♀; Tibet Autonomous Region, Chayu County, Xiachayu Farm Hydropower Station; 28°30'19"N, 97°01'25"E; 1520 m a.s.l.; 8 July 2016; Shaolin Han leg; CAU.

Diagnosis. *Antocha* (*A.*) *setigera* can be recognized by thorax with four brown stripes, wing lacking a stigma, basal section of M_3 as long as m-m, and slightly curved outer gonostylus with blackened, blunt tip. Aedeagal complex with interbase distally small and parameres apically fused, arch-shaped.

Description. Male. Body length 4.5–5.0 mm, wing length 5.0–6.0 mm, antenna length 1.5–1.8 mm.

Head (Fig. 4b). Dark brown with brown setae. Antenna brown with light brown scape. Scape cylindrical; pedicel and flagellomeres elongate oval, apically tapering; terminal segment short, about half as short as other segments. Rostrum yellow; palpus light brown; setae on rostrum and palpus brown.

Thorax (Fig. 4c). Pronotum brown. Prescutum and presutural scutum brown four brown stripes. The central stripes fused in the anterior third, the rest is separated by pale narrow vitta. Postsutural scutum dark brown, middle area yellow, scutal lobes each with brown spot. Scutellum pale yellow, with side edges dark brown. Mediotergite brown to dark brown. Pleuron brown (Fig. 4a). Legs with fore coxa brown; mid coxa brownish yellow; hind coxa yellow; trochanters yellow; femora and tibiae brownish yellow; tarsi brown with terminal segments darker brown. Wing light brown, without stigma; anal angle nearly right-angled (Fig. 4d). Veins brown. Venation: Sc ending nearly at fork of Rs; basal section of R_5 about twice as long as r-m; m-cu shortly before fork of M, distance approximately 1/3 its own length; basal section of M_3 as long as m-m; cell m_1 longer than cell dm. Halter pale with stem light yellow.

Abdomen. Tergites dark brown. Sternites 1–6 brown with side edges yellow, sternites 7 and 8 dark brown.

Hypopygium (Figs 4e, 5). Yellow. Posterior margin of tergite 9 convex with middle slightly emarginate (Fig. 5a). Gonocoxite nearly cylindrical with long brown setae (Figs 4e, 5). Outer gonostylus slightly curved, with blackened distal half and tip sclerotized and blunt. Inner gonostylus slightly curved. Interbase distally flattened, small and horn-like with tip sharp (Figs 4e, 5). Parameres apically fused, arch-shaped. Inner branch of paramere elongated, with tip narrowly obtuse (Figs 4e, 5). Aedeagus curved ventrally, tip bifid (Figs 4e, 5).

Female. Body length 4.5–5.5 mm, wing length 5.0–6.0 mm. Generally similar to male by body coloration.

Ovipositor (Fig. 4f). Tergite 10 yellowish brown with base darker. Cercus brown, tip raised and tapering, apex acute. Hypogynial valve yellowish, reaching sub-tip of cercus.

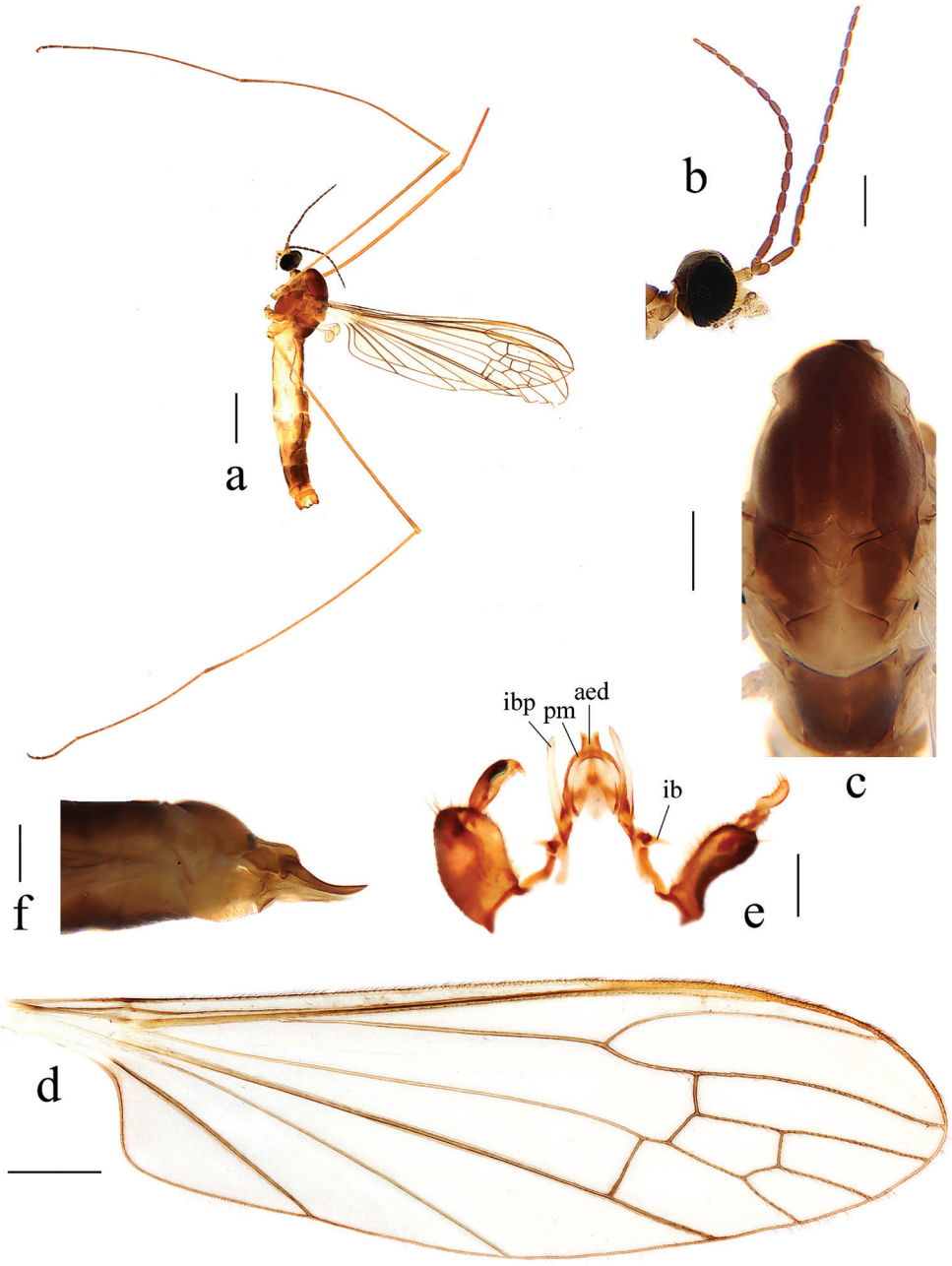

Figure 4. *Antocha* (*Antocha*) *setigera* **a** habitus of male, lateral view **b** male head, lateral view **c** male thorax, dorsal view **d** male wing **e** aedeagus complex with gonocoxite and gonostyli, dorsal view **f** female ovipositor, lateral view. Scale bars: 1.0 mm (**a**); 0.2 mm (**b, c**); 0.5 mm (**d**); 0.2 mm (**e, f**).

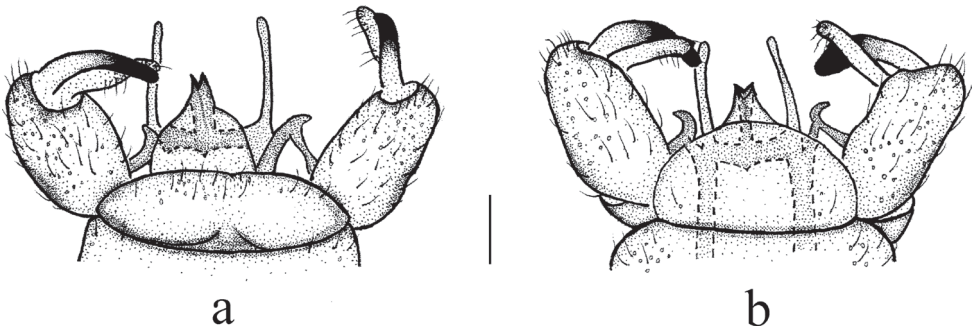

Figure 5. *Antocha* (*Antocha*) *setigera* **a** male hypopygium, dorsal view **b** male hypopygium, ventral view. Scale bar: 0.1 mm.

Distribution. China (Sichuan, Tibet).

Remarks. In China, this species was previously only known in Sichuan province and is now recorded in Tibet for the first time. For descriptions and illustrations of this species, also see Alexander (1933b) and Markevičiūtė et al. (2019, 2021).

Antocha (*Antocha*) *spiralis* Alexander

Figs 6, 7

Antocha (*Antocha*) *spiralis* Alexander 1932: 389 (original description).

Material examined. China • 9 ♂♂ 1 ♀; Tibet Autonomous Region, Bayi District, Pailong; 30°01'25"N, 95°00'32"E; 2003 m a.s.l.; 20 June 2018; Liang Wang leg.; CAU.

Diagnosis. *Antocha* (*A.*) *spiralis* can be recognized by thorax having no stripes, wing without stigma, basal section of M_3 about one and half times as long as m-m, posterior margin of tergite 9 having shallow, median emargination and slightly curved, blackened in distal 2/3 of outer gonostylus. Aedeagal complex with interbase nearly U-shaped; paramere apically slender and twisted into a spiral; inner branch of paramere with bifid tip.

Description. Male. Body length 4.5–5.5 mm, wing length 5.0–6.0 mm, antenna length 1.0–1.2 mm.

Head (Fig. 6b). Black with brown setae. Antenna brown, with dark brown pedicel. Scape cylindrical; pedicel and flagellomeres oval; terminal two segments slender. Rostrum yellow; palpus light brown; setae on rostrum and palpus brown.

Thorax (Fig. 6c). Pronotum brown. Prescutum and presutural scutum dark brown, without stripe. Postsutural scutum brownish yellow in middle; scutal lobes each with brown spot. Scutellum brown with middle of base brownish yellow. Mediotergite dark brown, with middle brownish yellow. Pleuron brown (Fig. 6a). Legs with fore and mid coxae brown; hind coxa yellow; trochanters yellow with side

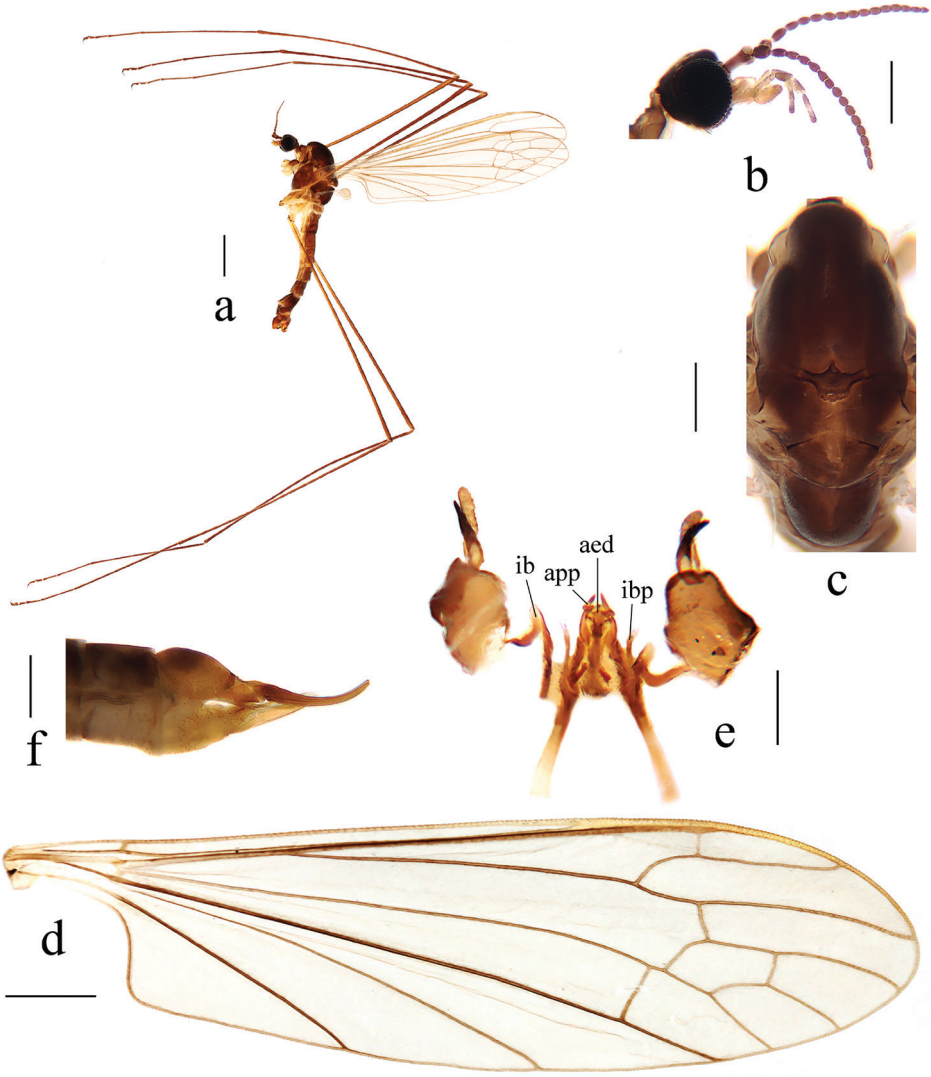

Figure 6. *Antocha* (*Antocha*) *spiralis* **a** habitus of male, lateral view **b** male head, lateral view **c** male thorax, dorsal view **d** male wing **e** aedeagus complex with gonocoxite and gonostyli, dorsal view **f** female ovipositor, lateral view. Scale bars: 1.0 mm (**a**); 0.3 mm (**b**); 0.4 mm (**c**); 0.6 mm (**d**); 0.2 mm (**e, f**).

edges brown; femora brownish yellow to brown; remaining segments dark brown. Wing light brown, without stigma; anal angle nearly right-angled (Fig. 6d). Veins brown. Venation: Sc ending before fork of Rs, at about 5/6 of Rs; basal section of R_5 about 1½ times as long as r-m; m-cu shortly before fork of M, distance approximately 1/4 its own length; basal section of M_3 about 1½ as long as m-m; cell m_1 longer than cell dm. Halter pale.

Abdomen. Tergites 1–6 brown, tergites 7 and 8 dark brown. Sternites 1–6 brownish yellow to light brown; sternites 7 and 8 dark brown.

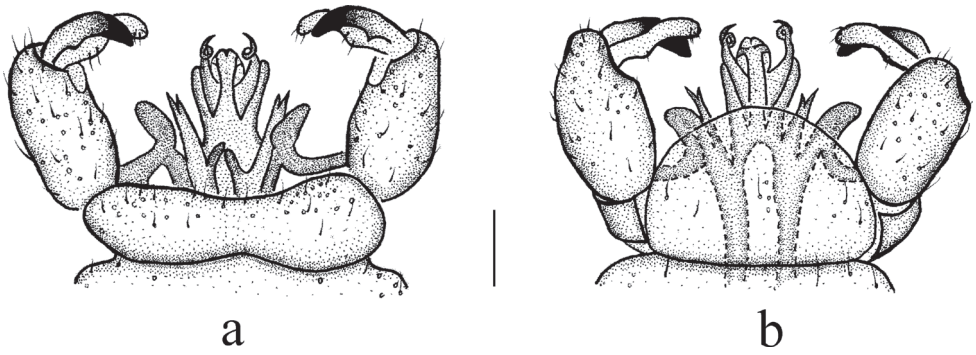

Figure 7. *Antocha* (*Antocha*) *spiralis* **a** male hypopygium, dorsal view **b** male hypopygium, ventral view. Scale bar: 0.1 mm.

Hypopygium (Figs 6e, 7). Posterior margin of tergite 9 with broad and shallow emargination (Fig. 7a). Gonocoxite nearly cylindrical with brown setae (Figs 6e, 7). Outer gonostylus slightly curved; base yellowish brown; distal 2/3 blackened, narrowing towards obtuse apex. Interbase nearly U-shaped, distal part flattened and oval (Figs 6e, 7). Paramere with rod-shaped base; apical part slender and twisted into spiral; tip sharp. Inner branch of paramere with tip bifid; outer tooth longer than inner one (Figs 6e, 7). Aedeagus with two projections near tip (Figs 6e, 7).

Female. Body length 4.5–5.5 mm, wing length 5.0–6.0 mm. Generally similar to male by body coloration.

Ovipositor (Fig. 6f). Tergite 10 brownish yellow, with brown base. Cercus yellowish brown, with base darker, slender, and curved; tip raised and tapering. Hypogynial valve yellow, reaching approximately middle of cercus.

Distribution. China (Sichuan, Tibet), India.

Remarks. In China, this species was previously only known in Sichuan and is now recorded in Tibet for the first time. For descriptions and illustrations of this species, also see Alexander (1932) and Markevičiūtė et al. (2019, 2021). Both *A.* (*A.*) *spiralis* and *A.* (*A.*) *bella* from China have the twisted structure of the hypopygium. In *A.* (*A.*) *spiralis*, the apical part of the paramere is slender and twisted into a spiral, and the tip of the inner branch of the paramere is bifid (Figs 6e, 7), while in *A.* (*A.*) *bella*, the tip of the inner branch of the paramere is twisted (Markevičiūtė et al. 2019).

Antocha (*Antocha*) *tibetana* Lv & Zhang, sp. nov.

https://zoobank.org/81CC7F50-E60F-47BD-A80C-A206C006D2FA
Figs 8, 9

Type material. ***Holotype*****:** China • ♂; Tibet Autonomous Region, Medog County, 80k; 29°28'47"N, 96°05'19"E; 2104 m a.s.l.; 30 July 2014; Tingting Zhang leg; CAU. ***Paratypes*****:** China • 1 ♂ 2 ♀♀; Tibet Autonomous Region, Medog County, 80k; 29°28'47"N, 96°05'19"E; 2104 m a.s.l.; 1 Aug. 2014; Tingting Zhang leg; CAU.

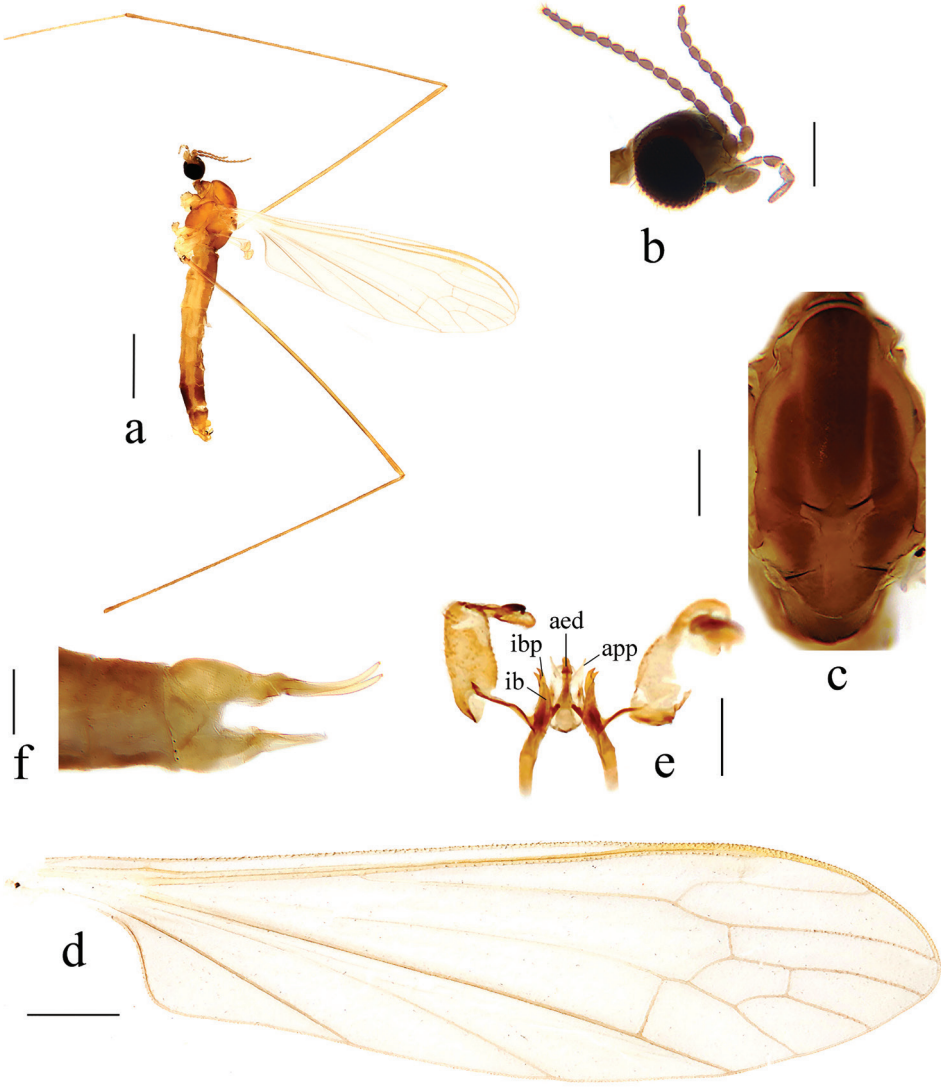

Figure 8. *Antocha* (*Antocha*) *tibetana* sp. nov. **a** habitus of male, lateral view **b** male head, lateral view **c** male thorax, dorsal view **d** male wing **e** aedeagus complex with gonocoxite and gonostyli, dorsal view **f** female ovipositor, lateral view. Scale bars: 1.0 mm (**a**); 0.3 mm (**b, c**); 0.5 mm (**d**); 0.2 mm (**e, f**).

Diagnosis. *Antocha* (*A.*) *tibetana* sp. nov. can be recognized by thorax with three dark brown stripes, wing having indistinct stigma, basal section of M_3 about twice as long as m-m, posterior margin of tergite with shallow emargination and outer gonostylus apically claw-shaped. Aedeagal complex with interbase distally horn-like; paramere apically flattened and triangular; inner branch of paramere with tip bifid into two teeth.

Description. Male. Body length 4.5–5.0 mm, wing length 5.1–5.5 mm, antenna length 1.0–1.2 mm.

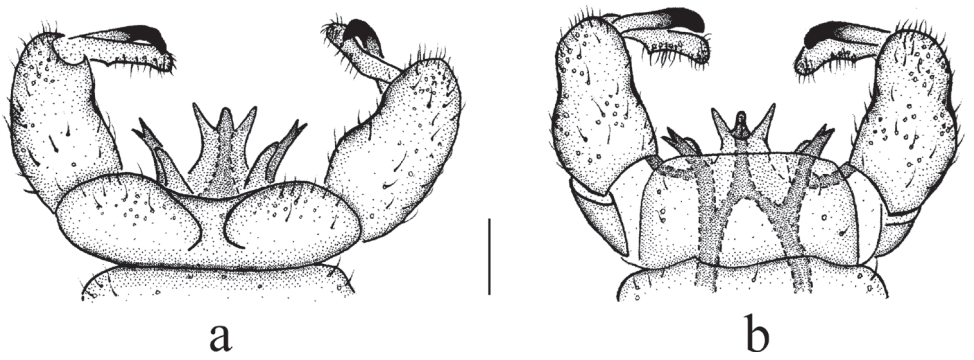

Figure 9. *Antocha* (*Antocha*) *tibetana* sp. nov. **a** male hypopygium, dorsal view **b** male hypopygium, ventral view. Scale bar: 0.1 mm.

Head (Fig. 8b). Dark brown, with brown setae. Antenna brown, with brown setae. Scape nearly cylindrical; pedicel oval; flagellomeres oval, apically shortened. Rostrum and palpus brown, with brown setae.

Thorax (Fig. 8c). Pronotum brown. Prescutum and presutural scutum brownish yellow, with three dark brown stripes. Postsutural scutum brownish yellow; scutal lobes each with a brown spot. Scutellum brown, with middle brownish yellow. Mediotergite brown with side edges light brown. Pleuron brownish yellow (Fig. 8a). Legs with coxae and trochanters yellow; rest of segments brownish yellow. Wing light brownish yellow, with very indistinct stigma; anal angle nearly right-angled (Fig. 8d). Veins brownish yellow. Venation: Sc ending before fork of Rs, at about 5/6 of Rs; basal section of R_5 about 1½ as long as r-m; m-cu shortly before fork of M, distance approximately 1/3 its own length; basal section of M_3 about twice as long as m-m; cell m_1 longer than cell dm. Halter pale with stem light yellow.

Abdomen. Tergites 1–6 brown, tergites 7 and 8 dark brown. Sternites 1–6 brownish yellow; sternites 7 and 8 dark brown.

Hypopygium (Figs 8e, 9). Yellow. Posterior margin of tergite 9 with shallow emargination (Fig. 9a). Gonocoxite nearly cylindrical with brown setae (Figs 8e, 9). Outer gonostylus apically black with tip curved, claw-shaped. Inner gonostylus nearly straight with tip rounded. Interbase nearly V-shaped, distal part flattened and horn-like, with tip blunt (Figs 8e, 9). Paramere with base rod-shaped; apical part flattened, triangular in shape. Inner branch of paramere with tip bifid, two teeth almost equal in length (Figs 8e, 9). Aedeagus rod-shaped, curved ventrally (Figs 8e, 9).

Female. Body length 5.0–5.3 mm, wing length 5.5–5.7 mm. Generally similar to male by body coloration.

Ovipositor (Fig. 8f). Tergite 10 yellowish. Cercus pale yellow, with base darker; tip raised and tapering. Hypogynial valve yellowish, reaching approximately middle of cercus.

Etymology. The species is named after the type locality, Tibet.

Distribution. China (Tibet).

Remarks. The new species is somewhat similar to *A.* (*A.*) *spiralis* from China and India with the similar wing venation and bifid tip of inner branch of paramere, but it can be easily distinguished by the three stripes on the thorax (Fig. 8c) and the triangular apex of the paramere (Figs 8e, 9). In *A.* (*A.*) *spiralis*, the thorax has no obvious longitudinal stripes (Fig. 6c), while the apex of the paramere is slender and twisted into a spiral (Figs 6e, 7).

Acknowledgements

We express our sincere thanks to Qifei Liu, Sigitas Podenas, and Jon K. Gelhaus for their great help with the study of the type specimens in USNM. This work was supported by the National Natural Science Foundation of China (32100356) and the National Animal Collection Resource Center, China.

References

Alexander CP (1924) New or little-known crane flies from northern Japan (Tipulidae, Diptera). Philippine Journal of Science 24: 531–611.

Alexander CP (1931) New or little-known Tipulidae from eastern Asia (Diptera). IX. Philippine Journal of Science 44: 339–368.

Alexander CP (1932) New or little-known Tipulidae from eastern Asia (Diptera). XI. Philippine Journal of Science 49: 373–406.

Alexander CP (1933a) New or little-known Tipulidae from eastern Asia (Diptera). XIV. Philippine Journal of Science 51: 507–544.

Alexander CP (1933b) New or little-known Tipulidae from eastern Asia (Diptera). XII. Philippine Journal of Science 50: 129–162.

Alexander CP (1935) New or little-known Tipulidae from eastern Asia (Diptera). XXVI. Philippine Journal of Science 57: 195–225.

Alexander CP (1936) New or little-known Tipulidae from eastern Asia (Diptera). XXVIII. Philippine Journal of Science 58: 385–426.

Alexander CP (1938a) New or little-known Tipulidae from eastern Asia (Diptera). XXXVIII. Philippine Journal of Science 66: 309–342.

Alexander CP (1938b) New or little-known Tipulidae from eastern Asia (Diptera). XXXIX. Philippine Journal of Science 66: 439–478.

Alexander CP (1953) New or little-known Tipulidae (Diptera). XCIV. Oriental-Australasian species. Annals and Magazine of Natural History (Series 12) 6: 174–192. https://doi.org/10.1080/00222935308654410

Alexander CP (1963) Some Tipulidae from Tibet and upper Burma in the British museum (natural history) (Diptera). Bulletin of the British Museum (Natural History). Entomology 14: 319–340. https://doi.org/10.5962/bhl.part.8785

Alexander CP (1968) New or little-known species of exotic Tipulidae (Diptera). XV. Proceedings of the Royal Entomological Society of London (B) 37(3–4): 43–49. https://doi.org/10.1111/j.1365-3113.1968.tb00196.x

Alexander CP (1971) New or little-known species of exotic Tipulidae (Diptera). XVIII. Journal of Entomology (B) 40(2): 163–172. https://doi.org/10.1111/j.1365-3113.1971.tb00119.x

Brunetti E (1912) Diptera Nematocera (excluding Chironomidae and Culicidae). Fauna of British India, including Ceylon and Burma 1: 1–581. https://doi.org/10.5962/bhl.title.8711

Cumming JM, Wood DM (2017) Adult morphology and terminology. In: Kirk-Spriggs AH, Sinclair BJ (Eds) Manual of Afrotropical Diptera. Vol. 1. South African National Biodiversity Institute, Pretoria, 107–151.

de Jong H (2017) Limoniidae and Tipulidae. In: Kirk-Spriggs AH, Sinclair BJ (Eds) Manual of Afrotropical Diptera. Vol. 2. South African National Biodiversity Institue, Pretoria, 427–477.

Kato D, Tachi T (2019) Taxonomic notes on the genus *Elliptera* Schiner, 1863, of Japan. Makunagi / Acta Dipterologica 30: 1–7.

Markevičiūtė R, Podenas S, Saldaitis A, Bernotiene R (2019) A new species of *Antocha* Osten Sacken, 1860 (Diptera: Limoniidae) from Sichuan, China. Zootaxa 4661(1): 118–132. https://doi.org/10.11646/zootaxa.4661.1.5

Markevičiūtė R, Podenas S, Saldaitis A (2021) New *Antocha* Osten Sacken (Diptera: Limoniidae) from Sichuan, China. Zootaxa 4969(2): 280–292. https://doi.org/10.11646/zootaxa.4969.2.3

Oosterbroek P (2023) Catalogue of the Craneflies of the World (Diptera, Tipuloidea: Pediciidae, Limoniidae, Cylindrotomidae, Tipulidae). http://ccw.naturalis.nl/ [Accessed 2023-01-24]

Osten Sacken CR (1860) New genera and species of North American Tipulidae with short palpi, with an attempt at a new classification of the tribe. Proceedings of the Academy of Natural Sciences of Philadelphia 1859: 197–254.

Podenas S (2015) A new species of *Antocha* crane fly Osten Sacken, 1860 (Diptera: Limoniidae) for North Korea. Proceedings of the Academy of Natural Sciences of Philadelphia 164(1): 3–7. https://doi.org/10.1635/053.164.0102

Podenas S, Byun HW (2014) New species of *Antocha* Osten Sacken, 1860 crane flies (Diptera: Limoniidae) for South Korea. Zootaxa 3900: 117–126. https://doi.org/10.11646/zootaxa.3900.1.7

Podenas S, Young CW (2015) *Antocha* crane flies from Taiwan (Diptera: Limoniidae: Limoniinae). Zootaxa 4048(4): 523–537. https://doi.org/10.11646/zootaxa.4048.4.4

Torii T (1992a) Systematic study of the genus *Antocha* recorded from Japan and its adjacent area (Diptera, Tipulidae). Acta Zoologica Cracoviensia 35: 157–192.

Torii T (1992b) Three new species of the genus *Antocha* from Japan, with a note on the sugenera *Antocha* and *Proantocha* (Diptera, Tipulidae). Japanese Journal of Entomology 60: 1–9.

Torii T (1992c) Synonymic notes on three Japanese species of *Antocha* (Diptera, Tipulidae). Japanese Journal of Entomology 60: 867–868.

Torii T (1996) Cladistic analysis of the genus *Antocha* recorded from Japan and its adjacent area (Insecta: Diptera: Tipulidae). Zoological Science 13, Supplement 39.

Young CW (1994) A new species of *Antocha* (subgenus *Orimargula*) from Sulawesi (Diptera: Tipulidae) and its mate-clasping behavior. Annals of the Carnegie Museum 63(4): 319–325. https://doi.org/10.5962/p.215816

ZooKeys 1156: 71–85 (2023)
doi: 10.3897/zookeys.1156.96698
https://zookeys.pensoft.net

RESEARCH ARTICLE

A peer-reviewed open-access journal
ZooKeys
Launched to accelerate biodiversity research

A new hexactinellid-sponge-associated zoantharian (Porifera, Hexasterophora) from the northwestern Pacific Ocean

Hiroki Kise[1], Miyuki Nishijima[1], Akira Iguchi[1,2], Junpei Minatoya[3], Hiroyuki Yokooka[4], Yuji Ise[5], Atsushi Suzuki[1,2]

1 *Geological Survey of Japan, National Institute of Advanced Industrial Science and Technology (AIST), AIST Tsukuba Central 7, 1-1-1 Higashi, Tsukuba, Ibaraki 305-8567, Japan* **2** *Research Laboratory on Environmentally-conscious Developments and Technologies (E-code), National Institute of Advanced Industrial Science and Technology (AIST), Tsukuba 305-8567, Japan* **3** *Japan Organization for Metals and Energy Security (JOGMEC), 2-10-1 Minato-ku, Tokyo 105-0001, Japan* **4** *Institute of Environmental Ecology, IDEA Consultants, Inc., 1334-5 Riemon, Yaizu-shi, Shizuoka 421-0212, Japan* **5** *Kuroshio Biological Research Foundation, 560 Nishidomari, Otsuki, Hata, Kochi 788-0333, Japan*

Corresponding author: Hiroki Kise (h.kise@aist.go.jp)

Academic editor: B. W. Hoeksema | Received 25 October 2022 | Accepted 22 December 2022 | Published 24 March 2023

https://zoobank.org/1D88BB39-FB85-4795-9406-8DDC524394E5

Citation: Kise H, Nishijima M, Iguchi A, Minatoya J, Yokooka H, Ise Y, Suzuki A (2023) A new hexactinellid-sponge-associated zoantharian (Porifera, Hexasterophora) from the northwestern Pacific Ocean. ZooKeys 1156: 71–85. https://doi.org/10.3897/zookeys.1156.96698

Abstract

Symbiotic associations between zoantharians and sponges can be divided into two groups: those that associate with Demospongiae and those that associate with Hexactinellida. *Parachurabana shinseimaruae* Kise, **gen. nov. et sp. nov.**, a new genus and a new species of Hexactinellida-associated zoantharian from Japanese waters, is described. It is characterized by a combination of the following: i) its host hexactinellid sponge, ii) very flat polyps, iii) cteniform endodermal marginal muscles, and iv) characteristic mutations in three mitochondrial regions (including a unique 26-bp deletion in 16S ribosomal DNA) and three nuclear regions. *Parachurabana shinseimaruae* Kise, **gen. nov. et sp. nov.** is the third genus in the family Parazoanthidae that is reported to be associated with Hexasterophora sponges. Although specimens have so far only been collected on Takuyo-Daigo Seamount off Minami-Torishima Island in Japan, unidentified zoantharians of similar description have been reported from the waters around Australia, indicating that the species might be widespread across the Pacific.

Keywords
Glass sponge, Hexasterophora, host specificity, molecular phylogeny, symbiosis

Introduction

The family Parazoanthidae Delage & Hérouard, 1901 comprises 16 genera and more than 50 species (Reimer and Sinniger 2022). The Parazoanthidae usually form symbiotic relationships with various benthic invertebrates, including octocorals (Cutress and Pequegnat 1960; Reimer et al. 2008; Sinniger et al. 2013; Carreiro-Silva et al. 2017), antipatharians (Sinniger et al. 2010; Kise et al. 2017), and sponges (Duchassaing de Fonbressin and Michelotti 1860; Schmidt 1862; Montenegro et al. 2015). This allows them to capture plankton more effectively in environments where plankton are scarce by attaching themselves to benthic filter feeders (Di Camillo et al. 2010).

Sinniger et al. (2005, 2010) suggested that different genera within the Parazoanthidae share evolutionary histories with their associated host organisms, as these genera form monophyletic clades based on associated host organisms. Symbiotic associations between parazoanthids and sponges can be divided into two groups: those that associate with Demospongiae and those that associate with Hexactinellida. Demospongiae-associated zoantharians consist of *Bergia* Duchassaing & Michelotti, 1860, *Parazoanthus* Haddon & Shackleton, 1891, and *Umimayanthus* Montenegro, Sinniger & Reimer, 2015; Hexactinellida-associated zoantharians comprise *Churabana* Kise, Montenegro & Reimer, 2021, *Isozoanthus* Carlgren in Chun, 1903, and *Vitrumanthus* Kise, Montenegro & Reimer, 2021. *Churabana* and *Vitrumanthus* are recently established genera that are characterized by their association with the hexactinellid subclass Hexasterophora (Kise et al. 2022). *Churabana kuroshioae* Kise, Montenegro & Reimer, 2021 and *Vitrumanthus oligomyarius* (Wassilieff, 1908) are found in the Pacific Ocean, and *V. schrieri* Kise, Montenegro & Reimer, 2021 and *V. vanderlandi* Kise, Montenegro & Reimer, 2021 are found in the Atlantic Ocean, including the Dutch Caribbean and the western coast of Africa. Although Hexasterophora–zoantharian associations are relatively common and have been reported to occur circumglobally, potentially undescribed zoantharians have been observed on hexasterophoran sponges such as *Cyrtaulon caledoniensis* Reiswig & Kelly, 2017 in the Pacific Ocean (Reiswig and Kelly 2017). Thus, the diversity of Hexasterophora-associated zoantharians remains understudied in this region.

Recently, we collected a single specimen of parazoanthid associated with a hexactinellid sponge in the family Farreidae Gray, 1872 during a benthic survey of the Takuyo-Daigo Seamount in the western Pacific Ocean. On the basis of molecular phylogenetic analyses combined with morphological and ecological data, we formally describe it here as the new species *Parachurabana shinseimaruae* gen. nov. et sp. nov. (authored by Kise).

Materials and methods

Specimen collection

A single specimen was collected on 19 June 2020 by using a remotely operated submersible on Takuyo-Daigo Seamount off southwestern Minami-Torishima Island in the northwestern Pacific Ocean during a cruise aboard the RV *Shinsei-maru*. Photographs of the specimen were taken in situ for gross external morphological observation. The collected specimen was fixed in 99.5% EtOH and stored at –80 °C.

Molecular analyses

Genomic DNA was extracted from the tissue of the holotype specimen using a spin-column DNeasy Blood and Tissue Extraction Kit (Qiagen, Hilden, Germany) following the manufacture's protocol. PCR amplification using Takara Ex Taq DNA Polymerase Hot Start Version (TaKaRa Bio, Inc., Shiga, Japan) was conducted for mitochondrial cytochrome c oxidase subunit I (COI) with jgLCO1490 and jgHCO2198 (Geller et al. 2013), mitochondrial 12S ribosomal DNA (mt 12S-rDNA) with the primers 12S1a and 12S3r (Sinniger et al. 2005), mitochondrial 16S ribosomal DNA (mt 16S-rDNA) with the primers 16Sant0a (Sinniger et al. 2010) and 16SbmoH (Sinniger et al. 2005), nuclear 18S ribosomal DNA (18S-rDNA) with the primers 18SA and 18SB (Medlin et al. 1988), nuclear internal transcribed spacer region of ribosomal DNA (ITS-rDNA) with the primers ITSf and ITSr (Swain 2010), and nuclear 28S ribosomal DNA (28S-rDNA) with the primers 28Sf and 28Sr (Swain 2009). For 18S-rDNA, the primers 18SC, 18SL, 18SO, and 18SY (Apakupakul et al. 1999) were used for sequencing.

All PCR products were purified with ExoSAP-IT™ PCR Product Cleanup Reagent (Thermo Fisher Scientific, Waltham, MA, USA) at 37 °C for 15 min followed by 80 °C for 15 min. Purified PCR products were sequenced by Macrogen Japan, Inc. (Kyoto, Japan). Obtained sequences in this study were deposited in GenBank (Suppl. material 1)

Bidirectional sequences were assembled and edited in Geneious v. 10.2.3 (Kearse et al. 2012). Multiple sequence alignments were performed with previously published Parazoanthidae sequences obtained from GenBank (Suppl. material 1) using MAFFT v. 7.110 (Katoh and Standley 2013) with the auto algorithm under default parameters. Epizoanthidae Delage & Hérouard, 1901 and *Isozoanthus* Carlgren in Chun, 1903 were selected as outgroups. Although *Isozoanthus* is currently located in Parazoanthidae, recent studies suggest that *Isozoanthus* is phylogenetically closer to Epizoanthidae than Parazoanthidae (e.g., Swain 2010). All aligned datasets are available at figshare (https://doi.org/10.6084/m9.figshare.21673196).

Phylogenetic analyses were performed on the concatenated dataset using maximum likelihood (ML) and Bayesian inference (BI). ModelTest-NG v. 0.1.6 (Darriba et al. 2019) and the Akaike information criterion were used to independently select the best-fitting model for each molecular marker for both ML and BI. The best models

for ML and BI analyses were TrN+I+G (BI: HKY+I+G) for COI, TPM3uf+I+G (BI: HKY+G) for mt 12S-rDNA, GTR+G for mt 16S-rDNA, HKY+I+G for 18S-rDNA, TPM1uf+I+G (BI: GTR+I+G) for ITS-rDNA, and GTR+I+G for 28S-rDNA. Independent phylogenetic analyses were performed using models partitioned by region in RAxML-NG v. 0.9.0 (Kozlov et al. 2019) for ML, and MrBayes v. 3.2.6 (Ronquist and Huelsenbeck 2003) for BI. RAxML-NG was configured to use 12,345 initial seeds, search for the best tree among 100 preliminary parsimony trees, scale and automatically optimize branch length for each partition, and optimize the model parameters, with 1000 bootstrap replicates. MrBayes was configured as indicated by ModelTest-NG: 4 Markov chain Monte Carlo heated chains were run for 5,000,000 generations with the temperature of the heated chain set to 0.2. Chains were sampled every 200 generations. Burn-in was set to 1,250,000 generations, at which point the average standard deviation of split frequency was consistently below 0.01.

ITS-rDNA has been considered as a useful marker to delineate species in Zoantharia (Reimer et al. 2007). Therefore, additional ML phylogenetic analysis for ITS-rDNA was performed using PhyML v. 3.0 (Guindon et al. 2010) with the best model (GTR) inferred by Smart Model Selection (SMS) implemented in the PhyML, with 1000 bootstrap replicates.

Morphological observations

External morphological characters of the preserved specimen were examined using in-situ images and a dissecting microscope. Internal morphological characters were examined by using histological sections; 10–15 μm serial sections were made with a microtome (LEICA RM2145; Leica, Germany) and stained with haematoxylin and eosin after decalcification with Morse solution for 48 h (1:1 vol; 20% citric acid: 50% formic acid) and desilication with 20% hydrofluoric acid for 18–24 h. Classification of marginal muscle shapes followed the scheme described by Swain et al. (2015). Cnidae analysis was conducted using undischarged nematocysts from the tentacles, columns, actinopharynxes, and mesenterial filaments of two polyps of the holotype specimen under a Nikon Eclipse80i microscope (Nikon, Tokyo). Cnidae sizes were measured using ImageJ v. 1.45 (Rasband 2012). Cnidae classification followed England (1991) and Ryland and Lancaster (2004) except for the treatment of basitrichs and microbasic b-mastigophores as mentioned by Kise and Reimer (2019). Associated hexactinellid sponges were identified based on morphology (Reiswig and Wheeler 2002a, b).

Abbreviations

CMNH Coastal Branch of the Natural History Museum and Institute, Chiba, Japan;
NSMT National Science Museum, Tsukuba, Ibaraki, Japan;
RMNH Rijksmuseum van Natuurlijke Historie (now at the Naturalis Biodiversity Center), Leiden, the Netherlands;
RUMF Ryukyu University Museum (Fujukan), University of the Ryukyus, Okinawa, Japan.

Results

Taxonomic description

Order Zoantharia Rafinesque, 1815
Suborder Macrocnemina Haddon & Shackleton, 1891
Family Parazoanthidae Delage & Hérouard, 1901

Genus *Parachurabana* Kise, gen. nov.
https://zoobank.org/B0C6562D-BA20-42D5-B875-E91977F3C31F

Type species. *Parachurabana shinseimaruae* Kise sp. nov. by original designation.

Diagnosis. Parazoanthidae with symbiotic relationship with farreid sponges. Polyp cylindrical and flat when preserved. Preserved polyps 0.5–1.0 mm in height, 0.5–3.0 mm in diameter. Azooxanthellate. Cteniform endodermal marginal muscle.

Remarks. *Parachurabana* gen. nov. is differentiated from other sponge-associated parazoanthids based on a combination of host-sponge identity and morphological features. *Parachurabana* gen. nov. is easily distinguished from the genera *Bergia*, *Parazoanthus*, and *Umimayanthus* by its association with hexactinellid sponges, as the three other genera are associated with Demospongiae sponges. In Hexactinellida-sponge-associated Parazoanthidae genera, the association with subclass Amphidiscophora differentiates *Parachurabana* gen. nov. from *Isozoanthus*. Marginal muscle morphology differentiates *Parachurabana* gen. nov. (cteniform endodermal marginal muscles) from *Vitrumanthus* (cyclically transitional marginal muscles). *Parachurabana* gen. nov. can be distinguished from *Churabana* by polyp size, as *Parachurabana* gen. nov. has very flat polyps when preserved (0.5–1.0 mm in height, 0.5–3.0 mm in diameter) in comparison to *Churabana* (3.0–4.0 mm in height, 2.8–4.0 mm in diameter). In the16S-rDNA region, *Parachurabana* gen. nov. is characterized by a unique deletion of 26 bp (positions 136–150 and 168–178 in our alignment) (Suppl. material 2).

Etymology. *Parachurabana* alludes to its morphological similarities to *Churabana.* The Prefix "*para*" is a Greek word meaning "resembling."

***Parachurabana shinseimaruae* Kise, sp. nov.**
https://zoobank.org/908AC687-D304-4881-A097-F1BA98340F6D
Figs 1–3

Material examined. *Holotype*. NSMT-Co 1819, Takuyo-Daigo Seamount off southwestern Minami-Torishima Island, 23°23'N, 153°04'E, 935 m depth, coll. RV *Shinseimaru*, 19 June 2020, fixed in 99.5% ethanol.

Material examined for comparison. *Churabana kuroshioae* RUMF-ZG-04447 (holotype), collected from near Iejima Island, Motobu, Okinawa, Japan by T. Higashiji, 02 Mar. 2018. *Vitrumanthus schrieri* RMNH.COEL.42429 (holotype), collected from SubStation, Curaçao by B.W. Hoeksema, 31 Mar. 2014. *Vitrumanthus vanderlandi*

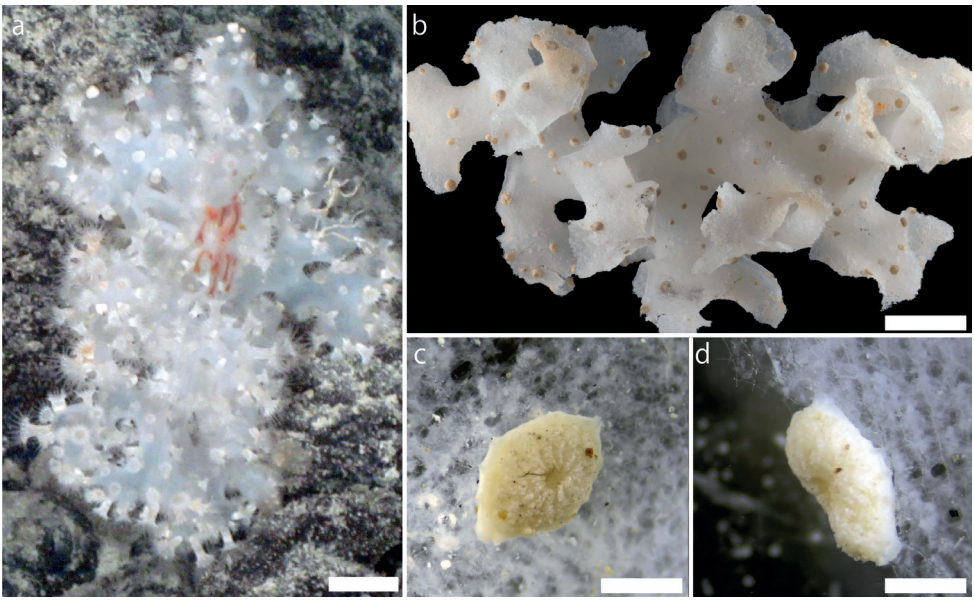

Figure 1. External morphology of *Parachurabana shinseimaruae* sp. nov. **a** photographic record from Takuyo-Daigo Seamount off southwestern Minami-Torishima Island **b–d** NSMT-Co 1819 **a** living polyps on a hexactinellid sponge *Farrea* sp. **b** preserved specimen **c** close-up image of a single preserved polyp **d** close-up, side-view image of a single preserved polyp attached to a hexactinellid sponge *Farrea* sp. Scale bars: 20 mm (**a, b**); 1 mm (**c, d**).

RMNH.COEL.42623 (holotype), Cape Verde Islands, São Tiago, Ilheus Rombos east of Cima by RV *HNIMS Tydeman*, 24 Aug. 1986. *Vitrumanthus oligomyarius* CMNH ZG-4785, off Katsuura, Chiba, Japan by A. Tamura, 19 Jan. 2006.

Description. ***External morphology.*** Cylindrical polyps that appear solitary and sparsely distributed on the hexactinellid sponge *Farrea* Bowerbank, 1862 (Fig. 1a, b). Surface of column rough, and ectoderm continuous. Polyps attached to hexactinellid sponge surfaces with pedal-disk-like structure (Fig. 1c, d). In contracted polyp, tentacles poorly covered by capitulum and actinopharynx visible. Preserved column creamy white in color and heavily encrusted with sand and silica particles. Capitulary ridges discernible, 12–14 in number (Fig. 1c). Tentacles 24–28 in number, shorter than or equal to expanded oral disk diameter. Living expanded polyps to ca. 10.0 mm in height and 5.0 mm in diameter. Preserved contracted polyps to 0.5–1.0 mm in height and 0.5–3.0 mm in diameter. Living column white and/or yellowish; capitulum and tentacle transparent (Fig. 1a).

Internal morphology. Zooxanthellae absent. Cteniform endodermal marginal muscle with comb-like mesogleal pleats (Fig. 2a). Ectoderm and mesoglea heavily encrusted with numerous sand and silica particles of various size (Fig. 2b, c). Basal canals of mesenteries absent and encircling sinus visible (Fig. 2c). Single siphonoglyph and complete mesenteries possibly fertile.

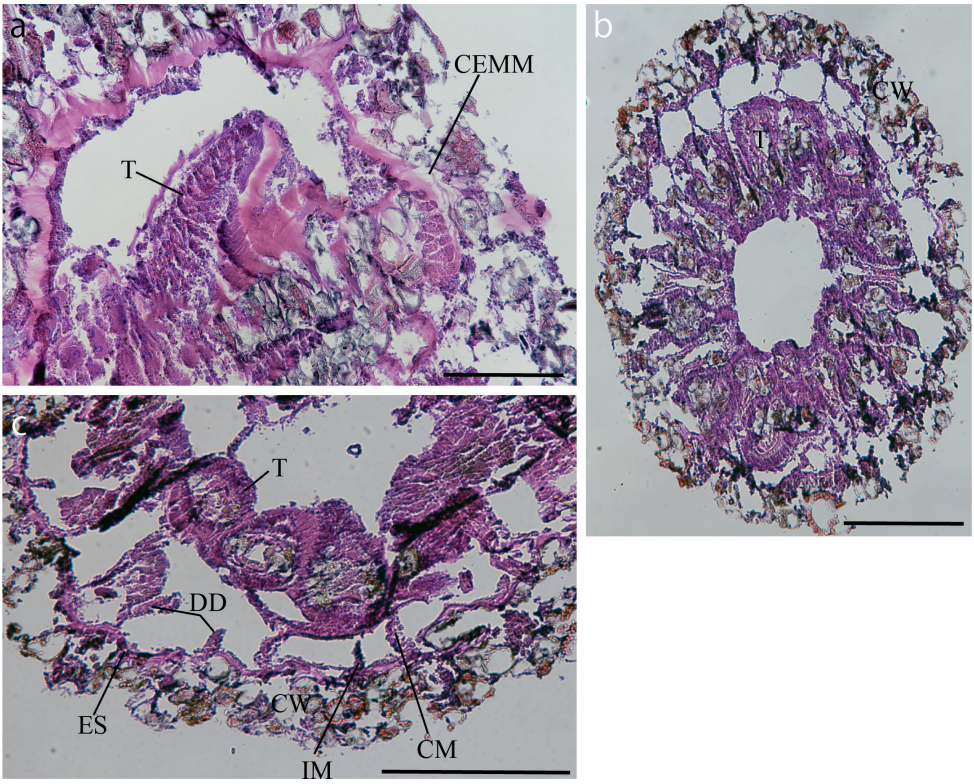

Figure 2. Images of the internal morphology of *Parachurabana shinseimaruae* sp. nov. NSMT-Co 1819 **a** close-up image of cteniform endodermal marginal muscle in a longitudinal polyp section **b** cross-section at the height of tentacles **c** cross-section at the height of the actinopharynx. Abbreviations: CEMM, cteniform endodermal marginal muscle; CM, complete mesentery; CW, column wall; DD, dorsal directives; ES, encircling sinus; IM, incomplete mesentery; T, tentacles. Scale bars: 200 μm (**a**); 500 μm (**b, c**).

***Cnidae*.** Basitrichs and microbasic b-mastigophores, microbasic p-mastigophores, holotrichs, special b-mastigophores, and spirocysts (See Fig. 3 and Table 1 for size).

Distribution and habitats. Northwestern Pacific Ocean: Takuyo-Daigo Seamount off southwestern Minami-Torishima Island at depths of 900–1000 m.

Associated host. *Farrea* sp. (Porifera: Hexactinellida)

Molecular phylogeny. Both ML and BI phylogenetic analyses using the concatenate dataset indicate that *Parachurabana shinseimaruae* sp. nov. is basal to the clade containing the genera *Bergia*, *Parazoanthus*, and *Umimayanthus* (Fig. 4; ML, 62%; BI, 0.99). ML phylogenetic analyses place *Churabana* and *Vitrumanthus* in a clade with octocoral-associated genera such as *Corallizoanthus* Reimer in Reimer, Nonaka, Sinniger & Iwase, 2008 with no support (ML < 50%), whereas BI phylogenetic analyses place *Churabana* and *Vitrumanthus* in a sister clade to that containing *Parachurabana*, *Bergia*,

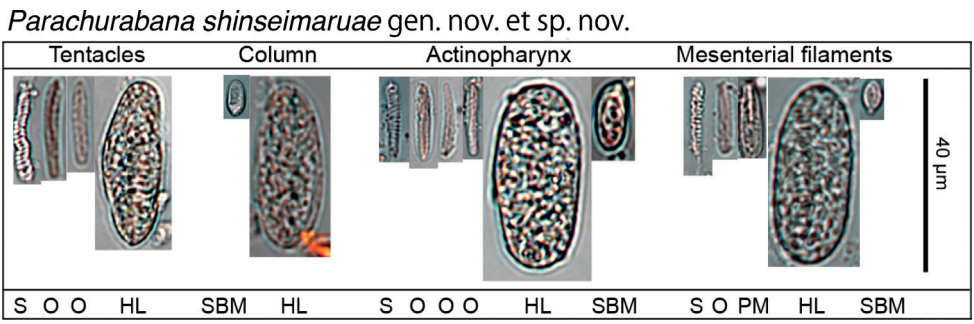

Figure 3. Cnidae in the tentacles, column, actinopharynx, and mesenterial filaments of the holotype of *Parachurabana shinseimaruae* sp. nov. Abbreviations: HL, holotrich large; O, basitrichs and microbasic b-mastigophores; SBM, special microbasic b-mastigophores; PM, microbasic p-mastigophores; S, spriocysts.

Table 1. Cnidae types and sizes observed in this study. Frequency: relative abundance of cnidae type in decreasing order; numerous, common, occasional, rare. *n* = number of cnidae measured.

Tissue	Type of cnidae	Length (min–max, mean)	Width (min–max, mean)	Frequency	*n*
Tentacle	Spirocysts	15.30–32.20, 23.40	2.22–4.81, 3.64	Numerous	195
	Basitrichs and microbasic b-mastigophores	15.31–25.12, 21.54	1.61–4.20, 3.38	Numerous	67
	Holotrichs (L)	27.97–44.58, 35.29	11.63–21.31, 15.20	Occasional	11
Column	Special microbasic b-mastigophores	11.56–16.84, 13.91	5.16–8.04, 6.01	Occasional	13
	Holotrich (L)	28.84–37.84, 32.00	10.72–18.72, 15.35	Common	18
Actinopharynx	Spirocysts	18.05–29.02, 23.73	2.03–4.62, 3.45	Numerous	45
	Basitrichs and microbasic b-mastigophores	18.29–27.64, 22.33	1.73–4.96, 3.30	Common	32
	Special microbasic b-mastigophores	17.88–19.09, 18.48	5.69–5.73, 5.71	Rare	2
	Holotrichs (L)	38.33–48.65, 43.00	11.08–17.51, 13.96	Rare	3
Mesenterial filaments	Spirocysts	19.31–32.17, 24.76	2.26–4.81, 3.40	Occasional	11
	Bastrichs and microbasic b-mastigophores	17.81–27.46, 22.45	3.38–4.57, 3.83	Common	15
	Microbasic p-mastigophores	14.04–23.25, 19.31	5.08–7.51, 5.96	Occasional	13
	Special microbasic b-mastigophores	5.84–10.71, 7.79	2.68–5.27, 4.21	Occasional	11
	Holotrichs (L)	33.13–48.86, 38.93	12.39–24.04, 16.39	Common	22

Parazoanthus, and *Umimayanthus* (Suppl. material 3). The topology of a phylogeny for ITS-rDNA dataset was similar with the concatenate dataset (Suppl. material 4).

Remarks. *Parachurabana shinseimaruae* sp. nov. has so far only been identified on one seamount off southwestern Minami-Torishima Island. However, *Parachurabana shinseimaruae* sp. nov. may be distributed across the Pacific Ocean, as several specimens associated with farreid sponges have been observed in Australian waters (M. Ekins personal communication). Although *Parachurabana shinseimaruae* sp. nov. is morphologically similar to *Vitrumanthus schrieri*, *Parachurabana shinseimaruae* sp. nov. and *V. schrieri* can be separated by marginal muscle (cteniform endodermal marginal muscle vs cycli-

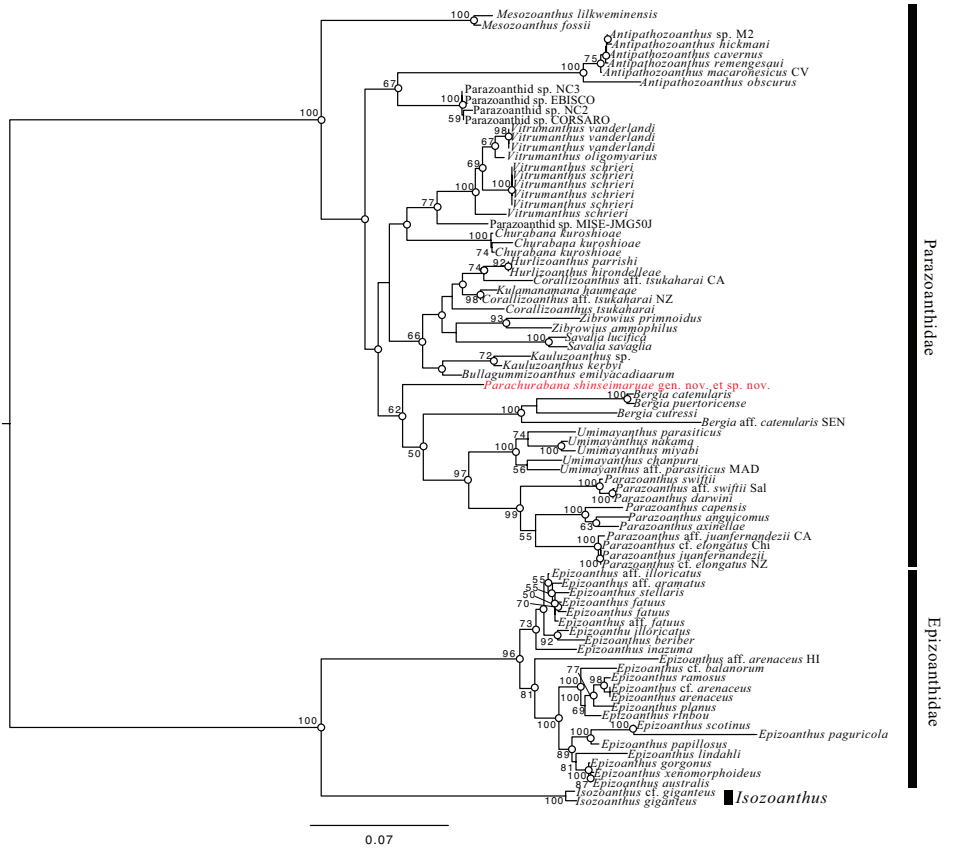

Figure 4. Maximum-likelihood tree based on combined dataset of COI, 12S-rDNA, 16S-rDNA, 18S-rDNA, 28S-rDNA, and ITS-rDNA sequences. Number at nodes represent ML bootstrap values (>50% are shown). White circles on nodes indicate high support of Bayesian posterior probabilities (>0.95).

cally transitional marginal muscle). Furthermore, *Parachurabana shinseimaruae* sp. nov. can be distinguished from *Churabana kuroshioae* by polyp size (0.5–1.0 mm in height by 0.5–3.0 mm in diameter vs 3.0–4.0 mm in height by 2.8–4.0 mm in diameter).

Etymology. The species is named after RV *Shinsei-maru*, as the type specimens were collected by this vessel.

Discussion

Parachurabana gen. nov. is the third Parazoanthidae genus known to associate with hexasterophoran sponges. Each of these three genera is associated with different hexasterophorans: *Parachurabana* gen. nov. is known to associate with *Farrea* (family Farreidae); *Churabana* with *Pararete* Ijima, 1927 (Euretidae); and *Vitrumanthus* with

Verrucocoeloidea Reid, 1969 (Euretidae), *Cyrtaulon* Schulze, 1886 (*Sceptrulophora incertae sedis*), *Aphrocallistes* Gray, 1858 (Aphrocallistidae), and *Tretochone* Reid, 1958 (Euretidae) (Kise et al. 2022). In addition, *Vitrumanthus* is also known to associate to *Parahigginsia* Dendy, 1924 within the Demospongiae (Kise et al. 2022). Although *Parachurabana* gen. nov. may be host specific to the genus *Farrea*, recent studies suggest that the association between zoantharians and host organisms can be more flexible than initially presumed (see Vaga et al. 2020). Further studies on more taxa are required to evaluate host specificity between zoantharians and hexasterophorans. Recent studies indicate that the deep sea harbors high levels of zoantharian diversity (e.g., Sinniger et al. 2013; Carreiro-Silva et al. 2017; Reimer et al. 2019). However, taxonomic studies on the deep-sea zoantharians are generally lacking and numerous undescribed species await formal description. This study contributes to filling this taxonomic gap.

Acknowledgements

This study was commissioned by the Agency for Natural Resources and Energy in the Ministry of Economy, Trade and Industry, Japan. This study was funded by Japan Organization for Metals and Energy Security (JOGMEC). Computations were partially performed on the NIG supercomputer at the ROIS National Institute of Genetics. We thank Dr Kyoko Yamaoka (AIST) for providing technical support. Comments from Dr James Davis Reimer, Dr Javier Montenegro, and an anonymous reviewer greatly improved this manuscript.

References

Apakupakul K, Siddall ME, Burreson EM (1999) Higher level relationships of leeches (Annelida: Clitellata: Euhirudinea) based on morphology and gene sequences. Molecular Phylogenetics and Evolution 12(3): 350–359. https://doi.org/10.1006/mpev.1999.0639

Bowerbank JS (1862) On the anatomy and physiology of the Spongiadae. Part III. Philosophical Transactions of the Royal Society 152(2): 1087–1135. https://doi.org/10.1098/rstl.1862.0044

Carreiro-Silva M, Ocaña O, Stanković D, Sampaio Í, Porteiro FM, Fabri M-C, Stefanni S (2017) Zoantharians (Hexacorallia: Zoantharia) associated with cold-water corals in the Azores region: new species and associations in the deep sea. Frontiers in Marine Science 4: e88. https://doi.org/10.3389/fmars.2017.00088

Chun C (1903) Aus den Tiefen des Weltmeeres Schilderungen von der Deutschen Tiefsee-Expedition. Gustav Fisher, Jena, 740 pp. https://doi.org/10.5962/bhl.title.14876

Cutress CE, Pequegnat WE (1960) Three new species of Zoantharia from California. Pacific Science 14: 89–100.

Darriba D, Posada D, Kozlov AM, Stamatakis A, Morel B, Flouri T (2019) ModelTest-NG: A new and scalable tool for the selection of DNA and protein evolutionary models. Molecular Biology and Evolution 37(1): 291–294. https://doi.org/10.1093/molbev/msz189

Delage Y, Hérouard E (1901) Zoanthidés. – Zoanthidae. In: Traité de Zoologie concrète (2eme partie). Les Cœlentérés. C. Reinwald, Paris, 654–667.

Dendy A (1924) Porifera. Part I. Non-Antarctic sponges. Natural History Report. British Antarctic ("Terra Nova") Expedition, 1910. Zoology (Jena, Germany) 6: 269–392.

Di Camillo CG, Bo M, Puce S, Bavestrello G (2010) Association between *Dentitheca habereri* (Cnidaria: Hydrozoa) and two zoanthids. The Italian Journal of Zoology 77(1): 81–91. https://doi.org/10.1080/11250000902740962

Duchassaing de Fonbressin P, Michelotti J (1860) Mémoire sur les coralliaires des Antilles. Memorie della Reale Accademia delle Scienzeai di Torino Serie Seconda 23: 270–365. https://doi.org/10.5962/bhl.title.11388

England KW (1991) Nematocysts of sea anemones (Actiniaria, Ceriantharia and Corallimorpharia: Cnidaria): nomenclature. Hydrobiologia 216(1): 691–697. https://doi.org/10.1007/BF00026532

Geller J, Meyer C, Parker M, Hawk H (2013) Redesign of PCR primers for mitochondrial cytochrome c oxidase subunit I for marine invertebrates and application in all-taxa biotic surveys. Molecular Ecology Resources 13(5): 851–861. https://doi.org/10.1111/1755-0998.12138

Gray JE (1858) On Aphrocallistes, a new genus of Spongiadae from Malacca. Proceedings of the Zoological Society of London 26(1): 114–115. https://doi.org/10.1111/j.1469-7998.1858.tb06352.x

Gray JE (1872) Notes on the classification of the sponges. Annals and Magazine of Natural History (Series 4) 9(54): 442–461. https://doi.org/10.1080/00222937208696616

Guindon S, Dufayard JF, Lefort V, Anisimova M, Hordijk W, Gascuel O (2010) New algorithms and methods to estimate maximum-likelihood phylogenies: Assessing the performance of PhyML 3.0. Systematic Biology 59(3): 307–321. https://doi.org/10.1093/sysbio/syq010

Haddon AC, Shackleton AM (1891) A revision of the British Actiniae. Part II. The Zoantheae. Scientific Transactions of the Royal Dublin Society 4: 609–672. https://doi.org/10.5962/bhl.title.46280

Ijima I (1927) Hexactinellida of the Siboga Expedition. In: Weber M (Ed.) Uitkomsten op Zoologisch, Botanisch, Oceanographisch en Geologisch Gebied Verzameld in Nederlandsch Oost-Indië 1899–1900, 6. Brill, Leiden.

Katoh K, Standley DM (2013) MAFFT multiple sequence alignment software version 7: Improvements in performance and usability. Molecular Biology and Evolution 30(4): 772–780. https://doi.org/10.1093/molbev/mst010

Kearse M, Moir R, Wilson A, Stones-Havas S, Cheung M, Sturrock S, Buxton S, Cooper A, Markowitz S, Duran C, Thierer T, Ashton B, Meintjes P, Drummond A (2012) Geneious Basic: An integrated and extendable desktop software platform for the organization and analysis of sequence data. Bioinformatics (Oxford, England) 28(12): 1647–1649. https://doi.org/10.1093/bioinformatics/bts199

Kise H, Reimer JD (2019) A new *Epizoanthus* species (Cnidaria: Anthozoa: Epizoanthidae) associated with the gastropod mollusk Guildfordia triumphans from southern Japan. Zoological Science 36(3): 259–265. https://doi.org/10.2108/zs180182

Kise H, Fujii T, Masucci G, Biondi P, Reimer JD (2017) Three new species and the molecular phylogeny of *Antipathozoanthus* from the Indo-Pacific Ocean (Anthozoa, Hexacorallia, Zoantharia). ZooKeys 725: 97–122. https://doi.org/10.3897/zookeys.725.21006

Kise H, Montenergro J, Santos MEA, Hoeksema BW, Ekins M, Ise Y, Higashiji T, Fernandez-Silva I, Reimer JD (2022) Evolution and phylogeny of glass-sponge-associated zoantharians, with a description of two new genera and three new species. Zoological Journal of the Linnean Society 194(1): 323–347. https://doi.org/10.1093/zoolinnean/zlab068

Kozlov AM, Darriba D, Flouri T, Morel B, Stamatakis A (2019) RAxML-NG: A fast, scalable and user-friendly tool for maximum likelihood phylogenetic inference. Bioinformatics (Oxford, England) 35(21): 4453–4455. https://doi.org/10.1093/bioinformatics/btz305

Medlin L, Elwood HJ, Stickel S, Sogin ML (1988) The characterization of enzymatically amplified eukaryotic 16S-like rRNA-coding regions. Gene 71(2): 491–499. https://doi.org/10.1016/0378-1119(88)90066-2

Montenegro J, Sinniger F, Reimer JD (2015) Unexpected diversity and new species in the sponge–Parazoanthidae association in southern Japan. Molecular Phylogenetics and Evolution 89: 73–90. https://doi.org/10.1016/j.ympev.2015.04.002

Rafinesque CS (1815) Analyse de la Nature ou Tableau de L'univers et des Corps Organisés. Palermo, 224 pp. https://doi.org/10.5962/bhl.title.106607

Rasband WS (2012) ImageJ: Image processing and analysis in Java. Astrophysics Source Code Library 1: e06013.

Reid REH (1958) A monograph of the upper cretaceous Hexactinellida of Great Britain and Northern Ireland. Part I. Paleontographical Society (Monographs) 111: 1–46. https://doi.org/10.1080/25761900.2022.12131673

Reid REH (1969) Notes on hexactinellid sponges: 5. *Verrucocoeloida* gen. nov., with a discussion of the genera *Verrucocoelia* Etallon and *Periphragella* Marshall. Journal of Natural History 3(4): 485–492. https://doi.org/10.1080/00222936900770411

Reimer JD, Sinniger F (2022) World list of Zoantharia. Zoantharia. World Register of Marine Species. https://www.marinespecies.org/aphia.php?p=taxdetails&id=100689 [on 2022-07-04]

Reimer JD, Takishita K, Ono S, Maruyama T (2007) Diversity and evolution in the zoanthid genus *Palythoa* (Cnidaria: Hexacorallia) based on nuclear ITS-rDNA. Coral Reefs 26(2): 399–410. https://doi.org/10.1007/s00338-007-0210-5

Reimer JD, Nonaka M, Sinniger F, Iwase F (2008) Morphological and molecular characterization of a new genus and new species of parazoanthid (Anthozoa: Hexacorallia: Zoantharia) associated with Japanese red coral (*Paracorallium japonicum*) in southern Japan. Coral Reefs 27(4): 935–949. https://doi.org/10.1007/s00338-008-0389-0

Reimer JD, Kise H, Santos MEA, Lindsay DJ, Pyle RL, Copus JM, Bowen BW, Nonaka M, Higashiji T, Benayahu Y (2019) Exploring the biodiversity of understudied benthic taxa at mesophotic and deeper depths: examples from the order Zoantharia (Anthozoa: Hexacorallia). Frontiers in Marine Science 6: e305. https://doi.org/10.3389/fmars.2019.00305

Reiswig HM, Kelly M (2017) Studies on Southwest Pacific Hexactinellida 1: Atlantisella lorraineae, a new glass sponge genus and species record for New Zealand. Memoirs of the Queensland Museum Nature 60: 91–99. https://doi.org/10.17082/j.2204-1478.60.2017.2016-16

Reiswig HM, Wheeler B (2002a) Family Euretidae Zittel, 1877. In: Hooper JNA, Van Soest RWM (Eds) Systema Porifera. A Guide to the Classification of Sponges. Plenum, New York, 1301–1331. https://doi.org/10.1007/978-1-4615-0747-5_135

Reiswig HM, Wheeler B (2002b) Family Tretodictyidae Schulze, 1886. In: Hooper JNA, Van Soest RWM (Eds) Systema Porifera. A Guide to the Classification of Sponges. Plenum, New York, 1341–1354. https://doi.org/10.1007/978-1-4615-0747-5_137

Ronquist FR, Huelsenbeck JP (2003) MRBAYES: Bayesian inference of phylogeny. Bioinformatics (Oxford, England) 19: 1572–1574. https://doi.org/10.1093/bioinformatics/btg180

Ryland JS, Lancaster JE (2004) A review of zoanthid nematocyst types and their population structure. Hydrobiologia 530(1–3): 179–187. https://doi.org/10.1007/s10750-004-2685-1

Schmidt O (1862) Die Spongien des adriatischen Meeres. Wilhelm Engelmann, Leipzig, viii + 1–88. [pls 1–7]

Schulze FE (1886) Über den Bau und das System der Hexactinelliden. Abhandlungen der Königlichen Akademie der Wissenschaften zu Berlin (Physikalisch-Mathematische Classe) 1886: 1–97.

Sinniger F, Montoya-Burgos JI, Chevaldonne P, Pawlowski J (2005) Phylogeny of the order Zoantharia (Anthozoa, Hexacorallia) based on the mitochondrial ribosomal genes. Marine Biology 147(5): 1121–1128. https://doi.org/10.1007/s00227-005-0016-3

Sinniger F, Reimer JD, Pawlowski J (2010) The Parazoanthidae (Hexacorallia: Zoantharia) DNA taxonomy: description of two new genera. Marine Biodiversity 40(1): 57–70. https://doi.org/10.1007/s12526-009-0034-3

Sinniger F, Ocaña OV, Baco AR (2013) Diversity of zoanthids (Anthozoa: Hexacorallia) on Hawaiian seamounts: description of the Hawaiian gold coral and additional zoanthids. PLoS ONE 8(1): e52607. https://doi.org/10.1371/journal.pone.0052607

Swain TD (2009) Phylogeny-based species delimitations and the evolution of host associations in symbiotic zoanthids (Anthozoa, Zoanthidea) of the wider Caribbean region. Zoological Journal of the Linnean Society 156(2): 223–238. https://doi.org/10.1111/j.1096-3642.2008.00513.x

Swain TD (2010) Evolutionary transitions in symbioses: Dramatic reductions in bathymetric and geographic ranges of Zoanthidea coincide with loss of symbioses with invertebrates. Molecular Ecology 19: 2587–2598. https://doi.org/10.1111/j.1365-294X.2010.04672.x

Swain TD, Schellinger JL, Strimaitis AM, Reuter KE (2015) Evolution of anthozoan polyp retraction mechanisms: convergent functional morphology and evolutionary allometry of the marginal musculature in order Zoanthidea (Cnidaria: Anthozoa: Hexacorallia.). BioMed Central Evolutionary Biology 15(1): 1–19. https://doi.org/10.1186/s12862-015-0406-1

Vaga CF, Santos MEA, Migotto AE, Reimer JD, Kitahara MV (2020) Octocoral-associated Parazoanthus cf. swiftii from the southwestern Atlantic. Marine Biodiversity 50(2): 17–17. https://doi.org/10.1007/s12526-020-01041-3

Wassilieff A (1908) Japanische actinien, in Doflein. Abhandlungen der Mathematisch-Physikalischen Klasse der Königlich Bayerischen Akademie der Wissenschaften 1: 1–49.

Supplementary material 1

GenBank accession numbers used for phylogenetic analyses in this study

Authors: Hiroki Kise, Miyuki Nishijima, Akira Iguchi, Junpei Minatoya, Hiroyuki Yokooka, Yuji Ise, Atsushi Suzuki

Data type: Accession numbers

Link: https://doi.org/10.3897/zookeys.1156.96698.suppl1

Supplementary material 2

Summary of deletions in the alignment of 16S-rDNA that characterize *Parachurabana* gen. nov.

Authors: Hiroki Kise, Miyuki Nishijima, Akira Iguchi, Junpei Minatoya, Hiroyuki Yokooka, Yuji Ise, Atsushi Suzuki

Data type: figure (eps file)

Link: https://doi.org/10.3897/zookeys.1156.96698.suppl2

Supplementary material 3

Bayesian-inference tree based on combined dataset of COI, 12S-rDNA, 16S-rDNA, 18S-rDNA, 28S-rDNA, and ITS-rDNA sequences. Number at nodes represent Bayesian posterior probabilities (>0.95)

Authors: Hiroki Kise, Miyuki Nishijima, Akira Iguchi, Junpei Minatoya, Hiroyuki Yokooka, Yuji Ise, Atsushi Suzuki

Data type: figure (pdf file)

Link: https://doi.org/10.3897/zookeys.1156.96698.suppl3

Supplementary material 4

Maximum-likelihood tree based on ITS-rDNA sequences. Number at nodes represent ML bootstrap values (>50% are shown)

Authors: Hiroki Kise, Miyuki Nishijima, Akira Iguchi, Junpei Minatoya, Hiroyuki Yokooka, Yuji Ise, Atsushi Suzuki

Data type: figure (pdf file)

Link: https://doi.org/10.3897/zookeys.1156.96698.suppl4

ZooKeys 1156: 87–106 (2023)
doi: 10.3897/zookeys.1156.101072
https://zookeys.pensoft.net

RESEARCH ARTICLE

A peer-reviewed open-access journal
ZooKeys
Launched to accelerate biodiversity research

Re-collected after 55 years: a new species of *Bembidion* (Coleoptera, Carabidae) from California

David R. Maddison[1], John S. Sproul[2], Kipling Will[3]

1 *Department of Integrative Biology, Oregon State University, Corvallis, OR 97331, USA* **2** *Department of Biology, University of Nebraska Omaha, Omaha, NE 68182, USA* **3** *Essig Museum of Entomology, University of California, Berkeley, CA 94720, USA*

Corresponding author: David R. Maddison (david.maddison@oregonstate.edu)

Academic editor: Borislav Guéorguiev | Received 27 January 2023 | Accepted 5 March 2023 | Published 27 March 2023

https://zoobank.org/1B321F54-0511-4933-9C86-9153655F0EA4

Citation: Maddison DR, Sproul JS, Will K (2023) Re-collected after 55 years: a new species of *Bembidion* (Coleoptera, Carabidae) from California. ZooKeys 1156: 87–106. https://doi.org/10.3897/zookeys.1156.101072

Abstract

A new species of the carabid beetle genus *Bembidion* Latreille is described from the Central Valley, Los Angeles Basin, and surrounding areas of California. *Bembidion brownorum* **sp. nov.** is a distinctive species, a relatively large member of the subgenus *Notaphus* Dejean, and within *Notaphus* a member of the *B. obtusangulum* LeConte species group. It has faint spots on the elytra and a large, convex, rounded prothorax. Of the 22 specimens from 11 localities, all but one were collected more than 55 years ago. Although the collection of the holotype in 2021 at UV light suggest the species is still extant, the lack of other recent specimens suggests the species may have a more restricted distribution than in the past, and its populations may be in decline.

Keywords

Bembidiini, DNA, ground beetle, molecular systematics, morphology, phylogeny, Trechinae

Introduction

Our knowledge of the North American carabid (ground beetle) fauna has benefitted from many decades of significant study and publication (e.g., Hatch 1953; Lindroth 1961–1969; Ball and Bousquet 2000; Bousquet 2012). However, the carabid fauna of the western and southern regions of the continent remains understudied, with distributional ranges, habitats, and life histories of the carabids in those regions still poorly documented and new species still to be discovered and described. To fill this knowledge gap, we have been sampling carabids in the western United States and Canada, frequently targeting areas that appear to have been little sampled.

With about 275 species described from the USA and Canada, *Bembidion* Latreille is the largest genus of carabid beetles in the region (and the world), and one of the groups most likely to contain undiscovered taxa (e.g., Maddison and Cooper 2014; Sproul and Maddison 2017a; Maddison 2020). These are small beetles, with adults of most species ranging between 3 and 6 mm in length. The majority of species live along the edges of bodies of water, from ocean shores and estuarian areas to pond shores and marshes, river and creek shores, and high-elevation snow fields, but some species are associated with grasslands, alpine meadows, and other areas far from open water. California has the richest fauna in North America, with over 120 species known.

Although within an hour's drive of the major metropolitan center of Sacramento, many parts of Colusa County, California remain unsampled and little represented in major California entomology collections. Most of the land in the county is privately owned and used for agricultural production, which limits opportunities for access and sampling. Somewhat serendipitously, access and permission to collect was obtained for a ranch, known locally as "Mountain House," in Colusa County. Over the course of two years, periodic sampling was conducted to determine the diversity of carabid beetles on the property.

Among the many insects sampled, a single specimen of *Bembidion* stood out as very distinctive (Fig. 1). It was somewhat similar in overall appearance to *Bembidion mormon* Hayward, *B. obtusangulum* LeConte, and *B. callens* Casey, all members of the subgenus *Notaphus* Dejean, but the specimen's morphological characteristics were unusual enough that it seemed likely that it belonged to a previously unknown species. Results of analyses of DNA sequence data from the specimen provided additional evidence that it was a new species.

The discovery of this single specimen motivated a search in major carabid collections in California for additional specimens. Only 21 additional specimens were located, all of which were collected more than 55 years ago. The distribution of specimens suggests this was a widespread species, but the lack of recently collected specimens suggests it may now be more restricted in distribution. Given the prospect of a declining and potentially threatened species, we felt it urgent to describe this species to spur the search for additional populations, and prompt research to better understand the species.

Figure 1. Holotype male of *Bembidion brownorum*.

Materials and methods

Members of *Bembidion* were examined from the collections listed below. Each collection's listing begins with the code used in the text.

BMEC Bohart Museum of Entomology, University of California, Davis, USA;
CAS California Academy of Sciences, San Francisco, USA;
CSAC California State Arthropod Collection, Sacramento, USA;
EMEC Essig Museum Entomology Collection, University of California, Berkeley, USA;
NMNH National Museum of Natural History, Washington, DC, USA;
OSAC Oregon State Arthropod Collection, Oregon State University, Corvallis, USA.

Morphological methods

General methods of specimen preparation for morphological work, and terms used, follow Maddison (1993, 2008). Genitalia were prepared, after dissection from the body, by treatment in 10% KOH at 65 °C for 10 minutes followed by multi-hour baths of distilled water, 5% glacial acetic acid, distilled water, and finally 100% ethanol. Male genitalia were then mounted in Euparal between two small coverslips attached to archival-quality heavyweight watercolor paper, and, once dried, pinned beneath the specimen.

Photographs of entire beetles, as well as the head and pronotum pictures, were taken with a Leica M165C dissecting scope and a Sony NEX-7 camera, and of male genitalia with a Leica DM5500B compound microscope and DMC425C camera. Microsculpture photographs were taken with a DMC425C camera attached to a DM5500B compound scope equipped with an X-Cite 110LED light source, which provides co-axial illumination, and a 20× epi-illumination objective lens. For all photographs of specimens or body parts, a stack of images from different focal positions was merged using the PMax procedure in Zerene Systems's Zerene Stacker; the final images thus potentially have some artefacts caused by the merging algorithm. Measurements were made using Leica Application Suite v. 4.9 from images acquired using either a Leica Z6 Apo lens and DMC4500 camera or a Leica DM5500B compound microscope and DMC425C camera.

Taxon sampling for DNA studies

We obtained new DNA sequence data for the holotype of *Bembidion brownorum* sp. nov. and 13 specimens of related species of *Bembidion*. These new data were combined with previously published data from six additional specimens (Maddison 2012; Sproul and Maddison 2017b). As *Bembidion flohri* Bates, *B. mormon*, *B. callens*, and *B. obtusangulum* appear to be the closest relatives of *B. brownorum* based upon a more extensive sampling of *Bembidion* (Maddison unpublished), we focused our sampling on those species, and included three additional species (*B. obtusidens* Fall, *B. scudderi* LeConte, and *B. consimile* Hayward) as outgroups (Tables 1, 2). All voucher specimens are deposited in OSAC except for the holotype of *B. brownorum* (deposited in EMEC) and the paralectotype of *B. callens* (specimen 4939, deposited in NMNH as specimen USNM.Ent.01114823).

Table 1. Sampling of members of *Bembidion* (*Notaphus*) for DNA-based study. Four-digit numbers under "#" are D.R. Maddison DNA voucher numbers, and an abbreviation for state or province of capture under "Loc"; further information on the newly sequenced specimens is given in Table 2. Other entries are GenBank accession numbers. Newly acquired sequences are those with accession numbers beginning with "OQ".

	#	Loc	28S	COI	CAD	Topo
Outgroups						
B. obtusidens	2042		KY246703	KY246743	KY246784	KY246824
B. scudderi	1471		OQ286105	OQ284076	OQ288589	OQ288575
B. consimile	2506		OQ286106	OQ284077	OQ288590	OQ288576
***obtusangulum* group**						
B. flohri	3049	AB	KY246708	KY246749	KY246789	KY246830
B. flohri	3046	OR	KY246707	KY246748	KY246788	KY246829
B. flohri	1753	NV	JN170340	JN171035	JN170807	JN171216
B. flohri	3061	UT	KY246709	KY246750	KY246790	KY246831
B. flohri	5234	NM	OQ286107	OQ284078	OQ288591	OQ288577
B. mormon	3044	OR	OQ286110	OQ284081	OQ288594	OQ288580
B. mormon	2142	UT	OQ286111	OQ284082	OQ288595	OQ288581
B. mormon	3045	UT	OQ286112	OQ284083	OQ288596	OQ288582
B. mormon	4977	NV	OQ286109	OQ284080	OQ288593	OQ288579
B. mormon	2039	CA	OQ286108	OQ284079	OQ288592	OQ288578
B. obtusangulum	2051	AB	JN170397	MF616907	JN170869	MF616774
B. obtusangulum	3151	AB	OQ286113	OQ284084	OQ288597	OQ288583
B. obtusangulum	3594	CO	OQ286115	OQ284086	OQ288599	OQ288585
B. obtusangulum	3043	CA	OQ286114	OQ284085	OQ288598	OQ288584
B. callens	4936	AZ	OQ286116	OQ284087	OQ288600	OQ288586
B. callens	4939	AZ	OQ286117	OQ284088	OQ288601	OQ288587
B. brownorum	5864	CA	OQ286118	OQ284089	OQ288602	OQ288588

Table 2. Locality information for specimens of *Bembidion* (*Notaphus*) analyzed for DNA. Four-digit numbers under "#" are D.R. Maddison DNA voucher numbers.

Species	#	Locality
B. obtusidens	2042	Canada: Alberta: Burbank, junction of Red Deer and Blindman Rivers, 52.3542°N, 113.7556°W
B. scudderi	1471	Canada: Alberta: Bow River at highway 36, 50.246°N, 112.077°W
B. consimile	2506	USA: Colorado: Huerfano Co., Butte Road at I-25, 1825m, 37.7454°N, 104.832°W
B. flohri	3049	Canada: Alberta: Birch Lake, 640 m, 53.362°N, 111.5231°W
B. flohri	3046	USA: Oregon: Harney Co., Harney Lake, NE corner, 1237 m, 43.2750°N, 119.0902°W
B. flohri	1753	USA: Nevada: Lyon Co., Carson River near Weeks, 390 m, 39.2866°N, 119.2778°W
B. flohri	3061	USA: Utah: Salt Lake Co., Great Salt Lake Marina, 1280 m, 40.7482°N, 112.1856°W
B. flohri	5234	USA: New Mexico: Torrance Co., Laguna del Perro, 1861 m, 34.6003°N, 105.9252°W
B. mormon	3044	USA: Oregon: Harney Co., 00 Ranch Road NW Harney Lake, 1240 m, 43.2804°N, 119.1976°W
B. mormon	2142	USA: Utah: Salt Lake Co., Great Salt Lake Marina, 390 m, 40.7482°N, 112.1856°W
B. mormon	3045	USA: Utah: Salt Lake Co., Great Salt Lake Marina, 1280 m, 40.7482°N, 112.1856°W
B. mormon	4977	USA: Nevada: Mineral Co., Walker Lake, Twenty Mile Beach, 1200 m, 38.7503°N, 118.7577°W
B. mormon	2039	USA: California: Inyo Co., Owens Lake, 1100 m, 36.4684°N, 117.8585°W
B. obtusangulum	2051	Canada: Alberta: Kenilworth Lake, 10.vi.1993. DRM 93.054
B. obtusangulum	3151	CANADA: Alberta: High Level, 330 m, 58.5073°N, 117.1385°W
B. obtusangulum	3594	USA: Colorado: Alamosa Co., Alamosa NWR, 2292 m, 37.4435°N, 105.7722°W
B. obtusangulum	3043	USA: California: Mono Co., Mono Lake, 1940 m, 37.97780°N, 119.13000°W
B. callens	4936	USA: Arizona: Coconino Co., Havasu Indian Reservation, Havasu Springs, 36.2176°N, 112.6871°W
B. callens	4939	USA: Arizona: Tucson
B. brownorum	5864	USA: California: Colusa Co. Antelope Valley, Freshwater Creek, 39.13841°N, 122.34621°W

DNA sequencing

Genes studied, and abbreviations used in this paper, are: **28S:** 28S ribosomal DNA (D1–D3 domains); **COI**: cytochrome c oxidase subunit I; **CAD**: part 4 of carbamoyl phosphate synthetase domain of the *rudimentary* gene; **Topo**: topoisomerase I.

For specimens collected into 95–100% ethanol (all but the paralectotype of *B. callens* DNA4939), DNA was extracted using a Qiagen DNeasy Blood and Tissue Kit. Fragments for the four genes were amplified using the Polymerase Chain Reaction on an Eppendorf Mastercycler Pro Thermal Cycler, using TaKaRa Ex Taq and the basic protocols recommended by the manufacturers. Primers and details of the cycling reactions used are given in Maddison (2012) and Maddison and Cooper (2014). The amplified products were then cleaned, quantified, and sequenced at the University of Arizona's Genomic and Technology Core Facility using a 3730 XL Applied Biosystems automatic sequencer. Assembly of multiple chromatograms for each gene fragment and initial base calls were made with Phred (Green and Ewing 2002) and Phrap (Green 1999) as orchestrated by Mesquite's Chromaseq package (Maddison and Maddison 2021a, c), with subsequent modifications by Chromaseq and manual inspection. Multiple peaks at a single position in multiple reads were coded using IUPAC ambiguity codes.

DNA extraction and sequencing of the paralectotype of *Bembidion callens* DNA4939 followed Sproul and Maddison (2017b). In brief, DNA in that specimen was extracted using the Qiagen QIAmp Micro Kit (using the standard protocol with carrier RNA added), with dual-index libraries prepared using the NEBNext DNA Ultra II kit (New England BioLabs), which were then sequenced on an Illumina HiSeq 3000, multiplexed on a 150-base paired-end lane at the Oregon State University Center for Quantitative Life Sciences. No other members of subgenus *Notaphus* were included on that lane. Approximately 66 million reads were obtained for the sample. Reads were processed in CLC Genomics Workbench (CLCGW) v. 22.0. Reads were trimmed to eliminate low-quality ends (limit = 0.000316, corresponding to a quality score of 35) and to remove adapter sequences. The number of reads left after trimming was approximately 46 million. De novo assemblies were generated using CLCGW from paired, trimmed reads using an automatic word and bubble size, with the minimum contig length set to 200. The de novo assemblies were converted to BLASTable databases using NCBI's makeblastdb tool and BLASTed using Mesquite's (Maddison and Maddison 2021c) local BLAST tool (1E-30 as the e-value cutoff for nuclear protein-coding genes, and 1E-100 the cutoff for COI and 28S) using as query sequences the sequences of the four target genes from *B. mormon* DNA3045. For each gene, only one contig was returned; these hits were BLASTed to NCBI's GenBank, and in all cases returned *Bembidion* as the top match.

Newly acquired sequences are all of "genseq-4" (Chakrabarty et al. 2013), except for those of the holotype of *B. brownorum* (specimen 5864) which are "genseq-1", and those of the paralectotype of *B. callens* (specimen 4939), which are "genseq-2".

Alignment and data exclusion

COI, CAD, and Topo were easily aligned by eye, as there were no insertions or deletions (indels) evident in the sampled sequences. Alignment of 28S was conducted in MAFFT v. 7.130b (Katoh and Standley 2013) using the L-INS-i search option and otherwise default parameter values. In general, no sites were excluded from analyses, except at the 5' and 3' ends of the alignments; those regions were excluded, as they were mostly missing data, containing data from only a small fraction of the samples because of variation in the length of the sequences that were obtained.

Phylogenetic analyses

A maximum-likelihood (ML) analysis was conducted for each gene individually using IQ-TREE v. 2.1.3 (Nguyen et al. 2015), as orchestrated by Mesquite's Zephyr package (Maddison and Maddison 2021b, c). The ModelFinder feature within IQ-TREE (Kalyaanamoorthy et al. 2017) was used to find the optimal character evolution models. The MFP model option was used for 28S, and the TESTMERGE option for protein-coding genes. The TESTMERGE option sought the optimal partition of sites, beginning with the codon positions in different parts. Fifty searches were conducted for the ML tree for each matrix analyzed. In addition, analyses of a matrix formed by concatenation of all four gene fragments were conducted, with the TESTMERGE option also being used, beginning with each codon position for each gene as a separate part (thus, the analysis began allowing for up to 10 parts: three for each of the three protein-coding genes, and one for 28S). Fifty searches were conducted for the ML tree. For standard, non-parametric bootstrap analysis of the concatenated data, 500 replicates were used.

Data availability

Sequences of the studied genes have been deposited in GenBank with accession numbers OQ284076 to OQ284089, OQ286105 to OQ286118, and OQ288575 to OQ288602. Files containing the untrimmed gene sequences for each specimen as well as the inferred trees for each gene have been deposited in Dryad (data available from the Dryad Digital Repository at https://doi.org/10.6078/D17416.

Results

Molecular and phylogenetic results

The single specimen of *Bembidion brownorum* sequenced is quite distinctive in DNA sequences of 28S, COI, and Topo, and clearly outside the bounds of sequence variation in the other species sampled. This is evident both by the gene trees (Fig. 2) and by the details

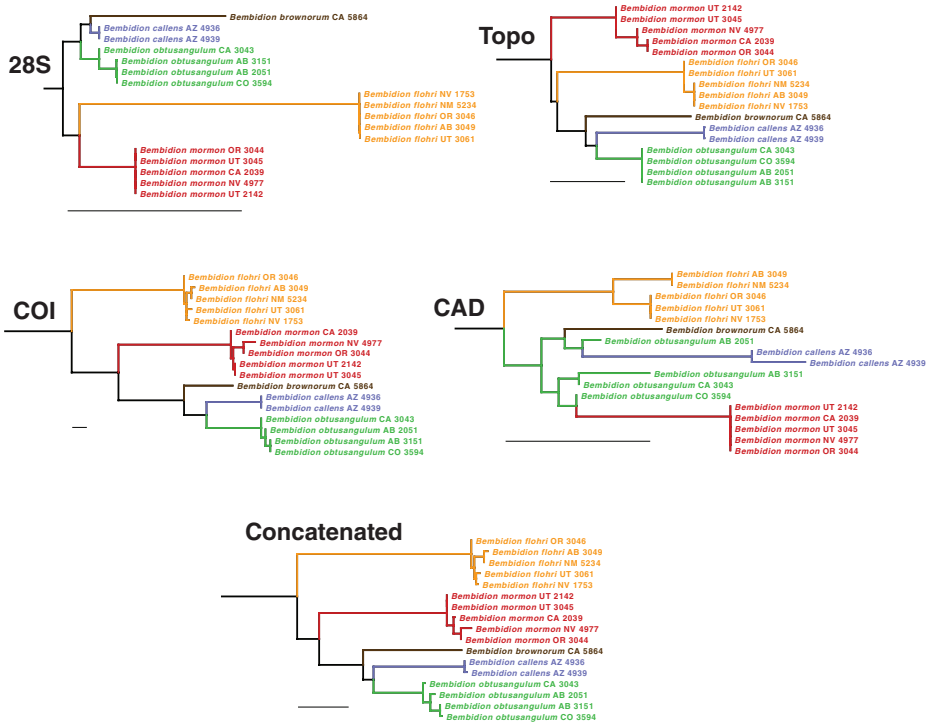

Figure 2. Maximum-likelihood trees of the *Bembidion obtusangulum* group for four individual genes as well as the concatenated matrix. Scale bars: 0.01 nucleotide substitutions per nucleotide site, as reconstructed by IQ-TREE. Outgroups not shown; in all single-gene and concatenated analyses, the five species shown here formed a clade, with a bootstrap value of 100% in the concatenated analysis.

of variation. *Bembidion brownorum* differs from all specimens of the morphologically most similar species, *B. mormon*, at 13 bases in 28S, 44 bases in COI (6.7% divergence), two amino acids in CAD, and one amino acid in Topo. It differs from *B. callens*, which appears as a member of its sister group, at seven bases in 28S, 28 bases in COI (4.3% divergence), and three amino acids in CAD, and from the other member of its sister group, *B. obtusangulum*, at nine bases in 28S, and 33 bases in COI (5.0% divergence).

Three of the genes (28S, COI, and Topo) individually suggest that the nearest relatives of *B. brownorum* are *B. callens* and *B. obtusangulum*; in the ML tree of the concatenated matrix of all four genes, the latter two species form a clade with *B. brownorum* as its sister group (Fig. 2). The bootstrap value for the concatenated matrix for this sister-group relationship is 68%.

Morphological results

Bembidion brownorum has a distinctively convex and rounded prothorax (Fig. 3A) in addition to other characteristics that distinguish it from additional members of the subgenus *Notaphus*, as documented in the Taxonomic Treatment section below.

Figure 3. Habitus of members of the *Bembidion obtusangulum* species group **A** *Bembidion brownorum*, holotype male **B** *Bembidion mormon* male **C** *Bembidion callens* (paralectotype) female **D** *Bembidion obtusangulum* male. Scale bars: 1 mm.

Taxonomic treatment

To accommodate *B. brownorum*, couplet 169 in Lindroth's (1963) key can be modified into a triplet as follows (figure numbers refer to those in Lindroth (1963) except as specified):

169 3.5–4.0 mm. Upper surface unmetallic. Prothorax with evident latero-basal carina (fig. 171b) ..... **102. *B. nudipenne***

– 4.4–5.0 mm. Upper surface unmetallic or only slightly metallic. Latero-basal carina evident, long (this paper, Fig. 4B). Prothorax broad and very convex (this paper, Fig. 1). California ..... ***B. brownorum***

– 4.3–5.9 mm. Metallic above. Latero-basal carina thin, usually rudimentary, or absent (fig. 187). Prothorax convex..... **171**

***Bembidion brownorum* Maddison, Sproul & Will, sp. nov.**
https://zoobank.org/3B2A0EB4-D01A-4FBA-AE98-6898FDAF878D

Type materials. ***Holotype.*** Male, in EMEC, herein designated, labeled: "39.13841/–122.34621 USA: California: Colusa Co. Antelope Valley, Freshwater Creek uv light pan trap 133 m. 1.vii.2021 K.Will [Cal2021.vii.1.2]", "David R. Maddison DNA5864 DNA Voucher" [pale green paper], "HOLOTYPE Bembidion brownorum Maddison, Sproul, & Will" [partly handwritten, on red paper], "UC Berkeley EMEC 347587" [with matrix code on right side]. Genitalia mounted in Euparal in between coverslips pinned with specimen; extracted DNA stored separately. GenBank accession numbers for DNA sequences of the holotype are OQ284089, OQ286118, OQ288588, and OQ288602.

Paratypes. (13 males, 8 females). "Borax Lake, Lower Lake, Lake Co., Cal. May 14 1922" (2, CAS). "Atwater, Merced Co., Calif 15 Aug 1966" (5, CAS, OSAC). "Wood L., Tulare Co., Calif. Rotary Trap V-22-1947 Norman W. Frazier, EMEC347588" (1, EMEC). "Wood L., Tulare Co., Calif. Rotary Trap V-24-1947 Norman W. Frazier EMEC347589" (1, EMEC). "Redondo, Cal." (1, CAS). "Pasadena, Cal." (3, CAS). "San Joaquin Mill Tulare Co., Calif. May 15, 3800 ft" (2, CAS). "Azusa, Cal." (1, CAS). "Riverside, Cal. F.E. Winters" (1, CAS). "CALIF: Forest Home, San Bernardino Mts, 6000 ft. May" (1, CAS). "Poway, San Diego Co., Cal." (2, CAS). "S. Cal" (1, CAS).

Type locality. USA: California: Colusa Co. Antelope Valley, Freshwater Creek, 39.13841°N, 122.34621°W (Fig. 5).

Derivation of specific epithet. The specific epithet *brownorum* is treated as a noun in the genitive case and refers to Jerry and Anne Brown, former Governor and First Lady of California, respectively. The name is formed in their honor as it was their hospitality and openness to allowing access for research of insects on their ranch, the type locality, which led to the discovery of this species. Additionally, this honors their long commitment to environmentalism and continued efforts in the international climate-change movement.

Diagnosis. A relatively large *Bembidion* (*Notaphus*), superficially similar to *B. mormon* (with which it has been confused in collections), with which it shares a pale subapical band on the elytra. However, *B. brownorum* has a much more convex pronotum, giving it an inflated appearance; the pronotum has more rounded sides and is more constricted posteriorly. From *B. callens* and *B. obtusangulum*, in addition to the prothorax shape, it is distinguished by presence of pale elytral spots, which those two species lack.

Description (based upon the holotype and 21 paratypes). Body length 4.4–5.0 mm. Body dark brown or dark reddish brown, with head and pronotum slightly darker than elytra; elytra each with one diffuse pale spot at about the posterior fourth. Legs uniform in color, reddish brown; antennae brown, with first antennomere paler, at least ventrally. Mentum with anterior lateral regions large, with apical portion broadly rounded, not angulate; medial tooth simple (not bifid) with truncate tip; frontal furrows weakly defined, shallow; eyes prominent (Fig. 4A). Prothorax large, notably convex, with sides strikingly rounded such that the width at middle is much greater than the width at the posterior margin, with sides immediately front of hind angle slightly sinuate (Fig. 4B); hind angle slightly obtuse; posterolateral carina well defined, moderately long; posterior region of pronotum slightly rugose. Elytra with lateral bead not prolonged medially at shoulder; all striae complete, striatopunctate, with much smaller punctures in the posterior half. Microsculpture present on most of the dorsal surface of the body except for the disc of the pronotum, which is glossy; evident in both sexes over entire surface of elytra, consisting of sculpticells that are slightly transverse, more deeply engraved in females (Fig. 6B) than in males (Fig. 6A); female elytra thus matte. Pronotum with two lateral setae on each side; elytron with two setae in third interval. Aedeagus (Fig. 6C) typical for a member of subgenus *Notaphus*.

Flight ability. All 18 specimens examined for wing condition are macropterous. The capture of two specimens from Woodlake in a rotary trap (Winkler 1949) and the capture of the holotype at a UV light both suggest that these beetles can fly.

Geographic variation. None noted.

Geographic distribution. Central Valley, Los Angeles Basin, and surrounding areas of California (Fig. 7). Two of the localities on the map are marked as uncertain: those labeled as from Forest Home and Redondo. The Forest Home locality is at much higher elevation than all other specimens (6000 ft). Based upon the labeling on other specimens from the F.E. Winters collection, the hand-written label attached to this specimen appears not to be an original label, and we have doubts about the validity of the data on the label. We have some doubts about the locality for the specimen labeled "Redondo", as there are at least seven localities in California that include "Redondo" in the name (USGS Geographic Names Information System, https://edits.nationalmap.gov/apps/gaz-domestic/public/search/names). An additional locality, "San Joaquin Mill Tulare Co., Calif 3800 ft" was not mapped as we could not determine the site with any certainty.

Figure 4. Head and pronotum of holotype of *Bembidion brownorum*. Scale bar: 0.5 mm.

Habitat. The only specimen with detailed collecting data including an exact locality is the holotype. Because it was collected at a UV light, the specimen was not found in its natural microhabitat, and we do not know how far it had flown from a suitable habitat.

Figure 5. Type locality of *Bembidion brownorum*. USA: California: Colusa Co. Antelope Valley, Freshwater Creek, 39.13841°N, 122.34621°W. Image taken November 2022.

However, the type locality might provide some hints about possible habitat of the species. The type locality lies on the east side of Antelope Valley in the northern part of the Cortina Ridge, which marks the western edge of the Colusa Basin region of the Sacramento Valley. The ridge is formed of tilted sandstone beds, mudstone, and siltstone formed from the eroded sediments of the Sierran–Klamath terrane. As members of subgenus *Notaphus* are almost universally found at the edges of bodies of water (with exceptions for some species found at high elevation), we expect *B. brownorum* to live on lake, pond, marsh, river, or creek shores. The UV light was set up next to Freshwater Creek (Fig. 5), which might be the habitat of the specimen. Freshwater Creek cuts through Cortina Ridge; its bed is composed of consolidated claystone and lenses of poorly hardened conglomerate, sandstone, and siltstone. The stream is somewhat trellis-like, with persistent pools, due to the presence of minor ridges of erosion-resistant materials. The current dominant vegetation consists of grasses, cattails, willows, and rushes near the stream. Sparsely set oaks line the stream edge and lateral drainages. Water is persistent and flows on the surface in portions of the stream throughout the year. Evaporation along the stream margin intermittently creates a hardened crust of white mineral deposits that often overlays a black, highly organic mud in depositional stretches. Narrow, steep-sided sections of the stream have banks composed of exfoliating claystone and

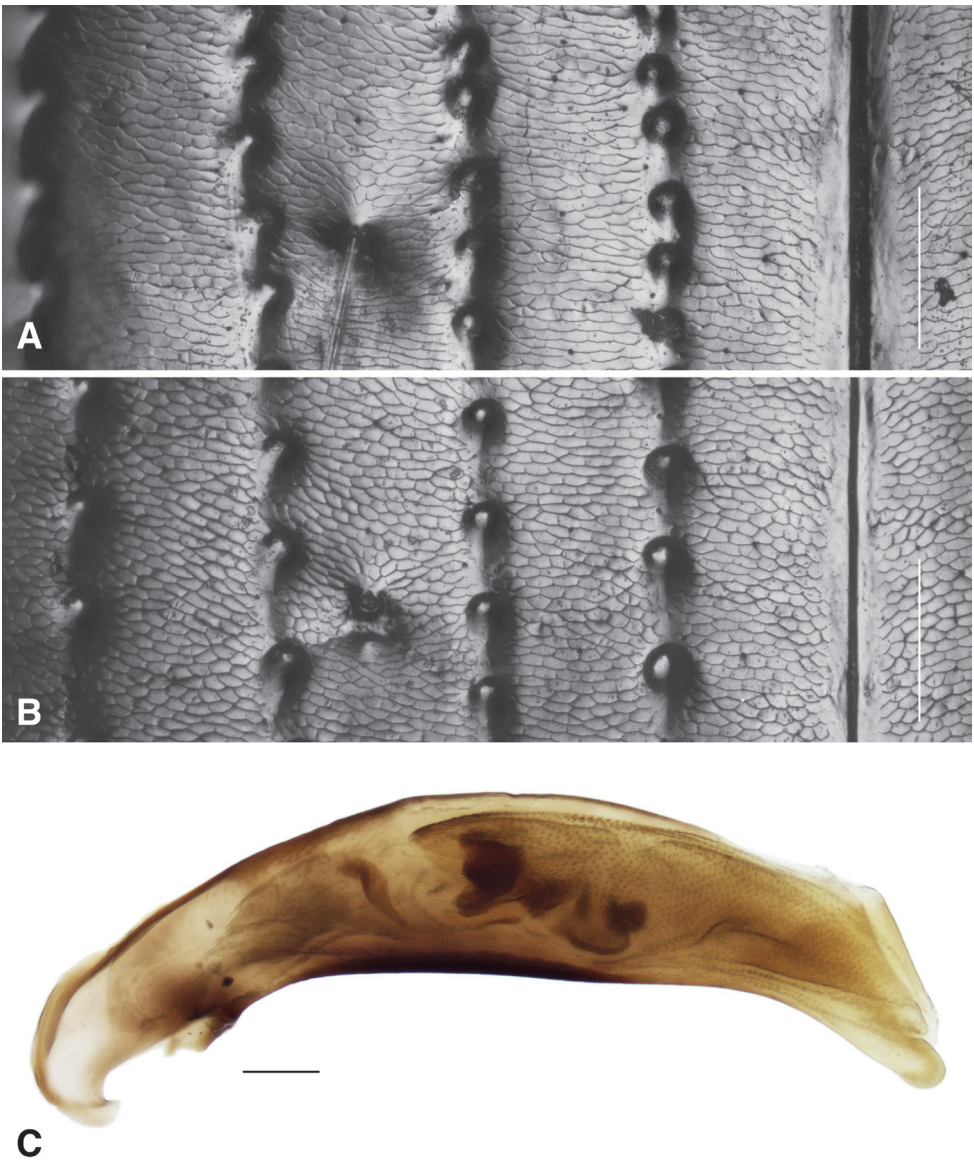

Figure 6. Microsculpture and aedeagus of *Bembidion brownorum* **A** elytral microsculpture around seta ed3 of holotype male **B** elytral microsculpture around seta ed3 of a female from Woodlake **C** aedeagus of holotype male. Scale bars: 100 μm.

mud from eroded topsoil. The adjacent land was historically used for crop production, e.g., barley, but the land and water has primarily been used for cattle ranching. Both the stream bed and adjacent area show the impact of many years of cattle grazing. There is an historical account of beaver damming (J. Brown pers. com.) but there is presently no impact of this event. There is no evidence that the water flow has been artificially dammed, channelized, or diverted in the collection area. As such, this stretch of

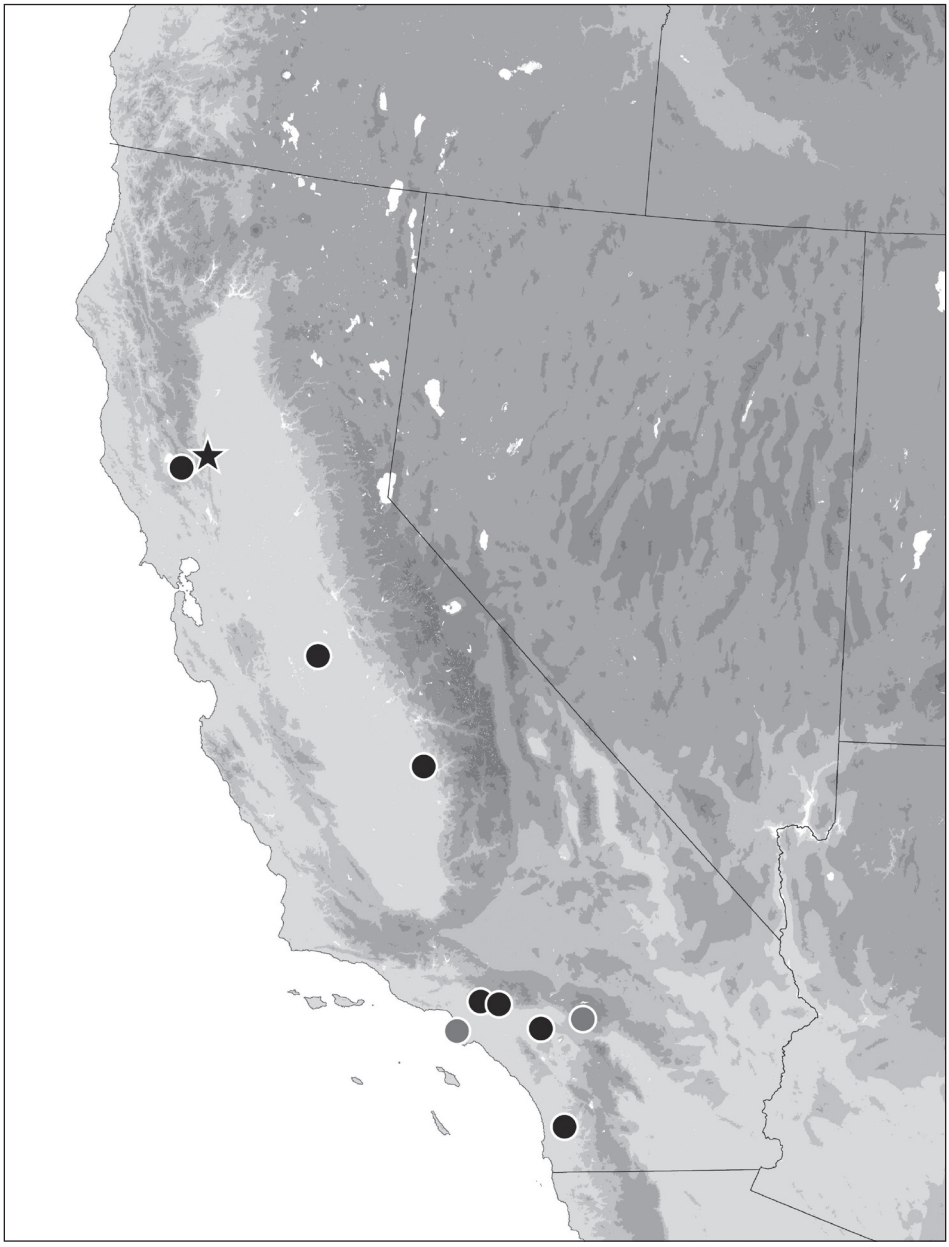

Figure 7. Geographic distribution of *Bembidion brownorum* in California. The locality indicated with a star is the type locality. The two localities indicated by gray dots are uncertain or doubtful. Darker gray areas in the base map represent higher elevations.

Freshwater Creek represents a relatively unaltered, natural, perennial source of surface water—unusual in the Central Valley and adjacent foothills of California. However, we consider evidence for *B. brownorum* being a stream-shore species very weak, as it is based upon only one specimen which might have flown in from some distance.

The other known localities do not clearly suggest a specific habitat, nor do the known localities of related species. *Bembidion brownorum* localities include a lake with sodium borate deposits (Borax Lake, Lake County), a city with a lake with extensive, flat shores (Bravo Lake in Woodlake), and a site near the Pacific Ocean that once had a salt lake (Redondo). At least the latter two are habitats similar to the saline, pond and lake shore habitats frequented by *B. obtusangulum* and *B. mormon*, near relatives of *B. brownorum*. The specimen labeled as from 6000 feet elevation at Forest Home, San Bernardino Mts (presumably around 34.083°N, 116.893°W) suggest instead a less saline, creek shore habit, but we doubt the veracity of that label (see above). The only specimen of the related *B. callens* with known habitat data is a specimen collected by Larry Stevens in gravel around the calcium-carbonate-rich waters of Havasu Springs, Arizona, at 36.2176°N, 112.6871°W (Larry Stevens pers. comm. 2022).

Discussion

Much attention has recently been drawn to the apparent decline of insect populations (Sánchez-Bayo and Wyckhuys 2019; Wagner 2020; Wagner et al. 2021). Given the many, significant changes brought about by human activities, which range in scale from local and ephemeral to global and long-term, substantial changes in insect abundance and species assemblages are not surprising. Even in the absence of apparent changes in measures like species richness, insect assemblages may be homogenized with increases in generalist species and species that can take advantage of human habitat alterations (Ball-Damerow et al. 2014). Among carabid beetles, species decline and apparent extinction have been recently documented (Kotze and O'Hara 2003; Knisley and Fenster 2005; Brandmayr et al. 2009), and a number of traits have been hypothesized as being linked to decline and extinction risk (Kotze and O'Hara 2003; Nolte et al. 2019). Examples of these risk-linked traits are (1) habitat specialization, (2) small distributional range, (3) large body size, and (4) being either monomorphic macropterous or brachypterous. Bad luck (sensu Samways 2006) also plays a role, in that narrow habitat requirements or restricted ranges may coincide with human land use priorities that impact beetles. Among carabid beetles, there are notable examples of unlucky species from California. For example, the southern subspecies of the Golden Bear Harpaline (*Dicheirus dilatatus angulatus* Casey) is hypothesized to have been impacted by annual fire break disturbance (Noonan 1968), transformation of seasonal wetlands to agricultural production that reduced available habitat significantly impacted the Delta Green Ground Beetle (*Elaphrus viridis* Horn) (Arnold and Kavanaugh 2021), and urban development and general habitat degradation have ongoing effects on the Ohlone Tiger Beetle (*Cicindela ohlone* Freitag & Kavanaugh) (Knisley and Arnold 2013).

It is likely that *B. brownorum* is yet another unlucky carabid beetle species. After our initial collection and recognition of *B. brownorum* we searched relevant collections for additional specimens. The small number of specimens located were only found in the EMEC and CAS collections, both with significant quantities of older material,

including substantial holdings from pre-1950 (https://essig.berkeley.edu/museum-history/, https://www.calacademy.org/scientists/entomology-information-page#history). Despite having considerable and important carabid beetle holdings, no specimens were found in the CSAC and BMEC collections, which almost exclusively have specimens collected after 1970. Prior to 2021, the most recent specimen is from Atwater, California, collected in 1966. The only other specimens with an explicit date are from the 1940s. The undated specimens have labels in styles that suggest they are at least as old or older than those with dates. For example, specimens of the F.E. Winters collection in CAS and EMEC are typically from collecting events in the early twentieth century, up to about 1930. Such a long gap in sampling may be indicative of species deterioration but can also be the result of a lack of sampling (i.e., "Wallacean extinction" of Ladle and Jepson 2008) or the lack of available taxonomic expertise (also a resource in significant decline). Various factors can affect repeat collection of a given species, such as range size, collecting effort, habitat access, and collectability (Ladle et al. 2011).

Bembidion brownorum's large range (Fig. 7) and small body size suggest that it should be resistant to decline, but its apparent monomorphic macroptery could be a risk factor (Kotze and O'Hara 2003; Scheffers et al. 2011; Nolte et al. 2019). Additionally, given its large range and that these beetles are attracted to lights, frequent collection would be expected even though its small size might cause it to be missed during visual-search collecting by general collectors and despite habitat access issues in California. Other species collected abundantly in light traps in 2021 from Colusa County, such as *Stenolophus* (*Stenolophus*) *anceps* LeConte, *Stenolophus* (*Stenolophus*) *limbalis* LeConte, and *Pseudaptinus* (*Pseudaptinus*) *tenuicollis* (LeConte), *Bembidion* (*Trepanedoris*) *connivens* (LeConte), *Bembidion* (*Furcacampa*) *timidum* (LeConte), and *Bembidion* (*Notaphus*) *approximatum* (LeConte), are represented in all the collections we surveyed, in very large numbers, and across the full distributional and temporal range. These observations suggest that *B. brownorum* has likely experienced a significant decline in population numbers, and that the lack of recently collected specimens is not simply because it has been missed or overlooked by collectors.

Though details on the microhabitat are unknown, it seems probable that habitat specialization and the degradation of that habitat led to this species' decline. At a very general level, most of the locations at which *B. brownorum* was historically collected presently have no apparent, natural habitat, and are entirely highly developed (Atwater, Woodlake, Redondo [Beach], Pasadena, and Azusa) or are largely developed with little potential habitat (Riverside and Poway). Perhaps the Borax Lake region, which is only 33 km southwest of the type locality, holds the best odds for a persistent population. In addition, lakes near previous localities may also harbor populations (e.g., Bravo Lake, within 4 km of the Woodlake collection site, or East Park Reservoir, about 25 km NNE of the type locality, or Indian Valley Reservoir, about 17 km W of the type locality).

The recent collection of *B. brownorum* raises our hopes that the species persists in more locations, and we encourage efforts to sample for it, but we are concerned that the species still has the potential to disappear forever. Rediscovery or re-collection does

not mean a species is doing well. As pointed out by Scheffers et al. (2011), "88% of rediscovered [vertebrate] species are currently threatened" and declining abundance leads to declining detectability, making the job of conservation even harder. Will populations of this, and other imperiled species, be located before the many sources of disturbance (e.g., invasive species, habitat loss, pesticide exposure, and climate change) drive them to extinction?

Acknowledgements

We thank Jerry and Anne Brown for allowing access to their property and encouraging collecting and research activities. We thank collection personnel of the entomological collections for allowing us to examine their holdings and borrow materials, in particular Christopher Grinter (CAS), Lynn Kimsey (BMEC), and Martin Hauser (CSAC). We thank Larry Stevens (Springs Stewardship Institute) for sending the specimen of *Bembidion callens* from Havasu Springs. For performing some of the PCR reactions on which the DNA sequence data in this paper is based, we thank Tiana S.L. Week, Danielle L. Mendez, Estany Campbell-Dunfee, and Joseph J. Dubie. We thank Borislav Guéorguiev, Luca Toledano, David H. Kavanaugh, and an anonymous reviewer for their thoughtful reviews of the manuscript.

This project was supported by the Harold E. and Leona M. Rice Endowment Fund at Oregon State University.

References

Arnold RA, Kavanaugh DH (2021) Geographic distribution and habitat characterization of the threatened Delta Green Ground Beetle, *Elaphrus viridis* Horn, 1878 (Coleoptera: Carabidae), in the Jepson Prairie Region of Solano County, California, USA. Coleopterists Bulletin 75(3): 519–530. https://doi.org/10.1649/0010-065X-75.3.519

Ball GE, Bousquet Y (2000) Carabidae Latreille, 1810. In: Arnett RH, Thomas Jr MC (Eds) American Beetles (Vol. 1). Archostemata, Myxophaga, Adephaga, Polyphaga: Staphyliniformia. CRC Press, Boca Raton, 32–132.

Ball-Damerow JE, M'Gonigle LK, Resh VH (2014) Changes in occurrence, richness, and biological traits of dragonflies and damselflies (Odonata) in California and Nevada over the past century. Biodiversity and Conservation 23(8): 2107–2126. https://doi.org/10.1007/s10531-014-0707-5

Bousquet Y (2012) Catalogue of Geadephaga (Coleoptera, Adephaga) of America, north of Mexico. ZooKeys 245: 1–1722. https://doi.org/10.3897/zookeys.245.3416

Brandmayr P, Pizzolotto R, Colombetta G, Zetto T (2009) In site extinction of carabid beetles and community changes in a protected suburban forest during the past century: The "Bosco Farneto" near Trieste (Italy). Journal of Insect Conservation 13(2): 231–234. https://doi.org/10.1007/s10841-008-9161-6

Chakrabarty P, Warren M, Page LM, Baldwin CC (2013) GenSeq: An updated nomenclature and ranking for genetic sequences from type and non-type sources. ZooKeys 346: 29–41. https://doi.org/10.3897/zookeys.346.5753

Green P (1999) Phrap. Version 0.990329. http://phrap.org

Green P, Ewing B (2002) Phred. Version 0.020425c. http://phrap.org

Hatch MH (1953) The Beetles of the Pacific Northwest. Part I: Introduction and Adephaga. University of Washington, Seattle, 340 pp.

Kalyaanamoorthy S, Minh BQ, Wong TKF, von Haeseler A, Jermiin LS (2017) ModelFinder: Fast model selection for accurate phylogenetic estimates. Nature Methods 14(6): 587–589. https://doi.org/10.1038/nmeth.4285

Katoh K, Standley DM (2013) MAFFT multiple sequence alignment software version 7: Improvements in performance and usability. Molecular Biology and Evolution 30(4): 772–780. https://doi.org/10.1093/molbev/mst010

Knisley CB, Arnold RA (2013) Biology and conservation of *Cicindela ohlone* Freitag and Kavanaugh, the endangered Ohlone Tiger Beetle (Coleoptera: Carabidae: Cicindelinae). I. Distribution and natural history. Coleopterists Bulletin 67(4): 569–580. https://doi.org/10.1649/0010-065X-67.4.569

Knisley CB, Fenster MS (2005) Apparent extinction of the tiger beetle, *Cicindela hirticollis abrupta* (Coleoptera: Carabidae: Cicindelinae). Coleopterists Bulletin 59(4): 451–458. https://doi.org/10.1649/799.1

Kotze DJ, O'Hara RB (2003) Species decline–But why? Explanations of carabid beetle (Coleoptera, Carabidae) declines in Europe. Oecologia 135(1): 138–148. https://doi.org/10.1007/s00442-002-1174-3

Ladle RJ, Jepson P (2008) Toward a biocultural theory of avoided extinction. Conservation Letters 1(3): 111–118. https://doi.org/10.1111/j.1755-263X.2008.00016.x

Ladle R, Jepson P, Malhado ACM, Jennings S, Barua M (2011) The causes and biogeographical significance of species' rediscovery. Frontiers of Biogeography 3(3): 111–118. https://doi.org/10.21425/F5FBG12432

Lindroth CH (1963) The ground-beetles (Carabidae, excl. Cicindelinae) of Canada and Alaska. Part 3. Opuscula Entomologica (Supplementum 24): 201–408.

Lindroth CH (1961–1969) The ground-beetles (Carabidae, excl. Cicindelinae) of Canada and Alaska. Parts 1–6. Opuscula Entomologica Supplementum 20, 24, 29, 33, 34, 35: 1–1192.

Maddison DR (1993) Systematics of the Holarctic beetle subgenus *Bracteon* and related *Bembidion* (Coleoptera: Carabidae). Bulletin of the Museum of Comparative Zoology 153: 143–299.

Maddison DR (2008) Systematics of the North American beetle subgenus *Pseudoperyphus* (Coleoptera: Carabidae: *Bembidion*) based upon morphological, chromosomal, and molecular data. Annals of the Carnegie Museum 77(1): 147–193. https://doi.org/10.2992/0097-4463-77.1.147

Maddison DR (2012) Phylogeny of *Bembidion* and related ground beetles (Coleoptera: Carabidae: Trechinae: Bembidiini: Bembidiina). Molecular Phylogenetics and Evolution 63(3): 533–576. https://doi.org/10.1016/j.ympev.2012.01.015

Maddison DR (2020) Shards, sequences, and shorelines: Two new species of *Bembidion* from North America (Coleoptera, Carabidae). ZooKeys 1007: 85–128. https://doi.org/10.3897/zookeys.1007.60012

Maddison DR, Cooper KW (2014) Species delimitation in the ground beetle subgenus *Liocosmius* (Coleoptera: Carabidae: *Bembidion*), including standard and next-generation sequencing of museum specimens. Zoological Journal of the Linnean Society 172(4): 741–770. https://doi.org/10.1111/zoj.12188

Maddison DR, Maddison WP (2021a) Chromaseq: a Mesquite package for analyzing sequence chromatograms. Version 1.53. http://chromaseq.mesquiteproject.org

Maddison DR, Maddison WP (2021b) Zephyr: a Mesquite package for interacting with external phylogeny inference programs. Version 3.20. http://zephyr.mesquiteproject.org

Maddison WP, Maddison DR (2021c) Mesquite: a modular system for evolutionary analysis. Version 3.70. http://www.mesquiteproject.org

Nguyen L-T, Schmidt HA, von Haeseler A, Minh BQ (2015) IQ-TREE: A fast and effective stochastic algorithm for estimating maximum-likelihood phylogenies. Molecular Biology and Evolution 32(1): 268–274. https://doi.org/10.1093/molbev/msu300

Nolte D, Boutaud E, Kotze DJ, Schuldt A, Assmann T (2019) Habitat specialization, distribution range size and body size drive extinction risk in carabid beetles. Biodiversity and Conservation 28(5): 1267–1283. https://doi.org/10.1007/s10531-019-01724-9

Noonan GR (1968) A revision of the genus *Dicheirus* Mannerheim 1843. Opuscula Entomologica 33: 281–304.

Samways MJ (2006) Insect extinctions and insect survival. Conservation Biology 20(1): 245–246. https://doi.org/10.1111/j.1523-1739.2006.00349.x

Sánchez-Bayo F, Wyckhuys KAG (2019) Worldwide decline of the entomofauna: A review of its drivers. Biological Conservation 232: 8–27. https://doi.org/10.1016/j.biocon.2019.01.020

Scheffers BR, Yong DL, Harris JBC, Giam X, Sodhi NS (2011) The world's rediscovered species: Back from the brink? PLoS ONE 6(7): e22531. https://doi.org/10.1371/journal.pone.0022531

Sproul JS, Maddison DR (2017a) Cryptic species in the mountaintops: species delimitation and taxonomy of the *Bembidion breve* species group (Carabidae: Coleoptera) aided by genomic architecture of a century-old type specimen. Zoological Journal of the Linnean Society 183: 556–583. https://doi.org/10.1093/zoolinnean/zlx076

Sproul JS, Maddison DR (2017b) Sequencing historical specimens: Successful preparation of small specimens with low amounts of degraded DNA. Molecular Ecology Resources 17(6): 1183–1201. https://doi.org/10.1111/1755-0998.12660

Wagner DL (2020) Insect declines in the Anthropocene. Annual Review of Entomology 65(1): 457–480. https://doi.org/10.1146/annurev-ento-011019-025151

Wagner DL, Grames EM, Forister ML, Berenbaum MR, Stopak D (2021) Insect decline in the Anthropocene: Death by a thousand cuts. Proceedings of the National Academy of Sciences of the United States of America 118(2): e2023989118. https://doi.org/10.1073/pnas.2023989118

Winkler A (1949) Pierce's disease investigations. Hilgardia 19(7): 207–264. https://doi.org/10.3733/hilg.v19n07p207

ZooKeys 1156: 107–131 (2023)
doi: 10.3897/zookeys.1156.84943
https://zookeys.pensoft.net

RESEARCH ARTICLE

A peer-reviewed open-access journal
ZooKeys
Launched to accelerate biodiversity research

Phylogeography of *Falagonia mexicana* Sharp, 1883 (Coleoptera, Staphylinidae, Aleocharinae)

Justo A. Reyes[1], Alejandro Espinosa de los Monteros[2], Quiyari J. Santiago-Jiménez[1]

1 *Facultad de Biología-Xalapa, Universidad Veracruzana, Zona Universitaria, Circuito Gonzalo Aguirre Beltrán s/n, Xalapa, Veracruz, 91090, Mexico* **2** *Departamento de Biología Evolutiva, Laboratorio de Sistemática Filogenética, INECOL, Carretera Antigua a Coatepec No. 351, Xalapa, Veracruz, 91070, Mexico*

Corresponding authors: Quiyari J. Santiago-Jiménez (qsantiago@uv.mx);
Alejandro Espinosa de los Monteros (alejandro.espinosa@inecol.mx)

Academic editor: Adam Brunke | Received 8 April 2022 | Accepted 28 February 2023 | Published 29 March 2023

https://zoobank.org/815F5618-30DE-4552-8A07-8BC3D042D97E

Citation: Reyes JA, Espinosa de los Monteros A, Santiago-Jiménez QJ (2023) Phylogeography of *Falagonia mexicana* Sharp, 1883 (Coleoptera, Staphylinidae, Aleocharinae). ZooKeys 1156: 107–131. https://doi.org/10.3897/zookeys.1156.84943

Abstract

Falagonia mexicana is an aleocharine distributed from northern Mexico to Guatemala and El Salvador. It is associated with *Atta mexicana* ants and lives within their piles of waste or external debris. The phylogeography and historical demography of 18 populations from Mexico, Guatemala, and El Salvador were studied. The data set encompasses a 472 bp fragment of the COI. Results suggest that *F. mexicana* was originated during Middle Pliocene (ca. 0.5 Mya), starting its diversification at the Upper Pleistocene and Holocene. Populations were recovered forming at least four main lineages, with a significant phylogeographic structure. Evidence of contemporary restricted gene flow was found among populations. The historical demography suggests that the geographic structure is due to recent physical barriers (e.g., Isthmus of Tehuantepec) rather than ancient geological events. Also, recent geological and volcanic events in the east of the Trans-Mexican Volcanic Belt and the Sierra Madre Oriental might be responsible for the restricted gene flow among populations. Skyline-plot analyses suggested that a demographic expansion event took place at the end of the Late Quaternary glacial-interglacial cycles.

Keywords

Cytochrome oxidase I, “false Lomechusini”, Mesoamerica, mtDNA

Introduction

Falagonia mexicana Sharp, 1883 is a species of Coleoptera that belongs to the subfamily Aleocharinae (Staphylinidae) (Bouchard et al. 2011). Particularly, the species is placed within Lomechusini, a tribe distinctive for having a 4–5–5 tarsal formula, metasternal process typically longer than mesosternal process, maxillar galea and lacinia moderately to considerably elongated, mesocoxae moderately to very widely separated by broad meso- and metaventral processes (Seevers 1965, 1978), among other characters. Several Lomechusini species are associated with termites and ants (Navarrete-Heredia et al. 2002), as is the case of *F. mexicana*. However, some recent studies have suggested that Lomechusini is not a monophyletic group and two clades have been proposed: the "true Lomechusini" whose species show a Holarctic distribution, and the "false Lomechusini" distributed in tropical America (Elven et al. 2010, 2012). Based on molecular data *F. mexicana* has been recovered as part of the "false Lomechusini" (unpublished data).

The genus *Falagonia* Sharp, 1883 included two species: *F. mexicana* and *F. crassiventris* Sharp, 1883. Currently, *F. crassiventris* is located in the genus *Pseudofalagonia* Santiago-Jiménez, 2010; therefore, *Falagonia* is now a monotypic genus (Santiago-Jiménez 2010; Santiago-Jiménez and Espinosa de los Monteros 2016). At a phylogenetic analysis, *Falagonia* was supported by seven autapomorphies: 1) epipharynx with a spinose process on the apico-medial margin; 2) with a pair of setae on the sensory area of ligula; 3) with simple punctures on elytral disc; 4) without tuberculate punctures on elytral disc; 5) tergite IV of male with a protuberance on each side of midline; 6) tergite VIII of male without lobes on posterior margin; and 7) tergite VIII of female without lobes on posterior margin. It is important to highlight that the specimens of *F. mexicana* are very homogeneous, except for some variation in size (4–7 mm); in color (from reddish to pale yellow in the tenerals); in the length of the α-sensilla of the epipharynx, as well as the length of the spines of the spinose process on the apico-medial margin of the epipharynx. Moreover, they present secondary sexual dimorphism. Males have a protuberance on each side of the midline of tergite IV, and a protuberance on the midline of tergite VIII.

From Mexico to El Salvador, *F. mexicana* has been recorded in a wide altitude range (from 50 to 2,000 m a.s.l.). This species has been recorded in diverse types of vegetation (Santiago-Jiménez 2010). According to Challenger and Soberón (2008) those habitats correspond to tropical evergreen forests, tropical deciduous forests, temperate coniferous and broadleaf forests, cloud forests, and scrub xerophytes. These types of vegetation in Mexico tend to present warm humid climates (Af, Am, Aw, BSh) to temperate climates (Cfb, Cwa, Cwb). Records in pine and oak forests do not exceed 2,000 m a.s.l. Thus, in general, they prefer warm humid climates with dry winter (Rzedowski 1994).

In Mexico, *F. mexicana* is found in the states of Colima, Guanajuato, Guerrero, Hidalgo, Jalisco, Michoacan, Morelos, Oaxaca, Queretaro, San Luis Potosi, Sinaloa,

Sonora, Tamaulipas, and Veracruz (Santiago-Jiménez 2010). This distribution corresponds to the biogeographic provinces of the Pacific, Trans-Mexican Volcanic Belt, Sierra Madre Oriental, Sierra Madre del Sur, Soconusco, and Tierras Altas de Chiapas. These regions are associated with physiographic provinces that show heterogeneous historical processes and dates of origin (e.g., de Cserna 1989; Mastretta-Yanes et al. 2015 for summaries). For instance, the most recent formation corresponds to the Trans-Mexican Volcanic Belt from the Miocene to the present day, with some stratovolcanoes forming in during the Pleistocene (Ferrari et al. 2012).

Falagonia mexicana lives in the debris produced by *Atta mexicana* (Smith, 1858) ants. The reddish color *F. mexicana* allows it to blend in with the debris. Apparently, despite having developed wings, this species does not fly. Flight intercept traps have been placed near the debris and we have not been able to catch them. Instead, by placing pit-fall traps in the vicinity of the detritus we have obtained some specimens. The nests of *A. mexicana* with its associated debris seems to be islands in the geographic distribution of *F. mexicana*, due to their presumed inability to fly and limited long-distance movement. Therefore, geographical barriers have a great effect in reducing gene flow between its populations, as well as restrictions on its geographical distribution. Physical barriers can lead to genetic isolation when they remain for an extended period of time, which is essential for lineage divergence (Saunders et al. 1991; Avise 2000).

Apparently, both *A. mexicana* and *F. mexicana* are incapable of surviving in areas above 2,300 m a.s.l. In the case of *F. mexicana*, its septentrional distribution is limited by the Tropic of Cancer, as is the case with other insect groups (e.g., Passalidae, Reyes-Castillo 2000). However, *A. mexicana* does reach the southern United States. It has been seen in the field that *F. mexicana* prefers debris that is under vegetal cover, with more shade and humidity. Usually, *F. mexicana* is found in *A. mexicana*'s detritus, but that does not mean that every *A. mexicana* nest has *F. mexicana* associated with it, especially when the detritus is exposed to desiccation.

Recently, some studies have been carried out to understand the biogeographical patterns of the biota in Middle America (e.g., Marshall and Liebherr 2000; Daza et al. 2010; Ornelas et al. 2013). With an average altitude of 200 m a.s.l. the Isthmus of Tehuantepec has been identified as an effective barrier for gene flow (Barrier et al. 1998). Likewise, the Trans-Mexican Volcanic Belt represents a biogeographical barrier (Marshall and Liebherr 2000) and a center for lineage diversification (Bryson et al. 2018). The use of coalescent and geographic structure models based on molecular data can be useful to test historical demographic scenarios where hypothesis of vicariance and dispersion can be contrasted (Knowles and Carstens 2007; Daza et al. 2010). Therefore, *F. mexicana* is an interesting model to study the relationship between genealogy and geography. The objectives of the present study are to estimate the date of the appearance of *Falagonia mexicana*, to evaluate the phylogenetic structure of *F. mexicana*, and to correlate the historic events that explain the divergence processes within the lineage.

Materials and methods

The sampling was carried out in 18 localities from El Salvador, Guatemala, and Mexico (Fig. 1, Table 1). The collection sites were selected based on previous records and potential suitable sites. Potential localities were identified based on their environmental and geographic conditions. This sampling covers most of the species' distribution. Field collections were carried out by direct collection on debris of *A. mexicana* using an aspirator. After its collection, the specimens were placed in 96% ethanol and stored at -20 °C. The material was deposited at the Phylogenetic Systematics Laboratory (INECOL, Xalapa).

From total genomic DNA, we obtained the sequence for a fragment of 472 base pairs (bp) of the Cytochrome Oxidase subunit I (COI) mitochondrial gene. This fragment is located between positions 250 and 720 of the COI gene. This gene was selected since it presents an adequate mutation rate for this kind of studies (Avise 2000). Sequences present extensive intraspecific polymorphisms, providing information between individuals. In addition, this molecular marker has been a useful tool for species' identification (Avise 2000). DNA extraction was performed using the kit Tissue & Insect DNA MicroPrep (Zymo Research Corp., Irvine, CA), following the protocol suggested by the manufacturer. DNA was extracted for amplification from 139 specimens. Amplification was performed using the S1718 (Normark 1996) and NANCY (Simon et al. 1994) primers designed for Coleoptera. PCR mix consisted of 5 µL of DNA, 3 µL of 5X Buffer, 3 µL of MgCl2 (25mM), 3 µL of dNTP's (8mM), 3 µL of each primer (10mM), 0.2 µL of Taq polymerase (5 U / µL) and 9.8 µL of ddH2O adding to a final volume of 30 µL. The PCR protocol consisted of an initial denaturation for 180 s at 94 °C; 35 cycles of 30 s at 94 °C as denaturing temperature, 30 s at 45 °C for primer annealing and 90 s at 74 °C for extension; followed by one final extension cycle of 300 s at 72 °C. PCR products were visualized in a 1% agarose gel stained with ethidium bromide and purified using the GeneJET Genomic DNA Purification Kit (Thermo Fisher Scientific Inc., Waltham, MA). The PCR samples were sent to the Macrogen company (South Korea) for sequencing. Sequences were assembled with the software SEQUENCHER v. 5.2.4 (Gene Codes Corporation). The alignment of the sequences was trivial; therefore, it was done manually using the software MEGA v. 7 (Kumar et al. 2016). All the sequences acquired for the first time were deposited in GenBank (OQ608846–OQ608984).

The identity of the sequences was corroborated by translating them into amino acids, verifying the absence of nonsense codons or intermediate stops, and by a BLAST search. Using the software PAUP v. 4.0 (Swofford 2002), the nucleotide proportion of each sequence was estimated, as well as their standard deviation and nucleotide bias. In turn, the first, second, and third positions were identified, and the same descriptors were calculated. The proportion of transitions and transversions were also calculated.

To identify genetically congruent geographic regions, a spatial analysis of molecular variance (SAMOVA) was conducted. This was performed with the aid of the software SAMOVA v. 1 (Dupanloup et al. 2002), using 100 banding steps to obtain

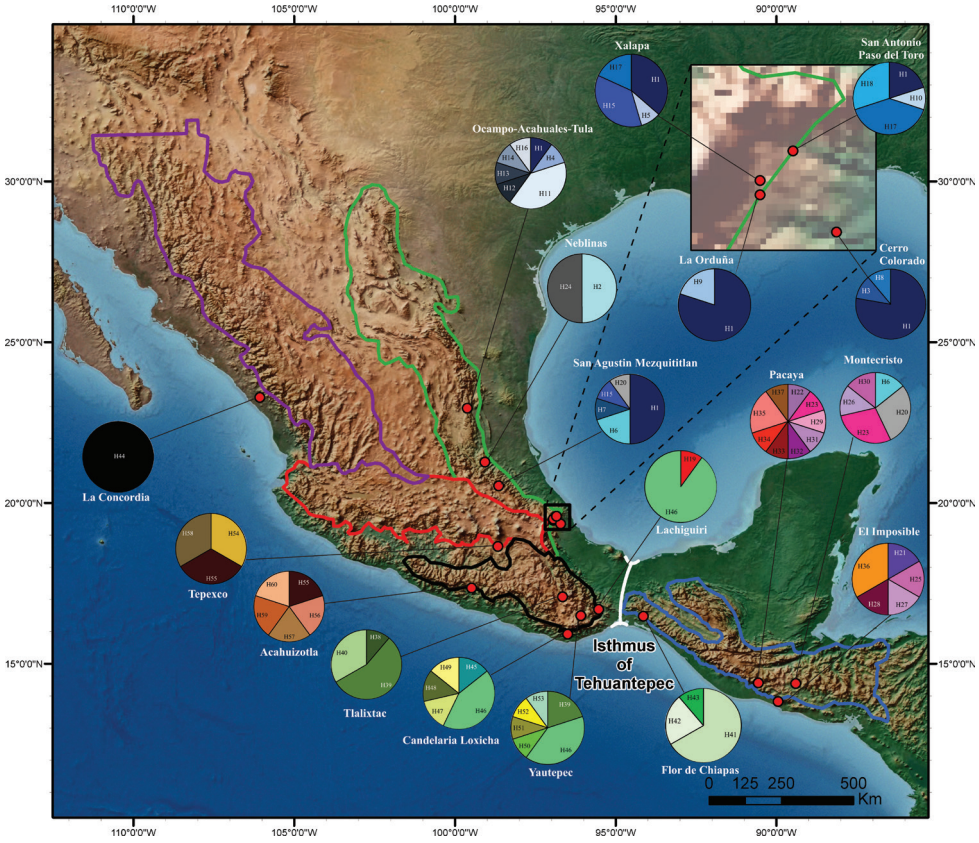

Figure 1. Distribution map showing the localities where individuals of *Falagonia mexicana* were sampled. Pie charts represent haplotypes sampled in each locality. Color on map indicates altitudinal changes every 500 m a.s.l. The polygons represent the main biogeographical regions: Sierra Madre del Sur (black), Sierra Madre Occidental (purple), Sierra Madre Oriental (green), Tierras Altas de Chiapas (blue), and Trans-Mexican Volcanic Belt (red). The white line represents the Isthmus of Tehuantepec.

the fixation index F_{CT} (Excoffier et al. 1992). Likewise, a non-hierarchical analysis of molecular variance (AMOVA) was carried out including every population, followed by an analysis between the statistically significant regions identified by the SAMOVA. This was conducted with 1000 permutations using the software ARLEQUIN v. 3.5 (Excoffier and Lischer 2010). A Mantel test was performed, based on the combined data set, to detect possible isolation by distance. Genetic variation within and between populations was evaluated using descriptive empirical values, such as number of haplotypes (*H*), haplotype diversity (*Hd*), nucleotide diversity (π) (Nei 1987), and segregated sites (*S*) (Nei and Kumar 2000). These values were estimated using the software DNASP v. 5.10 (Librado and Rozas 2009). This analysis was done for each population, as well as for each region inferred by the SAMOVA. The haplotype network was made with the software NETWORK v. 4.5 (Bandelt et al. 1999) using the Median Joining

Table 1. Collection sites for samples of *Falagonia mexicana* examined in the present study (*n* = 139).

Country	Locality	Region	*n*	Altitude (m a.s.l.)	Coordinates	Haplotypes
El Salvador	SAN: Montecristo	TAC	7	1340	14°23.18'N, 89°24.01'W	H6(1), H20(2), H23(2), H26(1), H30(1)
El Salvador	AHU: El Imposible	TAC	6	810	13°49.65'N, 89°56.84'W	H21(1), H25(1), H27(1), H28(1), H36(2)
Guatemala	GUA: Pacaya	TAC	10	1350	14°24.22'N, 90°33.61'W	H22(1), H23(1), H29(1), H31(1), H32(1), H33(1), H34(1), H35(2), H37(1)
Mexico	GUE: Acahuizotla	SMS	5	1100	17°21.32'N, 99°28.68'W	H55(1), H56(1), H57(1), H59(1), H60(1)
Mexico	HGO: San Agustin Mezquititlan	SMO	10	1350	20°31.90'N, 98°38.40'W	H1(5), H6(2), H7(1), H15(1), H20(1)
Mexico	OAX: Candelaria Loxicha	SMS	7	500	15°55.42'N, 96°29.33'W	H45(1), H46(3), H47(1), H48(1), H49(1)
Mexico	OAX: Flor de Chiapas	SOC	9	1130	16°28.48'N, 94°08.13'W	H41(6), H42(2), H43(1)
Mexico	OAX: Lachiguiri	SMS	10	810	16°41.39'N, 95°31.72'W	H19(1), H46(9)
Mexico	OAX: Tlalixtac	SMS: VCO	9	1590	17°04.86'N, 96°39.03'W	H38(1), H39(5), H40(3)
Mexico	OAX: Yautepec	SMS: VCO	10	760	16°29.84'N, 96°05.56'W	H39(2), H46(4), H50(1), H51(1), H52(1), H53(1)
Mexico	PUE: Tepexco	TMV	3	1290	18°39.03'N, 98°39.88'W	H54(1), H55(1), H58(1)
Mexico	QUE: Neblinas	SMO	2	650	21°16.08'N, 99°03.98'W	H2(1), H24(1)
Mexico	SIN: La Concordia	PAC	1	130	23°17.27'N, 106°03.98'W	H44(1)
Mexico	TAM: Ocampo-Acahuales-Tula	SMO	10	1030	22°56.17'N, 99°31.10'W	H1(1), H4(1), H11(4), H12(1), H13(1), H14(1), H16(1)
Mexico	VER: Cerro Colorado	SMO	9	520	19°21.15'N, 96°42.69'W	H1(7), H3(1), H8(1)
Mexico	VER: La Orduña	SMO	10	1210	19°27.64'N, 96°56.08'W	H1(8), H9(2)
Mexico	VER: San Antonio Paso del Toro	SMO	10	1010	19°35.28'N, 96°50.27'W	H1(2), H10(1), H17(4), H18(3)
Mexico	VER: Xalapa	SMO	11	1360	19°30.17'N, 96°56.05'W	H1(4), H5(1), H15(4), H17(2)

AHU Ahuachapan, SAN Santa Ana, GUA Guatemala, GUE Guerrero, HGO Hidalgo, OAX Oaxaca, PUE Puebla, QUE Queretaro, SIN Sinaloa, TAM Tamaulipas, VER Veracruz, TAC Tierras Altas de Chiapas, SMS Sierra Madre del Sur, SMO Sierra Madre Oriental, SOC Soconusco, TMV Trans-Mexican Volcanic Belt, PAC Pacific, VCO Valles Centrales de Oaxaca.

algorithm with a weight of 10 for all characters and an epsilon of 10 as suggested by the authors. Similarly, the Maximum Parsimony post-processing tool was used to eliminate all the superfluous intermediate haplotypes and the links that were not in the shortest network.

The genealogy of the sequences was estimated with a Bayesian inference analysis, using the software MRBAYES v. 3.2.3 (Ronquist et al. 2012). The best-fit nucleotide substitution model was selected using the Akaike information criterion through the software JMODELTEST v. 2.02 (Posada 2008). A homologous sequence of *Pseudofalagonia* sp. (acc. num. OL764948.1), a species closely related to *F. mexicana*, was used as outgroup. The Markov Monte Carlo Chains (MCMC) were run for 10 million generations sampling trees and parameters every 1000 generations. The consensus tree was obtained with their respective posterior probabilities after discarding the initial 25% of the stored trees (Ronquist et al. 2012). Likewise, an inference based on the Maximum Likelihood (ML) optimality criterion was carried out using the software RAXML v. 8 (Stamatakis 2014). The robustness of the nodes recovered in the ML tree was evaluated with 500 bootstrap replications.

To date and infer possible isolation events in *F. mexicana* populations, we used the software BEAST v. 1.10.4 (Drummond et al. 2012). To optimize tree search, the topology inferred from the Maximum Likelihood analysis was used as the tree prior. The ML tree was used instead of the Bayesian one because BEAST only accepts fully resolved trees as priors. To estimate the divergence times, we used a relaxed uncorrelated clock model.

A nucleotide substitution rate of 6.311 (10^{-2} subs/site/My/lineage) for the COI was used to date the genealogy of *Falagonia*. This rate between taxa is based on the substitution rate estimated by Pons et al. (2010) for the COI gene of the coleopteran mitochondrial genome. Alternatively, a more conserve substitution rate of 2.0 (10^{-2} subs/site/My/lineage) was used (chronogram available as Suppl. material 1). This rate closely matches the standard mitochondrial arthropod clock reported by Brower (1994), and the rates calculated in studies that compared closely related species of Coleoptera (e.g., Leys et al. 2003; Balke et al. 2009; Ribera et al. 2010). The BEAST MCMC ran for 10 million generations, sampling trees and parameters every 1000 generations. The software TRACER v. 1.6 (Rambaut et al. 2014) was used to evaluate stationarity of the MCMC parameters, sample sizes (ESSs > 200) and posterior intervals spanning the 95% of the highest posterior density. This analysis was repeated four times and the trees resulting from each run were combined using the software LOGCOMBINER v. 1.10.4 (Drummond et al. 2012), after applying an initial burn-in of 25%. The evaluated nodes were those that scored a posterior probability value higher than 0.9. The inferred chronogram was viewed and edited with the software FIGTREE v. 1.4.2 (Rambaut 2008). To determine the historical demography of the populations, we conducted a neutrality test with Fu's *F* statistics (Fu 1997). This was compared with the generalized skyline-plot analysis inferred with BEAST. The input parameters, as well as the molecular clock model, were identical to the ones used for the coalescence analysis for node dating.

Results

The alignment of the 139 COI sequences showed 417 constant positions (88%). The 55 remaining characters correspond to variable sites (See Suppl. material 2), of which 39 of them are potentially phylogenetically informative, while the other 16 are singletons. Sequences present a 0.27 nucleotide bias and the following nucleotide percentages: A 29.8%, C 17.2%, G 14.9%, and T 38.1%. Regarding codon positions, first positions show less nucleotide bias (0.11) and the following nucleotide proportion: A 25%, C 17.6%, G 25.0%, and T 31.2%. Second positions present an intermediate bias (0.28) and the following nucleotide percentages: A 13.3%, C 28.8%, G 17.2%, and T 40.7%. Lastly, third positions show the highest nucleotide bias (0.64) and this nucleotide composition: A 50.4%, C 17.2%, G 14.9%, and T 38.1%. Regarding base substitution mutations we found a total of 48 transitions and 30 transversions, resulting in a Ts:Tv = 1.6:1 ratio. Mutation transitions were as follows: 27 A-G and 21 C-T; while transversions: 10 A-T, 10 T-G, 7 A-C and 3 C-G.

The haplotype network (Fig. 2) contains 60 haplotypes distributed among the 18 localities. Most of the localities exhibited more than one haplotype. Two main haplotypes (i.e., H1, H46) connected by eleven mutations were recovered. Most of the Sierra Madre Oriental populations had haplotype H1 individuals; while haplotype H46 is shared by individuals from the Sierra Madre del Sur, and one population from the Valles Centrales de Oaxaca. Haplotypes H6 and H20 are shared between the Sierra Madre Oriental and Tierras Altas de Chiapas regions. Haplotypes H2 and H24 collected in Neblinas (Queretaro state) were recovered in the network as the most closely related to the haplotypes from Sierra Madre Oriental and Tierras Altas de Chiapas, respectively. Haplotype H19 from Lachiguiri (Oaxaca state) is an intermediate haplotype among those of Sierra Madre Oriental, Tierras Altas de Chiapas, and Sierra Madre del Sur in Valles Centrales de Oaxaca. Individuals from Tlalixtac and Yautepec (Valles Centrales de Oaxaca) shared Haplotype H39. Haplotypes H41, H42, and H43 are endemic to Flor de Chiapas. Haplotypes H38 and H40 are endemic to Tlalixtac. Haplotypes H45, H47, H48 and H49 are endemic to Candelaria Loxicha (Oaxaca state), and haplotypes H50 to H53 to Yautepec. Haplotypes H54 to H60 were found in individuals from the Sierra Madre del Sur (Acahuizotla, Guerrero state) and the Trans-Mexican Volcanic Belt (Tepexco, Puebla state) regions. Global and local haplotype frequencies can be consulted in Suppl. material 3.

Genetic variation descriptors (Table 2) show that within populations the number of segregated sites range from 1 to 16. The highest nucleotide variation value was found in the population of Neblinas (π = 0.0149, S = 7). This locality had nearly 30 times the nucleotide variation found in Flor de Chiapas (π = 0.0005, S = 1). The lowest value for haplotype diversity was at Lachiguiri (Hd = 0.2), while the highest value (i.e., 1) was at Acahuizotla (Guerrero), Neblinas (Queretaro) and Tepexco (Puebla). The global Fu's F value (i.e., -7.935; $p < 0.001$) is consistent with a significant demographic expansion history. However, none of the individual populations showed statistically significant values for this descriptor.

The SAMOVA (k change from 2 to 15) showed a gradual increase in the F_{CT} values (Table 3). The highest F_{CT} was reached with 15 groups, where the genetic variability among groups reached approximately 80%. This result suggests that practically every locality is an isolated group. The only two groups recovered were: Xalapa-La Orduña-San Antonio Paso del Toro (central Veracruz state) and Acahuizotla-Tepexco. The Mantel test revealed a significant positive correlation (r = 0.3756, $p < 0.0001$), which suggests isolation by distance. The AMOVA showed also significant genetic structure (F_{ST} = 0.77, $P < 0.0001$). Approximately 77% of molecular variance occurs among populations, while the remaining 23% is explained by the genetic differences within populations (Table 4). Population pairwise F_{ST} values revealed significant differentiation between most populations (Table 5). Gene flow estimations among populations were extremely varied, fluctuating from M = 0.000 (i.e., between Flor de Chiapas-San Antonio Paso del Toro) to a continuous exchange of individuals between Xalapa-La Orduña, and Xalapa-Cerro Colorado.

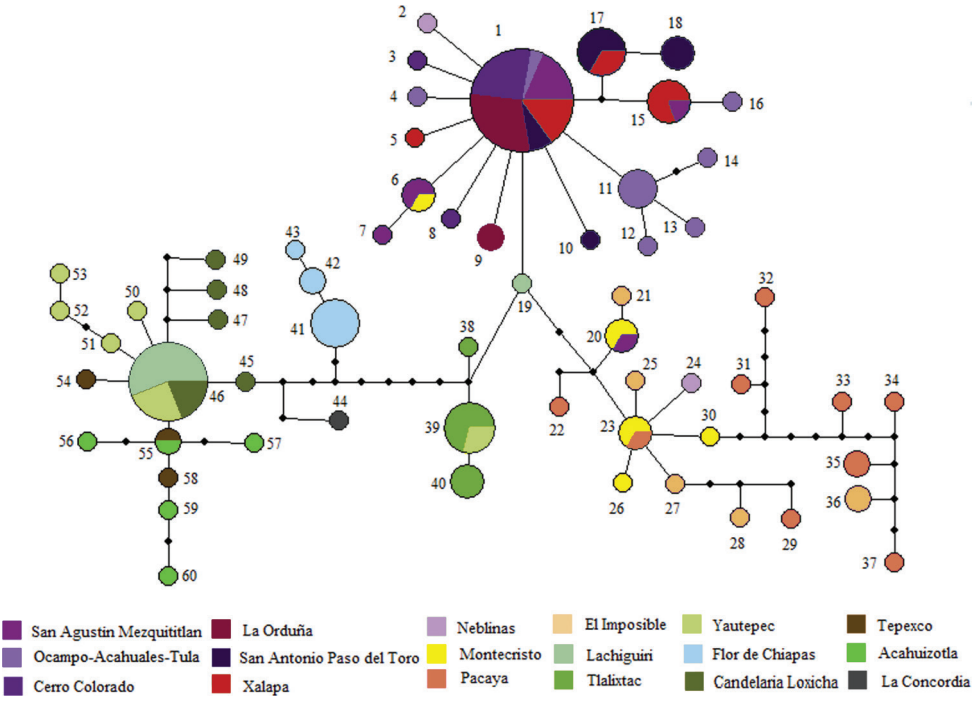

Figure 2. Haplotype network of *Falagonia mexicana*. The network was based on statistical parsimony for the 60 haplotypes retrieved from the COI sequences. Numbers indicate haplotype identity. Colors on network correspond to each locality as shown in the legend.

Table 2. Indices of genetic diversity from the sequences of the 472 bp fragment of COI from *F. mexicana*.

Population	*n*	*S*	π	S.D. π	*h*	*Hd*	S.D. *Hd*	Fu's *F*	*p*
Flor de Chiapas	9	1	0.0005	0.0004	2	0.222	0.166	-0.263	0.342
La Orduña	10	1	0.0008	0.0003	2	0.356	0.159	0.417	0.400
Cerro Colorado	9	2	0.0011	0.0005	3	0.417	0.191	-1.081	0.196
San Antonio Paso del Toro	10	2	0.0015	0.0005	3	0.511	0.164	-0.272	0.282
Xalapa	11	3	0.0029	0.0004	4	0.764	0.083	-0.290	0.251
Tepexco	3	4	0.0059	0.0022	3	1.000	0.272	-0.341	0.416
Tlalixtac	9	4	0.0025	0.0011	3	0.639	0.126	0.645	0.329
Candelaria Loxicha	7	5	0.0041	0.0012	4	0.714	0.181	-0.324	0.274
Neblinas	2	7	0.0149	0.0075	2	1.000	0.500	1.946	0.875
Acahuizotla	5	7	0.0069	0.0016	5	1.000	0.126	-2.238	0.096
El Imposible	6	7	0.0079	0.0015	4	0.867	0.129	0.426	0.352
Ocampo-Acahuales-Tula	10	7	0.0048	0.0010	7	0.867	0.107	-3.310	0.029
San Agustin Mezquititlan	10	8	0.0044	0.0018	5	0.756	0.130	-0.760	0.201
Montecristo	7	9	0.0078	0.0024	4	0.810	0.130	0.812	0.327
Pacaya	10	11	0.0079	0.0017	7	0.867	0.107	-1.744	0.109
Lachiguiri	10	12	0.0053	0.0041	2	0.200	0.154	4.582	0.069
Yautepec	10	16	0.0127	0.0039	6	0.844	0.103	0.778	0.272
La Concordia	1	0	0.0000	–	1	0	–	–	–
Xalapa, Orduña, and San Antonio Paso del Toro	31	4	0.0020	0.0003	5	0.652	0.063	-0.977	0.159
Acahuizotla and Tepexco	8	10	0.0064	0.0015	6	0.929	0.084	-1.785	0.113
Global	139	35	0.0161	0.0007	34	0.862	0.022	-7.935	< 0.001

n: samples number; *S*: number of segregating sites; π: nucleotide diversity; S.D.: standard deviation; *h*: haplotype numbers; *Hd*: haplotype diversity; *p*: probability value.

Table 3. Fixation index (F_{CT}) for population groups of *F. mexicana* recovered by the SAMOVA.

Population groups	*k*	F_{CT}	*p*
(Xal, Ord, CCo, Mez, OAT, Neb, Imp, Mon, Pac, SAPT, Tla) (Aca, CaL, Tep, Lac, FDC, Yau, Con)	2	0.613	< 0.00001
(Xal, Ord, Cco, Mez, OAT, Neb, SAPT y Tla) (Aca, CaL, Tep, Lac, FDC, Con) (Imp, Mon, Pac)	3	0.634	< 0.00001
(Xal, Ord, Cco, Mez, OAT, Neb, SAPT, Tla) (Imp) (Aca, CaL, Tep, Lac, FDC, Yau, Con) (Mon, PAC)	4	0.620	< 0.00001
(Xal, Ord, Cco, Mez, OAT, Neb, SAPT, Tla) (Imp, Mon) (Pac) (FDC) (Aca, CaL, Tep, Lac, Yau, Con)	5	0.680	< 0.00001
(Xal, Ord, Cco, Mez, OAT, Neb, SAPT) (Tla) (Imp, Mon, Pac) (Aca, Tep, Con) (CaL, Lac, Yau) (FDC)	6	0.760	< 0.00001
(Xal, Cco, Mez, OAT, Neb, SAPT) (Ord) (Tla) (Imp, Mon, Pac) (Aca, Tep, Con) (CaL, Lac, Yau) (FDC)	7	0.741	< 0.00001
(Xal, Ord, Cco, Mez, OAT, Neb, SAPT) (Tla) (Imp, Mon) (Pac) (Aca, Tep) (CaL, Lac, Yau) (Con) (FDC)	8	0.771	< 0.00001
(Xal, Ord, Cco, Mez, OAT, Neb, SAPT) (Tla) (Imp, Mon) (Pac) (Aca, Tep) (CaL) (Lac, Yau) (FDC) (Con)	9	0.767	< 0.00001
(Xal, Ord, Cco, Mez, SAPT) (OAT, Neb) (Tla) (Imp, Mon) (Pac) (Aca, Tep) (CaL) (Lac, Yau) (Con) (FDC)	10	0.774	< 0.00001
(Xal, Ord, Cco, Mez, SAPT) (Neb) (OAT) (Tla) (Imp, Mon) (Pac) (Aca, Tep) (CaL) (Lac, Yau) (Con) (FDC)	11	0.783	< 0.00001
(Xal, Ord, Cco, Mez, SAPT) (OAT) (Neb) (Tla) (Imp, Mon) (Pac) (Aca) (Tep) (CaL) (Lac, Yau) (Con) (FDC)	12	0.781	< 0.00001
(Xal, Ord, Cco, SAPT) (Mez) (OAT) (Neb) (Tla) (Imp) (Mon) (Pac) (Aca) (Tep) (CaL, Lac, Yau) (Con) (FDC)	13	0.780	< 0.00001
(Xal, Ord, Cco, Mez, SAPT) (OAT) (Neb) (Tla) (Imp) (Mon) (Pac) (Aca) (Tep) (CaL) (Lac) (Yau) (Con) (FDC)	14	0.792	< 0.00001
(Xal, Ord, SAPT) (Cco) (Mez) (OAT) (Neb) (Tla) (Imp) (Mon) (Pac) (Aca, Tep) (CaL) (Lac) (Yau) (Con) (FDC)	15	0.794	< 0.00001

k: number of groups; F_{CT}: genetic diversity between groups; *p*: p-value. Xal: Xalapa, Ord: La Orduña, CCo: Cerro Colorado, Mez: San Agustin Mezquititlan, OAT: Ocampo-Acahuales-Tula, Neb: Neblinas, Imp: El Imposible, Mon: Montecristo, Pac: Pacaya, SAPT: San Antonio Paso del Toro, Tla: Tlalixtac, Aca: Acahuizotla, CaL: Candelaria Loxicha, Tep: Tepexco, Lac: Lachiguiri, FDC: Flor de Chiapas, Yau: Yautepec, Con: La Concordia.

Table 4. Analysis of molecular variance (AMOVA) among the 18 populations of *F. mexicana*.

Variation Source	d. f.	Sum of squares	Variance components	Variation (%)	F_{ST}
Among populations	17	507.30	3.75	77.03	0.77*
Within populations	121	135.39	1.12	22.97	
Total	138	642.69	4.87		

*= Significance < 0.000001.

The best-fitting nucleotide substitution model was TrN+G+I. The model's specific parameters were: base frequency = 0.3175, 0.1536 0.1489, 0.38; nst = 2; ts:tv ratio = 4.7931; Gamma shape = 0.5600; ncat = 4; and pinvar = 0.7490. The trees recovered by Bayesian (Fig. 3) and ML (See Suppl. material 4) inferences have congruent topologies, with slight changes in the internal relationships. The base of the *F. mexicana* clade is a polytomy formed by individuals of populations mainly distributed in the Sierra Madre del Sur, Pacific and Trans-Mexican Volcanic Belt, a Flor de Chiapas clade (FDC [PP = 1]), and a "big clade" (PP = 1) that encompasses the populations from Tierras Altas de Chiapas (TAC) to Sierra Madre Oriental (SMO). This "big clade" presents a substructure recovering a monophyletic group formed by Valles Centrales de Oaxaca (SMS: VCO) which is the sister group to the clade containing the rest of the sampled populations.

The chronogram (Fig. 4) showed a radiation event during the Middle Pleistocene. The results showed that *F. mexicana* split from the outgroup approximately 450,000 years ago. The diversification events that originated the main lineages within the species occurred nearly 150,000 years ago. The skyline-plots showed that the populations were kept in stasis for the most part of the Pleistocene, followed by a demographic expansion period towards the end of this epoch. For the lineage of TAC, a small increase in *Ne* occurred 3,500 years ago. In the SMO lineage, the increase of *Ne* occurred approximately 1,000 years ago. For the species (global analysis) the skyline-plot showed a demographic increment process that started approximately 4,000 years ago (Fig. 4).

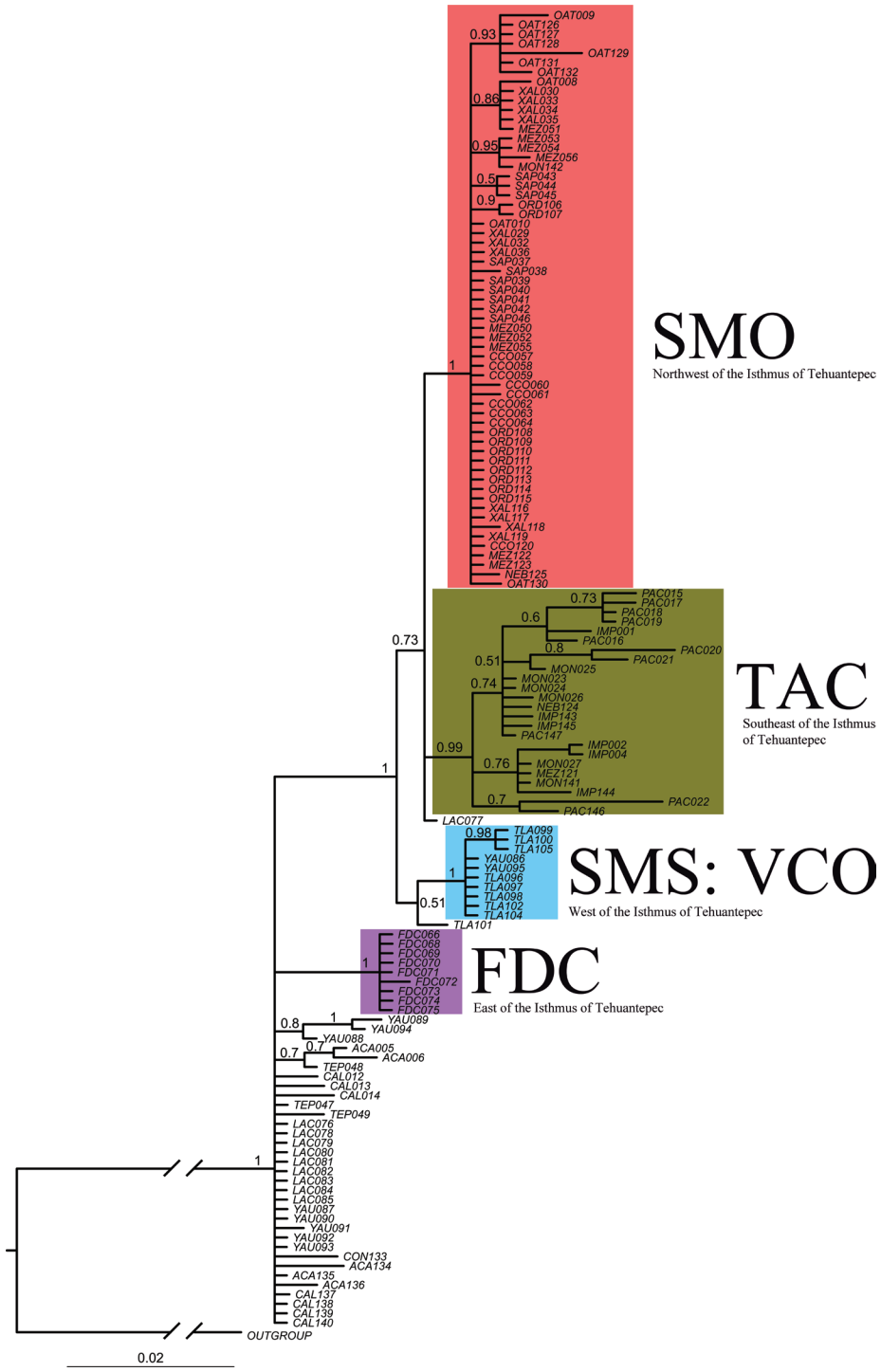

Figure 3. Genealogy recovered based on Bayesian inference. Numbers indicate the Bayesian posterior probabilities. The four main lineages are Flor de Chiapas (FDC), Sierra Madre del Sur that encompasses the Valles Centrales de Oaxaca (SMS: VCO), Tierras Altas de Chiapas (TAC), and Sierra Madre Oriental (SMO).

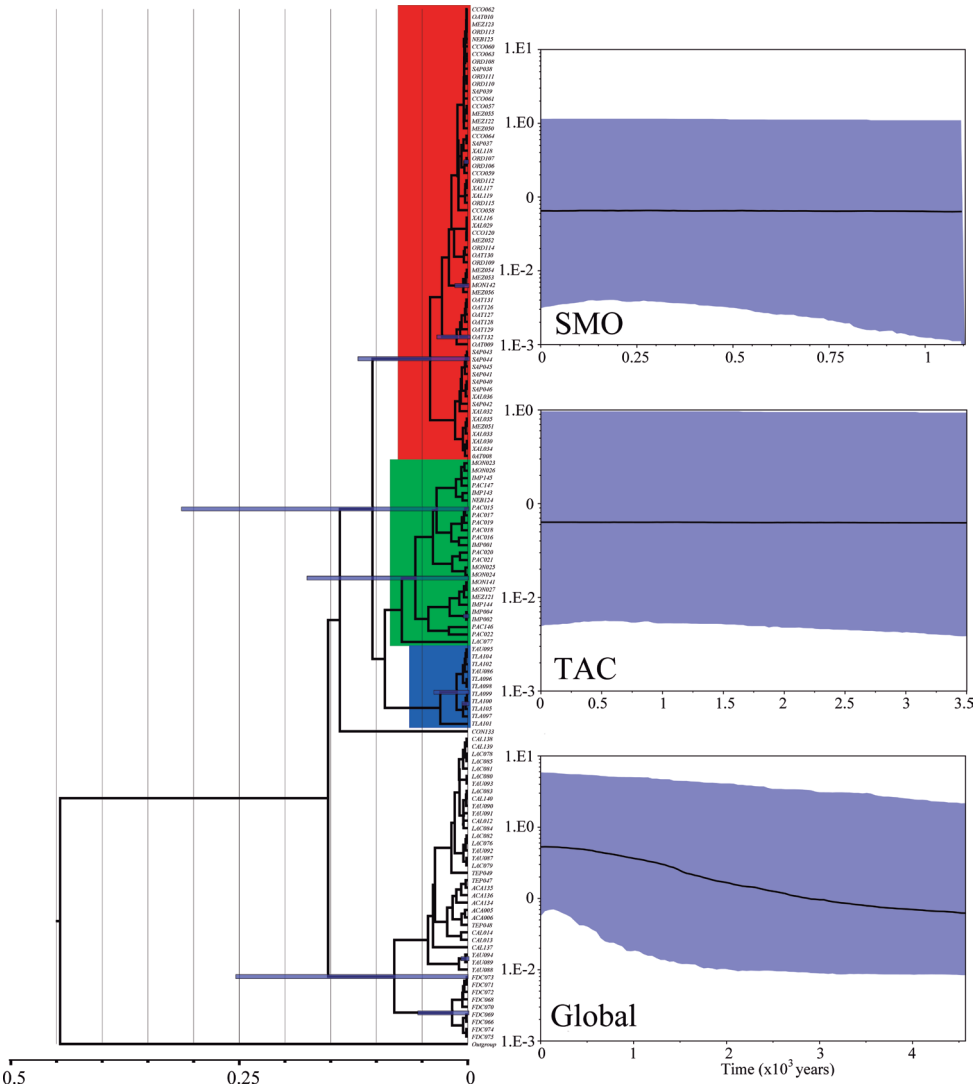

Figure 4. Chronogram and Skyline-plots based on COI sequences of *Falagonia mexicana*. For the chronogram the time is in millions of years. The Skyline-plots are shown for the clades going through demographic changes (SMO: Sierra Madre Oriental, TAC: Tierras Altas de Chiapas, and Global: Whole genealogy). Skyline-plots show mean *Ne*, plus 95% HDP confidence limit.

Discussion

Population structure and genetic diversity

Falagonia mexicana is a highly polymorphic species with sixty different haplotypes recovered. Nucleotide changes are dispersed geographically creating many endemic haplotypes, but despite this, there are two widely distributed haplotypes (i.e., haplotypes H1 and H46) suggesting effective gene flow. Possibly, these haplotypes are ancestral

that gave rise to the more recent ones. Gene flow is supported by the values obtained for migrants per generation (Table 5). Nonetheless, the low values of migrants per generation between the Sierra Madre Oriental (excluding Neblinas) and Tierras Altas de Chiapas (M = 0.113–0.643) suggest the existence of potential geographic barriers. The Isthmus of Tehuantepec could be such barrier. The gene flow is a complex process as suggested by the Mantel´s test. The mutation pattern observed in haplotypes H24 and H19 suggests that they might mediate the inferred gene flow. They are intermediate haplotypes between those from Sierra Madre Oriental, Tierras Altas de Chiapas, Tlalixtac, and Yautepec. There is a negative relationship between *Hd* and sample size (Table 2). High *Hd* values were obtained for populations of Tierras Altas de Chiapas, Ocampo-Acahuales-Tula, and Yautepec. Alternatively, populations closest to the Isthmus of Tehuantepec registered low *Hd* values. This occurs in the west (Lachiguiri) as well as in the east (Flor de Chiapas) of the Isthmus. However, the number of segregated sites and nucleotide diversity differ greatly within these two populations. The population of Lachiguiri has maintained gene flow with the Candelaria Loxicha and Yautepec populations (M = 9.323–inf; Table 5). Regarding to the population of Flor de Chiapas, it may have recently gone through a bottleneck reducing the genetic variability to a single segregated site. Such uneven genetic dynamic suggests that the Isthmus of Tehuantepec represents a geographic barrier that promoted differential effects on gene flow and demography.

The F_{ST} values (Table 5) and the AMOVA (Table 4) revealed a significant differentiation between most populations and a high genetic structure. We found a phylogeographic structure like that reported by Nolasco-Soto et al. (2017) for populations of the *Canthon cyanellus* beetle. According to these authors that species arose in the late Pliocene with radiation during the Pleistocene. The oldest lineages were recovered to the north of the Trans-Mexican Volcanic Belt (north of Sierra Madre Oriental) and in the Pacific, and the most recent lineage to the south of the Trans-Mexican Volcanic Belt, on the Coastal Plain of the Gulf of Mexico. Nolasco-Soto et al. (2017) reported limited historical gene flow with current genetic structure determined by isolation by distance and other contemporary processes. Anducho-Reyes et al. (2008) reported high F_{ST} for the bark beetle *Dendroctonus mexicanus*, reporting an allopatric fragmentation event among the populations to the north of the Trans-Mexican Volcanic Belt, and the Sierra Madre del Sur. They assumed a long-distance colonization process with continuous migration between populations of those geographic provinces. Another study by Sánchez-Sánchez et al. (2012) for the *Dendroctonus approximatus* beetle found differentiation between populations in the group of Sierra Madre Oriental-Sierra Madre del Sur with respect to the Sierra Madre Occidental-Trans-Mexican Volcanic Belt group. This divergence was estimated to have occurred 195,000 years ago in the late Pleistocene. They concluded that the populations of that species represent a model of geographic range expansion and contraction, with subsequent restricted gene flow among putative Pleistocene refuges. Apparently, a rapid genetic structure in space and time for Coleoptera, and possibly for insects in general, is feasible in the mountainous regions of Mexico. It is important to continue with studies like these that will allow us to reinforce possible dominant evolutionary patterns in Neotropical insects.

Table 5. Paired comparisons of *F. mexicana* populations. Above the diagonal: Number of migrants per generation (*M*). Below the diagonal: Fixation Index (F_{ST}).

	Xal	Ord	CCo	Mez	OAT	Neb	Aca	CaL	Imp	Mon	Pac	SAPT	Tep	Lach	Tlal	FDC	Yau	Con
Xalapa		inf	inf	6.100	0.713	0.252	0.028	0.026	0.139	0.214	0.214	inf	0.035	0.061	0.048	0.011	0.167	0.023
La Orduña	-0.01		4.578	3.102	0.523	0.152	0.014	0.015	0.113	0.178	0.193	inf	0.018	0.051	0.024	0.000	0.158	0.000
Cerro Colorado	-0.02	0.098		inf	1.168	0.504	0.048	0.041	0.198	0.308	0.274	4.578	0.060	0.080	0.082	0.023	0.209	0.057
San Agustin Mezquititlan	0.076	0.139	0.00		2.326	2.088	0.109	0.086	0.411	0.643	0.454	3.102	0.135	0.123	0.204	0.068	0.264	0.182
Ocampo-Acahuales-Tula	**0.412***	**0.489***	**0.300***	**0.177***		1.102	0.083	0.065	0.296	0.413	0.342	0.523	0.103	0.097	0.145	0.050	0.221	0.127
Neblinas	0.665	0.766	0.498	0.193	0.312		0.140	0.089	3.066	inf	814.4	0.152	0.274	0.153	0.237	0.047	0.520	1.250
Acahuizotla	**0.947***	**0.973***	**0.913***	**0.821***	0.858	0.781		0.192	0.106	0.133	0.145	0.014	inf	0.377	0.037	0.030	1.373	0.099
Candelaria Loxicha	**0.951***	**0.971***	**0.924***	**0.854***	**0.885***	0.848	**0.723***		0.077	0.098	0.108	0.015	0.337	inf	0.033	0.029	4.371	0.097
El Imposible	**0.782***	**0.816***	**0.716***	**0.549***	**0.628***	0.140	**0.825***	**0.866***		17.01	3.169	0.113	0.144	0.112	0.150	0.056	0.266	0.197
Montecristo	**0.700***	**0.738***	**0.619***	**0.438***	**0.548***	-0.05	**0.790***	**0.836***	0.029		3.625	0.178	0.179	0.137	0.246	0.081	0.319	0.277
Pacaya	**0.701***	**0.722***	**0.646***	**0.524***	**0.594***	0.001	**0.776***	**0.822***	0.136	0.121		0.193	0.180	0.140	0.223	0.093	0.283	0.235
San Antonio Paso del Toro	-0.01	0.000	0.098	0.139	**0.489***	0.766	**0.973***	**0.971***	**0.816***	**0.738***	**0.722***		0.018	0.051	0.024	0.000	0.158	0.000
Tepexco	**0.935***	**0.965***	**0.892***	**0.787***	**0.830***	0.646	-0.01	0.597	0.777	**0.737***	**0.736***	**0.965***		0.633	0.048	0.040	4.059	0.304
Lachiguiri	**0.892***	**0.907***	**0.862***	**0.803***	**0.837***	0.766	**0.570***	-0.05	**0.816***	**0.785***	**0.782***	**0.907***	0.441		0.075	0.089	9.323	0.294
Tlalixtac	0.913	**0.955***	**0.860***	**0.710***	**0.775***	0.678	**0.931***	**0.938***	**0.770***	**0.670***	**0.692***	**0.955***	**0.912***	**0.869***		0.016	0.264	0.032
Flor de Chiapas	**0.979***	**1.000***	**0.956***	**0.880***	**0.909***	0.913	**0.944***	**0.946***	**0.900***	**0.861***	**0.844***	**1.000***	**0.927***	**0.849***	**0.970***		0.287	0.000
Yautepec	**0.750***	**0.760***	**0.705***	**0.655***	**0.694***	0.490	0.267	0.103	**0.653***	**0.610***	**0.638***	**0.760***	0.110	0.051	**0.654***	**0.635***		3.368
La Concordia	0.955	1.000	0.897	0.733	0.798	0.286	0.835	0.838	0.717	0.644	0.680	1.000	0.622	0.629	0.940	1.000	0.129	

Bold values showed a significance value of $p < 0.01$. Abbreviations of the localities correspond to those used in Table 3.

Biogeography and diversification time

The biogeographic history of Middle America has been complex and intriguing. One of the main questions has been how many events of exchange of organisms between the Nearctic and Neotropical regions have happened. Recently, studies have focused on the Mexican and Central America highlands to understand the biogeographic history of this area (Mastretta-Yanes et al. 2015). The estimated divergence time suggests that the origin of *F. mexicana* occurred during the Middle Pliocene, followed by a radiation that begun in the Upper Pleistocene that persisted during the Holocene. Such time coincide with several of the glacial-interglacial cycles that took place during those periods (O'Dea et al. 2016). Although most of the volcanic activity in the Sierra Madre Occidental and the other great mountain chains of Mexico ceased between the Oligocene-Miocene boundary; however, many localized and significant tectonic events have occurred until present times (de Cserna 1989; Ferrari et al. 1999, 2005, 2012). For instance, different pulses have conformed the topology of the Trans-Mexican Volcanic Belt were some of the large stratovolcanoes were formed less than 1 Mya. It has been found that the Trans-Mexican Volcanic Belt constitutes a geographical barrier, separating two large biogeographical assemblages, one to the north and the other to the south of it. Our results suggest that the ancestral area of *F. mexicana* might be located between the Pacific, Trans-Mexican Volcanic Belt or Sierra Madre del Sur biogeographic regions (Fig. 4). One of the northernmost records of the species is Sierra Alamos, Sonora (Santiago-Jiménez 2010). This area is located on the border of the Sierra Madre Occidental and Pacific provinces. That population is geographically closer to that of La Concordia, Sinaloa, representing a cluster of Pacific affinities; whereas the taxa distributed in the southern portion of the Sierra Madre Occidental have a closer affinity to those in the Sierra Madre del Sur (Marshall and Liebherr 2000).

The Isthmus of Tehuantepec is a geographical barrier for gene flow between the east and west regions. Many vicariance events have been invoked for different lineages (Castoe et al. 2009; Barber and Klicka 2010; Daza et al. 2010; González et al. 2011; Gutiérrez-Rodríguez et al. 2011). The Isthmus of Tehuantepec is a valley, located near the triple junction of the North American, Cocos and Caribbean plates. It is approximately 200 km long and has an average altitude of 200 m a.s.l. Climatic and topographic conditions along with the glacial-interglacial cycles during the Pleistocene might explaine diversification patterns found at this area (Pringle et al. 2012; Ornelas et al. 2013; Rodríguez-Gómez et al. 2013; Pech-May et al. 2019). Our findings are consistent with such vicariance patterns. Approximately 100,000 years ago three main clades of *Falagonia* rose: a) a cladogenetic event occurred separating the FDC clade (east of the Isthmus of Tehuantepec) from its sister group, b) the SMS: VCO clade (west of the Isthmus) differentiated from the TAC clade, and c) the SMO clade (northwest of the Isthmus) split from the TAC- SMS: VCO clade. All this could be regulated by continental uplift and sea level oscillations, or glacial-interglacial cycles.

The Isthmus of Tehuantepec has an average altitude of 200 m a.s.l. Although this is within the low range of the altitudinal tolerance of *Falagonia*, the dry and harsh climatic

conditions of this area might create a barrier for this species. The northern area of the Isthmus is more humid due to the influence of the Gulf of Mexico. Until a century ago the predominant vegetation was tropical evergreen forest. In the past this vegetation was a continuum ecosystem from northern Veracruz to the northeast of Chiapas (Rzedowski 1994). However, anthropocentric activities (e.g., cattle ranching) have decreased the vegetation cover to near disappearance, altering the climatic conditions significantly. Such habitat modification indubitably is playing an important role in gene flow disruption among the populations of this staphylinid and many other species of flora and fauna. A more exhaustive population sampling at both sides of the Isthmus of Tehuantepec is necessary to understand the effects of deforestation and habitat fragmentation on *F. mexicana*.

For the SMO clade the Trans-Mexican Volcanic Belt constitutes a recent geographical barrier. One of the most relevant episodes occurred between the late Pliocene and the Quaternary in southern Veracruz (Palma Sola, Los Tuxtlas). Rodríguez et al. (2010) considered the Cofre de Perote-Pico de Orizaba volcanic range as the eastern end of the Trans-Mexican Volcanic Belt. The recent volcanic activity at this region and at the Sierra Madre Oriental allowed the SMO clade to finally establish during the Pleistocene, once geological, geographic, and climatic conditions were more stable. More recently, the volcanic activity to the east, at Chiconquiaco-Palma Sola, during the Quaternary, apparently constituted another barrier to the *F. mexicana* populations from the northeast of Mexico. The rocks of the Xalapa Monogenetic Volcanic Field, which comprises more than 59 volcanoes of the Quaternary, fall into three groups, the oldest with a little more than 2 Mya, others between 250 to 400 Kya, and others less than 100 Kya (Rodríguez et al. 2010). This recent geologic activity possibly has not allowed the differentiation of populations to the north (e.g., Ocampo-Acahuales-Tula) and south (e.g., Xalapa-La Orduña-San Antonio Paso del Toro) of Chiconquiaco-Palma Sola region.

The divergence times suggest an origin for the populations of *F. mexicana* in the western region of Mexico, where biogeographical assemblages from the southern Sierra Madre Occidental have been found more closely related to other assemblages to the south of the Trans-Mexican Volcanic Belt (Marshall and Liebherr 2000). Evidence of lineage diversification during the Pleistocene in Mexico and Central America has been found for different insects: dung beetles (Nolasco-Soto et al. 2017), bark beetles (Sánchez-Sánchez et al. 2012), edible crickets (Pedraza-Lara et al. 2015), dolichoderine ants (Pringle et al. 2012), and the *Triatoma dimidiate* vector (Pech-May et al. 2019), among others. This supports the hypothesis that the geo-climatic events that took place during the Pliocene, such as intense volcanic activity, glacial-interglacial cycles, and sea level fluctuations, represent a major driver for the diversification of different insects' lineages.

Historical demography

The population expansion processes inferred for *F. mexicana* during the Quaternary period might be the result of the end of the last glacial maximum. The climate on Earth has undergone very marked fluctuations in cycles of ≈ 100,000 years, during the last 400,000 years. The coldest stages (8 °C less on average) constitute the glacial cycles, while

the stages where the climates are equal to or warmer (2–3 °C higher) than the present, are the interglacials (Stute et al. 1995; Brown and Lomolino 1998). Glacial events in the Trans-Mexican Volcanic Belt produced a decrease in the Equilibrium Line Altitude of ~ 1,000 m from current levels in the main mountains. Therefore, not only the volcanic activity has contributed to the diversification of lineages in this area (Caballero et al. 2010). Such drastic changes in temperature also could have had an effect in fluctuations of the gene flow at the Isthmus of Tehuantepec region. Nowadays the lowlands that separate the higher altitude areas have arid zones with warmer climates, dry jungles, and tropical rain forests (Challenger and Soberón 2008; Mastretta-Yanes et al. 2015). During the last maximum glacial the paleolimnological and pollen data support drier and cooler conditions in central and eastern-central Mexico, particularly between 21,000 to 18,000 years ago. While deglaciation started earlier in temperate zones, conditions remained very similar to the last maximum glacial for the Trans-Mexican Volcanic Belt mountains (Caballero et al. 2010). *Falagonia mexicana* could have been distributed in a northwest-southeast sequence reaching northern Central America, pushed by the effects of the Wisconsin glaciation and other previous glaciations, while a displacement in the opposite direction (i.e., invasion of the Sierra Madre Oriental) occurred more recently. Other data obtained from the mtDNA from a variety of insect groups has revealed a general pattern where population expansions occurred during the Pleistocene (Pfeiler and Markow 2011; Pfeiler et al. 2013; Nolasco-Soto et al. 2017; Pech-May et al. 2019).

Association with ants

The larvae of *F. mexicana* are unknown; therefore, there is a lack of information about its natural history, behavior, and ecology. So far, the adults of this species have been only observed and collected in association or near by the nests of *Atta mexicana*. Santiago-Jiménez (2010) reports that the adults are active predator of these ants. However, alternative hypotheses exist to explain the association between *F. mexicana* with *A. mexicana*. The ant species of the tribe Attini depend strictly for their feeding on the cultivation of the *Leucoagaricus gongylophorus* fungi. Such agricultural practice creates particular micro environmental condition inside the ant´s nest as well as the continuous production of foliar debris. Temperature fluctuations had a harsh effect on insect population perhaps partly due to thermoregulation in conjunction with body mass, playing an important role at the level of ecological niche and geographic distribution patterns. Verdú et al. (2006) pointed out that dung beetles weighing less than 1.9 g, tend to be thermo-conformal or poikilotherms, only capable of maintaining a temperature similar to the environment at the time of flight. Márquez and Navarrete-Heredia (1994) reported that the debris maintain, most of the time, a temperature between 19–27 °C, usually higher than environmental temperature. This suggests that *F. mexicana* can use the nests of *A. mexicana* as a refuge to regulate their body temperature and, at the same time, be able to capture prey. Therefore, the external debris of *A. mexicana* may historically constitute a refuge without abrupt temperature changes, allowing this species to occupy higher altitudinal and wider latitudinal ranges in different vegetation types.

Final remarks

Falagonia mexicana is a species whose origin can be dated during the Pleistocene and diversified in at least four main haplogroups since then. Geographic barriers such as the Isthmus of Tehuantepec, Trans-Mexican Volcanic Belt and Sierra Madre Oriental have played a major role in the evolution of this species. Even though geographic regions define the haplogroups, evidence of contemporary restricted gene flow was found, which indicates that this lineage is in the process of genetic differentiation. The differentiation among populations was supported by significant values of pairwise F_{st}, and the global genetic structure revealed by the AMOVA. Also, a significantly positive correlation between genetic and geographic distances, suggesting isolation by distance is a process promoting its genetic structure. Finally, climatic, and volcanic events that occurred during the late Quaternary Period indubitably have shaped the distribution, genetic structure, and demography history of this elusive insect.

Acknowledgements

We thank Dr. Domínguez Martínez and Dr. Sánchez Palmeros for their pertinent comments on this paper, as well as Jonathan Sulvarán-Salazar for his assistance in field. QJSJ is indebted to Enio Cano and Eunice E. Echeverria for the facilities provided to collect in Guatemala and El Salvador, respectively. We are grateful to A. Valencia for helping us with the English version of this paper. Dr. Janet Nolasco-Soto provided technical and logistical aid during the lab work. We thank Dr. J. L. Navarrete-Heredia and Dr. L. Delgado for the donation of biological material from La Concordia and Tepexco, respectively. In addition, we thank Dr. Gusarov for allowing us to use the outgroup's sequence. Similarly, we thank the anonymous reviewers for their comments, as well as all the people who in any way helped us during the development of this research.

This work was partially supported by a CONACyT (Consejo Nacional de Ciencia y Tecnología) fellowship (# 164479) to QJSJ. Complementary financial support was obtained by the program "Apoyos Económicos para Estudiantes de Posgrado" (Instituto de Ecología, A. C.). QJSJ is grateful with IdeaWild organization for providing some equipment used during fieldwork and thanks the Universidad Veracruzana for the support to carry out a sabbatical stay at the Instituto de Ecología, A. C. to finish this manuscript. The funders were not involved in anyway regarding the study design, data collection and analysis, decision to publish, or preparation of the manuscript.

References

Anducho-Reyes MA, Cognato AI, Hayes JL, Zúñiga G (2008) Phylogeography of the bark beetle *Dendroctonus mexicanus* Hopkins (Coleoptera: Curculionidae: Scolytinae). Molecular Phylogenetics and Evolution 49(3): 930–940. https://doi.org/10.1016/j.ympev.2008.09.005

Avise JC (2000) Phylogeography: The history and formation of species. Harvard University Press, Cambridge, 447 pp. https://doi.org/10.2307/j.ctv1nzfgj7

Balke M, Ribera I, Hendrich L, Miller MA, Sagata K, Posman A, Vogler AP, Meier R (2009) New Guinea highland origin of a widespread arthropod supertramp. Proceedings of the Royal Society B: Biological Sciences 276(1666): 2359–2367. https://doi.org/10.1098/rspb.2009.0015

Bandelt HJ, Forster P, Röhl A (1999) Median-joining networks for inferring intraspecific phylogenies. Molecular Biology and Evolution 16(1): 37–48. https://doi.org/10.1093/oxfordjournals.molbev.a026036

Barber BR, Klicka J (2010) Two pulses of diversification across the Isthmus of Tehuantepec in a montane Mexican bird fauna. Proceedings of the Royal Society B: Biological Sciencies 277: 2675–2681. https://doi.org/10.1098/rspb.2010.0343

Barrier E, Velasquillo L, Chavez M, Gaulon R (1998) Neotectonic evolution of the Isthmus of Tehuantepec. Tectonophysics 287(1–4): 77–96. https://doi.org/10.1016/S0040-1951(98)80062-0

Bouchard P, Bousquet Y, Davies AE, Alonso-Zarazaga MA, Lawrence JF, Lyal CHC, Newton AF, Reid CAM, Schmitt M, Ślipiński SA, Smith ABT (2011) Family-group names in Coleoptera (Insecta). ZooKeys 88: 1–972. https://doi.org/10.3897/zookeys.88.807

Brower AVZ (1994) Rapid morphological radiation and convergence among races of the butterfly *Heliconius erato* inferred from patterns of mitochondrial DNA evolution. Proceedings of the National Academy of Sciences of the United States of America 91(14): 6491–6495. https://doi.org/10.1073/pnas.91.14.6491

Brown JH, Lomolino MV (1998) Biogeography. Sinauer Associates, Inc. Publishers, Sunderland, 691 pp.

Bryson Jr RW, Zarza E, Grummer JA, Parra-Olea G, Flores-Villela O, Klicka J, McCormack JE (2018) Phylogenomic insights into the diversification of salamanders in the *Isthmura bellii* group across the Mexican highlands. Molecular Phylogenetics and Evolution 125: 78–84. https://doi.org/10.1016/j.ympev.2018.03.024

Caballero M, Lozano-García S, Vázquez-Selem L, Ortega B (2010) Evidencias de cambio climático y ambiental en registros glaciales y en cuencas lacustres del centro de México durante el último máximo glacial. Boletín de la Sociedad Geológica Mexicana 62(3): 359–377. https://doi.org/10.18268/BSGM2010v62n3a4

Castoe TA, Daza JM, Smith EN, Sasa MM, Kuch U, Campbell JA, Chippindale PT, Parkinson CL (2009) Comparative phylogeography of pitvipers suggests a consensus of ancient Middle American highland biogeography. Journal of Biogeography 36(1): 88–103. https://doi.org/10.1111/j.1365-2699.2008.01991.x

Challenger A, Soberón J (2008) Los ecosistemas terrestres. In: Soberón J, Halffter G, Llorente-Bousquets J (Eds) Capital Natural de México, vol. I: Conocimiento Actual de la Biodiversidad. Comisión Nacional para el Conocimiento y Uso de la Biodibversidad, México, 87–108.

Daza JM, Castoe TA, Parkinson CL (2010) Using regional comparative phylogeographic data from snake lineages to infer historical processes in Middle America. Ecogeography 33: 343–354. https://doi.org/10.1111/j.1600-0587.2010.06281.x

de Cserna Z (1989) An outline of the geology of Mexico. In: Bally AW, Palmer AR (Eds) The Geology of North America: An Overview. The Geological Society of America, Inc., Boulder, 233–264. https://doi.org/10.1130/DNAG-GNA-A.233

Drummond AJ, Suchard MA, Xie D, Rambaut A (2012) Bayesian phylogenetics with BEAUti and BEAST 1.7. Molecular Biology and Evolution 29(8): 1969–1973. https://doi.org/10.1093/molbev/mss075

Dupanloup I, Schneider S, Excoffier L (2002) A simulated annealing approach to define the genetic structure of populations. Molecular Ecology 11(12): 2571–2581. https://doi.org/10.1046/j.1365-294X.2002.01650.x

Elven H, Bachmann L, Gusarov VI (2010) Phylogeny of the tribe Athetini (Coleoptera: Staphylinidae) inferred from mitochondrial and nuclear sequence data. Molecular Phylogenetics and Evolution 57(1): 84–100. https://doi.org/10.1016/j.ympev.2010.05.023

Elven H, Bachmann L, Gusarov VI (2012) Molecular phylogeny of the Athetini–Lomechusini–Ecitocharini clade of aleocharine rove beetles (Insecta). Zoologica Scripta 41(6): 617–636. https://doi.org/10.1111/j.1463-6409.2012.00553.x

Excoffier L, Lischer HEL (2010) Arlequin suite v3.5: A new series of programs to perform population genetics analyses under Linux and Windows. Molecular Ecology Resources 10(3): 564–567. https://doi.org/10.1111/j.1755-0998.2010.02847.x

Excoffier L, Smouse PE, Quattro JM (1992) Analysis of molecular variance inferred from metric distances among DNA haplotypes: Application to human mitochondrial DNA restriction data. Genetics 131(2): 479–491. https://doi.org/10.1093/genetics/131.2.479

Ferrari L, López-Martínez M, Aguirre-Díaz G, Carrasco-Núñez G (1999) Space-time patterns of Cenozoic arc volcanism in central Mexico: From the Sierra Madre Occidental to the Mexican Volcanic Belt. Geology 27(4): 303–306. https://doi.org/10.1130/0091-7613(1999)027<0303:STPOCA>2.3.CO;2

Ferrari L, Tagami T, Eguchi M, Orozco-Esquivel MT, Petrone CM, Jacobo-Albarrán J, López-Martínez M (2005) Geology, geochronology and tectonic setting of the late Cenozoic volcanism along the southwestern Gulf of Mexico: The Eastern Alakaline Province Revisited. Journal of Volcanology and Geothermal Research 146(4): 284–306. https://doi.org/10.1016/j.jvolgeores.2005.02.004

Ferrari L, Orozco-Esquivel T, Manea V, Manea M (2012) The dynamic history of the Trans-Mexican Volcanic Belt and the Mexico subduction zone. Tectonophysics 522–523: 122–149. https://doi.org/10.1016/j.tecto.2011.09.018

Fu YX (1997) Statistical tests of neutrality of mutations against population growth, hitchhiking and background selection. Genetics 147(2): 915–925. https://doi.org/10.1093/genetics/147.2.915

González C, Ornelas JF, Gutiérrez-Rodríguez C (2011) Selection and geographic isolation influence hummingbird speciation: Genetic, Acoustic and Morphological Divergence in the Wedge-Tailed Sabrewing (*Campylopterus curvipennis*). BMC Evolutionary Biology 11(1): 38. https://doi.org/10.1186/1471-2148-11-38

Gutiérrez-Rodríguez C, Ornelas JF, Rodríguez-Gómez F (2011) Chloroplast DNA phylogeography of a distylous shrub (*Palicourea padifolia*, Rubiaceae) reveals past fragmentation and demographic expansion in Mexican cloud forests. Molecular Phylogenetics and Evolution 61(3): 603–615. https://doi.org/10.1016/j.ympev.2011.08.023

Knowles LL, Carstens BC (2007) Estimating a geographically explicit model of population divergence. Evolution 61(3): 477–493. https://doi.org/10.1111/j.1558-5646.2007.00043.x

Kumar S, Stecher G, Tamura K (2016) MEGA7: Molecular Evolutionary Genetics Analysis version 7.0 for bigger datasets. Molecular Biology and Evolution 33: 1870–1874. https://doi.org/10.1093/molbev/msw054

Leys R, Watts CHS, Cooper SJB, Humphreys WF (2003) Evolution of subterranean diving beetles (Coleoptera: Dytiscidae: Hydroporini, Bidessini) in the arid zone of Australia. Evolution 57: 2819–2834. https://doi.org/10.1111/j.0014-3820.2003.tb01523.x

Librado P, Rozas J (2009) DnaSP v5: A software for comprehensive analysis of DNA polymorphism data. Bioinformatics 25(11): 1451–1452. https://doi.org/10.1093/bioinformatics/btp187

Márquez J, Navarrete-Heredia JL (1994) Especies de Staphylinidae (Insecta: Coleoptera) asociadas a detritos de *Atta mexicana* (F. Smith) (Hymenoptera: Formicidae) en dos localidades de Morelos, México. Folia Entomologica Mexicana 91: 31–46.

Marshall CJ, Liebherr JK (2000) Cladistic biogeography of the Mexican transition zone. Journal of Biogeography 27(1): 203–216. https://doi.org/10.1046/j.1365-2699.2000.00388.x

Mastretta-Yanes A, Moreno-Letelier A, Piñero D, Jorgensen TH, Emerson BC (2015) Biodiversity in the Mexican highlands and the interaction of geology, geography and climate within the Trans-Mexican Volcanic Belt. Journal of Biogeography 42(9): 1586–1600. https://doi.org/10.1111/jbi.12546

Navarrete-Heredia JL, Newton AF, Thayer MK, Ashe JS, Chandler DS (2002) Guía ilustrada para los géneros de Staphylinidae (Coleoptera) de México/Illustrated guide to the genera of Staphylinidae (Coleoptera) of Mexico. Universidad de Guadalajara and CONABIO, Guadalajara, 401 pp.

Nei M (1987) Molecular Evolutionary Genetics. Columbia University Press, New York, 514 pp. https://doi.org/10.7312/nei-92038

Nei M, Kumar S (2000) Molecular Evolution and Phylogenetics. Oxford University Press, New York, 333 pp.

Nolasco-Soto J, González-Astorga J, Espinosa de los Monteros A, Galante-Patiño E, Favila ME (2017) Phylogeographic structure of *Canthon cyanellus* (Coleoptera: Scarabaeidae), a Neotropical dung beetle in the Mexican Transition Zone: Insights on its origin and the impacts of Pleistocene climatic fluctuations on population dynamics. Molecular Phylogenetics and Evolution 109: 180–190. https://doi.org/10.1016/j.ympev.2017.01.004

Normark BB (1996) Phylogeny and evolution of parthenogenetic weevils of the *Aramigus tessellatus* species complex (Coleoptera: Curculionidae: Naupactini): Evidence from mitochondrial DNA sequences. Evolution 50(2): 734–745. https://doi.org/10.2307/2410846

O'Dea A, Lessios HA, Coates AG, Eytan RI, Restrepo-Moreno SA, Cione AL, Collins LS, de Queiroz A, Farris DW, Norris RD, Stallard RF, Woodburne MO, Aguilera O, Aubry MP, Berggren WA, Budd AF, Cozzuol MA, Coppard SE, Duque-Caro H, Finnegan S, Gasparini GM, Grossman EL, Johnson KG, Keigwin LD, Knowlton N, Leigh EG, Leonard-Pingel JS, Marko PB, Pyenson ND, Rachello-Dolmen PG, Soibelzon E, Soibelzon L, Todd JA, Vermeij GJ, Jackson JBC (2016) Formation of the Isthmus of Panama. Science Advances 2(8): e1600883. https://doi.org/10.1126/sciadv.1600883

Ornelas JF, Sosa V, Soltis DE, Daza JM, González C, Soltis PS, Gutiérrez-Rodríguez C, Espinosa de los Monteros A, Castoe TA, Bell C, Ruiz-Sanchez E (2013) Comparative phylogeographic analyses illustrate the complex evolutionary history of threatened Cloud

Forests of Northern Mesoamerica. PLoS ONE 8(2): e56283. https://doi.org/10.1371/journal.pone.0056283

Pech-May A, Mazariegos-Hidalgo CJ, Izeta-Alberdi A, López-Cancino SA, Tun-Ku E, De la Cruz-Félix K, Ibarra-Cerdeña CN, González RE, Ramsey JM (2019) Genetic variation and phylogeography of the *Triatoma dimidiata* complex evidence a potential center of origin and recent divergence of haplogroups having a differential *Trypanosoma cruzi* and DTU infections. PLoS Neglected Tropical Diseases 13(1): e0007044. https://doi.org/10.1371/journal.pntd.0007044

Pedraza-Lara C, Barrientos-Lozano L, Rocha-Sánchez AY, Zaldívar-Riverón A (2015) Montane and coastal species diversification in the economically important Mexican grasshopper genus *Sphenarium* (Orthoptera: Pyrgomorphidae). Molecular Phylogenetics and Evolution 84: 220–231. https://doi.org/10.1016/j.ympev.2015.01.001

Pfeiler E, Markow TA (2011) Phylogeography of the cactophilic *Drosophila* and other arthropods associated with cactus necroses in the Sonoran Desert. Insects 2(2): 218–231. https://doi.org/10.3390/insects2020218

Pfeiler E, Johnson S, Richmond MP, Markow TA (2013) Population genetics and phylogenetic relationships of beetles (Coleoptera: Histeridae and Staphylinidae) from the Sonoran Desert associated with rotting columnar cacti. Molecular Phylogenetics and Evolution 69(3): 491–501. https://doi.org/10.1016/j.ympev.2013.07.030

Pons J, Ribera I, Bertranpetit J, Balke M (2010) Nucleotide substitution rates for the full set of mitochondrial protein-coding genes in Coleoptera. Molecular Phylogenetics and Evolution 56(2): 796–807. https://doi.org/10.1016/j.ympev.2010.02.007

Posada D (2008) jModelTest: Phylogenetic model averaging. Molecular Biology and Evolution 25(7): 1253–1256. https://doi.org/10.1093/molbev/msn083

Pringle EG, Ramírez SR, Bonebrake TC, Gordon DM, Dirzo R (2012) Diversification and phylogeographic structure in widespread *Azteca* plant-ants from the northern Neotropics. Molecular Ecology 21: 3576–3592. https://10.1111/j.1365-294X.2012.05618.x

Rambaut A (2008) Fig Tree ver. 1.3.1. http://tree.bio.ed.ac.uk/software/figtree/

Rambaut A, Suchard MA, Xie D, Drummond AJ (2014) Tracer v1.6. http://tree.bio.ed.ac.uk/software/tracer/

Reyes-Castillo P (2000) Coleoptera Passalidae de México. In: Martín-Piera F, Morrone JJ, Melic A (Eds) Hacia un Proyecto CYTED para el Inventario y Estimación de la Diversidad Entomológica en Iberoamérica: PrIBES-2000. Monografías Tercer Milenio, vol. 1, Sociedad Entomológica Aragonesa, Zaragoza, 171–182.

Ribera I, Fresneda J, Bucur R, Izquierdo A, Vogler AP, Salgado JM, Cieslak A (2010) Ancient origin of a Western Mediterranean radiation of subterranean beetles. BMC Evolutionary Biology 10(1): 29. https://doi.org/10.1186/1471-2148-10-29

Rodríguez SR, Morales-Barrera W, Layer P, González-Mercado E (2010) A quaternary monogenetic volcanic field in the Xalapa region, eastern Trans-Mexican volcanic belt: Geoology, distribution and morphology of the volcanic vents. Journal of Volcanology and Geothermal Research 197(1–4): 149–166. https://doi.org/10.1016/j.jvolgeores.2009.08.003

Rodríguez-Gómez F, Gutiérrez-Rodríguez C, Ornelas JF (2013) Genetic, phenotypic and ecological divergence with gene flow at the Isthmus of Tehuantepec: The case of the

azure-crowned hummingbird (*Amazilia cyanocephala*). Journal of Biogeography 40(7): 1360–1373. https://doi.org/10.1111/jbi.12093

Ronquist F, Teslenko M, van der Mark P, Ayres DL, Darling A, Höhna S, Larget B, Liu L, Suchard MA, Huelsenbeck JP (2012) MrBayes 3.2: Efficient Bayesian phylogenetic inference and model choice across a large model space. Systematic Biology 61(3): 539–542. https://doi.org/10.1093/sysbio/sys029

Rzedowski J (1994) Vegetación de México. Limusa and Grupo Noriega Editores, México, D. F., 432 pp.

Sánchez-Sánchez H, López-Barrera G, Peñaloza-Ramírez JM, Rocha-Ramírez V, Oyama K (2012) Phylogeography reveals routes of colonization of the dark beetle *Dendroctonus approximatus* Dietz in Mexico. Journal of Heredity 103: 638–650. https://doi.org/10.1093/jhered/ess043

Santiago-Jiménez QJ (2010) Revision of the genus *Falagonia* (Coleoptera: Staphylinidae: Aleocharinae: Lomechusini), with description of related genera. Sociobiology 55: 643–723.

Santiago-Jiménez QJ, Espinosa de los Monteros A (2016) Exploring myrmecophily based on the phylogenetic interrelationships of *Falagonia* Sharp, 1883 (Coleoptera: Staphylinidae: Aleocharinae) and allied genera. Systematic Entomology 41(4): 794–807. https://doi.org/10.1111/syen.12191

Saunders DA, Hobbs RJ, Margules CR (1991) Biological consequences of ecosystem fragmentation: A review. Conservation Biology 5(1): 18–32. https://doi.org/10.1111/j.1523-1739.1991.tb00384.x

Seevers CH (1965) The systematics, evolution and zoogeography of staphylinid beetles associated with army ants (Coleoptera, Staphylinidae). Fieldiana, Zoology 47: 137–351. https://doi.org/10.5962/bhl.title.3063

Seevers CH (1978) A generic and tribal revision of the North American Aleocharinae (Coleoptera: Staphylinidae). Fieldiana, Zoology 71: 1–289. https://doi.org/10.5962/bhl.title.3136

Sharp D (1883) Fam. Staphylinidae. In: Godman FD, Salvin O (Eds) Biologia Centrali-Americana, Insecta, Coleoptera, Vol. 1 (2). Taylor & Francis, London, 145–312.

Simon C, Frati F, Beckenbach A, Crespi B, Liu H, Flook P (1994) Evolution, weighting and phylogenetic utility of mitochondrial gene sequences and a compilation of conserved polymerase chain reaction primers. Annals of the Entomological Society of America 87(6): 651–701. https://doi.org/10.1093/aesa/87.6.651

Smith F (1858) Catalogue of hymenopterous insects in the collection of the British Museum. Part. VI. Formicidae. Taylor and Francis, London, 216 pp.

Stamatakis S (2014) RAxML Version 8: A tool for Phylogenetic Analysis and Post-Analysis of Large Phylogenies. Bioinformatics 30(9): 1312–1313. https://doi.org/10.1093/bioinformatics/btu033

Stute M, Forster M, Frischkorn H, Serejo A, Clark JF, Schlosser P, Broecker WS, Bonani G (1995) Cooling of tropical Brazil (5 °C) during the Last Glacial Maximum. Science 269(5222): 379–383. https://doi.org/10.1126/science.269.5222.379

Swofford DL (2002) PAUP*. Phylogenetic Analysis Using Parsimony (*and other methods). Version 4. Sinauer Associates.

Verdú JR, Arellano L, Numa C (2006) Thermoregulation in endothermic dung beetles (Coleoptera: Scarabaeidae): Effect of body size and ecophysiological constraints in flight. Journal of Insect Physiology 52: 854–860. https://10.1016/j.jinsphys.2006.05.005

Supplementary material 1

Chronogram and Skyline-plots based on COI sequences of *Falagonia mexicana*

Authors: Justo A. Reyes, Alejandro Espinosa de los Monteros, Quiyari J. Santiago-Jiménez

Data type: chronogram

Explanation note: For the chronogram the time is in millions of years. The Skyline-plots are shown for the clades going through demographic changes (i.e., Sierra Madre Oriental, Tierras Altas de Chiapas, and global genealogy). On each Skyline-plot, the red line shows the trend of the mean Ne, and blue lines represent 95% HDP confidence limit. Substitution rate of 2.0 (10-2 subs/site/My/lineage) was used.

Link: https://doi.org/10.3897/zookeys.1156.84943.suppl1

Supplementary material 2

Variable sites of the COI nucleotide sequences of *F. mexicana*

Authors: Justo A. Reyes, Alejandro Espinosa de los Monteros, Quiyari J. Santiago-Jiménez

Data type: nucleotides

Explanation note: Variable sites of the COI nucleotide sequences from *F. mexicana*.

Link: https://doi.org/10.3897/zookeys.1156.84943.suppl2

Supplementary material 3

Table of haplotype frequencies found in COI sequences of *F. mexicana* by population

Authors: Justo A. Reyes, Alejandro Espinosa de los Monteros, Quiyari J. Santiago-Jiménez

Data type: haplotype frequencies

Explanation note: Haplotype frequencies found in the 472 bp fragment of COI sequences from *F. mexicana* by population.

Link: https://doi.org/10.3897/zookeys.1156.84943.suppl3

Supplementary material 4

Maximum likelihood tree recovered from sequences of the 472 bp fragment of COI from *Falagonia mexicana*

Authors: Justo A. Reyes, Alejandro Espinosa de los Monteros, Quiyari J. Santiago-Jiménez

Data type: phylogenetic tree

Explanation note: Ln likelihood= -1606.43. The four main lineages identified are Flor de Chiapas (FDC), Sierra Madre del Sur that encompasses the Valles Centrales de Oaxaca (SMS: VCO), Tierras Altas de Chiapas (TAC), and Sierra Madre Oriental (SMO).

Link: https://doi.org/10.3897/zookeys.1156.84943.suppl4

Supplementary material 5

Matrix

Authors: Justo A. Reyes, Alejandro Espinosa de los Monteros, Quiyari J. Santiago-Jiménez

Data type: matrix

Explanation note: Matrix used in the analyses.

Link: https://doi.org/10.3897/zookeys.1156.84943.suppl5

ZooKeys 1156: 133–158 (2023)
doi: 10.3897/zookeys.1156.97768
https://zookeys.pensoft.net

RESEARCH ARTICLE

A peer-reviewed open-access journal
ZooKeys
Launched to accelerate biodiversity research

Diversity and larval leaf-mining habits of Japanese jewel beetles of the tribe Tracheini (Coleoptera, Buprestidae)

Makoto Kato[1], Atsushi Kawakita[2]

1 *Graduate School of Human and Environmental Studies, Kyoto University, Sakyo 606-8501, Kyoto, Japan*
2 *The Botanical Gardens, Graduate School of Science, The University of Tokyo, Tokyo, 112-0001, Japan*

Corresponding author: Makoto Kato (kato@zoo.zool.kyoto-u.ac.jp)

Academic editor: C. Majka | Received 20 November 2022 | Accepted 22 February 2023 | Published 29 March 2023

https://zoobank.org/16142395-CE44-4A1F-A6C7-A3CE32FC108C

Citation: Kato M, Kawakita A (2023) Diversity and larval leaf-mining habits of Japanese jewel beetles of the tribe Tracheini (Coleoptera, Buprestidae). ZooKeys 1156: 133–158. https://doi.org/10.3897/zookeys.1156.97768

Abstract

From the Japanese Archipelago, 12 *Habroloma* and 20 *Trachys* species (Buprestidae: Tracheini) have been recorded. Two new *Habroloma* species were found, which are associated with Elaeocarpaceae and Loranthaceae, also new host plant families/orders for Tracheini. The two new species are described as *Habroloma elaeocarpusi* **sp. nov.** and *Habroloma taxillusi* **sp. nov.**, and the latter is the first Tracheini species shown to be associated with epiphytes. Leaf mines of 31 Tracheini species are also reported in this work, including new records of leaf mines for 16 Tracheini species. The larvae of all these recorded species are full-depth linear-blotch mesophyll miners of mature leaves and pupate within their mines. The mining habits of *Habroloma* species associated with *Symplocos* (Symplocaceae) are unique: the young larvae bore into midribs and petioles and cause leaf fall, and the larvae then mine the fallen leaves.

Keywords

Agrilinae, *Habroloma*, leaf miner, mining pattern, *Symplocos*, *Trachys*

Introduction

The coleopteran family Buprestidae is a species-rich clade whose larvae are xylophagous wood-borers, while the leaf-mining habit has evolved (Hering 1951). The tribe Tracheini of the subfamily Agrilinae is one of these leaf-mining clades and has great diversity, especially in Asia, Europe, and Africa. The two genera of Tracheini, *Trachys* and

Habroloma, comprise more than 650 and 300 species worldwide, respectively (Bellamy 2008). Continental Asia is home to diverse trachyine species (Obenberger 1918, 1929) and the number of trachyine species has been underestimated. In recent years, 14 *Trachys* and 33 *Habroloma* species have been newly described from China (Peng 2020, 2021a, b, c, d, 2022a, b). By contrast, the Japanese Archipelago harbors 20 *Trachys* and 12 *Habroloma* species (Buprestidae: Tracheini) (Ohmomo and Fukutomi 2013), and no new taxa have been added since the monograph by Kurosawa (1959).

Leaf-mining habits in Buprestidae are believed to have evolved from wood-boring habits (Frost 1924), and the switch from wood-boring to leaf-mining has occurred several times in Buprestidae (Evans et al. 2015). The leaf-mining habits of Japanese trachyine species are characterized by full-depth blotch mining of the leaves of woody plants such as *Malus*, *Rosa*, *Prunus*, *Ulmus*, *Zelkova*, *Aphananthe*, *Broussonetia*, *Quercus*, *Castanopsis*, *Platycarya*, *Salix*, and *Deutzia*, or subwoody climbing plants such as *Pueraria*, *Amphicarpaea*, and *Desmodium* (Yano 1952), while in Europe many leaf-mining trachyine species are associated with herbaceous plants such as *Fragaria*, *Potentilla*, *Scabiosa*, *Stachys*, *Malva* (Frost 1924), and *Geranium* (Schaefer 1950).

Of the 32 Japanese trachyine species, host plants have been reported for 28 (Ohmomo and Fukutomi 2013). The known host plants belong to seven angiosperm orders: Fabales (3 spp.), Rosales (13. spp.), Fagales (5 spp.), Malpighiales (2 spp.), Malvales (1 sp.), Cornales (2 spp.), and Ericales (2 spp.). The host plant records are based mainly on observations of adult beetles feeding, with immature stages and leaf mines being reported only for nine *Trachys* and four *Habroloma* species in Japan (Yano 1952).

To shed light on the diversity and host plant associations of trachyine species in Japan, we have conducted extensive rearing of leaf-mining larvae on diverse plants and a substantial collection of mined leaves. From the accumulated materials, we identified two undescribed trachyine species. The two new species are associated with two new plant orders and families for Tracheini: Oxalidales (Elaeocarpaceae) and Santalales (Loranthaceae). Furthermore, we detected leaf mines for 31 trachyine species, including new leaf mine records for 18 trachyine species. In this paper, we describe the two new species, as well as the leaf mines of 31 trachyine species, and discuss the diversity and evolution of plant utilization patterns of trachyine species in the Japanese Archipelago.

Materials and methods

We have conducted extensive sampling of buprestid leaf mines from the Japanese Archipelago since the 1980s. By rearing the leaf-mining larvae, we obtained 400 adult buprestid beetles. All of the specimens were collected by MK unless otherwise noted. The leaves containing leaf mines were dried, and the dried herbarium specimens have been deposited in the Kyoto University Museum (**KUM**).

The morphology of adult specimens was examined under a microscope (VHS-7000; Keyence). Specimens were photographed by synthesizing virtual images from

a sequence of corresponding depth images. To observe male genitalia, the specimens were macerated in hot water and dissected under a microscope. The abdomen was removed from the body and then cleaned in 5% KOH solution for ~ 12 h at room temperature. After washing in distilled water, the terminalia extracted from the abdomen were mounted on slides with glycerol.

Results

Systematics of Japanese *Habroloma* Thomson, 1864

Among adult beetles that emerged from collected leaf mines, we identified two new *Habroloma* species. We describe the two species using the following key to Japanese species. In this key, *Habroloma hikosanensis* is missing because it is within the morphological variation of *Habroloma yuasai*.

Key to the Japanese *Habroloma* Thomson, 1864 species

1 Pronotum with a large distinct fovea at the post-inferior side of each anterior angle ..... ***bifrons*** **(Kiesenwetter, 1879)**

– Pronotum with a shallow depression at the post-inferior side of each anterior angle **2**

2 Ventral surface of body flattened; thickness index (body thickness/body length) less than 0.36 (Fig. 2A–D); prosternal process inverted trapezoid, posterior margin linearly truncated (Fig. 3A–D) **3**

– Ventral surface of body convex ventrally; thickness index (body thickness/body length) greater than 0.37; prosternal process round or lingulate, longer than wide, posterior margin often rounded (Fig. 3E–J) **6**

3 Elytra clothed with greyish golden hairs except silvery vitta (Fig. 1A, B) **4**

– Elytra clothed with greyish hairs except silvery vitta (Fig. 1C, D) **5**

4 Elytra with a distinct V-shaped silvery vitta (Fig. 1B) ..... ***eximium*** **(Lewis, 1892) [host:** ***Symplocos***]

– Elytra without a distinct V-shaped silvery vitta (Fig. 1A) ..... ***liukiuensis*** **Obenberger, 1940 [host:** ***Symplocos***]

5 Elytra with a V-shaped silvery vitta, which neighboring a V-shaped black vitta ahead (Fig. 1C); prosternal process slightly expanded posteriorly (Fig. 3C) ... ***griseonigra*** **(E. Saunders, 1873) [host:** ***Quercus***]

– Elytra with two waving transverse silvery vittae on posterior half; anterior vitta M-shaped (Fig. 1D); prosternal process strongly expanded posteriorly (Fig. 3D) ..... ***elaeocarpusi*** **Kato, sp. nov. [host:** ***Elaeocarpus***]

6 Basal 2/3 of elytra with a steel-blue patch (Fig. 1E) ..... ***lewisii*** **(E. Saunders, 1873) [host:** ***Rosa***].

– Elytra without steel-blue patch **7**

7 Elytra with three wavy silvery and golden transverse vittae on posterior 2/3 (Fig. 1F); prosternal process round (Fig. 3F) ..... ***taxillusi* Kato, sp. nov. [host: *Taxillus*]**

– Elytra with two wavy silvery or golden transverse vittae on posterior half (Fig. 1G–K); prosternal process lingulate, longer than wide (Fig. 3G–J) **8**

8 Body subovate, less attenuated posteriorly, margins nearly parallel in basal half (Fig. 1G); prosternal process narrowest at base, with rounded posterior margin (Fig. 3G)..... ***nixilla* (Obenberger, 1929) [host: *Lagerstroemia*]**

– Body cuneiform, attenuating toward posterior end even from basal half (Fig. 1H–K); prosternal process with linearly truncated posterior margin (Fig. 3H–J) **9**

9 Anterior wavy transverse silverly/golden band of posterior elytra complete (Fig. 1H, I); prosternal process with posterior margin linearly truncated (Fig. 3H, I) **10**

– Anterior wavy transverse silverly/golden band of posterior elytra disconnected midway (Fig. 1J, K); prosternal process with posterior margin arched (Fig. 3J) **12**

10 Anterior wavy transverse band silvery (Fig. 1I) ..... ***marginicolle* (Fairmaire, 1888) [host: *Rubus*]**

– Anterior wavy transverse band grayish-golden and partly silvery (Fig. 1H)... **11**

11 Elytra with the sides constricted behind humeri; prosternal process as long as wide..... ***asahinai* Y. Kurosawa, 1959 [host: *Rubus*]**

– Elytra with the sides not constricted behind humeri (Fig. 1H); prosternal process longer than wide (Fig. 3H) ..... ***yuasai* Y. Kurosawa, 1976 [host: *Platycarya*]**

12 Elytra strongly attenuate from base to the apex, with the sides less arcuate and distinctly constricted behind humeri (Fig. 1J) ..... ***subbicorne* (Motschulsky, 1860) [host: *Rubus*]**

– Elytra attenuate from the base to the apex, with the sides not constricted behind humeri (Fig. 1K)..... ***atronitidum* (Gebhardt, 1929) [host: *Rubus*]**

***Habroloma elaeocarpusi* sp. nov.**

https://zoobank.org/13395C99-4CB0-48AB-8BAA-5BA2C4799DEF

Figs 1D, 2D, 3D, K–M

Material examined. ***Holotype*:** Japan: ♂ (MK-BP-a327), Mt. Osuzu, Tsuno-cho, Miyazaki Pref. (32.262°N, 131.471°E, 230 m above sea level), 14-VII-2021 (as larva on *Elaeocarpus japonicus*), emerged on 27-VII-2021, NSMT-I-C-200265.

***Paratypes*:** Japan: 1♂(MK-BP-a360), same data as holotype, emerged on 30-VII-2021, NSMT-I-C-200266; 1♀ (MK-BP-k35), Isso, Yakushima-cho, Yaku Island (30.440°N, 130.472°E, 60 m above sea level), 11-VI-1993 (as larva on *Elaeocarpus japonicus*), emerged on 26-VI-1993, NSMT-I-C-200267.

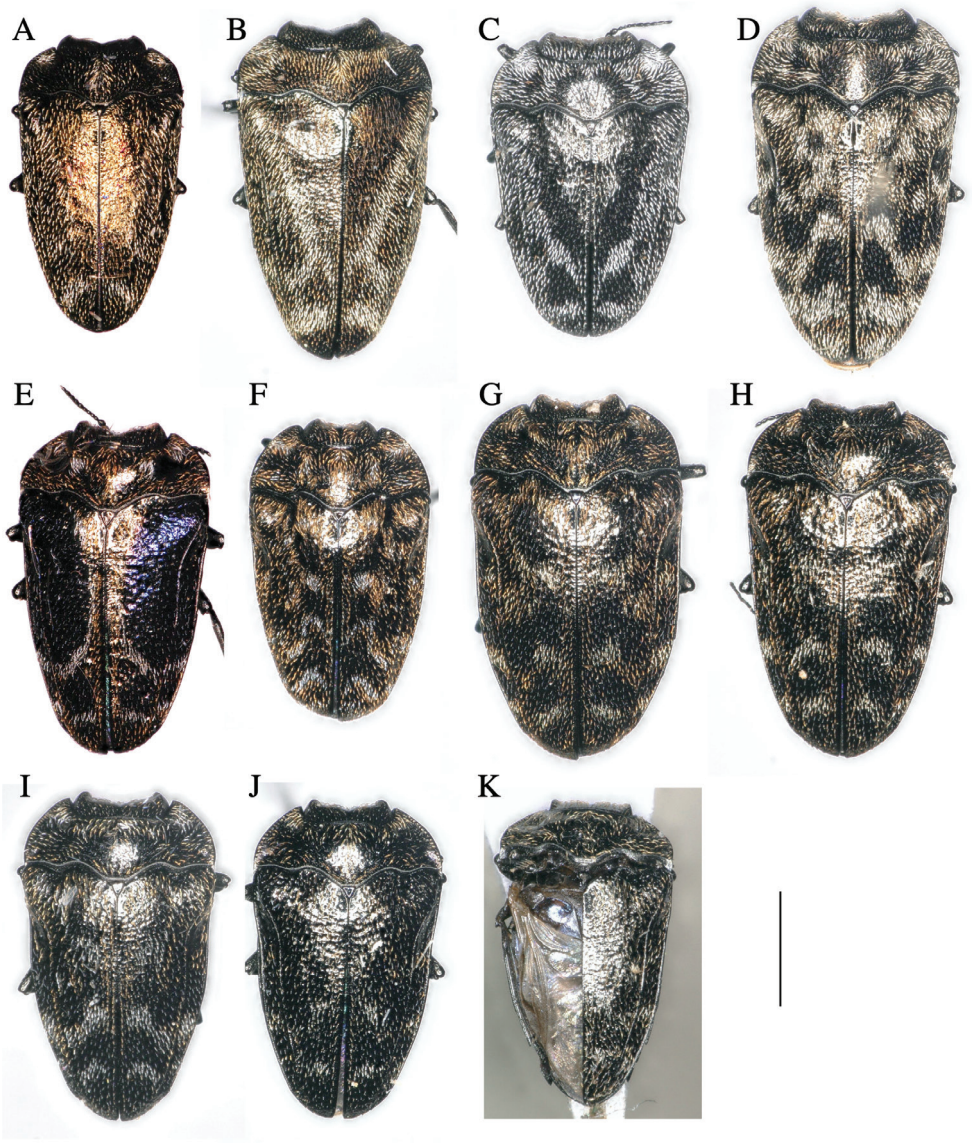

Figure 1. *Habroloma* species of Japan, adult dorsal views **A** *H. liukiuense* **B** *H. eximium eupoetum* **C** *H. griseonigrum* **D** *H. elaeocarpusi* **E** *H. lewisii* **F** *H. taxillusi* **G** *H. nixilla insulicola* **H** *H. yuasai* **I** *H. marginicolle* **J** *H. subbicorne* **K** *H. atronitidum*. Scale bar: 1 mm.

Other material. Japan: 2♂2♀, same data as holotype, emerged on 27-VII–2-VI-II-2021.

Diagnosis. A small wedge-shaped species (length 3.1–3.3 mm) having pronotum with posterior margin trisinuate. Elytra rather flattened, ornamentation consisting of white pubescence; on posterior half with three transverse bands, anterior one obliquely

zigzag, two posterior ones transversely straight. Male genitalia with slender tegmen with paramere setiferous on anterior margin and slender pennis with rounded apex. Larvae mine leaves of *Elaeocarpus japonicus*.

Description. Adult male: (Figs 1D, 2D, 3D) ***Body*** somewhat wedge-shaped and attenuated posteriorly; above entirely black-aeneous; body beneath, legs, and antennae black, with a very slight aeneous tinge, except tarsal lamellae brownish.

Head, seen from above, transverse, broadly and sharply excavated between the eyes, with the inferior rim of the eyes strongly and rather suddenly produced; frons with the median impression distinct; fovea just above each antennal cavity obsolete and indistinct; surface rather smooth, sparsely scattering laterally with traces of variolate and ocellate punctures, and sparsely clothed with whitish recumbent hairs; clypeal suture transverse, somewhat arcuate exteriorly; clypeus transverse, ~ 2.6× as wide as long, with the anterior margin somewhat arcuately emarginate; antennal cavities surrounded posteriorly with elevated carina; antennae short and compact, with the third segment ~ 1.5× as long as the fourth, with apical five segments serrated.

Pronotum transverse, widest just before the base, distinctly wider than elytra, and ~ 3.2× as wide as long; sides slightly but distinctly expanded just before the base, then crescent-shaped and strongly attenuated to the anterior angles, which are acute and strongly produced in dorsal aspect; anterior margin deeply, broadly and arcuately emarginate; posterior margin trisinuate, produced and subtruncate, narrowly and slightly emarginate just before scutellum; posterior angles acute and produced posteriorly; disk dilated laterally, broadly and obsoletely depressed at the anterior half of the lateral dilation on each side, but without fovea, and obsoletely impressed along the basal lobe causing the middle of the disk to be somewhat convex; surface lustrous, punctured with traces of large, obsolete, shallow, somewhat ocellate punctures, and sparsely clothed with whitish hairs. Scutellum smooth and triangular.

Elytra rather deplanate, widest at the base, ~ 1.3× as long as wide and ~ 4.3× as long as pronotum; sides feebly sinuate and narrowed or subparallel to the anterior 2/5, and then arcuately attenuated to the apex, but the attenuation somewhat angulate near the apex; sutural margin not elevated entirely; humeri slightly prominent; basal depressions along the base transverse; lateral carinae subparallel to the lateral margin; disk constricted behind humeri, narrowly and obsoletely impressed along the inferior side of each lateral carina; surface rather uniformly but coarsely punctate with shallow, ill-defined, irregularly sized punctures, with the punctuation being somewhat rugous at the sides; ornamentation consisting of white, yellowish-grey, and blackish hairs, with the whitish hairs being predominant. Ornamentation consisting of white pubescence arranged on each elytron as follows: at base with two irregular spots, at mid length near suture with one irregular spot, toward side with one narrow, wavy, and irregular strip, on posterior half with three transverse bands, anterior one obliquely zigzag, two posterior ones transversely straight.

Body beneath scattered with very fine inconspicuous cinereous hairs. Prosternal process inverted trapezoidal, narrow toward the base, ~ 1.3× broader than long, with the apex almost truncate. Metasternum slightly convex coarsely punctate with variolate

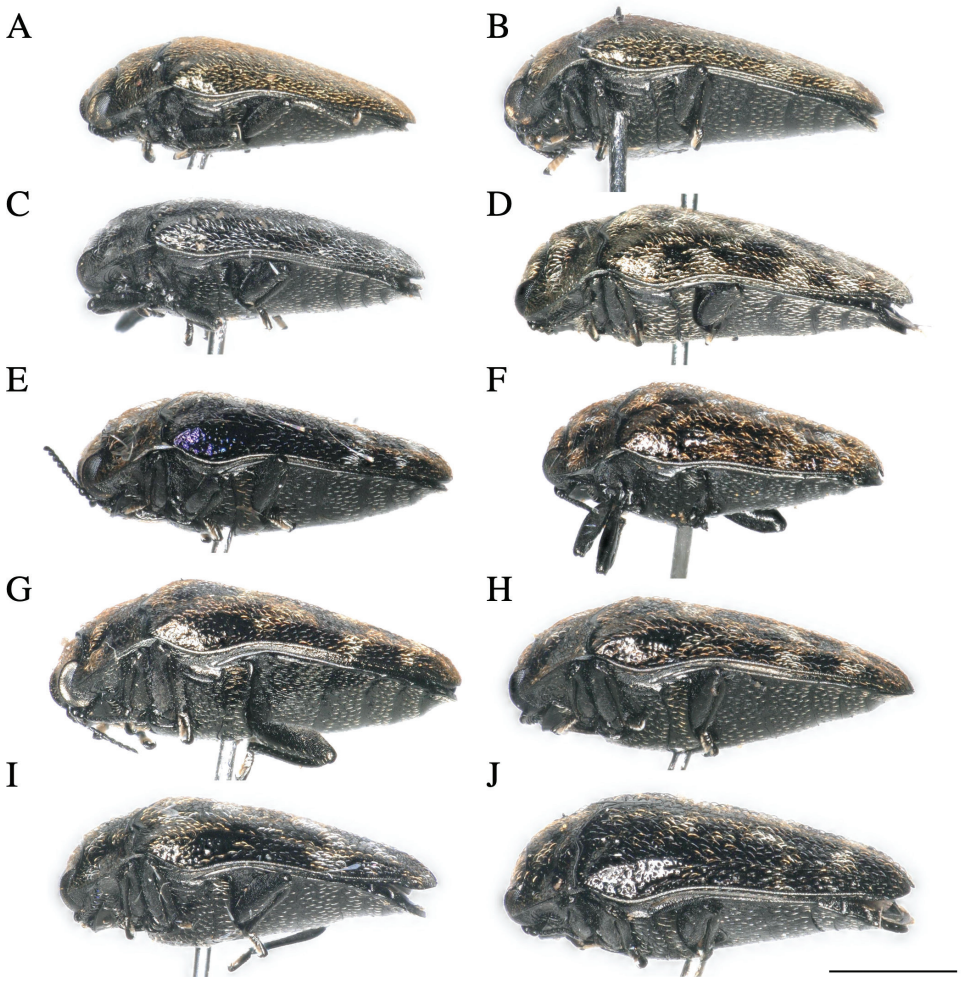

Figure 2. *Habroloma* species of Japan, adult lateral views **A** *H. liukiuense* **B** *H. eximium eupoetum* **C** *H. griseonigrum* **D** *H. elaeocarpusi* **E** *H. lewisii* **F** *H. taxillusi* **G** *H. nixilla insulicola* **H** *H. yuasai* **I** *H. marginicolle* **J** *H. subbicorne*. Scale bar: 1 mm.

and obsolete punctures at the middle. Abdomen beneath rather uniformly punctate with shallow, obsolete variolate punctures. Legs normal; posterior coxae depressed entirely, with the latero-posterior angles acute and produced latero-posteriorly.

Male genitalia (Fig. 3K–M). Sternite VIII wide, roundly arcuated along anterior margin, furnished with several setae on each side of anterior margin. Tegmen slender; paramere setiferous on anterior margin; phallobase wide, ~ 1/5 length of tegmen. Penis slender, slightly shorter than tegmen; round at apex, basally with median struts ~ 1/3 length of penis.

Female. Like the male, but more robust. Length: 3.1–3.3 mm, width: 1.8–1.9 mm.

Etymology. The name indicates the host plant genus, *Elaeocarpus*.

Japanese name. Kobanmochi-hiratachibi-tamamushi.
Host plant. *Elaeocarpus japonicus* Sieb. et Zucc.
Habitat. Primary evergreen forests dominated by *Castanopsis sieboldii* subsp. *sieboldii*.
Distribution. Japan (Kyushu and Yaku Island).

***Habroloma taxillusi* sp. nov.**
https://zoobank.org/3A0F84C8-254D-4F21-AD10-90501E54DB37
Figs 1F, 2F, 3F

Material examined. ***Holotype*:** Japan: ♂ (MK-BP-k40), Yakukachi, Amami-shi, Kagoshima Pref. (28.228°N, 129.347°E, 40 m above sea level), 23-V-2009 (as larva on *Taxillus yadoriki* collected by A. Kawakita), emerged on 7-VI-2009, NSMT-I-C-200268.

***Paratype*:** Japan: 1♀(MK-BP-k39), same data as holotype, emerged on 2-VI-2009, N NSMT-I-C-200269.

Diagnosis. A small wedge-shaped species (length 2.5–2.7 mm) having pronotum with posterior margin trisinuate. Elytra slightly convex around base, ornamentation consisting of yellowish-grey pubescence; on posterior 2/3 with three transverse bands, first two obliquely zigzag, apical one slightly transversely waved. Larvae mine leaves of a mistletoe species, *Taxillus yadoriki*.

Description. Adult male: (Figs 1F, 2F, 3F) ***Body*** somewhat wedge-shaped and attenuated posteriorly; above entirely black-aeneous; body beneath, legs, and antennae black, with a very slight aeneous tinge, except tarsal lamellae dark brownish.

Head, seen from above, transverse, broadly excavated between the eyes, with the inferior rim of the eyes strongly produced; frons with the median impression distinct; fovea just above each antennal cavity obsolete and indistinct; surface rather smooth, sparsely scattered laterally with traces of variolate and ocellate punctures, and sparsely clothed with recumbent yellowish-grey hairs; clypeal suture transverse, somewhat arcuate exteriorly; clypeus transverse, ~ 2.6× as wide as long, with the anterior margin somewhat arcuately emarginate; antennal cavities surrounded posteriorly with elevated carina; antennae short and compact, with the third segment ~ 1.5× as long as the fourth, and five apical serrated segments.

Pronotum transverse, widest just before the base, as wide as elytra, and ~ 2.4× as wide as long; sides slightly but distinctly expanded just before the base, then crescent-shaped and strongly attenuated to the anterior angles, which are acute and strongly produced in dorsal aspect; anterior margin deeply, broadly, and arcuately emarginate; posterior margin trisinuate and subtruncate, narrowly and slightly emarginate just before scutellum; posterior angles acute and produced posteriorly; disk dilated laterally, broadly and obsoletely depressed at the anterior half of the lateral dilation on each side, but without fovea, and obsoletely impressed along the basal lobe causing the middle of the disk to be somewhat convex; surface lustrous, punctured the traces of large, obsolete, shallow, somewhat ocellate structures, and sparsely clothed with yellowish gray hairs. Scutellum smooth and triangular.

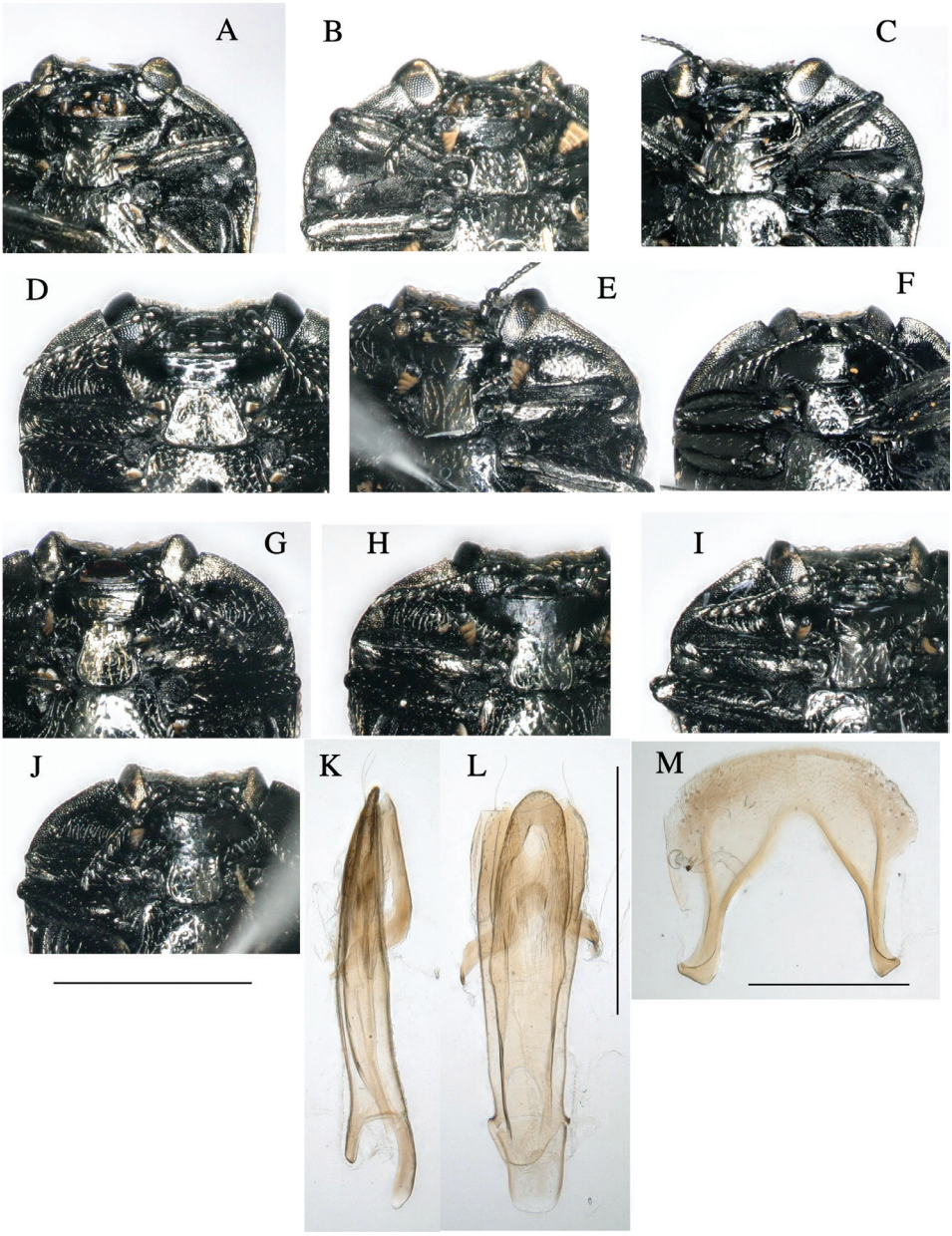

Figure 3. *Habroloma* species of Japan, adult ventral views (**A–J**) and male genitalia of *H. elaeocarpusi* (**K–M**). **A** *H. liukiuense* **B** *H. eximium eupoetum* **C** *H. griseonigrum* **D** *H. elaeocarpusi* **E** *H. lewisii* **F** *H. taxillusi* **G** *H. nixilla insulicola* **H** *H. yuasai* **I** *H. marginicolle* **J** *H. subbicorne* **K, L** lateral and ventral views of tegmen, pennis and sternite IX **M** tergite VIII. Scale bars 1 mm (**A–J**); 0.5 mm (**K–M**).

Elytra slightly convex along base, widest at the base, ~ 1.4× as long as wide and ~ 3.3× as long as pronotum; sides feebly sinuate and narrowed or subparallel to the anterior 2/5, and then arcuately attenuated to the apex but with the attenuation somewhat an-

gulate near the apex; humeri slightly prominent; basal depressions along the base transverse; lateral carinae subparallel to the lateral margin; disk constricted behind humeri, narrowly and obsoletely impressed along the inferior side of each lateral carina; surface rather uniformly but coarsely punctate with shallow, ill-defined, irregularly sized punctures, but the punctuation somewhat rugous at the sides. Ornamentation consisting of yellowish grey pubescence arranged on each elytron as follows: at base with two irregular spots, on posterior 2/3 with three transverse bands, first and second ones obliquely zigzag, apical one slightly transversely waved; with transverse irregular spot apically.

Body beneath scattered with very fine inconspicuous cinereous hairs. Prosternal process rounded, ~ 1.27× broader than long. Metasternum slightly convex and coarsely punctate, with variolate and obsolete punctures at the middle. Abdomen beneath rather uniformly punctate with shallow, obsolete variolate punctures. Legs normal; posterior coxae depressed entirely, with the latero-posterior angles acute and produced latero-posteriorly.

***Male genitalia*:** not studied.

Female. Like the male, but more robust. Ornamentation of elytra is similar but pubescence more whitish in female. Body length: 2.5–2.7 mm, width: 1.5–1.7 mm.

Etymology. The specific name indicates host plant genus, *Taxillus*.

Japanese name. Obayadorigi-hiratachibi-tamamushi.

Host plant. *Taxillus yadoriki* (Maxim.) Danser [Loranthaceae]

Habitat. Canopy of primary evergreen forests dominated by *Castanopsis sieboldii* subsp. *lutchuensis* (Fig. 5L).

Distribution. Japan (Amami-Oshima Island, known only from the type locality).

Leaf mines of Japanese Tracheini species

Leaf mines of Tracheini species have the following characteristics. The mined leaves are mature leaves that have completed expansion and hardening. An egg is laid on the upper side of a leaf and covered by a circular brown glossy coating, which is secreted by an adult female. Pupation takes place within the mine. Hereafter, we describe leaf mines of the 14 *Habroloma* and 20 *Trachys* species in Japan.

Habroloma species checklist

1. *Habroloma subbicorne* (Motschulsky, 1860)
Fig. 4A–E

Host plant. Rosaceae: *Rubus parvifolius* (Yano 1952), *Rubus palmatus*, *Rubus buergeri* (Kurosawa 1959).

Leaf mine. Brown full-depth blotch mine on mature leaf. Egg is laid at a distance from leaf margin and the mine expands in the leaf blade. Frass is thread-like.

Material examined. Nishihoragawa, Kiso, Nagano Pref. 6-VIII-2015 (as larva on *Rubus palmatus* var. *coptophyllus*), emerged on 27-VIII-2015 (Fig. 4A); Sakai-gawa, Takaoka, Miyazaki, Miyazaki Pref., 21-IX-2020 (as larva on *R. buergeri*), emerged on 7-VII-

2020 (Fig. 4B, C); Seikandoro, Kumanogawa, Shingu, Wakayama Pref., 14-VII-2021 (as larva on *R. buergeri*), emerged on 31-VII-2021 (Fig. 4D); Furubokke, Kasai, Hyogo Pref., 11-IX-2018 (as pupa on *R. parvifolius parvifolius*), emerged on 15-IX-2018 (Fig. 4E).

2. *H. atronitidum* (Gebhardt, 1929)
Fig. 4F

Host plant. Rosaceae: *Rubus vernus* (new record).

Leaf mine. Brown full-depth blotch mine on mature leaf. Egg is laid near leaf margin, and the mine expands along the leaf margin. Frass is thread-like.

Material examined. Mumyo-dani, Niimi, Okayama Pref., 9-VII-1991 (as pupa on *Rubus vernus*), emerged on ?-VIII-1991 (Fig. 4F).

3. *H. marginicolle* (Fairmaire, 1888)
Fig. 4G–I

Host plant. Rosaceae: *Rubus sieboldii* (Kurosawa 1959), *Rubus buergeri* (new record).

Leaf mine. Brown blotch mine on mature leaf. Egg is laid at a distance from leaf margin, and the mine expands in the leaf blade. Frass is thread-like.

Material examined. Modo, Minamata, Kumamoto Pref., 26-V-2018 (vacant mine of *Rubus sieboldii*) (Fig. 4G); Inohae, Kitago, Nichinan, Miyazaki Pref., 16-VI-2019 (as larva on *Rubus sieboldii*), emerged on 19-VII-2019; Inohae, Kitago, Nichinan, Miyazaki Pref., 16-VI-2019 (as larva on *R. buergeri*), emerged on 21-VII-2019 (Fig. 4H, I).

4. *H. asahinai* Y. Kurosawa, 1959
Fig. 4J

Host plant. Rosaceae: *Rubus sieboldii* (Ohmomo and Fukutomi 2013).

Leaf mine. Brown full-depth blotch mine on mature leaf. Egg is laid near leaf margin, and the mine expands along the leaf margin. Frass is thread-like.

Material examined. Okuma, Kunigami, Okinawa Pref., 30-III-2018 (vacant mine of *Rubus sieboldii*) (Fig. 4J).

5. *H. lewisii* (E. Saunders, 1873)
Fig. 4K–M

Host plant. Rosaceae: *Rosa multiflora* (Yano 1952).

Leaf mine. Brown, full-depth sometimes bluish, linear-blotch mine on mature leaf. Egg is laid along leaf margin, and the mine expands along leaf margin. Frass is thread-like, coiling or undulating for an extended length.

Material examined. Sabushi-gawa, Niimi, Okayama Pref., 1-VII-2018 (as larva on *Rosa multiflora*), emerged on 18-VII-2018 (Fig. 7K); Shimotokuyama, Hiruzen, Maniwa, Okayama Pref., 1-VII-2018 (as larva on *Rosa multiflora*) (Fig. 4L, M).

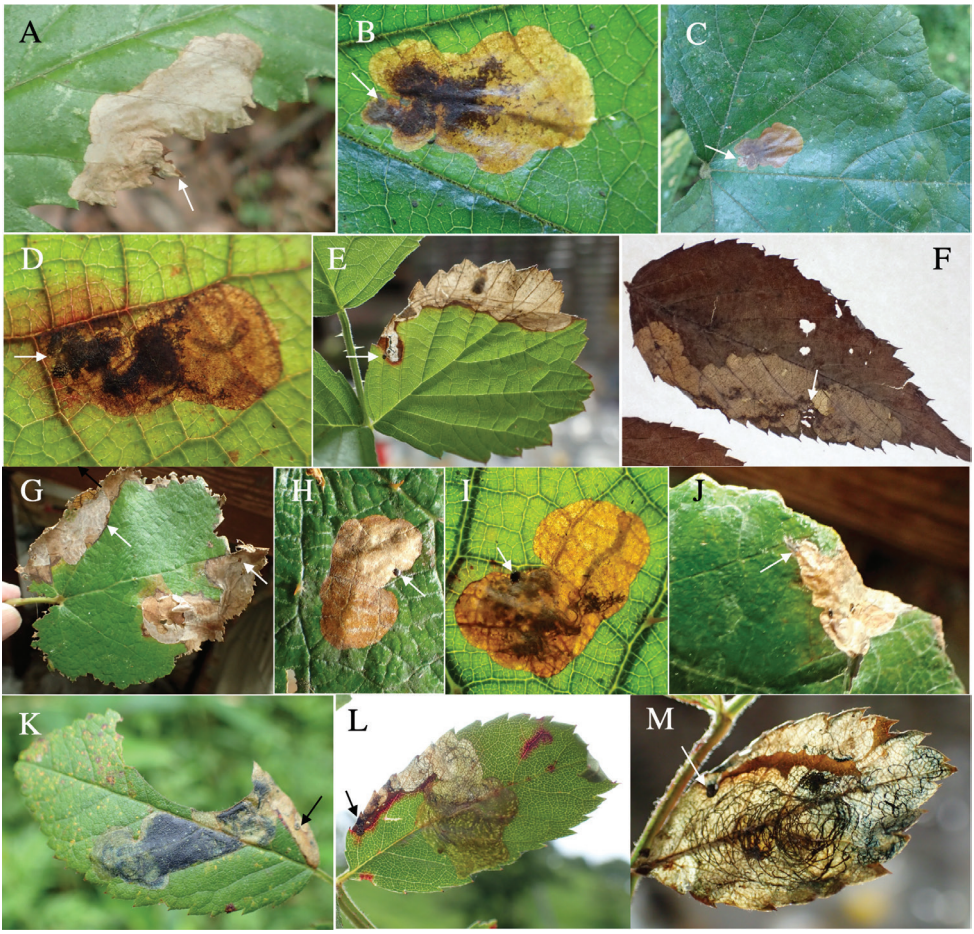

Figure 4. Leaf mines of *Habroloma* spp. on leaves of Rosaceae **A–E** *H. subbicorne* on *Rubus palmatus* var. *coptophyllus* (**A**), *Rubus buergeri* (**B–D**), and *Rubus parvifolius* (**E**) **F** *H. atronitidum* on *Rubus vernus* **G–I** *H. marginicolle* on *Rubus sieboldii* **J** *H. asahinai* on *Rubus sieboldii* **K–M** *H. lewisii* on *Rosa multiflora.* Arrows indicate oviposition scars.

6. *H. griseonigrum* (E. Saunders, 1873)

Fig. 5A

Host plant. Fagaceae: *Quercus glauca*, *Q. acutissima*, *Q. serrata* (Yano 1952), *Quercus acuta* (Ohmomo and Fukutomi 2013), *Quercus hondae* (new record).

Leaf mine. Brown full-depth blotch mine on mature leaf. Egg is laid near leaf margin of leaf base, and the mine expands upwards along leaf margin. Frass is thread-like.

Material examined. Gion, Yayoi, Saeki, Ooita Pref., 14-VI-1998 (as larva on *Quercus hondae*); emerged on 8-VII-1998 (Fig. 5A).

7. *H. yuasai* Y. Kurosawa, 1976
Fig. 5B–D

Host plant. Juglandaceae: *Platycarya strobilacea* (Yano 1952).

Leaf mine. Brown full-depth linear-blotch mine on mature leaf. Egg is laid near leaf margin, and the mine expands along leaf margin. Frass is thread-like, excreted from the mine through cracks of upper epidermis.

Material examined. Makido, Niimi, Okayama Pref., 22-VI-2020 (as larva on *Platycarya strobilacea*), emerged on 20-VII-2020 (Fig. 5B–D).

8. *H. elaeocarpusi* sp. nov
Fig. 5E–G

Host plant. Elaeocarpaceae: *Elaeocarpus japonicus* (new record).

Leaf mine. Pale brown full-depth linear-blotch mine on mature leaf. Egg is laid just beside midrib of leaf base, and the mine expands along midrib or along leaf margin. Frass is thread-like; frass line iterating arc-shaped reciprocating motion.

Material examined. Mt. Osuzu, Tsuno-cho, Miyazaki Pref., 14-VII-2021 (as larva on *Elaeocarepus japonicus*), emerged on 27-VII-2021 (Fig. 5E–G).

9. *H. bifrons* (Kiesenwetter, 1879)

Host plant. Unknown, while related species in Europe is associated with *Geranium* (Geraniaceae).

Leaf mine. Unknown.

10. *H. nixilla insulicola* Y. Kurosawa, 1959
Fig. 5H, I

Host plant. Lythraceae: *Lagerstroemia subcostata* (Kurosawa 1959).

Leaf mine. Brown full-depth linear-blotch mine on mature leaf. Egg is laid along leaf margin of leaf base, and the mine expands along leaf margin. Frass is thread-like, coiling in the mine.

Material examined. Sumiyo, Amami, Kagoshima Pref., 23-V-2009 (as larva on *Lagerstroemia subcostata*), emerged on 6-VI-2009 (Fig. 8H, I).

11. *H. taxillusi* sp. nov.
Fig. 5J–L

Host plant. Loranthaceae: *Taxillus yadoriki* (new record).

Leaf mine. Brown full-depth linear-blotch mine on mature leaf. Egg is laid along leaf margin of leaf base, and the mine expands along leaf margin. Frass is granular, accumulated in the center of the mine.

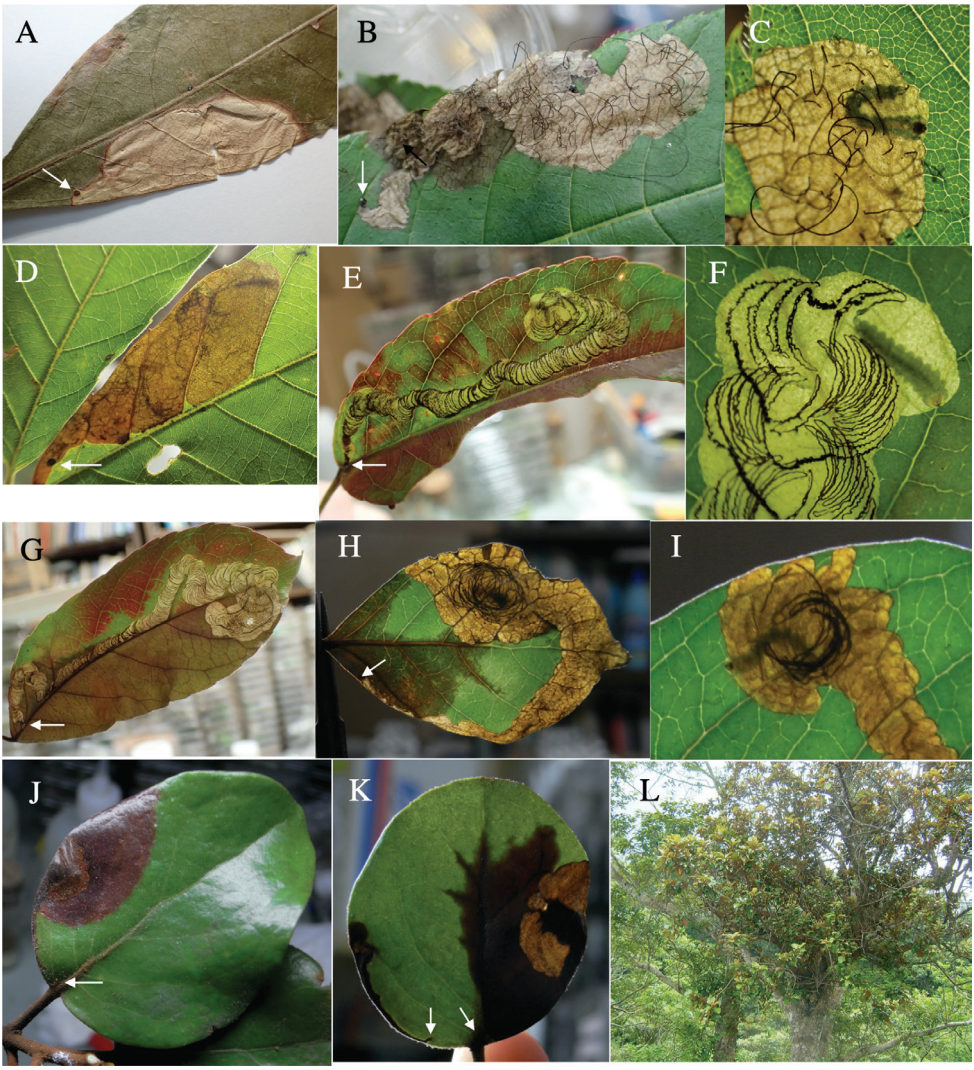

Figure 5. Leaf mines of *Habroloma* spp. on leaves of Fagaceae, Juglandaceae, Elaeocarpaceae, Lythraceae, and Loranthaceae **A** *H. griseonigrum* on *Quercus hondae* **B–D** *H. yuasai* on *Platycarya strobilacea* **E–G** *H. elaeocarpusi* on *Elaeocarpus japonicus* **H, I** *H. nixilla* on *Lagerstroemia subcostata* **J–L** *H. taxillusi* on *Taxillus yadoriki*. Arrows indicate oviposition scars.

Material examined. Yakukachi, Amami-shi, Kagoshima Pref., 23-V-2009 (as larva on *Taxillus yadoriki*), emerged on 7-VI-2009 (Fig. 5J–L).

12a. *H. eximium eximium* (Lewis, 1893)

Host plant. Symplocaceae: *Symplocos lancifolia* (Kurosawa 1959).

Leaf mine. Unknown.

12b. *H. eximium eupoetum* (Obenberger, 1929**)**
Fig. 6A–C

Host plant. Symplocaceae: S*ymplocos prunifolia* (Kurosawa 1976), while the identification seems to be incorrect; *S. caudata* (new record).

Leaf mine. Pale brown full-depth linear-blotch mine on mature leaf. Egg is laid near midrib of leaf base, and the hatched larva enters midrib and bores into petiole, causing the leaf to fall off from the branch by being abscised at the petiole base. After the leaf-fall, the mine departs from the midrib and slowly expands upwards along leaf margin or along midrib. After advancing halfway, the mine abruptly expands to become a blotch mine. Frass is thread-like, going in a zigzag in the early linear mine, and becomes thick cord-like without undulating as the mine expands. The fallen leaf is kept green for ca. two weeks, during which the larva completes its development.

Material examined. Komi, Iriomote Is., Yaeyama, Okinawa Pref., 10-V-2020 (as larva on *Symplocos caudata*), emerged on 15-VI-2020 (Fig. 6A–C).

13. *H. liukiuense* (Obenberger, 1940)
Fig. 6D–I

Host plant. Symplocaceae: S*ymplocos okinawensis* (Ohmomo and Fukutomi 2013), *S. microcalyx* (Ohmomo and Fukutomi 2013).

Leaf mine. Pale brown full-depth linear-blotch mine on mature leaf. Egg is laid near midrib of leaf base, and the hatched larva enters midrib and bores into petiole, causing the leaf to fall off from the branch by being abscised at the petiole base. After the leaf-fall, the mine departs from the midrib and slowly expands upwards along leaf margin or along midrib. After advancing halfway, the mine abruptly expands to become a blotch mine. Frass is thread-like, going in a zigzag in the early linear mine, and becomes granular. The fallen leaf is kept green for ca. two weeks, during which the larva completes its development.

Material examined. Foothill of Mt. Yonaha, Kunigami, Okinawa Pref., 6-VI-2018 (as larva on *Symplocos microcalyx*), emerged on 12-VII-2018 (Fig. 6D–I).

14. *H. hikosanense* Y. Kurosawa, 1959

Host plant. Unknown.

Leaf mine. Unknown.

Trachys species checklist

1. *Trachys auricollis* E. Saunders, 1873
Fig. 7A

Host plant. Fabaceae: *Pueraria montana* var. *lobata* (Yano 1952).

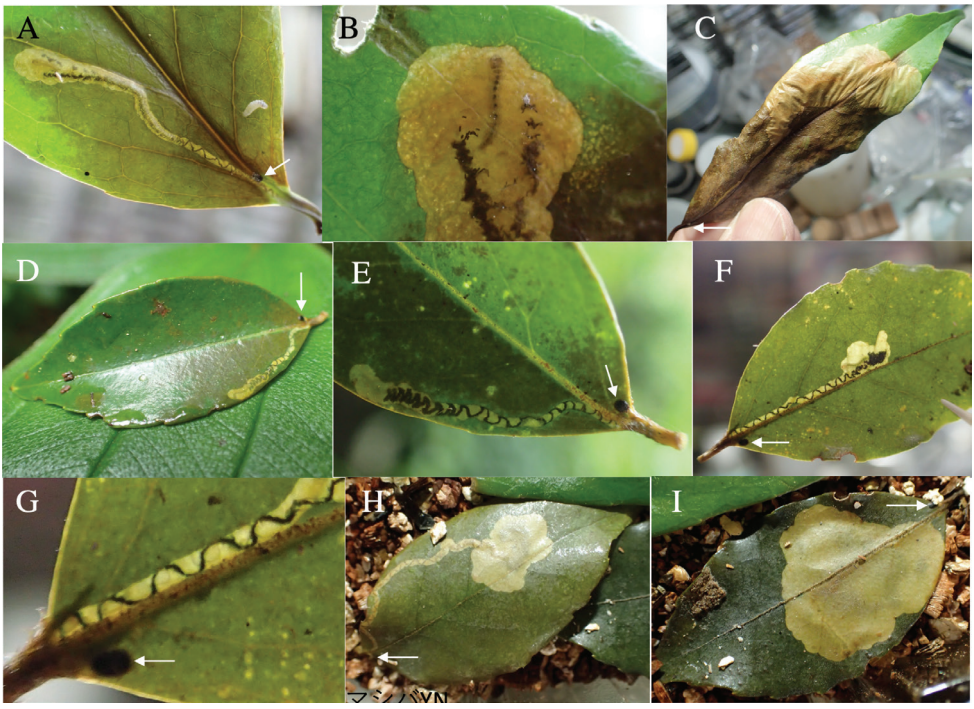

Figure 6. Leaf mines of *Habroloma* spp. on leaves of Symplocaceae **A–C** *H. eximium* on *Symplocos caudata* **D–I** *H. liukiuense* on *Symplocos microcalyx*. Arrows indicate oviposition scars.

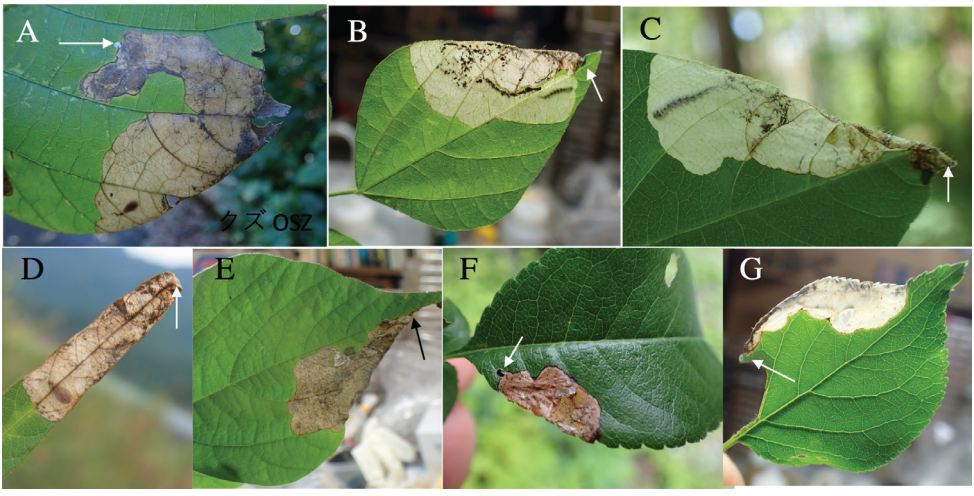

Figure 7. Leaf-mines of *Trachys* spp. on leaves of Fabaceae and Rosaceae **A** *T. auricollis* on *Pueraria montana* var. *lobata* **B–D** *T. reitteri* on *Amphicarpaea edgeworthii* (**B, C**) and *Glycine soja* (**D**) **E** *T. tokyoensis* on *Desmodium podocarpum* subsp. *fallax* **F** *T. toringoi* on *Chaenomeles japonica* **G** *T. inconspicuus* on *Prunus mume*. Arrows indicate oviposition scars.

Leaf mine. Gray full-depth blotch mine on mature leaflet. Egg is laid in an inner area of leaf blade, and mine expands toward leaf margin. Frass is granular and distributed all over the mine.

Material examined. Mt. Osuzu, Tsuno, Miyazaki Pref., 14-VII-2021 (as larva), emerged on 30-VII-2021 (Fig. 3A).

2. *Trachys reitteri* Obenberger, 1930
Fig. 7B–D

Host plant. Fabaceae: *Amphicarpaea edgeworthii* (Yano 1952), *Pueraria montana* var. *lobata*, *Rhynchosia volubilis*, *Glycine max* (Ohmomo and Fukutomi 2013), *Glycine soja* (new record).

Leaf mine. White full-depth blotch mine on mature leaflet. Egg is laid along anterior margin of a leaflet, and the mine expands toward leaf base. Frass is granular and distributed all over the mine.

Materials examined. Kiso-Fukushima, Nagano Pref., 10-VIII-2019 (as larva on *A. edgeworthii*), emerged on 23-VII-2019 (Fig. 7B) Hirogawara, Yamanashi Pref., 30-VII-2018 (as larva on *A. edgeworthii*) (Fig. 7C); Kawaguchi-ko Lake, Yamanashi Pref., 20-IX-2014 (as pupa on *G. soja*), emerged on 1-X-2014 (Fig. 7D).

3. *Trachys tokyoensis* Obenberger, 1940
Fig. 7E

Host plant. Fabaceae: *Desmodium podocarpum* subsp. *oxyphyllum* (Yano 1952), *Desmodium podocarpium* subsp. *fallax* (new record).

Leaf mine. Brown full-depth blotch mine on mature leaflet. Egg is laid along anterior margin of a leaflet, and the mine expands toward leaf base. Frass is granular and distributed all over the mine.

Material examined. Kawaguchi-ko Lake, Yamanashi Pref., 19-IX-2017 (as pupa on *Desmodium podocarpium* subsp. *fallax*), emerged on 10-X-2017 (Fig. 7E).

4. *Trachys toringoi* Y. Kurosawa, 1951
Fig. 7F

Host plant. Rosaceae: *Chaenomeles japonica*, *Malus sieboldii* (Yano 1952), *Cydonia oblonga*, *Malus pumila*, *Pyrus pyrifolia*, *Amelanchier asiatica* (Kurosawa 1959).

Leaf mine. Brown blotch mine on mature leaf. Egg is laid in an inner basal area of leaf blade, and the mine expands toward leaf top. Frass is granular and distributed all over the mine.

Material examined. Hara-mura, Suwa, Nagano Pref., 15-VIII-2018 (as vacant mine of *Chaenomeles japonica*) (Fig. 7F).

5. *Trachys inconspicuus* E. Saunders, 1873
Fig. 7G

Host plant. Rosaceae: *Prunus mume*, *P. salicina* (Yano 1952).

Leaf mine. White full-depth blotch mine on mature leaf. Egg is laid along leaf margin, and the mine expands along leaf margin. Frass is granular and distributed all over the mine.

Material examined. Kamikoma, Yamashiro, Kizugawa, Kyoto Pref., 17-VI-2016 (as pupa on *Prunus mume*), emerged on 19-VI-2016 (Fig. 7G).

6. *Trachys pecirkai* Obenberger, 1925
Fig. 8A

Host plant. Ulmaceae: *Ulmus davidiana* var. *japonica* (Ohmomo and Fukutomi 2013).

Leaf mine. Brown full-depth blotch mine on mature leaf. Egg is laid near midrib, and the mine expands along lateral vein and then along leaf margin. Frass is granular and distributed all over the mine.

Material examined. Suekawa, Kaida, Kiso, Nagano Pref., 5-VIII-2022 (as vacant mine of *Ulmus davidiana* var. *japonica*) (Fig. 8A).

7. *Trachys cupricolor* E. Saunders, 1873
Fig. 8B, C

Host plant. Ulmaceae: *Zelkova serrata* (Ohmomo and Fukutomi 2013).

Leaf mine. Dark brown full-depth blotch mine on mature leaf. Egg is laid along midrib, and the mine expands along leaf margin. Frass is granular and distributed all over the mine.

Material examined. Mt. Ibuki, Maibara, Shiga Pref., 29-VII-2020 (as pupa on *Zelkova serrata*), emerged on 25-VIII-2020 (Fig. 8B, C).

8. *Trachys yanoi* Y. Kurosawa, 1959
Fig. 8D–F

Host plant. Ulmaceae: *Zelkova serrata* (Kurosawa 1959).

Leaf mine. Brown full-depth blotch mine on mature leaf. Egg is laid along leaf margin, and the mine expands along leaf margin. Frass is granular and distributed all over the mine.

Material examined. Mt. Shizuhata, Aoi-ku, Shizuoka, Shizuoka Pref., 27-VI-2018 (as pupa on *Zelkova serrata*), emerged on 12-VII-2018 (Fig. 8D–F).

9. *Trachys griseofasciatus* E. Saunders, 1873
Fig. 8G, H

Host plant. Cannabaceae: *Aphananthe aspera* (Yano 1952), *Celtis sinensis* (Ohmomo and Fukutomi 2013).

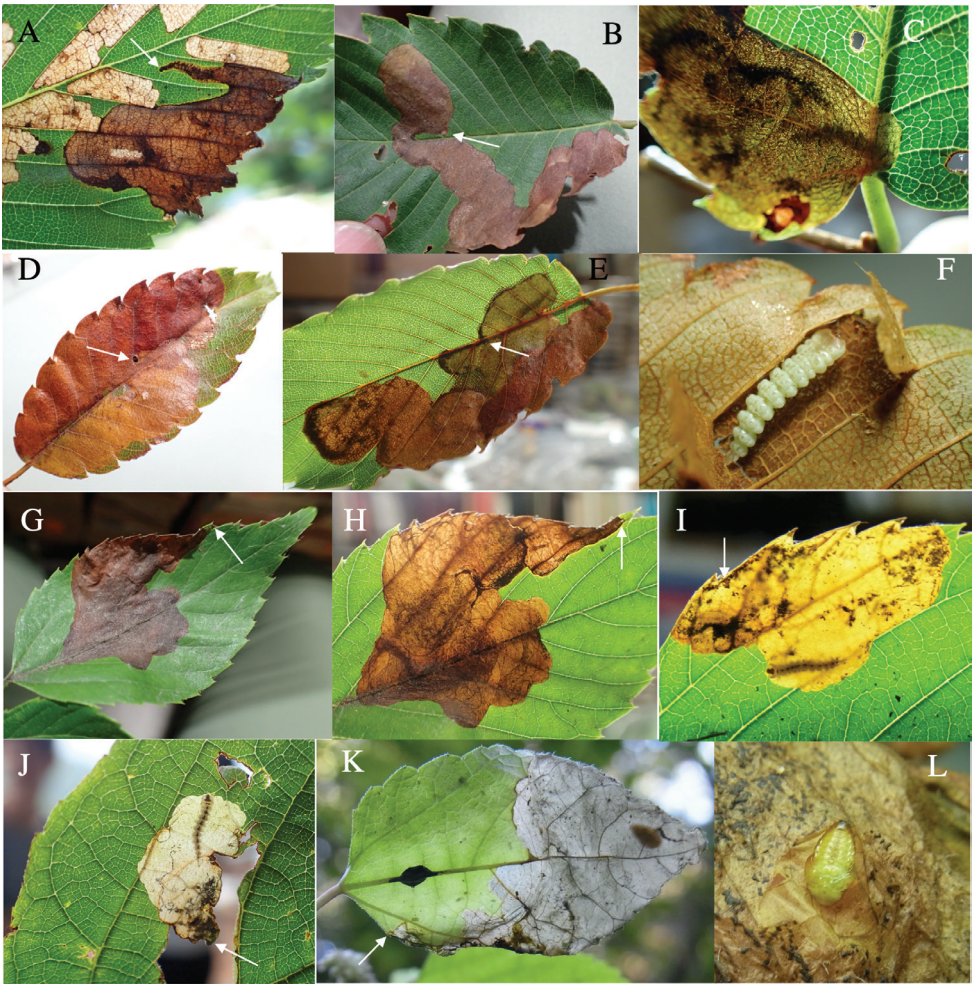

Figure 8. Leaf mines of *Trachys* spp. on leaves of Ulmaceae and Cannabaceae **A** *T. pecirkai* on *Ulmus davidiana* var. *japonica* **B–D** *T. yanoi* on *Zelkova serrata* **E, F** *T. cupricolor* on *Zelkova serrata* **G, H** *T. griseofasciatus* on *Aphananthe aspera* **I** *T. ineditus* on *A. aspera* **J–L** *T. broussonetiae* on *Broussonetia kazinoki* (**J**) and *Fatoua villosa* (**K, L**). Arrows indicate oviposition scars.

Leaf mine. Dark brown full-depth blotch mine on mature leaf. Egg is laid along anterior leaf margin, and the mine expands along leaf margin. Frass is thread-like and distributed all over the mine.

Material examined. Demachi-yanagi, Shimogamo, Sakyo, Kyoto Pref., 1-VII-2020 (as pupa on *Aphananthe aspera*), emerged on 7-VIII-2020 (Fig. 8G, H).

10. *Trachys ineditus* E. Saunders, 1873

Fig. 8I

Host plant. Cannabaceae: *Aphananthe aspera* (Ohmomo and Fukutomi 2013).

Leaf mine. White full-depth blotch mine on mature leaf. Egg is laid along leaf margin, and the mine expands along leaf margin. Frass is granular and distributed all over the mine.

Material examined. Mukoujima, Uji, Kyoto Pref., 15-VII-2012 (as larva on *Aphananthe aspera*), emerged on 28-VII-2012 (Fig. 8I).

11. *Trachys broussonetiae* Y. Kurosawa, 1985

Fig. 8J–L

Host plant. Moraceae: *Broussonetia kazinoki* (Yano 1952), *Fatoua villosa* (new record). The latter species is unique for host plants of Tracheini, because it is a herbaceous species.

Leaf mine. White full-depth blotch mine on mature leaf. Egg is laid along leaf margin, and the mine expands along leaf margin. Frass is granular and distributed all over the mine.

Materials examined. Chigonosawa, Kiso-fukushima, Kiso, Nagano Pref., 4-VIII-2018 (as larva on *Broussonetia kazinoki*), emerged on 30-VIII-2018 (Fig. 8J); Mumyodani, Niimi, Okayama Pref., 27-IX-2013 (as larva on *Fatoua villos*), emerged on 5-X-2013 (Fig. 8K, L).

12. *Trachys variolaris* E. Saunders, 1873

Fig. 9A–C

Host plant. Fagaceae: *Quercus glauca*, *Q. serrata*, *Q. variabilis* (Yano 1952), *Q. hondae* (new record).

Leaf mine. Gray full-depth blotch mine on mature leaf. Egg is laid near leaf margin, and the mine expands along leaf margin. Frass is granular and distributed all over the mine.

Material examined. Inohae-keikoku, Kitago, Nichinan, Miyazaki Pref., 16-VI-2019 (as larva on *Quercus hondae*), emerged on 19-VII-2019 (Fig. 9A, B); Suizu, Tsuruga, Fukui Pref., 14-VII-2021 (as larva on *Q. glauca*), emerged on 21-VII-2021 (Fig. 9C); Suizu, Tsuruga, Fukui Pref., 19-VIII-2019 (as pupa on *Q. serrata*), emerged on 23-VIII-2019.

13. *Trachys dilaticeps* Gebhardt, 1929

Fig. 9D–F

Host plant. Fagaceae: *Castanopsis sieboldii* subsp. *lutchuensis* (Ohmomo and Fukutomi 2013).

Leaf mine. Gray full-depth linear-blotch mine on mature leaf. Egg is laid along midrib near leaf tip, and the mine expands downwards along leaf margin. Frass is granular and distributed all over the mine.

Material examined. Mt. Nishime, Kunigami, Okinawa Pref., 6-VI-2018 (as larva on *Castanopsis sieboldii* subsp. *lutchuensis*), emerged on 6-VII-2018 (Fig. 9D, E); Komi, Iriomote Is., Yaeyama, Okinawa Pref., 4-VI-2018 (as vacant mine of *C. sieboldii* subsp. *lutchuensis*); Yakukachi, Sumiyo, Amami, Kagoshima Pref., 25-V-2017 (as larva on *Castanopsis sieboldii* subsp. *lutchuensis*), emerged on 15-VI-2017 (Fig. 9F).

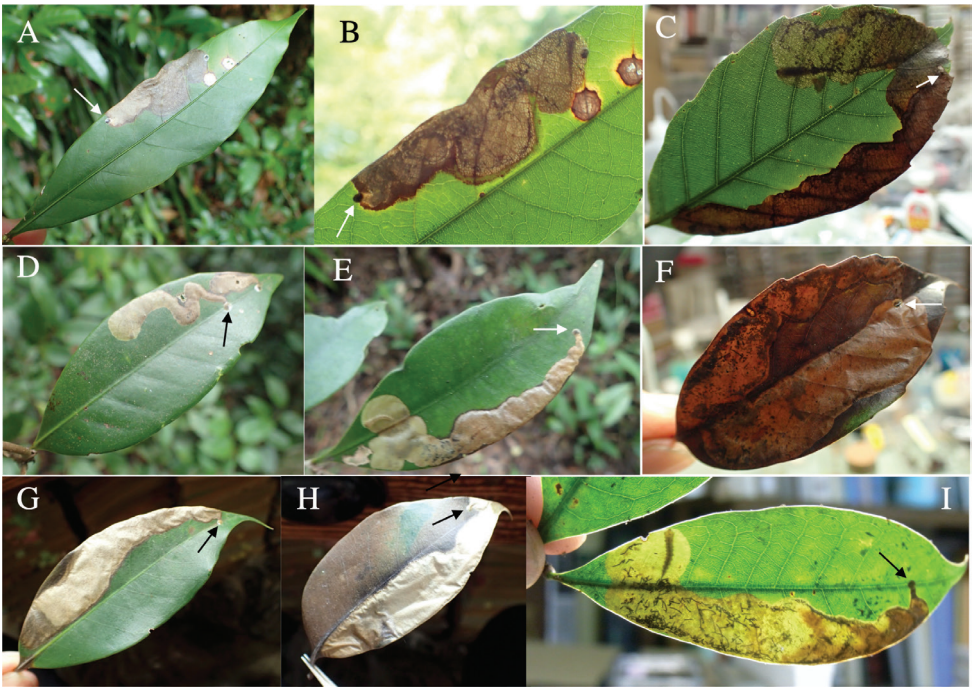

Figure 9. Leaf mines of *Trachys* spp. on leaves of Fagaceae **A–C** *T. variolaris* on *Quercus hondae* (**A, B**) and *Quercus serrata* (**C**) **D–F** *T. dilaticeps* on *Castanopsis sieboldii* subsp. *lutchuensis* **G–I** *T. robustus* on *Castanopsis sieboldii* subsp. *sieboldii*. Arrows indicate oviposition scars.

14. *Trachys robustus* E. Saunders, 1873

Fig. 9G–I

Host plant. Fagaceae: *Castanopsis sieboldii* subsp. *sieboldii* (Yano 1952).

Leaf mine. Gray full-depth linear-blotch mine on mature leaf. Egg is laid along midrib near leaf tip, and the mine expands downwards along leaf margin. Frass is granular and distributed all over the mine.

Material examined. Mt. Shizuhata, Aoi-ku, Shizuoka, Shizuoka Pref., 27-VI-2018 (as larva on *Castanopsis sieboldii* subsp. *sieboldii*), emerged on 13-VII-2018 (Fig. 9G, H); Suizu, Tsuruga, Fukui Pref., 11-VIII-2018 (as larva on *C. sieboldii* subsp. *sieboldii*), emerged on 5-X-2018 (Fig. 9I).

15. *Trachys minutus salicis* (Lewis, 1893)

Fig. 10A–C

Host plant. Salicaceae: *Salix caprea*, *S. miyabeana* subsp. *gymnolepis*, *S. vulpina*, *Populus maximowiczii* (Yano 1952), *Salix reinii* (new record).

Leaf mine. Brown full-depth blotch mine on mature leaf. Egg is laid just near leaf tip, and the mine expands downwards along leaf margin. Frass is granular and connected.

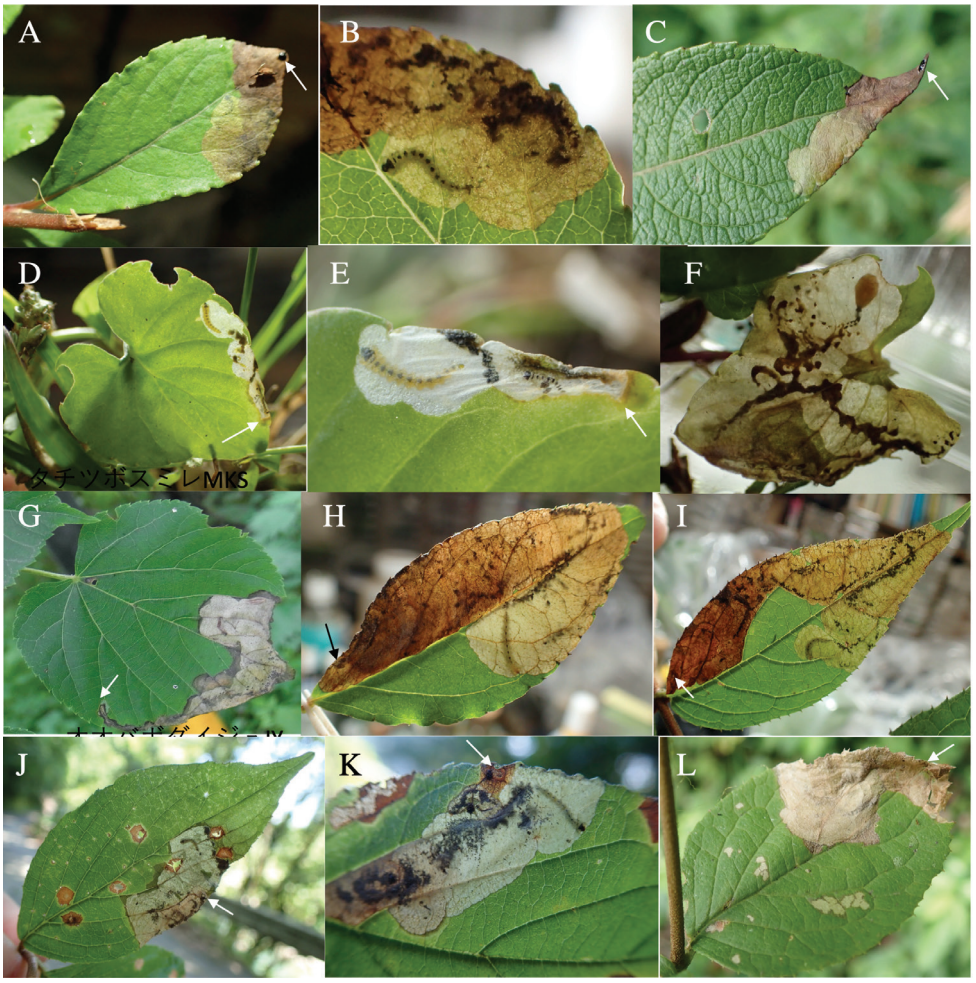

Figure 10. Leaf mines of *Trachys* spp. on leaves of Salicaceae, Violaceae, Malvaceae, and Hydrangeaceae. **A–C** *T. minutus* on *Salix reinii* (**A, B**) and *Salix vulpina* (**C**) **D–F** *T. pseudoscrobiculatus* on *Viola grypoceras* **G** *T. aurifluus* on *Tilia maximowicziana* **H, I** *T. saundersi* on *Deutzia crenata* (**H**) and *Deutzia gracilis* (**I**) **J–L** *T. tsusimae* on *Deutzia scabra*. Arrows indicate oviposition scars.

Material examined. Matsuo-kozan, Hachimantai, Iwate Pref., 7-VII-2018 (as larva on *Salix reinii*), emerged on 30-VII-2018 (Fig. 10A, B); Toyohara, Nasu, Nasu-gun, Tochigi Pref., 7-VII-2022 (as larva on *Salix caprea*) (Fig. 10C).

16. *Trachys pseudoscrobiculatus* Obenberger, 1940

Fig. 10D–F

Host plant. Violaceae: *Viola grypoceras*.

Leaf mine. White full-depth linear-blotch mine on mature leaf. Egg is laid along leaf margin near leaf tip, and the mine expands downwards along leaf margin. Frass is granular and connected.

Material examined. Mt. Mikusa, Kato-shi, Hyogo Pref., 20-V-2018 (as larva on *Viola grypoceras*), emerged on 8-VI-2018 (Fig. 10D–F).

17. *Trachys aurifluus* Solsky, 1875
Fig. 10G

Host plant. Malvaceae: *Tilia maximowicziana*, *T. japonica* (Kurosawa 1959).

Leaf mine. Brown full-depth linear-blotch mine on mature leaf. Egg is laid near leaf margin, and the mine expands along leaf margin. Frass is granular and distributed all over the mine.

Material examined. Iyari, Inao, Omachi, Nagano Pref., 1-VII-2013 (vacant mine of *Tilia maximowicziana*) (Fig. 10G).

18. *Trachys saundersi* Lewis, 1893
Fig. 10H, I

Host plant. Hydrangeaceae: *Deutzia crenata* (Yano 1952), *D. gracilis* (new record).

Leaf mine. Brown full-depth blotch mine of whole layers of leaf blade. Egg is laid along leaf margin near leaf base, and the mine expands upwards along leaf margin. Frass is granular and loosely connected.

Material examined. Makido, Niimi, Okayama Pref., 1-VII-2018 (as larva on *Deutzia crenata*), emerged on 17-VII-2018 (Fig. 10H); Donden, Sado, Niigata Pref., 13-VII-2019 (as larva on *Deutzia crenata*), emerged on 16-VIII-2019; Mt. Toyoguchi, Ooshika, Shimoina, Nagano Pref., 2-VIII-2020 (as larva on *Deutzia gracilis*), emerged on 5-IX-2020 (Fig. 10I).

19. *Trachys tsusimae* Obenberger, 1922
Fig. 10J–L

Host plant. Hydrangeaceae: *Deutzia crenata* (Ohmomo and Fukutomi 2013), but this record may be doubtful. *Deutzia scabra* (new record). We obtained adults from only *D. scabra*.

Leaf mine. Brown full-depth blotch mine on mature leaf. Egg is laid along leaf margin, and the mine expands along leaf margin. Frass is granular and distributed all over the mine.

Material examined. Mt. Osuzu, Tsuno, Miyazaki Pref., 14-VII-2021 (as larva on *Deutzia scabra*), emerged on 27-VII-2021 (Fig. 10J, K); Sakai-gawa, Takaoka, Miyazaki, Miyazaki Pref., 18-VII-2018 (as larva on *Deutzia scabra*), emerged on 1-VIII-2018 (Fig. 10L).

20. *Trachys cuneiferus* Y. Kurosawa, 1959

Host plant. Unknown.

Leaf mine. Unknown.

Discussion

After adding the two new species, we counted 34 trachyine species in the Japanese Archipelago (Table 1). Among these 34 species, host plants are known for 32, which are narrowly host-specific. All host plants are angiosperms belonging to ten orders of eudicots (Rosales, Fabales, Fagales, Malpighiales, Malvales, Cornales, Oxalidales, Myrtales, Santalales, and Ericales), suggesting that they are not associated with basal angiosperms, monocots, Saxifragales, Caryophyllales, or euasterids. From the standpoint of the life form of the host plant, 28 trachyine species are associated with woody plants (18 with trees, 10 with shrubs), three with subwoody climbing plants, and one with herbaceous plants. These results suggest that trachyine species have evolved from wood-borers associated with eudicots.

Table 1. A list of Japanese species of the tribe Trachyini, with their host plant species.

Buprestids		Host plants				
Genus	**Species**	**Subclass**	**Order**	**Family**	**Genera**	**Habit**
Habroloma	*subbicorne*	Rosids	Rosales	Rosaceae	*Rubus*	evergreen/ deciduous shrub
	atronitidum			Rosaceae	*Rubus*	deciduous shrub
	marginicolle			Rosaceae	*Rubus*	evergreen shrub
	asahinai			Rosaceae	*Rubus*	evergreen shrub
	lewisii			Rosaceae	*Rosa*	deciduous shrub
	griseonigrum		Fagales	Fagaceae	*Quercus*	evergreen/ deciduous tree
	yuasai			Juglandaceae	*Platycarya*	deciduous tree
	elaeocarpusi n. sp		Oxalidales*	Elaeocarepaceae*	*Elaeocarpus**	evergreen tree
	bifrons		Geraniales?	Geraniaceae ?	*Geranium*?	perennial ?
	nixilla insuicola		Myrtales	Lythraceae	*Lagerstroemia*	deciduous tree
	taxillusi n. sp		Santalales*	Loranthaceae*	*Taxillus**	evergreen epiphyte
	eximium eximium	Asterids	Ericales	Symplocaceae	*Symplocos*	evergreen tree
	eximium eupoetum			Symplocaceae	*Symplocos*	evergreen tree
	liukiuense			Symplocaceae	*Symplocos*	evergreen shrub
	hikosanense			?	?	?
Trachys	*auricollis*	Rosids	Fabales	Fabaceae	*Pueraria*	deciduous liana
	reitteri			Fabaceae	*Amphicarpaea*, *Glycine*, *Pueralia*, *Rhynchosia*	deciduous liana
	tokyoensis			Fabaceae	*Desmodium*	perennial
	toringoi		Rosales	Rosaceae	*Amelanchier*, *Chaenomeles*, *Cydonia*, *Malus*, *Pyrus*	deciduous tree
	inconspicuus			Rosaceae	*Prunus*	deciduous tree
	pecirkai			Ulmaceae	*Ulmus*	deciduous tree
	cupricolor			Ulmaceae	*Zelkova*	deciduous tree
	yanoi			Ulmaceae	*Zelkova*	deciduous tree
	griseofasciatus			Cannabaceae	*Aphananthe*, *Celtis*	deciduous tree
	ineditus			Cannabaceae	*Aphananthe*	deciduous tree
	broussonetiae			Moraceae	*Broussonetia*, *Fatoua**	deciduous tree/ annual
	variolaris		Fagales	Fagaceae	*Quercus*	evergreen tree
	dilaticeps			Fagaceae	*Castanopsis*	evergreen tree
	robustus			Fagaceae	*Castanopsis*	evergreen tree
	minutus salicis		Malpighiales	Salicaceae	*Salix*, *Poplus*	deciduous tree
	pseudoscrobiculatus			Violaceae	*Viola*	perennial
	aurifluus		Malvales	Malvaceae	*Tilia*	deciduous tree
	saundersi	Asterids	Cornales	Hydrangeaceae	*Deutzia*	deciduous shrub
	tsusimae			Hydrangeaceae	*Deutzia*	deciduous shrub
	cuneiferus		?	?	?	?

* new records.

The host plant genera of the two new trachyine species are *Elaeocarpus* and *Taxillus*, belonging to Elaeocarpaceae (Oxalidales) and Loranthaceae (Santalales), respectively, and representing the first records in Tracheini for both families and orders, while both plant families have been recorded as hosts for *Agrilus* (Jendek & Poláková, 2014). The record on *Taxillus* is also the first record of buprestids associated with epiphytic, plant-parasitic plants.

Our records of leaf mines suggest that those of trachyine species are generally full-depth blotch mines on mature leaves of woody or subwoody plants, except for one species (*Trachys pseudoscrobiculatus*) associated with *Viola*. These leaf mines contrast with upper-layer mines on young leaves formed by agromyzids, epidermal/mesophyll mines on young leaves formed by gracillariids, thin full-depth linear mines formed by Lyonetiidae, and full-depth linear-blotch mines on young leaves formed by Eriocraniidae.

Acknowledgements

One of the authors (MK) is indebted to the late Prof. Yoshihiko Kurosawa for helping to obtain references on Buprestidae in 1990s. This work was supported by a Japan Ministry of Education, Culture, Science, Sports, and Technology Grant-in-Aid for Scientific Research (#15H02420, #20H03321).

References

Bellamy CL (2008) A World Catalogue and Bibliography of the Jewel Beetles (Coleoptera: Buprestoidea), Volume 4: Agrilinae: Agrilina through Trachyini. Pensoft Publishers, Sofia/Moscow, 722 pp.

Evans AM, Mckenna DD, Bellamy CL, Farrell BD (2015) Large-scale molecular phylogeny of metallic wood-boring beetles (Coleoptera: Buprestoidea) provides new insights into relationships and reveals multiple evolutionary origins of the larval leaf-mining habit. Systematic Entomology 40(2): 385–400. https://doi.org/10.1111/syen.12108

Frost SW (1924) The leaf mining habit in the Coleoptera. Part I. Annals of the Entomological Society of America 17(4): 457–468. https://doi.org/10.1093/aesa/17.4.457

Hering EM (1951) Biology of the leaf miners. Dr. W. Junk, Uitgeverij, 420 pp. https://doi.org/10.1007/978-94-015-7196-8

Jendek E, Poláková J (2014) Host Plants of World *Agrilus* (Coleoptera, Buprestidae). A critical review, Springer, Heidelberg/New York/Dordrecht/London, 706 pp. https://doi.org/10.1007/978-3-319-08410-7

Kurosawa Y (1959) A revision of the leaf-mining buprestid-beetles from Japan and the Loo-Choo Islands. Bulletin of the National Science Museum (Tokyo) (N.S.) 4: 202–268.

Kurosawa Y (1976) Notes on the Oriental species of the Coleopterous family Buprestidae (II). Bulletin of the National Science Museum Series A (Zoology) 2(2): 129–136.

Obenberger J (1918) Revision der paläarktischen Trachydinen (Coleoptera-Buprestidae), mit Einschluss einiger Beschreibungen exotischer Arten. Archiv für Naturgeschichte 82(11): 1–74.

Obenberger J (1929) Révision des espèces exotiques du genre *Trachys* Fabr. du continent asiatique. Přehled exotických druhůrodu *Trachys* Fabr. asijské pevniny. Acta Entomologica Musei Nationalis Pragae 7: 5–106.

Ohmomo S, Fukutomi H (2013) The buprestid beetles of Japan. Mushi-Sha, Tokyo, 206 pp. [In Japanese]

Peng Z (2020) Studies on the genus *Habroloma* Thomson from China (1) – Discussion on the taxonomic characters and descriptions of seven new species (Coleoptera: Buprestidae: Agrilinae: Tracheini). Annales Zoologici 70(4): 697–710. https://doi.org/10.3161/00034541ANZ2020.70.4.013

Peng Z (2021a) Studies on the genus *Habroloma* Thomson from China (2) – New taxonomic characters introduction and descriptions of nine new species (Coleoptera: Buprestidae: Agrilinae: Tracheini). Annales Zoologici 71(1): 179–194. https://doi.org/10.3161/00034541ANZ2021.71.1.008

Peng Z (2021b) Studies on the genus *Habroloma* Thomson from China (3) –Descriptions of Twelve New Species (Coleoptera: Buprestidae: Agrilinae: Tracheini). Annales Zoologici 71(3): 607–626. https://doi.org/10.3161/00034541ANZ2021.71.3.002

Peng Z (2021c) Studies on the genus *Trachys* Fabricius from China (1) – Discussion of taxonomic characters and descriptions of eight new species (Coleoptera: Buprestidae: Agrilinae: Tracheini). Coleopterists Bulletin 75(2): 313–329. https://doi.org/10.1649/0010-065X-75.2.313

Peng Z (2021d) Studies on the genus *Trachys* Fabricius from China (2) – Descriptions of six new species (Coleoptera: Buprestidae: Agrilinae: Tracheini). Coleopterists Bulletin 75(4): 749–757. https://doi.org/10.1649/0010-065X-75.4.749

Peng Z (2022a) Studies on the genus *Habroloma* Thomson from China (4) – A faunal survey of Fujian Province and descriptions of five new species (Coleoptera: Buprestidae: Tracheini). Annales Zoologici 72(2): 299–312. https://doi.org/10.3161/00034541ANZ2022.72.2.013

Peng Z (2022b) Studies on the genus *Trachys* Fabricius from China (3)–A faunal survey of Hunan province and descriptions of four new species (Coleoptera: Buprestidae: Agrilinae: Tracheini). Coleopterists Bulletin 76(2): 263–272. https://doi.org/10.1649/0010-065X-76.2.263

Schaefer L (1950) Les Buprestides de France. Tableaux analytiques des Coléoptères de la faune francorhénane. Miscellanea Entomologica, Supplement, Paris, 511 pp.

Yano T (1952) The developmental stages of two genera of Trachyinae, *Trachys* and *Habroloma*, of Shikoku, Japan (Coleoptera: Buprestidae). Transactions of the Shikoku Entomological Society 3(2): 17–40.

ZooKeys 1156: 159–190 (2023)
doi: 10.3897/zookeys.1156.98930
https://zookeys.pensoft.net

RESEARCH ARTICLE

A peer-reviewed open-access journal
ZooKeys
Launched to accelerate biodiversity research

Two new species of *Tmethypocoelis* Koelbel, 1897 (Decapoda, Brachyura, Dotillidae) from Sulawesi, Indonesia

Dewi Citra Murniati[1,2,3], Akira Asakura[3], Peter J. F. Davie[4]

1 *Research Center for Biosystematics and Evolution, National Research and Innovation Agency (BRIN), Jl. Raya Jakarta Bogor Km 46, Cibinong, Bogor, Indonesia* **2** *Department of Zoology, Division of Biological Science, Graduate School of Science, Kyoto University, 606-8501, Yoshida-honmachi, Sakyo-ku, Kyoto-shi, Japan* **3** *Seto Marine Biological Laboratory, Field Science Education and Research Center, Kyoto University, 459 Shirahama, Nishimuro, Wakayama 649-2211, Japan* **4** *Queensland Museum, PO Box 3300, South Brisbane, Qld 4101, Australia*

Corresponding author: Dewi Citra Murniati (dewicitramurniati@gmail.com)

Academic editor: Sameer Pati | Received 16 December 2022 | Accepted 3 March 2023 | Published 30 March 2023

https://zoobank.org/2C1EAA98-1515-4873-872B-426299C98FAD

Citation: Murniati DC, Asakura A, Davie PJF (2023) Two new species of *Tmethypocoelis* Koelbel, 1897 (Decapoda, Brachyura, Dotillidae) from Sulawesi, Indonesia. ZooKeys 1156: 159–190. https://doi.org/10.3897/zookeys.1156.98930

Abstract

Tmethypocoelis Koelbel, 1897, is a central Indo-West Pacific genus of small intertidal, soft sediment dotillid crabs that includes five recognised species. Two new species, *Tmethypocoelis simplex* **sp. nov.** and *T. celebensis* **sp. nov.**, are here described from Sulawesi, Indonesia. *Tmethypocoelis simplex* **sp. nov.** is found on the west coast of Central Sulawesi, while *T. celebensis* **sp. nov.** occurs in the north-eastern part of Sulawesi. Both new species differ from each other and known congeners by the male cheliped, male pleon, and male first gonopod characters. The differences in gastric mill morphology further confirm the two species as new. The distinct water current patterns in the Makassar Strait and the Maluku Channel might have contributed to the evolution of these two sibling species.

Keywords

Biogeography, Celebes, dotillid crabs, gastric mill, morphology

Introduction

Crabs of the dotillid genus, *Tmethypocoelis* Koelbel, 1897, are small and found on intertidal mudflats and estuarine mud or sandy-mud banks, often extending into low salinity (Dutreix 1992). *Tmethypocoelis* is unique among confamilials by having a long narrow apical styliform projection on the eyestalks that extends beyond the cornea (Davie 1990).

The first species to be described was *Tmethypocoelis ceratophora* (Koelbel, 1897) from Hong Kong. Although it was initially placed in *Dioxippe* de Man, 1888, Koelbel (1897, 1898) remarked that its unique characters deserved the recognition of a new subgenus *Dioxippe* (*Tmethypocoelis*) Koelbel, 1897. Five species are currently known in *Tmethypocoelis: T. ceratophora* (Koelbel, 1897) from China; *T. koelbeli* Davie, 1990, from Northern Territory, Australia (Davie 1990; Davie and Kosuge 1995); *T. odontodactylus* Davie, 1990, from Madang, Papua New Guinea (Davie 1990; Davie and Kosuge 1995); *T. choreutes* Davie & Kosuge, 1995, from Japan (Davie and Kosuge 1995); *T. liki* Murniati, Asakura, Nugroho, Hernawan & Dharmawan, 2022, from Papua, eastern Indonesia (Murniati et al. 2022). The previous records of *T. ceratophora* from Japan and Indonesia (Dutreix 1992; Huang et al. 1992; Murniati 2015) would appear to be misidentifications, and the Japanese specimens have since been described as *T. choreutes* Davie & Kosuge, 1995. The specimen first recorded from Lombok, Indonesia, is also likely to be a new species and will be further discussed in a subsequent paper with other potential new species from the Indonesian region following ongoing revisionary work on this genus.

Fieldwork by the first author to investigate the systematics of the Dotillidae Stimpson, 1858, of Indonesia has resulted in the discovery of populations of two species occurring on opposite coasts of Sulawesi Island, Indonesia, here described as both new to science and compared with the previously known species of *Tmethypocoelis*.

Materials and methods

Sampling

Fieldwork to Sulawesi Island was conducted in September 2020 and June 2021 at six sampling estuarine sites: Moletang River (estuary), Kema Tiga, North Minahasa, North Sulawesi, 1°21'59.6"N, 125°04'38.9"E; Iyok Beach, East Bolang Mongondow, North Sulawesi, 0°35'06.0"N, 124°31'58.6"E; Towale River, Central Banawa District, Donggala, Central Sulawesi, 0°43'29.3"S, 119°40'43.9"E; Tosale, Banawa District, Donggala, Central Sulawesi, 0°45'57.1"S, 119°40'58.4"E; Tuladenggi Sibatang, Parigi Moutong, Central Sulawesi, 0°24'41.0"N, 121°07'43.9"E; Maleyali, Sausu, Parigi Moutong, Central Sulawesi, 1°05'31.0"S, 120°33'39.6"E (Fig. 1). The crab specimens were collected by hand during diurnal low tide periods. All specimens were preserved in 90% ethanol.

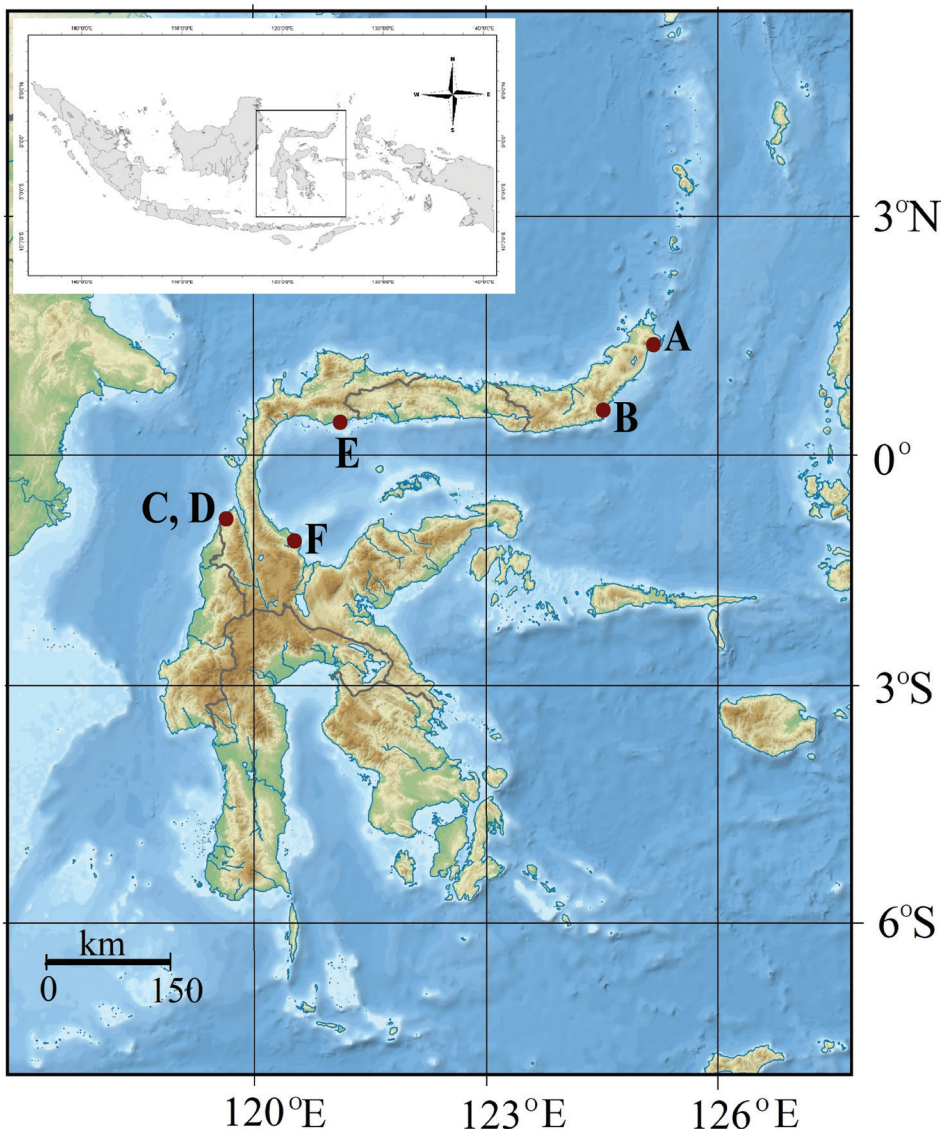

Figure 1. Map of Sulawesi. Sampling stations **A** Moletang Beach, Kema Tiga,North Minahasa, North Sulawesi **B** Iyok Beach, East Bolang Mogondow, North Sulawesi **C** Towale, CentralBanawa District, Donggala, Central Sulawesi **D** Tosale, Central Banawa District, Donggala, Central Sulawesi **E** Tuladenggi Sibatang, Parigi Moutong, Central Sulawesi **F** Maleyali, Sausu, Parigi Moutong, Central Sulawesi (derived from Wikipedia 2022).

Morphology

The crabs were observed, measured, and photographed using either a stereo microscope (Olympus SZ) connected with a digital camera (Olympus E-330), or a Leica Z6 microscope connected to a computer using LAS Core v. 4.13 software.

Measurements in millimeters (mm) were of carapace width (**cw**, measured across at the widest point) and carapace length (**cl**, measured from the mid-front to the mid-posterior margin). Smaller specimens and body parts were examined under a Nikon SMZ 800 stereo Microscope equipped with a camera lucida drawing tube. Drawings were made by hand and enhanced using a Wacom drawing pad and Adobe Illustrator CC2015 software.

Morphological terminology for the teeth of the gastric mill follows Davie et al. (2015). The G1 and teeth on the gastric mill were removed, fixed in glutaraldehyde and cacodylate buffer, serially dehydrated in ethanol (50%, 70%, 85%, 90%, 100%), and vacuum-dried using TITEC VC-96N for 10 minutes. Each prepared sample was then mounted on a specimen stub and coated with gold at 5–8 mA for 5 min using ion coater (Dewi and Purwaningsih 2020). The detailed photos of the teeth plate of the gastric mills and gonopods were captured using a scanning electron microscope (SEM), JEOL JSM-IT 200, at an accelerating voltage of 5 kV. The photographs of the teeth plate are presented with posterior portion upper-most.

Specimens have been deposited in the following repositories: Directorate of Scientific Collection Management, BRIN, Cibinong, Bogor, Indonesia (**MZB**); Lee Kong Chian Natural History Museum, National University of Singapore, Singapore (**ZRC**); Osaka Museum of Natural History, Japan (**OMNH**); Naturalis Biodiversity Center, The Netherlands (**RMNH**); and Queensland Museum, Australia (**QM**).

Abbreviations

Pl pleonite;
P pereiopod;
G1 male first gonopod;
ovig ovigerous.

Taxonomy

Dotillidae Stimpson, 1858

Tmethypocoelis Koelbel, 1897.
Dioxippe (*Tmethypocoelis*) Koelbel, 1897: 715; 1898: 574.
Tmethypocoelis – Shen 1935: 33. — Sakai 1939: 643; 1976: 625. — Davie 1990: 463; 2002: 347. — Dai et al. 1986: 451. — Dai and Yang 1991: 495. — Huang et al. 1992: 150 (key), 154. — Wada 1995: 415 (key). — Davie and Kosuge 1995: 208. — Ng et al. 2008: 235. — Shih et al. 2015: 61.

Type species. *Dioxippe* (*Tmethypocoelis*) *ceratophora* Koelbel, 1897, by original designation, subsequently elevated to generic status by Shen (1935); gender feminine.

Remarks. The genus name *Dioxippe* de Man 1888, to which the type species was originally placed, is pre-occupied by *Dioxippe* Thomson, 1860 [Coleoptera]; and therefore, a replacement name, *Tympanomerus*, was proposed by Rathbun (1897), and subsequently used by Tesch (1918) in his account of *Tympanomerus ceratophora*. However, *Tympanomerus* Rathbun, 1897, is itself currently considered a junior synonym of *Ilyoplax* Stimpson, 1858. Shen (1935) was the first to formally elevate *Tmethypocoelis* to full generic rank.

The year of publication of *Tmethypocoelis ceratophora* has usually been wrongly attributed to Koelbel (1898); the 1898 paper is actually a German translation of Koelbel's original paper published in 1897 in Hungarian. The name should thus be cited as *Tmethypocoelis ceratophora* (Koelbel, 1897).

Tmethypocoelis simplex sp. nov.

https://zoobank.org/F7FC7DED-1435-42E8-8428-5B38FF061959
Figs 2–9, 17A, C

Material examined. ***Holotype*.** Indonesia • 1 ♂ (7.7 × 4.4 mm); Tosale, Banawa District, Donggala, Central Sulawesi; 0°45'57.1"S, 119°40'58.4"E; 17 Sep. 2020; coll. DC. Murniati, D. Permatasari, Hairul, A. Padju; MZB.Cru.5573.

***Paratypes*.** Indonesia • 12 ♂ (4.0 × 2.5 – 7.9 × 4.6), 6 ♀ (5.8 × 3.6 – 6.5 × 4.0 mm); Towale River, Central Banawa District, Donggala, Central Sulawesi; 0°43'29.3"S, 119°40'43.9"E; 17 Sep. 2020; coll. DC. Murniati, D. Permatasari, Hairul, A. Padju; MZB.Cru.5182 • 15 ♂ (4.1 × 2.6 – 7.7 × 4.4 mm), 4 ♀ (3.8 × 2.6 – 6.1 × 3.9 mm); same data as for holotype; MZB.Cru.5183 • 4 ♂ (4.7 × 3.0 – 5.3 × 3.3 mm), 4 ♀ (4.0 × 2.5 – 5.6 × 3.3 mm); Towale River, Central Banawa District, Donggala, Central Sulawesi; 0°43'29.3"S, 119°40'43.9"E; 17 Sep. 2020; coll. DC. Murniati, D. Permatasari, Hairul, A. Padju; ZRC 2023.0055 • 4 ♂ (4.0 × 2.5 – 5.1 × 3.0 mm); Towale River, Central Banawa District, Donggala, Central Sulawesi; 0°43'29.3"S, 119°40'43.9"E; 17 Sep. 2020; coll. DC. Murniati, D. Permatasari, Hairul, A. Padju; OMNH-Ar.12758–12761 • 4 ♀ (5.8 × 3.5 – 6.6 × 4.0 mm); Towale River, Central Banawa District, Donggala, Central Sulawesi; 0°43'29.3"S, 119°40'43.9"E; 17 Sep. 2020; coll. DC. Murniati, D. Permatasari, Hairul, A. Padju; OMNH-Ar.12762–12765 • 6 ♂ (5.5 × 3.4 – 6.7 × 4.0 mm), 5 ♀ (5.0 × 3.1 – 5.8 × 3.5 mm); Towale River, Central Banawa District, Donggala, Central Sulawesi; 0°43'29.3"S, 119°40'43.9"E; 17 Sep. 2020; coll. DC. Murniati, D. Permatasari, Hairul, A. Padju; RMNH.CRUS.D.58046 • 3 ♂ (6.5 × 3.7 mm – 7.5 × 4.3 mm); Tosale, Banawa District, Donggala, Central Sulawesi; 0°45'57.1"S, 119°40'58.4"E; 17 Sep. 2020; coll. DC. Murniati, D. Permatasari, Hairul, A. Padju; QM W29642.

Comparative material. *Tmethypocoelis liki* Murniati, Asakura, Nugroho, Hernawan & Dharmawan, 2022: Indonesia • paratypes 5 ♂ (5.3 × 3.1 mm – 5.5 × 3.2 mm); Liki Village, Sarmi District, Sarmi Municipality, Liki Island, Papua Province; 01°37'25.29"S, 138°44'26.54"E; 21 Nov. 2018; coll. DC. Murniati; MZB.Cru.5012.

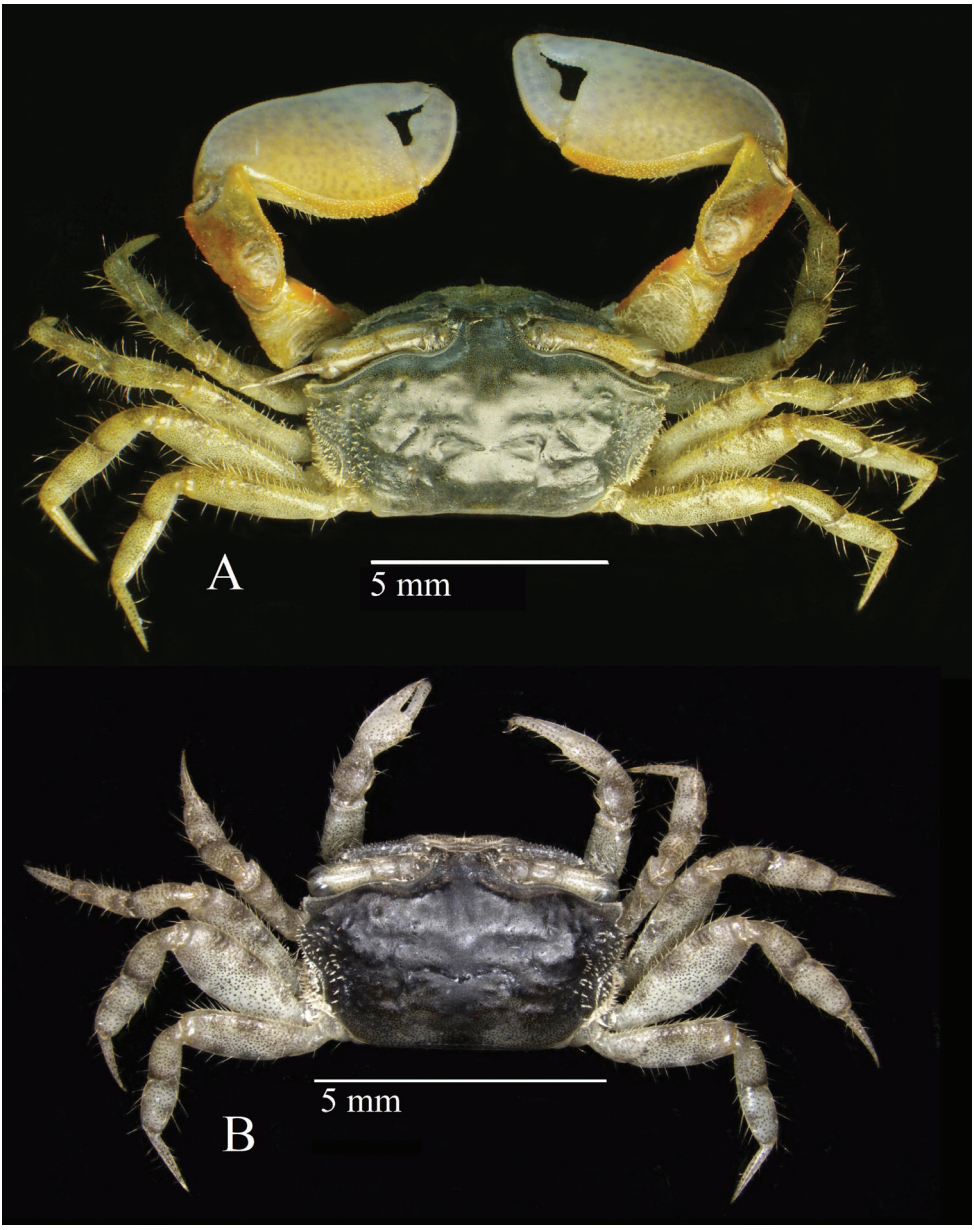

Figure 2. Dorsal habitus of *Tmethypocoelis simplex* sp. nov. from Towale River, Central Banawa District, Donggala, Central Sulawesi **A** holotype, male (7.7 × 4.4 mm) (MZB.Cru.5573) **B** paratype, female (5.8 × 3.6 mm) (MZB.Cru. 5182).

Diagnosis. Carapace pentagonal, ca. 1.7× as wide as long (Fig. 2A). Branchial regions sloping; protobranchial, mesobranchial and metabranchial regions well-defined. Sub-branchial region bulging, bearing regular setae and tubercles. Posterior margin

Figure 3. *Tmethypocoelis simplex* sp. nov. Holotype, male (7.7 × 4.4 mm) (MZB.Cru.5573), Towale River, Central Banawa District, Donggala, Central Sulawesi **A** in-situ with live coloration **B** front area **C** merus of left cheliped held against external orbital angle.

slightly concave, ca. 0.53 distance between exorbital angles. Exorbital angle triangular, acute, directed forward (Fig. 4A). Second anterolateral tooth of carapace slightly acute, slightly shorter than exorbital angle. Male pleon ca. 2× as long as wide (Fig. 4E). Male chelipeds long (Fig. 5); palm bulky, ca. 1.4× as long as wide; fingers shorter than palm; pollex short, triangular, cutting margin gently convex over entire length, without differentiated tooth or lobe; dactylus cutting margin evenly dentate, one enlarged wide convex tooth over proximal half, upper margin with one median row of granules in simple row, narrower distally (Fig. 5O). G1 long, curved, conspicuously slender; apical portion forming two poorly defined lobes, with three conspicuously curved setae on outer margin becoming slightly longer distally, two or three long setae apically, and four short setae on inner margin (Fig. 8A–E).

Description. Carapace (Fig. 2A, B) pentagonal, weakly convex along mid-dorsal line, weakly convex laterally, ca. 1.7× as wide as long. Dorsal surface smooth, lateral portion with granules, regions semi-defined; epigastric lobe poorly defined. Cervical grooves well-marked. Cardiac region with slight central depression. Branchial regions

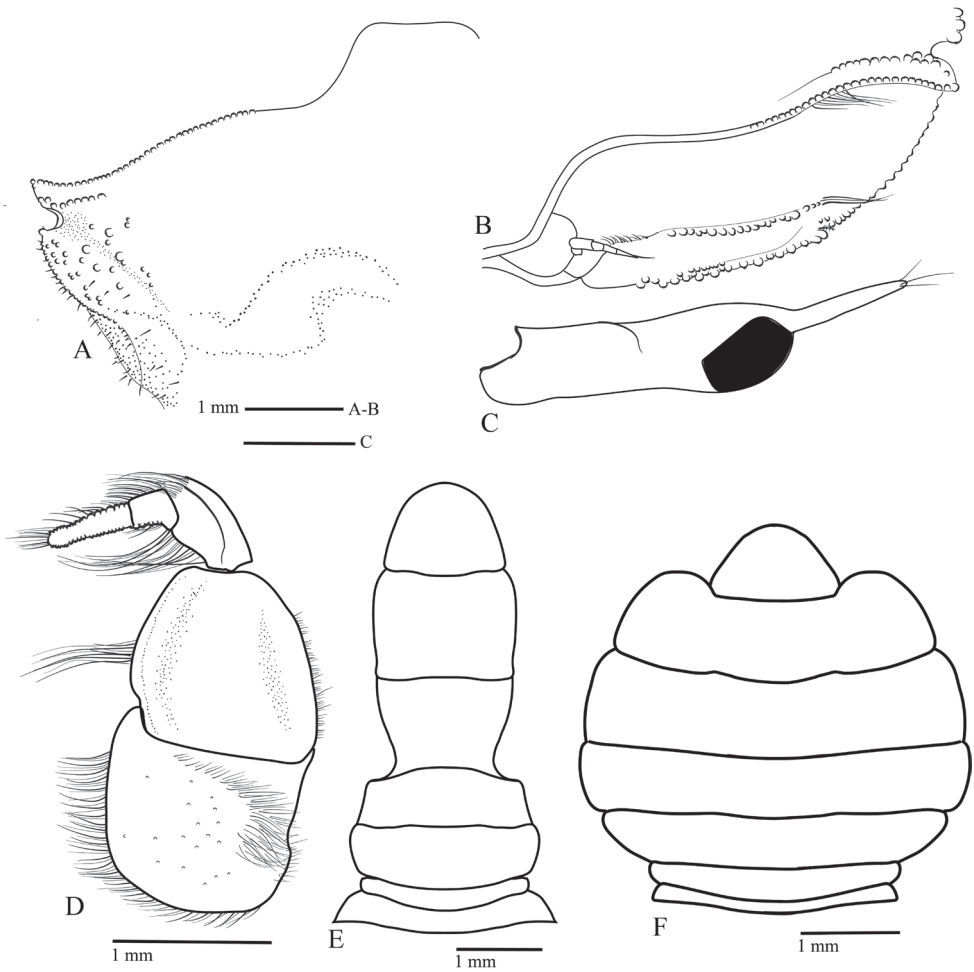

Figure 4. *Tmethypocoelis simplex* sp. nov. Holotype, male (7.7 × 4.4 mm) (MZB.Cru.5573), Towale River, Central Banawa District, Donggala, Central Sulawesi **A** external orbital angle **B** orbit area **C** eyestalk **D** third maxilliped **E** pleon. Paratype, female (5.8 × 3.6 mm) (MZB.Cru. 5182), Towale River, Central Banawa District, Donggala, Central Sulawesi **F** pleon.

sloping; protobranchial, mesobranchial and metabranchial regions well-defined. Subbranchial region bulging, bearing regular setae and tubercles. Carapace widest between exorbital angles. Intestinal and branchial borders poorly defined. Lateral margin of carapace recurved, with row of tubercles and short stout setae. Posterior margin weakly concave, ca. 0.53 distance between exorbital angles; fine ridge parallel to posterior margin forming broad rim. Front with lateral border moderately converging, width at base ca. 0.24× distance between exorbital angles, ca. 0.21 at anterior margin; frontal angle rounded; anterior margin with small central blunt prominence (Fig. 3B). Exorbital angle triangular, acute, directed forward; anterior margin with microscopic tubercles, lateral margin glabrous; one short tubercular ridge parallel to supraorbital margin;

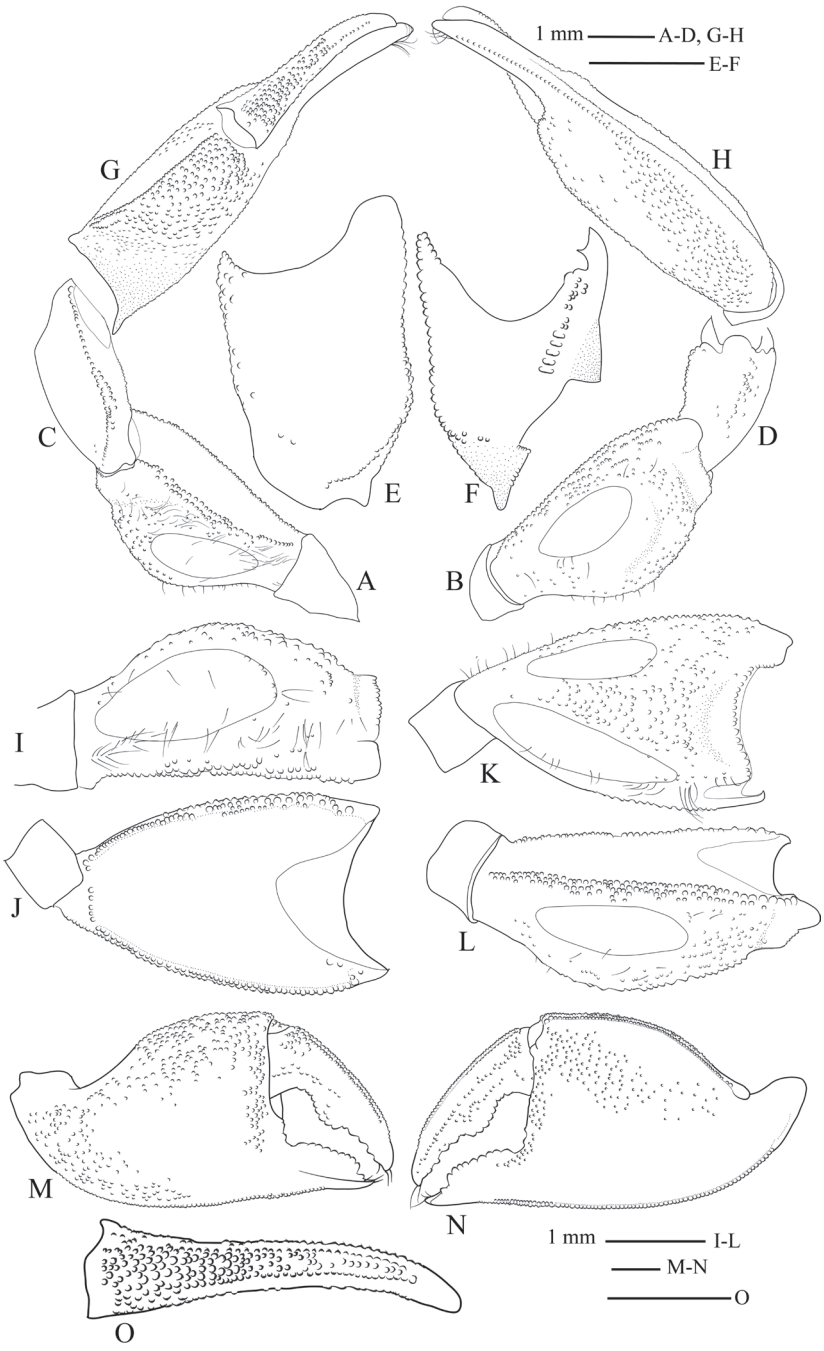

Figure 5. *Tmethypocoelis simplex* sp. nov. Holotype, male (7.7 × 4.4 mm) (MZB.Cru.5573), Towale River, Central Banawa District, Donggala, Central Sulawesi. Left cheliped **A** merus lower margin **B** merus outer surface. Carpus **C** outer surface **D** inner surface **E** upper surface **F** lower surface. Chela **G** upper margin **H** lower margin. Merus **I** upper surface **J** lower surface **K** upper margin **L** outer margin. Chela **M** inner surface **N** outer surface **O** dactylus upper margin.

posteriorly followed by broad U-shaped sinus. Second anterolateral tooth slightly acute, slightly shorter than exorbital angle. Posterolateral facet well-defined by crest originating anteriorly from base of exorbital angle (Fig. 4A). Supraorbital margin sinuous, sloping backward, microscopically tubercular. Infraorbital margin with medial notch; pterygostome with inwardly directed oblique channel; inner portion consisting of two granular ridges separated by shallow channel; upper ridge granular, with one row of setae; lower ridge granular, granules larger than those of upper ridge, without setation; outer portion granular, concave, ending in broad notch below exorbital angle (Fig. 4B).

Eyestalks long, not reaching exorbital angle, medial and distal diameters of similar width; projecting ocular style as long as cornea, tipped with setae; medial slope giving twisted appearance; cornea slightly bulging (Figs 2, 3B, 4C).

Third maxillipeds slightly vaulted, not completely covering buccal cavern. Ischium subquadrate; upper-mesial angle with wide triangular lobe; anterolateral angle narrow and triangular; mesial and lower margins with dense setae; lateral margin with setation medially; outer surface with oblique row of dense long setae, scattered granules distributed unevenly (Fig. 4D). Merus slightly larger than ischium; lateral margin convex, narrower distally, covered with short setae; mesial margin straight, with long setae; outer surface covered with scattered short setae (Fig. 4D). Carpus trihedral in cross section, mesial margin with dense long setae (Fig. 4D). Propodus short, margins tubercular and covered with dense setae (Fig. 4D). Dactylus slender, long, twice as long as propodus, margins tubercular, with long dense setae (Fig. 4D).

Male pleon (Fig. 4E) ca. 2× longer than wide; noticeably constricted at base of pleonite 5 (Pl5). Pl1 trapezoidal, narrow, ca. 9.5× wider than long; anterior margin ca. 0.7× as long as posterior margin; ca. 1.3× wider than Pl2. Pl2 ca. 7.5× as wide as long. Pl3 ca. 3.0× wider than long, anterior margin nearly straight, posterior margin convex. Pl4 ca. 2.9× as wide as long, widest proximally, narrowing distally, distolateral angle pointed. Pl5 ca. 1.4× wider than long (widest distally), markedly constricted at base. Pl6 ca. 1.4× as wide as long; widest sub-distally; 1.1× longer than Pl5; lateral margins subparallel, slightly concave. Male telson rounded, ca. 1.4× wider than long (Fig. 4E).

Female pleon conspicuously broad (Fig. 4F). Pl1 shortest; Pl2 distinctly longer, as wide as Pl1; Pl3 trapezoidal, longer than Pl2; Pl4 rectangular, slightly longer than Pl3, lateral margins convex; Pl5 longer than Pl4; Pl6 distinctly longest. Female telson triangular (Fig. 4F).

Male chelipeds stout, long, equal. Merus cross-section triangular; standing higher than exorbital angle (Fig. 3C); lower margin covered with granules extending entire length, granulation branched sub-medially into two rows (Fig. 5A); upper margin narrower proximally, wider distally, with irregular rows of granules on distal half, proximal portion smooth (Fig. 5K); outer margin with a single row of granules extending whole length, granulation branched proximally (Fig. 5L); upper surface slightly convex, with ovate tympanum, microscopic granules outside tympanum, granulation mainly on distal portion, scattered setae (Fig. 5I); lower surface smooth, flattened, without tympanum (Fig. 5J); outer surface slightly convex, wider than upper surface,

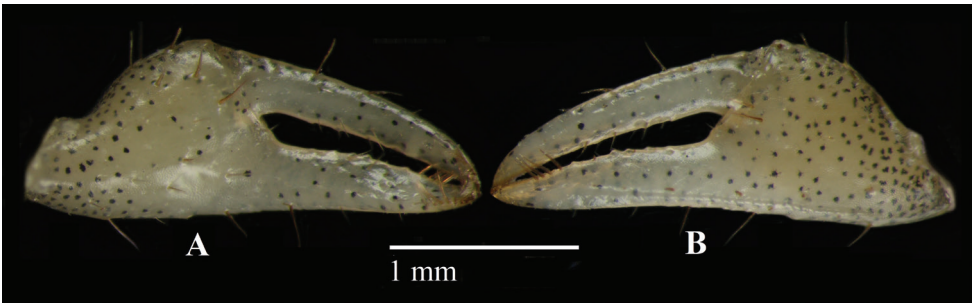

Figure 6. *Tmethypocoelis simplex* sp. nov. Paratype female (5.8 × 3.6 mm) (MZB.Cru. 5182), Towale river, Central Banawa District, Donggala, Central Sulawesi. Left chela **A** inner surface **B** outer surface.

tympanum smaller than on upper surface, granules outside tympanum distributed evenly (Fig. 5B). Carpus shorter than merus, elongate, ca. 1.5× as long as wide; upper and lower margins tubercular (Fig. 5C, D); outer surface rectangular, convex, microscopic granules only (Fig. 5E); inner surface shiny, with one oblique row of granules (Fig. 5F). Palm bulky, ca. 1.4× wider than long; upper margin with one row of granules, distinct groove extending below granular rows forming clear granular string (Fig. 5G); lower margin granular, granulation branched into two rows medial to distal portion (Fig. 5H); inner surface irregularly granular, upper granulation extending over median portion, curved to sharply cut upper margin of outer surface and base of fingers, lower granulation extending near lower margin from proximal portion to base of pollex (Fig. 5M); outer surface distinctly granular over upper half to base of pollex, lower half smooth (Fig. 5N). Fingers shorter than palm, broadly gaping at base; curved inwards, expanded distally forming spooned-tip; cutting margins evenly serrated; inner margin at tip of both fingers with short row of stout setae. Pollex short, triangular, cutting margin evenly dentate; long flat enlarged dentate tooth over most of length, ca. 0.4× as wide as palm; inner surface smooth (Fig. 5M); outer surface granular proximally parallel to cutting margin (Fig. 5N); lower margin granular nearly whole length (Fig. 5H). Dactylus ca. 0.6× as wide as palm; cutting margin evenly dentate; one enlarged wide convex tooth over proximal half; inner surface granular from proximal to median portion near cutting margin, one clutch of granules proximally near upper margin (Fig. 5M); outer surface with 1 row of granules medially, densest on proximal portion of surface, granulation extending nearly entire length, irregular granulation near cutting margin, a single row of spaced tubercles medially, parallel to upper margin (Fig. 5N); upper margin with median row of granules, narrower distally matching shape of upper margin (Fig. 5O).

Female chelipeds small, of typical dotillid type (Figs 2B, 6). Merus with ovate tympanum on upper and lower surfaces. Fingers longer than palm, spooned-tip (Fig. 6). Pollex outer surface with one tubercular ridge parallel to lower margin; lower margin entire; cutting margin with very low denticles. Dactylus cutting margin without denticles.

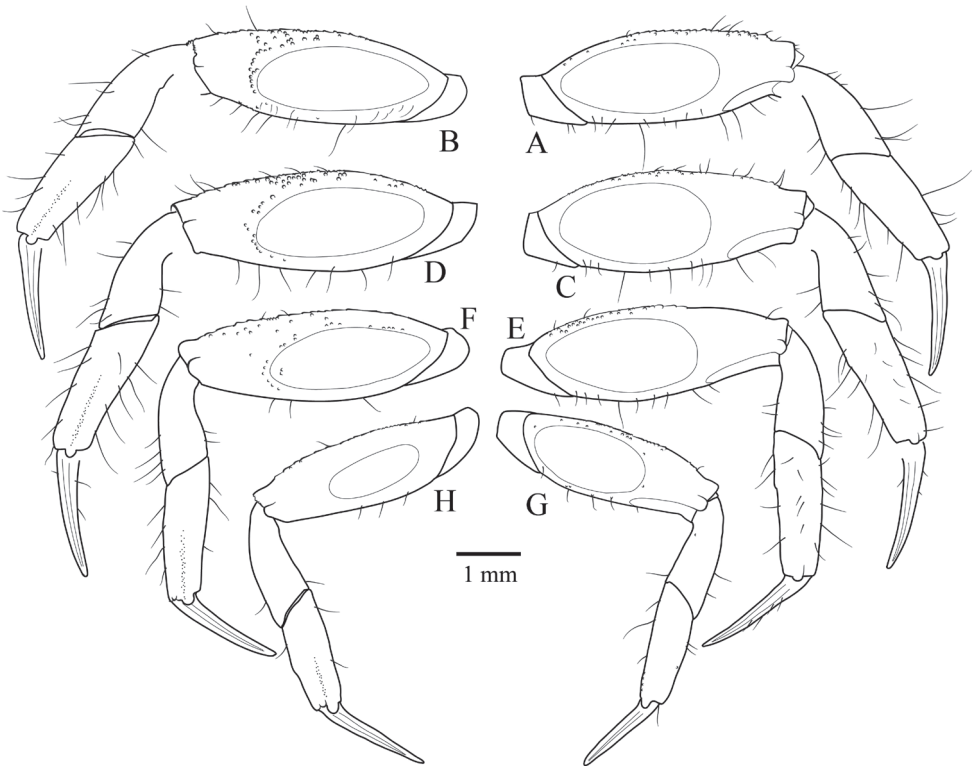

Figure 7. Left pereiopods of *Tmethypocoelis simplex* sp. nov. Holotype, male (7.7 × 4.4 mm) (MZB. Cru.5573), Towale River, Central Banawa District, Donggala, Central Sulawesi **A, B** P2 **C, D** P3 **E, F** P4; **G, H** P5. Right side, anterior surface; left side, posterior surface.

Pereiopods slender, elongate, P2–P5 similar; smooth ovate tympanum on anterior and posterior surfaces of meri. Tympani on posterior surfaces becoming progressively smaller from P2–P5. Dactyli nearly straight, pointed, shorter than propodi.

P2 (Fig. 7A, B) shorter than P3; merus ca. 2.84× longer than wide; anterior surface with scattered granules mainly near upper margin; posterior surface with sparse granules mainly near distal portion of tympanum; upper margin serrated, sparse long setae; lower margin smooth, sparse setae. Carpus subequal in length to propodus, surfaces smooth; margins smooth, sparse setae. Propodus with anterior and posterior surfaces bearing scattered granules; margins with sparse long setae.

P3 (Fig. 7C, D) longest; merus ca. 2.67× longer than wide; anterior surface with scattered granules, denser near upper margin; posterior surface with sparse granules denser distal to tympanum; upper margin serrated, sparse long setae; lower margin smooth, sparse setae. Carpus shorter than propodus, surfaces smooth; margins smooth, sparse setae. Propodus with anterior surface bearing sparse granules; posterior surface with sparse setae and granules; margins with sparse long setae.

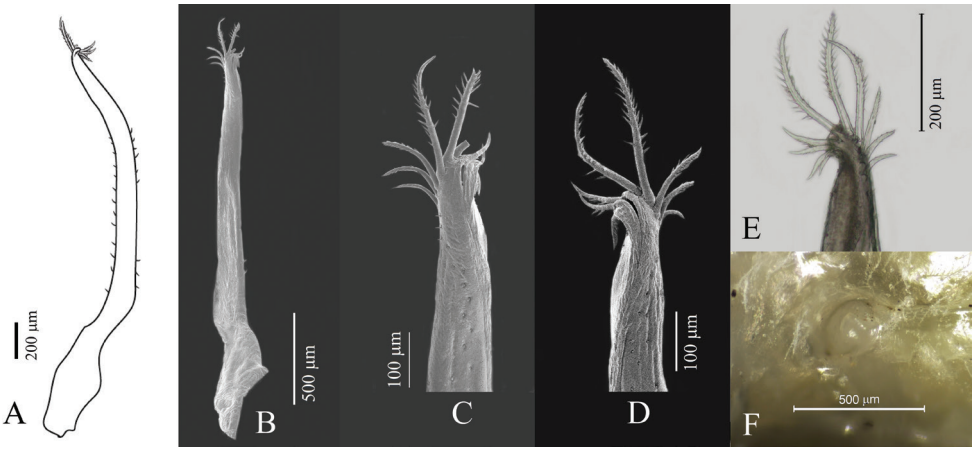

Figure 8. Reproductive organs of *Tmethypocoelis simplex* sp. nov. Paratype, males (**A–D** 4.1 × 2.6 mm **E** 6.9 × 4.0 mm) (MZB.Cru.5183), Tosale, Banawa District, Donggala, Central Sulawesi, left G1 **A** dorsal view **B** apical (dorsal view) **C, D** apical (ventral view) **E** mesial view. Paratype female (5.8 × 3.6 mm) (MZB.Cru.5182), Towale river, Central Banawa District, Donggala, Central Sulawesi **F** vulva.

P4 (Fig. 7E, F) merus ca. 2.78× longer than wide; anterior surface with scattered granules denser near upper margin; posterior surface sparsely granulate, denser towards upper margin; upper margin serrated, sparse long setae; lower margin smooth, sparse setae. Carpus shorter than propodus, surfaces smooth; margins smooth, sparse setae. Propodus with anterior surface with sparse setae and granules; posterior surface with granules; margins with sparse long setae.

P5 (Fig. 7G, H) shortest; merus ca. 2.71× longer than wide; anterior surface with scattered granules, denser near upper margin; posterior surface sparsely granulate, denser toward upper margin; upper margin serrated, sparse long setae; lower margin smooth, sparse setae. Carpus shorter than propodus, surfaces smooth; margins smooth, sparse setae. Propodus with anterior and posterior surfaces smooth; margins with sparse long setae.

Reproductive organs. G1 (Fig. 8A–E) long, curved, very slender; sub-proximal bulge (Fig. 8A, B); apical portion forming two poorly defined lobes, with three conspicuous curved setae on outer margin becoming slightly longer distally, two or three long setae apically, and four short setae on inner margin (Fig. 8C–E). Vulva (Fig. 8F) rounded, projecting.

Gastric mill (Fig. 17A, C). Median tooth plate simple, without defined ridges. Urocardiac ossicle relatively broad throughout length. Propyloric ossicle semi-circular, relatively flat and broad; posterior margin curved; anterior margin with one pointed lobe medially; lateral margins slightly truncated, evenly convex (Fig. 17A). Lateral zygocardiac tooth plate with nine slender teeth, four anterior teeth largest (Fig. 17C).

Habitat. *Tmethypocoelis simplex* sp. nov. lives in estuarine conditions on both sandy and muddy substrata (Fig. 9). At Towale Village, it inhabits sandy substrates alongside

Figure 9. Habitat of *Tmethypocoelis simplex* sp. nov. at mouth of Towale River, Central Banawa District, Donggala, Central Sulawesi.

other ocypodoids, *Austruca annulipes* (H. Milne Edwards, 1837) and *Scopimera intermedia* Balss, 1934, but also in muddier areas where it co-occurs with *Tubuca dussumieri* (H. Milne Edwards, 1852). At Tosale Village, it was typically collected on sandy substrates. While not collected, it was also observed along a small muddy canal near local residences. It was recorded approximately 1 km further upstream beyond the estuary in non-tidal area.

Etymology. The name *simplex* refers to the simple form of the cheliped dactylus that lacks a conspicuous outer subdistal dorsal projection, a character that is characteristic of other described species.

Remarks. Differences to distinguish and separate the species from *T. celebensis* sp. nov. and other congeners are given under "Remarks" for *T. celebensis* sp. nov.

Tmethypocoelis celebensis sp. nov.

https://zoobank.org/FA9B855D-5FE2-4007-BE15-EA27215DFD7E
Figs 10–16, 17B, D

Material examined. *Holotype*. Indonesia • 1 ♂ (7.4 × 4.3 mm); Moletang River estuary, Kema Tiga, North Minahasa, North Sulawesi; 1°21'59.6"N, 125°04'38.9"E; 12 Sep. 2020; coll. DC. Murniati and D. Nurdiansyah; MZB.Cru.5574.

Paratypes. **Indonesia** • 10 ♂ (2.8 × 1.8 – 7.2 × 4.3 mm), 8 ♀ (4.8 × 3.6 – 5.7 × 3.7 mm); Moletang River estuary, Kema Tiga, North Minahasa, North Sulawesi; 1°21'59.6"N, 125°04'38.9"E; 12 Sep. 2020; coll. DC. Murniati and D. Nurdiansyah; MZB.Cru.5180 • 10 ♂ (5.4 × 3.2 – 6.5 × 3.7 mm); Iyok Beach, East Bolang Mongondow, North Sulawesi; 0°35'06.0"N, 124°31'58.6"E; 17 Sep. 2020; coll. D. Nurdiansyah; MZB.Cru.5181 • 11 ♂ (6.3 × 3.8 – 7.9 × 4.8 mm); Tuladenggi Sibatang, Parigi Moutong, Central Sulawesi; 0°24'41.0"N, 121°07'43.9"E; 10 Jun. 2021; coll. DC. Murniati; MZB.Cru.5575 • 10 ♂ (7.3 × 3.8 – 7.4 × 4.3 mm); Maleyali, Sausu, Parigi Moutong, Central Sulawesi; 1°05'31.0"S, 120°33'39.6"E; 25 Jun. 2021; coll. DC. Murniati, Muslihun, M. Ikram; MZB.Cru.5576 • 5 ♂ (5.2 × 3.0 – 6.0 × 3.4 mm); Iyok Beach, East Bolang Mongondow, North Sulawesi; 0°35'06.0"N, 124°31'58.6"E; 17 Sep. 2020; coll. D. Nurdiansyah; ZRC 2023.0056 • 4 ♂ (6.6 × 3.8 – 7.2 × 4.1 mm); Maleyali, Sausu, Parigi Moutong, Central Sulawesi; 1°05'31.0"S, 120°33'39.6"E; 25 Jun. 2021; coll. DC. Murniati, Muslihun, M. Ikram; ZRC. 2023.0057 • 5 ♂ (4.7 × 3.0 – 6.0 × 3.7 mm); Iyok Beach, East Bolang Mongondow, North Sulawesi; 0°35'06.0"N, 124°31'58.6"E; 17 Sep. 2020; coll. D. Nurdiansyah; OMNH-Ar.12770–12774 • 4 ♂ (6.6 × 3.8 – 7.8 × 4.4 mm); Maleyali, Sausu, Parigi Moutong, Central Sulawesi; 1°05'31.0"S, 120°33'39.6"E; 25 Jun. 2021; coll. DC. Murniati, Muslihun, M. Ikram; OMNH-Ar. 12766–12769 • 4 ♂ (6.2 × 3.7 – 7.4 × 4.5 mm); Maleyali, Sausu, Parigi Moutong, Central Sulawesi; 1°05'31.0"S, 120°33'39.6"E; 25 Jun. 2021; coll. DC. Murniati, Muslihun, M. Ikram; RMNH.CRUS.D.58047 • 3 ♂ (4.3 × 3.8 – 4.9 × 3.8 mm); Tuladenggi Sibatang, Parigi Moutong, Central Sulawesi; 0°24'41.0"N, 121°07'43.9"E; 10 Jun. 2021; coll. DC. Murniati; QM W29643.

Comparative material. *Tmethypocoelis liki* Murniati, Asakura, Nugroho, Hernawan & Dharmawan, 2022: Indonesia • paratypes 5 ♂ (5.3 × 3.1 mm – 5.5 × 3.2 mm); Liki Village, Sarmi District, Sarmi Municipality, Liki Island, Papua Province; 01°37'25.29"S, 138°44'26.54"E; 21 Nov. 2018; coll. DC. Murniati; MZB.Cru.5012.

Diagnosis. Carapace pentagonal, ca. 1.6–1.7× as wide as long (Fig. 10A). Branchial region sloping, protobranchial, mesobranchial and metabranchial regions well-defined. Sub-branchial region bulging, bearing regular setae and tubercles. Posterior margin slightly concave, ca. 0.64 distance between exorbital angles. Exorbital angle triangular, acute, directed forward (Fig. 12A). Second anterolateral tooth less acute, slightly shorter. Male pleon ca. 2.0× longer than wide (Fig. 12E). Male chelipeds long. Palm bulky, ca. 1.3× longer than wide (Fig. 13M, N). Fingers shorter than palm. Pollex short, triangular, cutting margin slightly oblique, without large differentiated tooth or lobe (Fig. 13M); cutting margin of dactylus with large teeth over proximal half, small teeth on distal half, without median lobe, upper margin with row of fine tubercles; one triangular, upturned tooth subdistally (Fig. 13M–O). G1 long, recurved, very slender; sub-proximal portion bulging (Fig. 15A, B); apical portion forming two lobes, with three short setae on outer margin, two or three long setae apically, four or five short setae on inner margin (Fig. 15C, D).

Description. Carapace (Figs 10A, 12A) pentagonal; weakly convex laterally and longitudinally; ca. 1.6–1.7× wider than long. Dorsal surface smooth, regions semi-

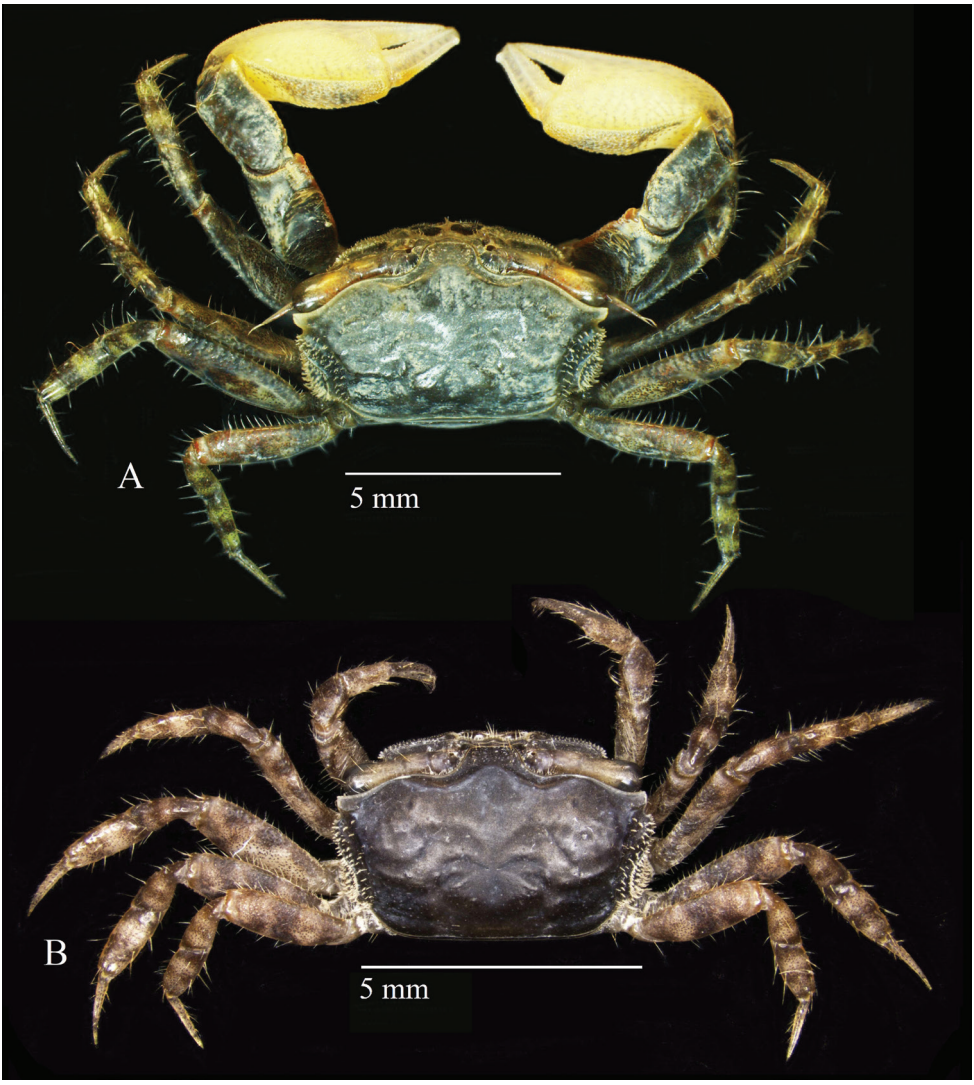

Figure 10. Habitus dorsal of *Tmethypocoelis celebensis* sp. nov. Moletang River (estuary), Kema Tiga, North Minahasa, North Sulawesi **A** holotype, male (7.2 × 4.4 mm) (MZB.Cru.5574) **B** paratype, female (5.5 × 3.5 mm) (MZB.Cru.5180).

defined; epigastric lobe poorly defined. Cervical grooves, well-marked; cardiac region slightly depressed. Branchial regions sloping, protobranchial, mesobranchial and metabranchial regions well-defined. Carapace widest between exorbital angles. Sub-branchial region bulging, bearing regular setae and tubercles. Intestinal and branchial regions well-defined. Posterior margin weakly concave, ca. 0.6× distance between exorbital angles; fine ridge parallel with posterior margin forming broad rim. Lateral margin recurved with row of tubercles and short stout setae. Frontal margin rounded, mod-

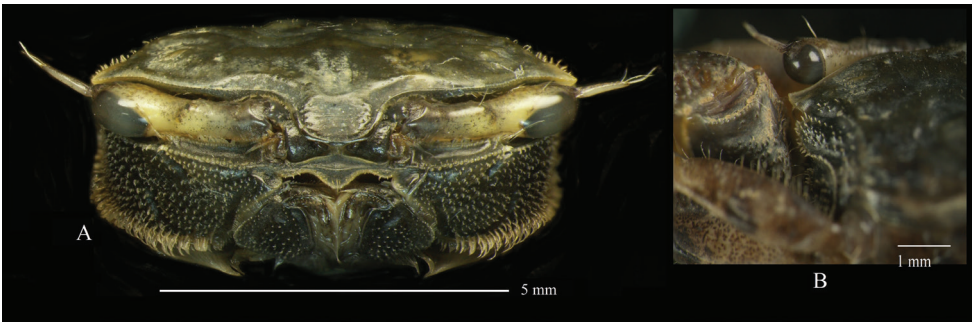

Figure 11. *Tmethypocoelis celebensis* sp. nov. Holotype, male (7.2 × 4.4 mm) (MZB.Cru.5574), Moletang River (estuary), Kema Tiga, North Minahasa, North Sulawesi **A** front area **B** left merus held against external orbital angle.

erately convergent, basal width ca. 0.19× distance between exorbital angles, ca. 0.13× at anterior margin; anterior margin with small central blunt prominence (Fig. 11A). Exorbital angle triangular, acute, directed forwardly; anterior margin with microscopic tubercles, lateral margin slightly tubercular; posteriorly followed by broad U-shaped sinus. Epibranchial tooth less acute, slightly shorter. Posterolateral facet well-defined by a crest originating anteriorly from base of exorbital angle (Fig. 12A). Supra-orbital borders sinuous, sloping backward, microscopically tubercular. Infra-orbital border with medial notch; pterygostome with inwardly directed oblique channel. Inner part of infra-orbital border with two granular ridges separated by shallow channel; upper ridge with row of setae; granules on lower ridge larger than that of upper ridge, without setation. Outer part of infra-orbital border granular, concave, ending in broad notch below exorbital angle (Fig. 12B).

Eyestalks (Figs 10, 11A, 12C) reaching exorbital angle, medial and distal diameters similar size; ocular style as long as cornea, tipped with setae; medial slope gives twisted appearance; cornea bulging.

Third maxillipeds (Fig. 12D) slightly vaulted, not completely covering buccal cavern. Ischium subquadrate, outer surface covered with spaced long setae, with one oblique row of long setae near upper margin, upper margin concave, upper-mesial angle with narrow, rounded lobe; lower-mesial angle curved; inner and lower margins with dense setae; lateral margin without setation (Fig. 12D). Merus slightly larger than ischium, ca. 1.3× longer; outer surface with regularly scattered short setae; lateral margin convex, narrower distally, covered with short setae; mesial margin straight with long setae (Fig. 12D). Carpus trihedral, subequal in length to propodus and dactylus together; mesial margin and distal portion with dense long setae (Fig. 12D). Propodus shorter than dactylus; margins entire, with long dense setae (Fig. 12D). Dactylus slender, with long dense setae laterally (Fig. 12D).

Male pleon (Fig. 12E) ca. 2.0× longer than wide. Pl1 trapezoidal, ca. 8.0× wider than long; ca. 1.3× wider than pl2. Pl2 very narrow, ca. 10× wider than long. Pl3 ca. 3× wider than long. Pl4 ca. 3.2× wider than long, lateral margins convergent distally, dis-

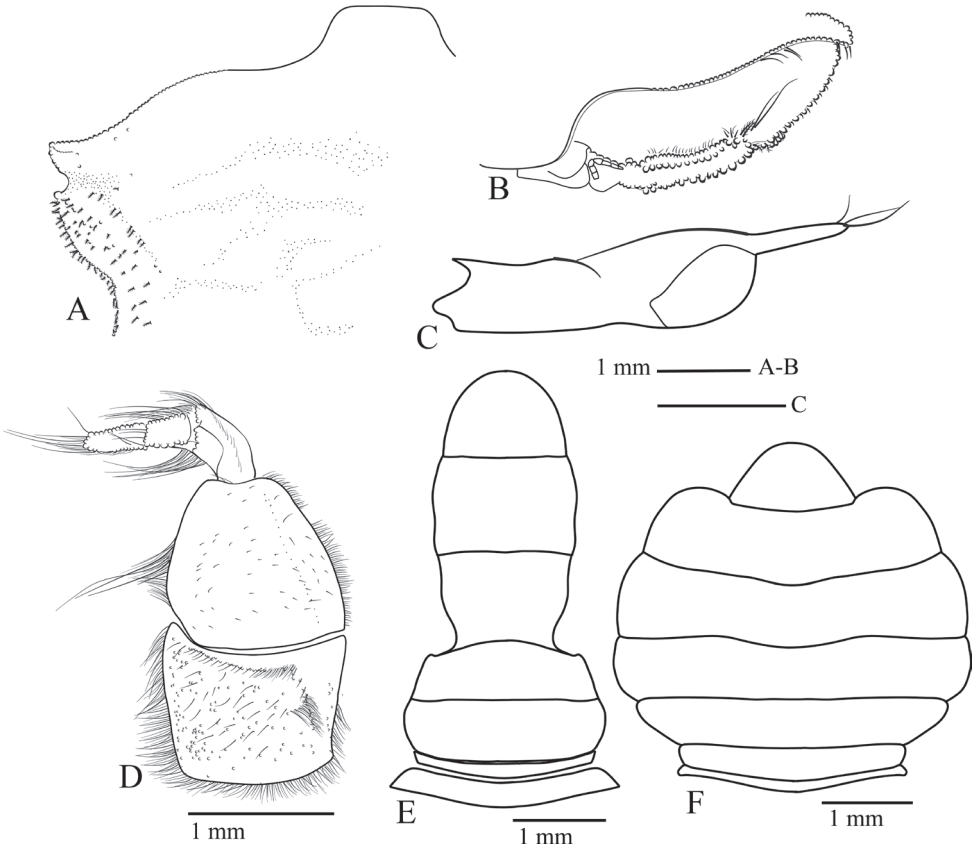

Figure 12. *Tmethypocoelis celebensis* sp. nov. Holotype, male (7.2 × 4.4 mm) (MZB.Cru.5574), Moletang River (estuary), Kema Tiga, North Minahasa, North Sulawesi **A** exorbital angle **B** orbit area **C** eyestalk **D** third maxilliped **E** pleon. Paratype, female (5.5 × 3.5 mm) (MZB.Cru.5180), Moletang River (estuary), Kema Tiga, North Minahasa, North Sulawesi **F** pleon.

tolateral angle pointed. Pl5 ca. 1.5× wider than long (at widest point), markedly constricted at base. Pl6 ca. 1.5× wider than long; widest sub-distally; subequal in length to pl5. Male telson rounded, ca. 1.4× wider than long (Fig. 12E).

Female pleon (Fig. 12F) conspicuously broad. Pl1 shortest; pl2 distinctly longer, as wide as pl1; pl3 trapezoidal, longer than pl2; pl4 rectangular, slightly longer than pl3, lateral margins convex; pl5 longer than pl4; pl6 distinctly longest. Female telson (Fig. 12F) triangular.

Male chelipeds stout, long, equal. Merus triangular in cross-section; standing higher than exorbital angle (Fig. 11B); lower margin with two rows of granules extending whole length of margin (Fig. 13A); upper margin narrowing proximally, with irregular rows of granules on distal half (Fig. 13K); outer margin with one row of granules extending whole length (Fig. 13L); upper surface flattened, ovate smooth tympanum, scattered long setae around tympanum, more setation distally, microscopically tuberculate (Fig. 13I); lower surface flattened, nearly smooth, with scattered granules, lacking

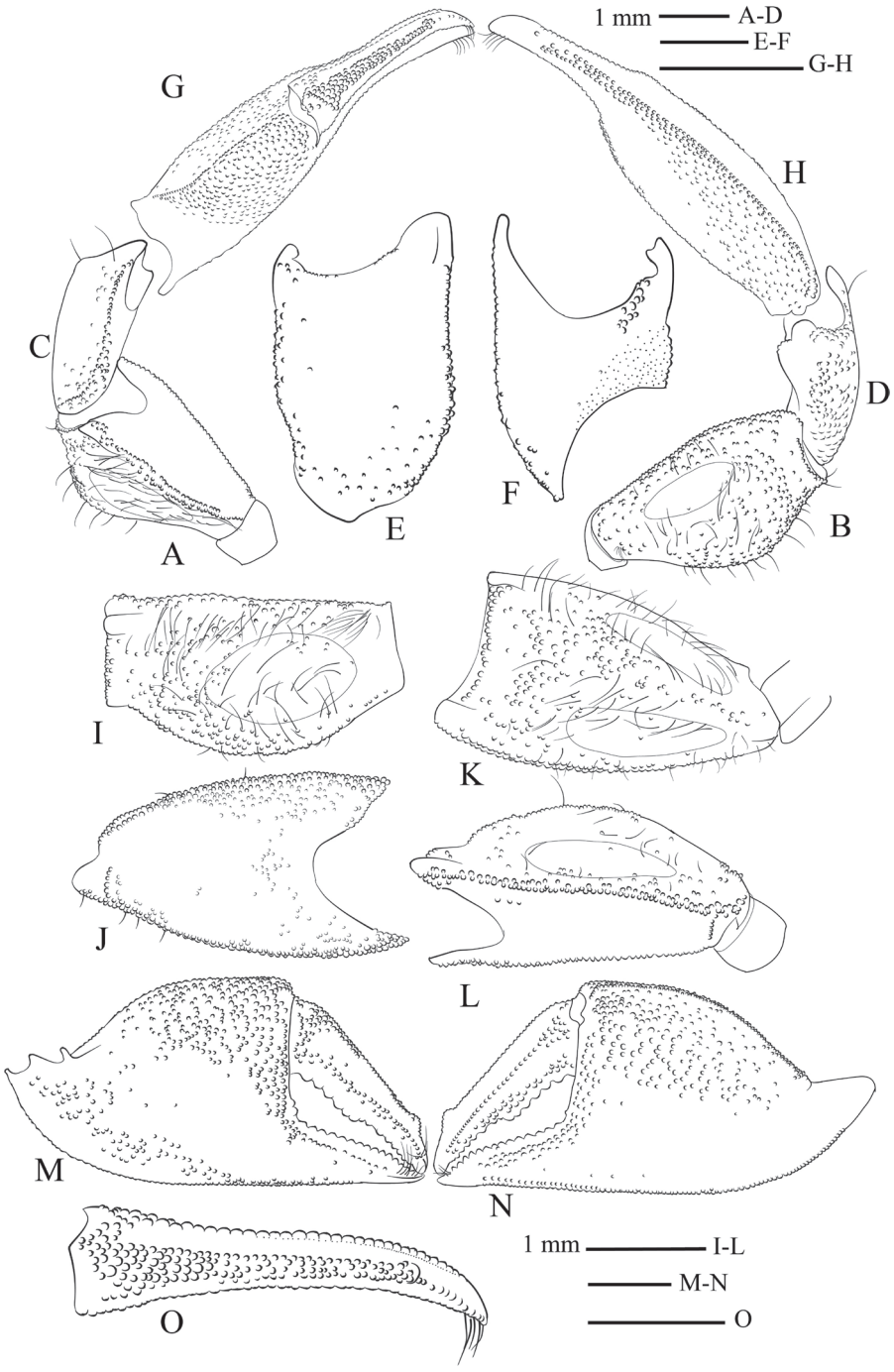

Figure 13. *Tmethypocoelis celebensis* sp. nov. Holotype, male (7.2 × 4.4 mm) (MZB.Cru.5574), Moletang River (estuary), Kema Tiga, North Minahasa, North Sulawesi. Left cheliped. Merus **A** lower margin **B** outer surface. Carpus **C** upper margin **D** lower margin **E** outer surface **F** inner surface. Chela **G** upper margin **H** lower margin. Merus **I** upper surface **J** lower surface **K** upper margin **L** outer margin. Chela **M** inner surface **N** outer surface **O** dactylus upper margin.

tympanum (Fig. 13J); outer surface convex, tympanum smaller than that of upper surface, evenly distributed granules and setae (Fig. 13B). Carpus shorter than merus, elongate, ca. 1.4× longer than wide; upper and lower margins tubercular (Fig. 13C, D); outer surface rectangular, scattered microscopic granules near upper and lower margins, median portion without microscopic tubercles (Fig. 13E); lower surface smooth, with one longitudinal row of granules, one patch of tubercles on proximal part (Fig. 13F). Palm bulky, ca. 1.3× longer than wide; inner surface granular over upper half, with granules extending over upper margin and curved to sharply cut upper margin of outer surface, distally with one row of regular granules reaching pollex, smaller granules near lower margin, median portion smooth (Fig. 13M); outer surface distinctly granular over upper half reaching to base of pollex, lower half smooth (Fig. 13N); upper margin with one row of granules, distinct groove extending below granular rows forming clear granular string (Fig. 13G); lower margin with granulation extending to lower part of inner surface (Fig. 13H). Fingers shorter than palm, lacking obvious basal gape, curved inwards, spooned-tip; cutting margins evenly serrated; inner margin at tip of both fingers with short row of stout setae. Pollex short, triangular, cutting margin slightly oblique, without large differentiated tooth or lobe, ca. 0.5× as long as palm; inner surface nearly smooth, one row of granules over proximal half (Fig. 13M); outer surface granular parallel to cutting margin, granules with similar size (Fig. 13N); lower margin granulated only along proximo-medially (Fig. 13H). Cutting margin of dactylus with teeth, larger teeth over proximal half, smaller teeth over distal half, without median lobe; inner surface with one row of granules parallel to upper margin, granulation extending from proximal to distal, one patch of granules proximally (Fig. 13M); band of granules on outer surface near cutting margin and junction to palm, one tubercular ridge extending medially parallel to upper margin (Fig. 13N); upper margin with row of tubercles terminating with triangular upturned tooth subdistally (Fig. 13O).

Female chelipeds small dotillid type (Figs 10B, 14). Not conspicuously different from *T. simplex* sp. nov. (see description for *T. simplex* sp. nov.).

Pereiopods (Fig. 15) slender, elongate, P2–P5 similar; smooth ovate tympanum on anterior and posterior surfaces of meri. Tympani on posterior surfaces becoming progressively smaller from P2–P5. Dactyli nearly straight, pointed, shorter than propodi.

P2 (Fig. 15A, B) shorter than P3; merus ca. 2.7× longer than wide; anterior surface bearing scattered granules outside tympanum, granules denser near lower margin, sparse setae near lower margin; posterior surface sparsely granulate, denser distal to tympanum; upper margin convex, sparse long setae, distally tubercular; lower margin smooth, sparse setae. Carpus shorter than propodus, surfaces smooth; margins without granules, sparse setae. Propodus with anterior and posterior surfaces with few small granules only; margins with sparse long setae.

P3 (Fig. 15C, D) longest; merus ca. 2.7× longer than wide; anterior surface scarcely granular; posterior surface sparsely granulate, denser near upper margin; upper and lower margins convex; upper margin tubercular distally, sparse long setae; lower margin smooth, sparse setae. Carpus shorter than propodus, surfaces nearly smooth, sparse setae distally; margins without tubercles, sparse setae. Propodus with anterior and posterior surfaces smooth; margins with sparse long setae.

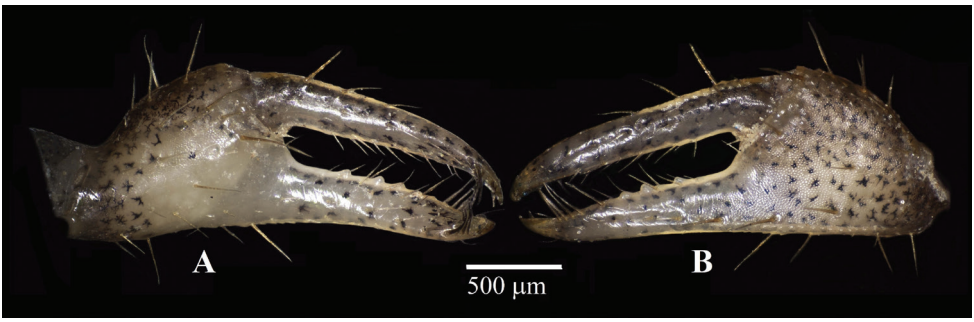

Figure 14. *Tmethypocoelis celebensis* sp. nov. Paratype, female (5.5 × 3.5 mm) (MZB.Cru.5180), Moletang river (estuary), Kema Tiga, North Minahasa, North Sulawesi. Left chela **A** inner surface **B** outer surface.

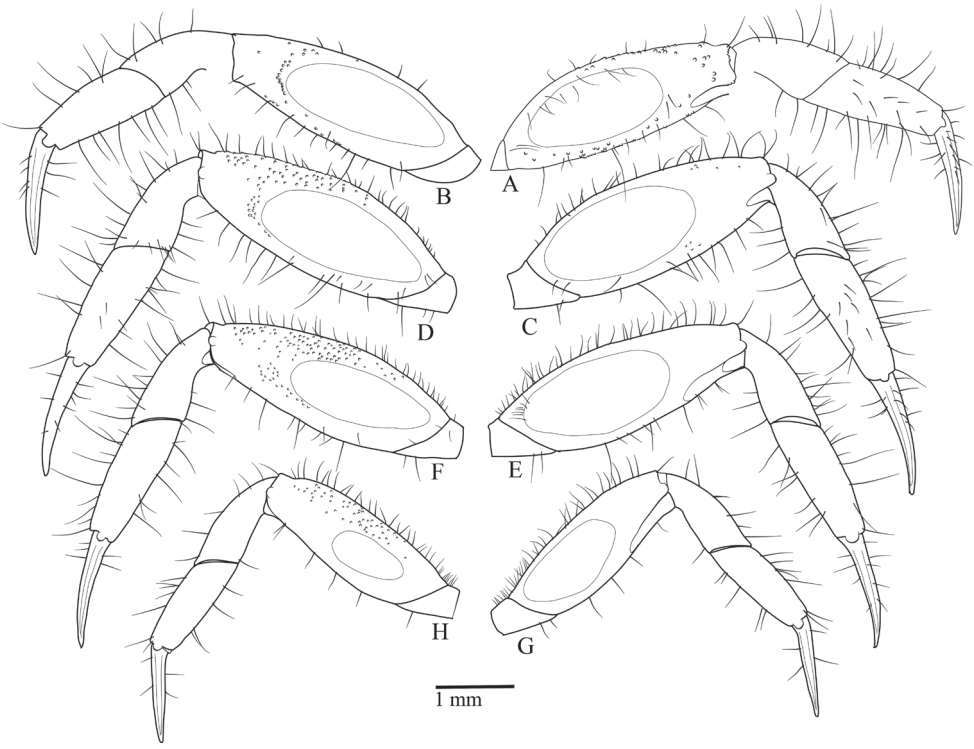

Figure 15. Left pereiopods of *Tmethypocoelis celebensis* sp. nov. Holotype, male (7.2 × 4.4 mm) (MZB. Cru.5574), Moletang River (estuary), Kema Tiga, North Minahasa, North Sulawesi **A, B** P2 **C, D** P3 **E, F** P4 **G, H** P5. Right side, anterior surfaces; left side, posterior surfaces.

P4 (Fig. 15E, F) nearly as long as P2; merus ca. 2.6× longer than wide; anterior surface scarcely granular; posterior surface with evenly distributed granules; upper and lower margins convex; upper margin tubercular distally, spaced long setae extending whole length; lower margin smooth, sparse setae. Carpus shorter than propodus, surfaces smooth; margins smooth, sparse setae. Propodus with anterior and posterior surfaces smooth; margins with sparse long setae.

P5 (Fig. 15G, H) shortest; merus ca. 2.8× longer than wide; anterior surface without granules; posterior surface granulate, granules denser near upper margin; upper and lower margins convex; upper margin sparsely tubercular, with sparse long setae, short setae proximally; lower margin smooth, with sparse setae. Carpus shorter than propodus, surfaces smooth; margins smooth, with sparse setae. Propodus with anterior and posterior surfaces smooth; margins with sparse long setae.

Reproductive organs. G1 long, recurved, very slender; sub-proximal portion bulging (Fig. 16A, B); apical portion forming two lobes, with three short setae on outer margin, two or three long setae apically, four or five short setae on mesial margin (Fig. 16C, D). Vulva (Fig. 16E) rounded, projecting.

Gastric mill. Median tooth plate simple, without defined ridges. Urocardiac ossicle relatively narrower throughout length. Propyloric ossicle semi-circular, relatively narrow and protruding; posterior margin curved; anterior margin with one pointed lobe medially; lateral margins quadrate with anterior lobes discrete, prominent, and rounded (Fig. 17B). Lateral zygocardiac tooth plate with eight slender teeth, three anterior teeth large (Fig. 17D).

Habitat. *Tmethypocoelis celebensis* sp. nov. inhabits sandy substrata in estuarine areas (Fig. 18).

Etymology. The species name is derived from the type locality. Celebes is the former name of Sulawesi Island, one of the great islands in Indonesia.

Remarks. The two new species described here differ from each other and from the other known species by numerous characters compared below. In general, the species of *Tmethypocoelis* are all extremely similar in general morphology with only small differences in male cheliped shape and dentition (Table 1), differences in the apical setal ornamentation of the male first gonopod, and sometimes differences in the proportions of the somites of the male pleon.

A comparison of male first gonopod setation patterns of described species suggests that the possession of two or three of markedly elongated apical setae (Figs 8C–E, 16C, D; Davie 1990: fig. 2), common to both *Tmethypocoelis simplex* sp. nov. and *T. celebensis* sp. nov., is so far shared with *T. liki* from Papua and *T. koelbeli* from the Northern Territory, NW Australia. Therefore, these four species may be more closely related to each other than they are to *T. ceratophora*, *T. choreutes*, and *T. odontodactylus*, which all share a coronet of shorter more evenly sized stout setae on the tip of the G1. A more thorough analysis of relationships within the genus will be undertaken as part of a larger revision of the genus, and with the help of DNA sequencing data.

Both *Tmethypocoelis simplex* sp. nov. and *T. celebensis* sp. nov. differ significantly from *T. koelbeli* in the shape of the male pleon, with that of *T. koelbeli* being relatively narrower, and in particular Pl5 being more constricted proximally (Table 2). The pleons of *T. simplex* sp. nov. and *T. celebensis* sp. nov. are similar, however, both Pl6 and the telson are slightly proportionately wider in *T. celebensis* sp. nov.

Tmethypocoelis simplex sp. nov. differs from *T. celebensis* sp. nov., *T. koelbeli*, and *T. liki* in the form and number of the apical setae of the G1. The G1 of *T. simplex* sp. nov.

Table 1. Comparison of male chelipeds in the species of *Tmethypocoelis*.

Species	*T. simplex* sp. nov.	*T. celebensis* sp. nov.	*T. koelbeli*	*T. liki*	*T. ceratophora*	*T. choreutes*	*T. odontodactylus*
Dactylus dorsal and outer armature	Upper margin finely tuberculate; lacking differentiated subdistal tooth; outer surface with semi-defined granular row medially; irregular granulation near cutting margin (Fig. 5M–O)	Upper margin finely tuberculate; culminating in subdistal upward, upwardly projecting triangular tooth of variable size from high and distinct to low; size not correlated with crab size; outer surface with medial granular row over entire length (Fig. 13M–O)	Dorsal band of fine granules; superior border straight, terminating in overhanging triangular tooth at about ¾ length; outer surface with 2 subregular lines of granules, superior one may extend ¾ length to tip, lower one less than that of superior	Upper margin with median row of granules, culminating into 1 prominent tooth	Finely tuberculate ridge on upper margin of dactylus terminates in outwardly directed flat triangular tooth (see Davie and Kosuge 1995: fig. 1 A, C)	Finely tubercular ridge on the upper margin continues evenly distally; outer surface has separate ridge ending in prominent triangular subdistal protrusion (see Davie and Kosuge 1995: fig. 1 B, D)	Full length medial granulate ridge; superior granulate crest terminating subdistally in strong upturned tooth (Davie 1990: fig. 3C)
Dactylus cutting margin	Evenly dentate; one wide enlarged convex tooth over proximal half	Evenly dentate, larger over proximal half, then finger narrower over distal half	Evenly dentate; smaller males with raised platform of teeth differentiated in proximal half, but less evident in mature chela	Wide and blunt irregular serrations	One small low tooth proximally	Low broad triangular convexity but lacking clearly differentiated tooth	Evenly dentate; slightly deeper medially, but without obvious differentiated tooth
Pollex cutting margin	Evenly dentate; long flat enlarged dentate tooth over most of length	Evenly dentate; straight, without differentiated tooth or lobe	Evenly dentate	Irregularly dentate	Prominent enlarged convex tooth medially	Lacking a defined tooth; slightly convex	Weakly convex; evenly dentate
Gape at base of fingers	Large	Poorly developed	Moderate	Poorly developed	Wide	Not strongly developed	Not strongly developed

Table 2. Comparison of pleonal somite proportions of *Tmethypocoelis simplex* sp. nov. and *T. celebensis* sp. nov. with the closely related *T. koelbeli* (proportions of latter taken from Davie 1990: fig. 1A).

Species	*T. koelbeli*	*T. liki*	*T. simplex* sp. nov.	*T. celebensis* sp. nov.
Pleonite 5 width/length	1.1	1.3	1.5	1.5
Pleonite 5 narrowest proximal width to distal width	0.6	0.8	0.7	0.7
Pleonite 6 width/length	1.2	1.2	1.4	1.5
Telson width/length	1.2	1.4	1.4	1.4

typically has two or three very long setae apically (Fig. 8C–E), and subapically there are three shorter stout setae on the outer margin increasing in length distally, and four short, downwardly reflexed setae on inner lobe. The G1 of *T. celebensis* sp. nov. has two or three very long recurved setae apically (Fig. 16B–D), and subapically there are also three stout setae on the outer margin, though the proximal seta is much smaller and less prominent than on *T. simplex* sp. nov., and also four or five short, downwardly reflexed setae on the inner lobe. The G1 of *T. koelbeli* similarly has two long apical setae but lacks a row of outer subapical setae and has a row of five short distally pointed setae on the inner lobe (Davie 1990: fig. 2). The G1 of *T. liki* has one long and five short apical setae (Murniati et al. 2022: fig. 20C).

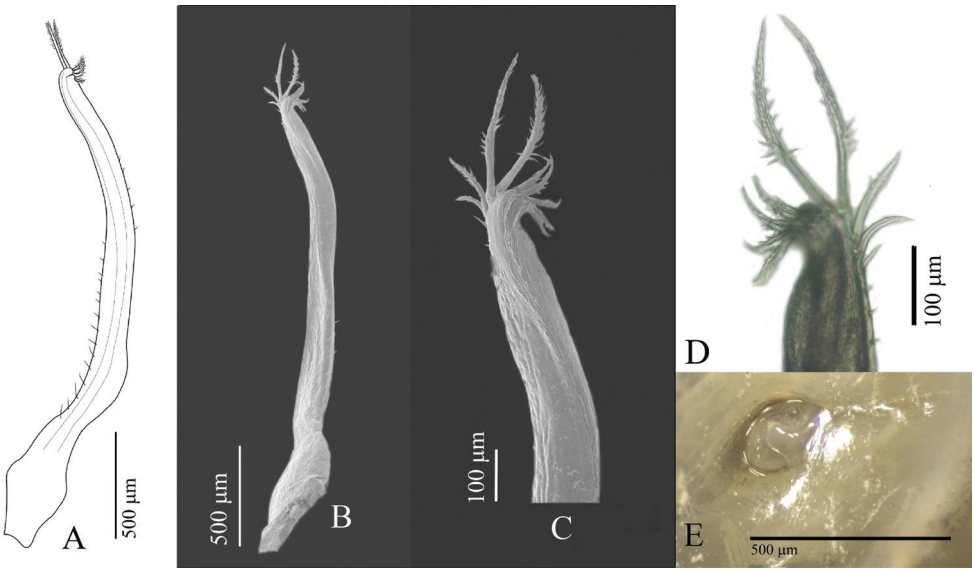

Figure 16. Reproductive organs of *Tmethypocoelis celebensis* **b** paratype, male (7.3 × 4.4 mm) (MZB. Cru.5180), Moletang River (estuary), Kema Tiga, North Minahasa, North Sulawesi, left G1 **A** mesial view **B** dorsal view **C, D** apical portion **C** dorsal view **D** ventral view. Paratype, female (5.5 × 3.5 mm) (MZB.Cru.5180), Moletang River (estuary), Kema Tiga, North Minahasa, North Sulawesi **E** vulva.

Discussion

Tmethypocoelis for many years included only the type species *Tmethypocoelis ceratophora* (Koelbel, 1897), which was believed to be widespread from Hong Kong, China, Japan, and south to Lombok in Indonesia (Tesch 1918; Dutreix 1992; Huang et al. 1992; Murniati 2015). In recent years, however, four new species have been described (see Introduction), and the distribution of *T. koelbeli* has become more restricted (Davie 1990; Davie and Kosuge 1995; Murniati et al. 2022). Nevertheless, the genus is outwardly morphologically relatively homogenous, with only small differences among the species most obviously related to chela dactylar tooth shape, and differences in the apical setae of the G1. This is particularly exemplified by the separation of the pseudocryptic *T. choreutes*, that had long been confused with *T. ceratophora*, but the morphological differences were shown to correlate with the evolution of a different male courtship waving display (Davie and Kosuge 1995).

The relative morphological homogeneity within the genus is also an indication that *Tmethypocoelis* species have undergone relatively recent speciation based around small-scale biogeographic restrictions. With the complex evolving paleogeography of land-connections and sea-level changes throughout the Indo-Malaysian Archipelago over the last two million years, it can be expected that the genus may have speciated much more than previously thought. Careful collecting across a broad range of areas within the region and more careful observations of populations, including finer scale morphological investigations, behavioural analyses and genetic studies are indeed revealing this pattern, and further new species will be described by the present authors as part of ongoing revisionary work.

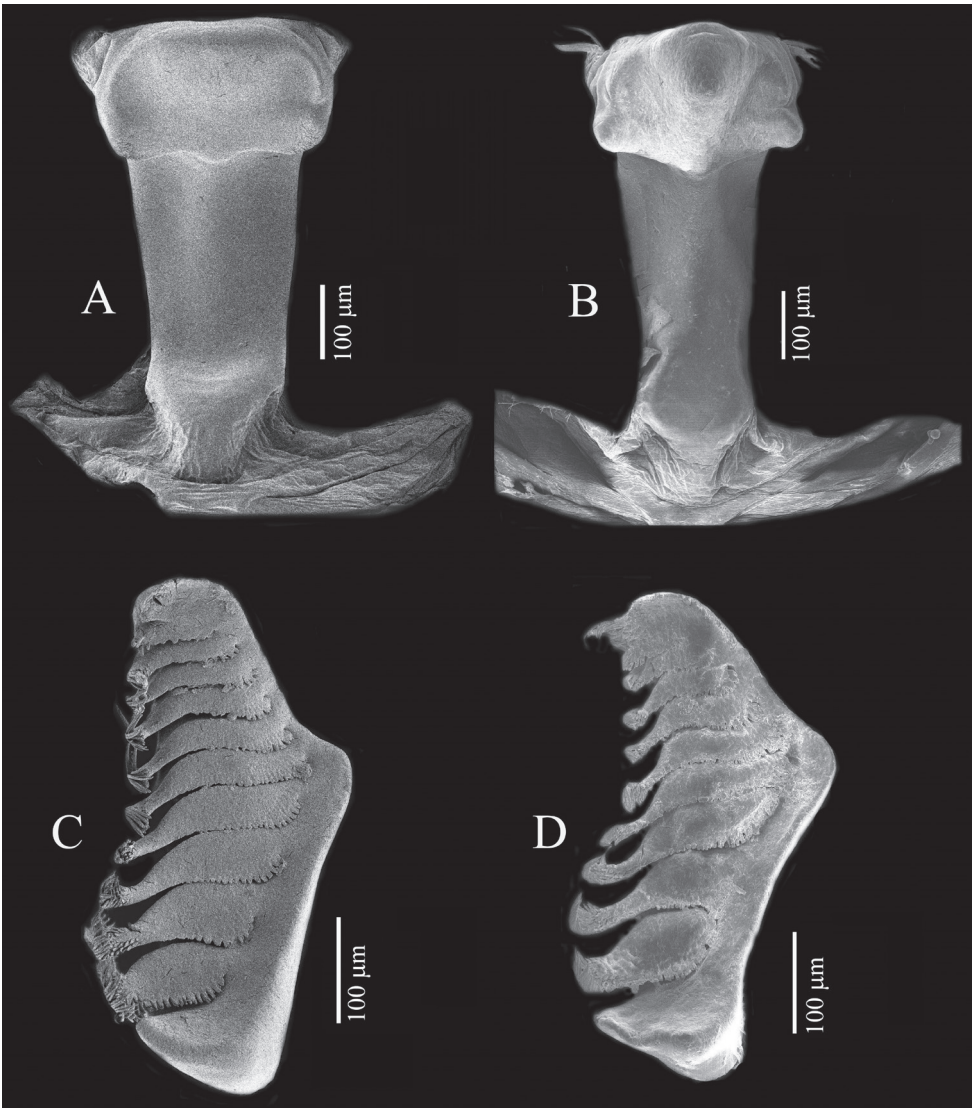

Figure 17. Teeth of gastric mill (posterior portion on upper part). *Tmethypocoelis simplex* sp. nov., paratype, male (6.9 × 4.0 mm) (MZB.Cru. 5183) (**A, C**). *Tmethypocoelis celebensis* sp. nov., paratype, male (7.3 × 4.4 mm) (MZB.Cru.5180) (**B, D**). **A, B** median tooth **C, D** lateral tooth.

General morphology

It is interesting to note that the tympani on the anterior and posterior surfaces of the pereiopods are essentially the same between the present two new species; and while the tympani are very similar on both faces of P2 and P3, on both P4 and P5 the anterior tympani are markedly smaller in size with P5 the smallest; the posterior tympani on P2 and P5 are much larger and cover a proportionately similar surface area to the first two pereiopods (Figs 7, 15). This is simply an observation, and no physiological explanation can be offered.

Figure 18. Habitat of *Tmethypocoelis celebensis* sp. nov. at Moletang River (estuary), Kema Tiga, North Minahasa, North Sulawesi.

Feeding morphology

Speciation in ocypodoid crabs seems to have commonly involved variations in structures related to feeding and adaptations to different sediment particle sizes or food types on which each species feeds. For example, both the setation of the second maxillipeds and the shape of the grinding plates inside the gastric mill, have proven useful in distinguishing closely related species (Davie et al. 2015). The second maxilliped has specialized "spoon shaped" setae for sorting organic matter and microorganisms from the sand (e.g., Icely and Jones 1978; Vogel 1984; Colpo and Negreiros-Fransozo 2013). Spoon-tipped setae mostly occur on the inside margins of the second maxillipeds where they hold sand grains that are then brushed by short stiff setae on the outer faces of the first maxillipeds. Such setal structures have been well studied especially in species of *Dotilla* Stimpson, 1858 and *Uca* Leach, 1848 sensu lato, and vary according to the preferred substrate particle-size composition, and the distribution of the species on the shore (Icely and Jones 1978). Murniati and Wowor (2017) were the first to use second maxilliped setation to successfully separate three species of *Tmethypocoelis* occurring in Indonesia, and to help infer micro-ecological niche separation.

Although, the second maxillipeds have not been examined as a part of the present species descriptions, the gastric mill structure has been included, and equally shows that the two new species described here have adapted to different dietary requirements

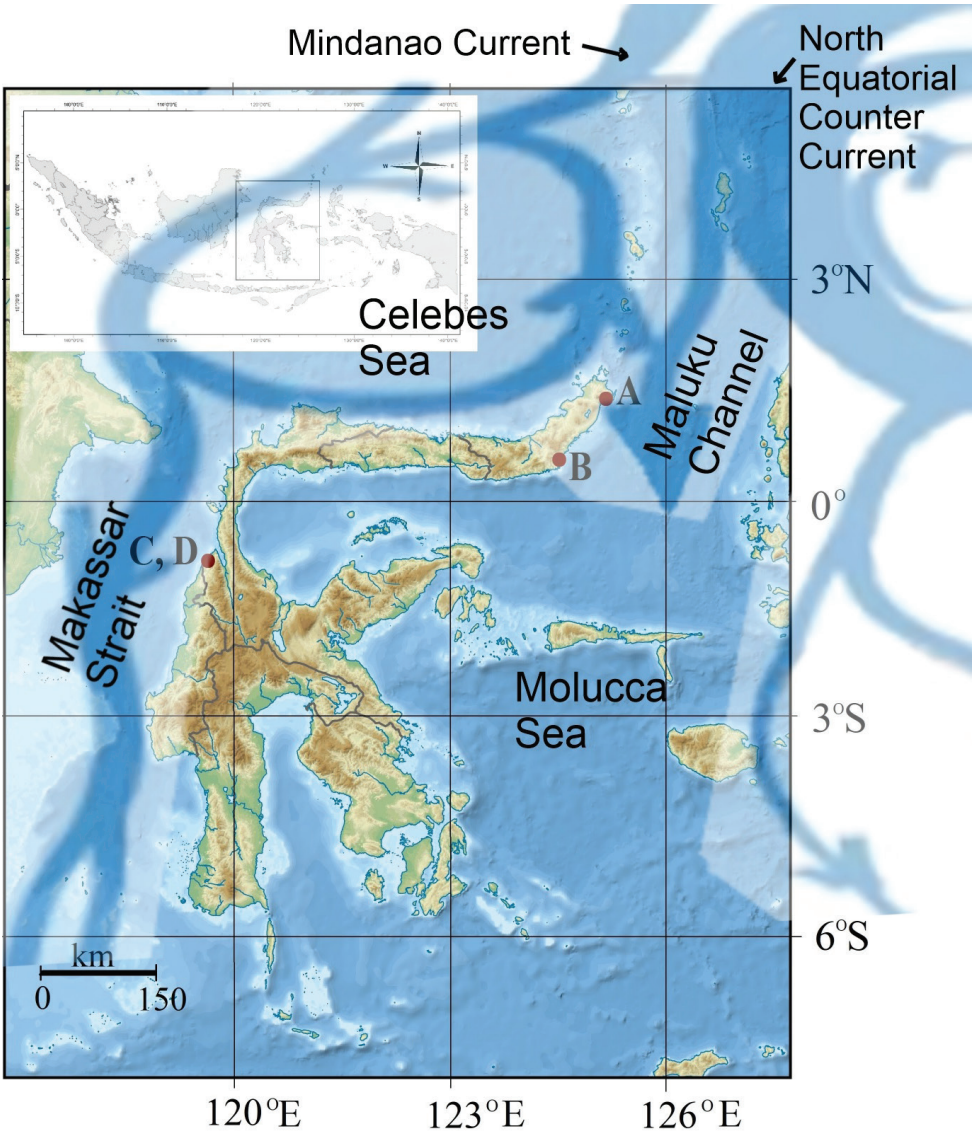

Figure 19. Map showing sea-current circulation patterns in the waters surrounding Sulawesi (derived from Wijeratne et al. 2018 and Sprintall et al. 2019).

(e.g., see Kosuge and Davie 2001), and this is the first study to report species-specific gastric mill differences within *Tmethypocoelis* (Fig. 17A–D). The main trunk of the urogastric ossicle is noticeably broader in *T. simplex* sp. nov. than in *T. celebensis* sp. nov.; in both species, the medial tooth plate is simple and without defined ridges. However, the lateral margins are evenly convex in *T. simplex* sp. nov., versus more quadrate margins with anterior lobes discrete, prominent, and rounded in *T. celebensis* sp. nov.; the propyloric ossicle is also flatter and broader in *T. simplex* sp. nov., versus narrower and more protruding in *T. celebensis* sp. nov. In lateral zygocardiac teeth, there are also

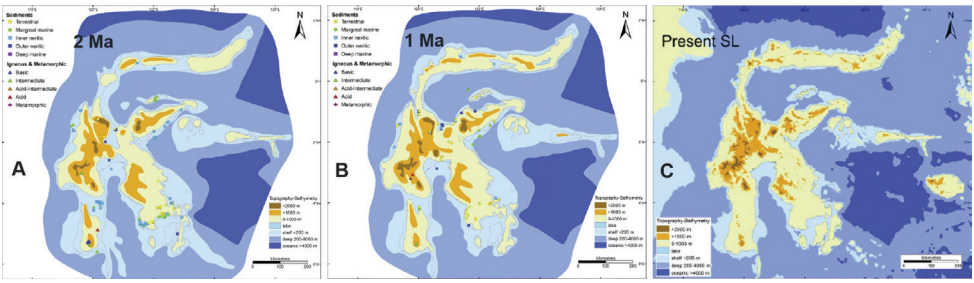

Figure 20. Paleogeography of Sulawesi. **A** 2 Mya **B** 1 Mya map **C** present time (after Nugraha and Hall 2018).

significant differences: in particular, *T. simplex* sp. nov. has nine accessory teeth that have a broader thicker brush of apical setae than *T. celebensis* sp. nov., which has only eight accessory teeth, each with a narrower brush of apical setae. While these differences would need a more specialized study to understand the dietary implications, nevertheless, it is apparent that although *Tmethypocoelis* species are deposit feeders, the lack of fine transverse median ridges on the urocardiac ossicle (as one would find on deposit feeding ocypodids such as *Uca*; see Icely and Nott 1992) would seem to indicate that the particulate organic matter that they are consuming does not require fine grinding, and the brushes of setae and fine scales on the accessory teeth of the zygocardiac ossicles serve more of a brushing function.

Biogeography

Tmethypocoelis species are essentially estuarine animals, living abundantly on estuarine mud flats and able to tolerate low salinities. Davie (1985) and Davie et al. (2010) have postulated that a short larval life in combination with local hydrological factors may be enough to lead to the allopatric separation of two geographically close taxa. Davie and Kosuge (1995) remarked that *Tmethypocoelis ceratophora* and their new species *T. choreutes* are separated by the relatively narrow strait between Taiwan and the Japanese Yaeyama Islands. Davie et al. (2010) described a similar disjunction between the Chinese/Taiwanese *Mictyris brevidactylus* Simpson, 1858, and their new species *Mictyris guinotae* Davie, Shih & Chan, 2010, as well as citing a number of other similar cases of closely related sibling species on either side of the aforesaid strait. They concluded that the Ryukyus appear to be much more influenced by the main Kuroshio Current in contrast to the continental coastline, which is impacted mainly by the South China Sea Current and westerly flowing Kuroshio Branch Current (Jan et al. 2002), and that the deep-water strait between Taiwan and the Yaeyama Islands plays an important additional role in the local circulation patterns of the region, so as to become an effective barrier for species that may have rapid larval development and/or abbreviated life cycles. Thus, this narrow passage of water has functioned as a barrier against genetic flow between the two regions, and allowed the allopatric speciation of sibling taxa.

In the case of the two new species described here, *T. simplex* sp. nov. and *T. celebensis* sp. nov., there is good evidence that a similar pattern of local current flow may have led to their separate evolutionary development (Fig. 19). Sprintall et al. (2019) have published an interesting map of current circulation patterns within the Indonesian Archipelago that shows the southerly flowing Mindanao current forming a counter-clockwise circulation flow within the Celebes Sea as well as flowing south through the Makassar Strait. The Celebes Sea is bordered to the east by a shallow ridge and island chain extending northwards from the tip of north Sulawesi to Mindanao in the southern Philippines; whereas the east coast of Sulawesi, home to *T. celebensis* sp. nov., is instead under the influence of an off-shoot of the North Equatorial Counter Current that flows southwards through the Maluku Channel. There are, therefore, two major separate southerly flowing current systems on either side of the island of Sulawesi, and this appears to effectively separate larval dispersal of both species to the east and west coasts, respectively.

While no genetic clock estimates have yet been applied to the two species studied here, it can be presumed that their evolutionary separation has been recent, i.e., within the last 2 million years. This time-frame has precedent in other recent speciation events that have occurred in the Indo-West Pacific region. For example, based on the molecular clock of COI mutation rates suggested by Schubart et al. (1998), Ragionieri et al. (2009, 2010, 2012) found that the sister sesarmid species *Neosarmatium africanum* Ragionieri, Fratini & Schubart, 2012, and *N. meinerti* (De Man, 1887) became isolated between 1.6–1.96 ± 0.34 mya (1.6% divergence); and similarly, Lai et al. (2010) estimated that the portunids *Portunus armatus* (A. Milne-Edwards, 1861) and *P. reticulatus* (Herbst, 1799) became established around 0.78–2.5 mya, based on a 1.8% CO1 divergence.

Given our assumption that species separation has been caused by differences in circulation patterns, then it is important to understand the geological history of the Indonesian archipelago and the geological changes that have led to the current shape of the island of Sulawesi. Nugraha and Hall (2018) have studied the Late Cenozoic palaeogeography of Sulawesi, and it is clear that it is only within the last 2 million years (since the Early Pleistocene) that, Sulawesi began to resemble its present form (Fig. 20A–C). By the Early Pleistocene, paleogeographic change across Sulawesi included the rise of high mountains and the rapid subsidence in offshore basins; much of the North Arm and most of the southern South Arm appear to have emerged although the northern part of the South Arm was still a shallow marine area. Between 1.8–1.0 mya subsidence in the southern SE Arm continued, and by 1 Mya, Sulawesi was very similar in form to the present. The inter-arm basins were close to their present depths of 1.5 to 2.0 km. The North Arm was largely emergent, and there was a land connection between the North Arm and western Central Sulawesi as the Neck elevation increased. Therefore, this pattern of recent island emergence and sea basin separation supports our contention that speciation of *T. simplex* sp. nov. and *T. celebensis* sp. nov. began as a vicariant event within the last 2 million years.

Studies of survivorships of pelagic larvae under various salinity regimes, and analyses of genetic structure among different island populations throughout the Indonesian Archipelago will provide exciting insights into the speciation of coastal crabs and the evolutionary impacts of paleogeography throughout this region.

Acknowledgements

We would like to thank our colleagues, Dr. Annawati and Fahri M.Si. from Tadulako University, Palu, Central Sulawesi for facilitating us during fieldwork. Thanks to Directorate of Scientific Collection Management, BRIN, Cibinong, Bogor, Indonesia for depositing the specimens. Martin Low of the Lee Kong Chian Natural History Museum, Singapore, is thanked for his research into clarifying the dates of publication of Koelbel's 1897/1898 publications in which *Tmethypocoelis* was first described. We are thankful to Sameer Kumar Pati, Peter Kee Lin Ng, and the other anonymous reviewer for comments on the manuscript. We also thank the Indonesia Endowment Fund for Education (LPDP), Ministry of Finance of the Republic of Indonesia for the PhD scholarship and research fund awarded to DCM. The present study was also supported by Seto Marine Biological Laboratory, Kyoto University, Japan.

References

Colpo KD, Negreiros-Fransozo ML (2013) Morphological diversity of setae on the second maxilliped of fiddler crabs (Decapoda: Ocypodidae) from the southwestern Atlantic coast. Invertebrate Biology 132(1): 38–45. https://doi.org/10.1111/ivb.12004

Dai AY, Yang S (1991) Crabs of the China Seas. China Ocean Press, Beijing, China, 608 pp. [74 pls]

Dai AY, Yang SL, Song YZ, Chen GX (1986) Crabs of the China Seas. China Ocean Press, Beijing, 11 + 642 pp. [In Chinese]

Davie PJF (1985) The biogeography of littoral crabs (Crustacea: Decapoda: Brachyura) associated with tidal wetlands in tropical and sub-tropical Australia. In: Bardsley KN, Davie JDS, Woodroffe CD (Eds) Coasts and tidal wetlands of the Australian Monsoon region. Mangrove Monograph No. 1. Australian National University, North Australia Research Unit, 259–275.

Davie PJF (1990) New and rare crabs of the subfamily Dotillinae (Crustacea: Ocypodidae) from northern Australia and Papua New Guinea. Memoirs of the Queensland Museum 28: 463–473.

Davie PJF (2002) Crustacea: Malacostraca: Eucarida (Part 2): Decapoda-Anomura, Brachyura). In: Wells A, Houston WWK (Eds) Zoological Catalogue of Australia. Vol. 19.3B. CSIRO Publishing, Melbourne, 1–641.

Davie PJF, Kosuge T (1995) A new species of *Tmethypocoelis* (Crustacea: Brachyura: Ocypodidae) from Japan. The Raffles Bulletin of Zoology 43(1): 207–215.

Davie PJF, Shih H-T, Chan B (2010) A new species of *Mictyris* (Crustacea: Decapoda: Brachyura: Mictyridae) from the Ryukyus Islands, southern Japan. In: Castro P, Davie PJF, Ng PKL, Richer de Forges B (Eds) Studies on Brachyura: a homage to Danièle Guinot. Crustaceana Monographs 11. Brill, Leiden, 83–105. https://doi.org/10.1163/ej.9789004170865.i-366.61

Davie PJF, Guinot D, Ng PKL (2015) Anatomy and functional morphology of Brachyura. In: Castro P, Davie PJF, Guinot D, Schram FR, Von Vaupel Klein JC (Eds) Decapoda: Brachyura (Part 1). Treatise on Zoology — anatomy, taxonomy, biology. The Crustacea. Vol. 9C-I. Brill, Leiden, 11–163. https://doi.org/10.1163/9789004190832_004

Dewi K, Purwaningsih E (2020) Three new species of Cloacininae (Nematoda: Strongyloidea) parasitic in *Dorcopsis muelleri* (Schlegel, 1866) from Papua and Salawati Island, Indonesia. Zootaxa 4747(3): 535–546. https://doi.org/10.11646/zootaxa.4747.3.7

Dutreix E (1992) Experimental study of the impact of hydrocarbons on the intertidal benthic community: The Mahakam Delta (East Kalimantan, Indonesia). Oceanologica Acta 15(2): 197–209.

Huang JF, Yu HP, Takeda M (1992) A review of the ocypodid and mictyrid crabs (Crustacea: Decapoda: Brachyura) in Taiwan. Bulletin of the Institute of Zoology, Academia Sinica 31(3): 141–161.

Icely JD, Jones DA (1978) Factors affecting the distribution of the genus *Uca* (Crustacea: Ocypodidae) on an East African shore. Estuarine and Coastal Marine Science 6(3): 315–325. https://doi.org/10.1016/0302-3524(78)90019-1

Icely JD, Nott JA (1992) Digestion and absorption: digestive system and associated organs. In: Harrison FW (Ser. Ed.) Microscopic anatomy of invertebrates. Harrison FW, Humes AG (Vol. Eds) Decapod Crustacea. John Wiley, New York, 147–201.

Jan S, Wang J, Chern C-H, Chao S-Y (2002) Seasonal variations of circulation in the Taiwan Strait. Journal of Marine Systems 35(3–4): 249–268. https://doi.org/10.1016/S0924-7963(02)00130-6

Koelbel K (1897) Rákok [= Crabs]. In: Széchenyi B [Count], 1890–1897. Gróf keletázsiai utjának tudományos eredménye, 1877–1880 [= Count Béla Széchenyi's Scientific Results of the East Asian passage, 1877–1880]. Vol. 2. K. F. E. K. [= Kilián Frigyes Egyetemi Könyvárus] Bizományában, Budapest, 709–718. [pl. I] [In Hungarian]

Koelbel K (1898) Beschreibung der Krebse. In: Széchenyi B [Count], 1893–1899. Die wissenschaftlichen Ergebnisse der Reise des Grafen Béla Széchenyi in Ostasien, 1877–1880 [= The Scientific Results of the Voyage of Count Bela Szechenyi in East Asia 1877–1880]. Vol. 2. Commission der Verlagsbuchhandlung von E. Holzel, Wien, 707–718. [pl. I.] [pp. 567–579 on separate] [German translation of Koelbel 1897]

Kosuge T, Davie PJF (2001) Redescription of *Macrophthalmus boteltobagoe* and *M. holthuisi* with notes on their ecology (Brachyura: Ocypodidae). Journal of Crustacean Biology 21(2): 545–555. https://doi.org/10.1163/20021975-99990155

Lai JCY, Ng PKL, Davie PJF (2010) A revision of the *Portunus pelagicus* species complex (Crustacea: Brachyura: Portunidae), with the recognition of four species. The Raffles Bulletin of Zoology 58(2): 199–237.

Murniati DC (2015) Distribution and characteristic of deposit feeder crabs (Crustacea: Brachyura) in some mangrove ecosystem types in Lombok Island. Journal of Biological Research (Thessaloniki) 21(1): 24–29. https://doi.org/10.23869/bphjbr.21.1.20155

Murniati DC, Wowor D (2017) Second maxilliped setation in genus *Tmethypocoelis* Koelbel, 1897 (Brachyura: Dotillidae) characterizes its microhabitat. Poster presented at the Third International conference on Southeast Asian Gateway Evolution (SAGE 2017). https://doi.org/10.13140/RG.2.2.19568.76806

Murniati DC, Asakura A, Nugroho DA, Hernawan UE, Dharmawan IWE (2022) On a collection of thoracotreme crabs (Crustacea: Brachyura: Ocypodidae, Macrophthalmidae, Dotillidae) from two offshore islands of Papua, eastern Indonesia, with descriptions of two new species. The Raffles Bulletin of Zoology 70: 461–491. https://doi.org/10.26107/RBZ-2022-0026

Ng PKL, Guinot D, Davie PJF (2008) Systema Brachyororum: Part I. An annotated checklist of extant brachyuran crabs of the world. The Raffles Bulletin of Zoology (Supplement 17): 1–286.

Nugraha AMS, Hall R (2018) Late cenozoic palaeogeography of Sulawesi, Indonesia. Palaeogeography, Palaeoclimatology, Palaeoecology 490: 191–209. https://doi.org/10.1016/j.palaeo.2017.10.033

Ragionieri L, Fratini S, Vannini M, Schubart CD (2009) Phylogenetic and morphometric differentiation reveal geographic radiation and pseudo-cryptic speciation in a mangrove crab from the Indo-West Pacific. Molecular Phylogenetics and Evolution 52(3): 825–834. https://doi.org/10.1016/j.ympev.2009.04.008

Ragionieri L, Cannicci S, Schubart CD, Fratini S (2010) Gene flow and demographic history of the mangrove crab *Neosarmatium meinerti:* A case study from the western Indian Ocean. Estuarine, Coastal and Shelf Science 86(2): 179–188. https://doi.org/10.1016/j.ecss.2009.11.002

Ragionieri L, Fratini S, Schubart CD (2012) Revision of the *Neosarmatium meinerti* species complex (Decapoda: Brachyura: Sesarmidae), with descriptions of three pseudocryptic Indo-West Pacific species. The Raffles Bulletin of Zoology 60: 71–87.

Rathbun MJ (1897) A revision of the nomenclature of the Brachyura. Proceedings of the Biological Society of Washington 11: 153–167.

Sakai T (1939) Studies on the Crabs of Japan. IV. Brachygnatha, Brachyrhyncha. Yokendo Co., Ltd., Tokyo, 365–741. [pls. 42–111]

Sakai T (1976) Crabs of Japan and the Adjacent Seas. Kodansha Ltd., Tokyo, 773 pp. [251 pls]

Schubart CD, Diesel R, Hedges SB (1998) Rapid evolution to terrestrial life in Jamaican crabs. Nature 393(6683): 363–365. https://doi.org/10.1038/30724

Shen CJ (1935) On some new and rare crabs of the families Pinnotheridae, Grapsidae and Ocypodidae from China. Dongwuxue Zazhi 1: 19–40.

Shih HT, Chan BKK, Teng SJ, Wong KJH (2015) Crustacean Fauna of Taiwan: Brachyuran Crabs. Volume II-Ocypodoidea. National Chung Hsing University, Taiwan, 303 pp.

Sprintall J, Gordon AL, Wijffels SE, Feng M, Hu S, Koch-Larrouy A, Phillips H, Nugroho D, Napitu A, Pujiana K, Susanto RD, Sloyan B, Peña-Molino B, Yuan D, Riama NF, Siswanto S, Kuswardani A, Arifin Z, Wahyudi AJ, Zhou H, Nagai T, Ansong JK, Bourdalle-Badié R, Chanut J, Lyard F, Arbic BK, Ramdhani A, Setiawan A (2019) Detecting change in the Indonesian seas. Frontiers in Marine Science 6: 257. https://doi.org/10.3389/fmars.2019.00257

Tesch JJ (1918) Hymenosomidae, Retroplumidae, Ocypodidae, Grapsidae and Gecarcinidae. The Decapoda Brachyura of the Siboga-Expedition. I. Siboga Expeditie Monografie, XXXIXc1, 1–148. [pls. 1–6] [Feb.1918] https://doi.org/10.5962/bhl.title.10267

Vogel F (1984) Comparative and functional morphology of the spoon-tipped setae on the second maxillipeds in *Dotilla* Stimpson, 1858 (Decapoda, Brachyura, Ocypodidae). Crustaceana 47(3): 225–234. https://doi.org/10.1163/156854084X00487

Wada K (1995) Brachyura. In: Nishimura S (Ed.) Guide to seashore animals of Japan with color pictures and keys. Hoikusha, Osaka, 2: 379–418. [pls. 101–118] [In Japanese]

Wijeratne S, Pattiaratchi C, Proctor R (2018) Estimates of surface and subsurface boundary current transport around Australia. Journal of Geophysical Research: Oceans 123: 3444–34466. https://doi.org.10.1029/2017JC013221

Wikipedia (2022) File:Sulawesi topography plain.png. https://commons.wikimedia.org/wiki/File:Sulawesi_topography_plain.png [accessed 22 September 2022]